MICHIGAN STATE UNIVERSITY

CYCLOTRON LABORATORY HENRY G. BLOSSER

Operating Proposal for the

NSCL Research Facility

and

MSU Nuclear Science Program

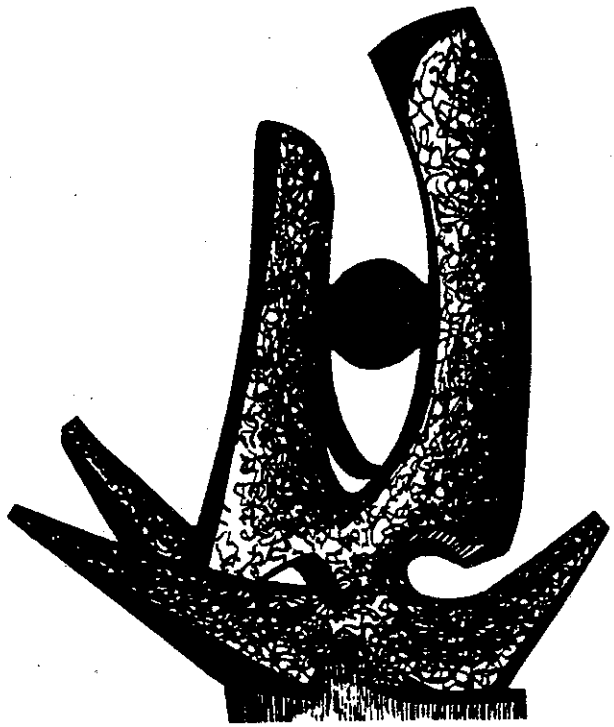

March 1986

MSUCL-552

PROPOSAL

to the

NATIONAL SCIENCE FOUNDATION

for

OPERATING SUPPORT

of the

NATIONAL SUPERCONDUCTING CYCLOTRON LABORATORY
RESEARCH FACILITY

and the

MICHIGAN STATE UNIVERSITY
NUCLEAR SCIENCE PROGRAM

Period: November 1, 1986 - October 31, 1989

Submitted by

Michigan State University

East Lansing, Michigan 48824-1321, USA

PRINCIPAL INVESTIGATORS

Nuclear Science:

S.M. Austin
W. Benenson
H.G. Blosser
G.M. Crawley
A.I. Galonsky
C.K. Gelbke
M.M. Gordon
E. Kashy
W.C. McHarris
J.A. Nolen, Jr.
D.K. Scott

Facility Operation:

R. Au
P. Miller

EXHIBIT II-1
Form Approved
OMB No. 3145-0058

PROPOSAL TO THE NATIONAL SCIENCE FOUNDATION
Cover Page

FOR CONSIDERATION BY NSF ORGANIZATIONAL UNIT (Indicate the most specific unit known, i.e. program, division, etc.)	IS THIS PROPOSAL BEING SUBMITTED TO ANOTHER FEDERAL AGENCY? Yes ___ No X ; IF YES, LIST ACRONYM(S):
NUCLEAR PHYSICS PROGRAM DIVISION OF PHYSICS	

PROGRAM ANNOUNCEMENT/SOLICITATION NO.:	CLOSING DATE (IF ANY):

NAME OF SUBMITTING ORGANIZATION TO WHICH AWARD SHOULD BE MADE (INCLUDE BRANCH/CAMPUS/OTHER COMPONENTS)

MICHIGAN STATE UNIVERSITY

ADDRESS OF ORGANIZATION (INCLUDE ZIP CODE)
NATIONAL SUPERCONDUCTING CYCLOTRON LABORATORY
MICHIGAN STATE UNIVERSITY
EAST LANSING, MI 48824-1321

TITLE OF PROPOSED PROJECT
Operation of the National Superconducting Cyclotron Laboratory Research Facility and the Michigan State University Nuclear Science Program.

REQUESTED AMOUNT	PROPOSED DURATION	DESIRED STARTING DATE
$25,215,700	3 years	1 November 1986

PI/PD DEPARTMENT	PI/PD ORGANIZATION	PI/PD PHONE NO.
National Superconducting Cyclotron Laboratory	Michigan State University	517-355-7602

PI/PD NAME	SOCIAL SECURITY NO.*	SIGNATURE	MALE*	FEMALE*
Sam M. Austin			X	
Henry G. Blosser			X	
ADDITIONAL PI/PD R. Au			X	
W. Benenson			X	
G. Crawley			X	
ADDITIONAL PI/PD A. Galonsky			X	
C.K. Gelbke			X	
M.M. Gordon			X	
ADDITIONAL PI/PD E. Kashy			X	
Wm. McHarris			X	
ADDITIONAL PI/PD P. Miller			X	
J. Nolen			X	
D. Scott			X	

FOR RENEWAL OR CONTINUING AWARD REQUEST, LIST PREVIOUS AWARD NO.:	SUBMITTING ORGANIZATION IS: ☐ For-Profit Organization; ☐ Small Business; ☐ Minority Business; ☐ Woman-Owned Business; (See cover page instructions)
PHY83-12245	

*Submission of social security numbers is voluntary and will not affect the organization's eligibility for an award. However, they are an integral part of the NSF information system and assist in processing the proposal. SSN solicited under NSF Act of 1950, as amended.

CHECK APPROPRIATE BOX(ES) IF THIS PROPOSAL INCLUDES ANY OF THE ITEMS LISTED BELOW:

☐ Animal Welfare ☐ Human Subjects ☐ National Environmental Policy Act
☐ Endangered Species ☐ Marine Mammal Protection ☐ Research Involving Recombinant DNA Molecules
☐ Historical Sites ☐ Pollution Control ☐ Proprietary and Privileged Information

PRINCIPAL INVESTIGATOR/ PROJECT DIRECTOR	AUTHORIZED ORGANIZATIONAL REP.	OTHER ENDORSEMENT (optional)
NAME S.M. Austin H.G. Blosser	NAME Howard G. Grider	NAME
SIGNATURE S.M. Austin Jerry Blosser	SIGNATURE Howard G. Grider	SIGNATURE
TITLE Co-Directors	TITLE Director, Contract and Grant Administration	TITLE
DATE 3/14/86	DATE 3/14/86	DATE
TELEPHONE NO. AREA CODE: 517 355-7602	TELEPHONE NO. AREA CODE: 517 355-5040	TELEPHONE NO. AREA CODE:

TABLE OF CONTENTS

NATIONAL SCIENCE FOUNDATION

PROJECT SUMMARY

FOR NSF USE ONLY			
DIRECTORATE/DIVISION	PROGRAM OR SECTION	PROPOSAL NO.	F.Y.

NAME OF INSTITUTION (INCLUDE BRANCH/CAMPUS AND SCHOOL OR DIVISION)

MICHIGAN STATE UNIVERSITY

ADDRESS (INCLUDE DEPARTMENT)

NATIONAL SUPERCONDUCTING CYCLOTRON LABORATORY (NSCL)
MICHIGAN STATE UNIVERSITY
EAST LANSING, MI 48824-1321

PRINCIPAL INVESTIGATOR(S)

Sam M. Austin, Co-Director
Henry G. Blosser, Co-Director

TITLE OF PROJECT

Operation of the National Superconducting Cyclotron Laboratory Research Facility and the Michigan State University Nuclear Science Program.

TECHNICAL ABSTRACT (LIMIT TO 22 PICA OR 18 ELITE TYPEWRITTEN LINES)

The National Superconducting Cyclotron Laboratory (NSCL) of Michigan State University is a national users facility for fundamental research in nuclear science. This proposal requests funds for operation of the NSCL, for support of its users and for support of the research of the MSU staff in nuclear science and in accelerator and instrumentation physics. Facilities at the Laboratory include an extremely compact superconducting cyclotron of NSCL design and construction, the world's first superconducting cyclotron. A larger superconducting cyclotron and a flexible array of detection equipment (the Phase II facility) are being constructed at the Laboratory. When complete the NSCL will be an exceptionally powerful international facility for research on nucleus-nucleus collisions. It will make possible detailed study of nuclear phenomena in the transition region where the projectile velocity crosses the velocity of nuclear sound, and nuclear shock waves compress the nuclear material.

The present cyclotron supports a users program in heavy ion physics, providing beams of the lighter heavy ions which are presently unique in the U.S. Demand for accelerator time far exceeds supply. The research program has been unusually influential, for such an early stage of the facility's life, in setting the directions of research with heavy ions. A measure of this influence is that over 100 invited talks have been given by NSCL users at national and international meetings during the past three year period. The funds requested will make possible continuation of this program and its expansion to a much more powerful facility when the larger cyclotron is finished during the first year of the grant period. A greatly expanded user community is expected when the second cyclotron comes into operation and brings high quality beams at supersonic velocities over the whole range of projectile mass, from hydrogen to uranium.

0. RESULTS FROM PRIOR NSF SUPPORT

A. Grant Details

At present the NSCL is supported by NSF Co-operative Agreement No. PHY-8312245 for "Operation of the National Superconducting Cyclotron Laboratory and an Associated Research Program (Physics)". The period of this agreement is from 1 October 1983 to 31 October 1986, plus the usual six months extension, and the total amount granted to date is $14,410,400. The purpose of this section is to summarize the work performed under this grant. However, a short summary such as this is necessarily incomplete; we refer the reader to the body of the proposal for more detail. Since the grant was for continuing operation of the laboratory over a three year period, we describe here, as in the remainder of this proposal, the work performed during the three year period 1 January 1983 to 31 December 1985.

B. Summary of Results

The past three year period has seen a great qualitative change in the laboratory. Successful operation of the K500 cyclotron, the world's first superconducting cyclotron, occurred on 31 August 1982, and regular operation began in January 1983. Since that time the NSCL has operated as a national users facility for research with heavy ions using the K500 cyclotron. The K500 has also served as an extremely valuable prototype for the larger K800 cyclotron that is the heart of the Phase II construction project.

1. Instrumentation Development

In the three year period the laboratory commissioned a substantial array of detection equipment. The S320 spectrograph is an easy-to-use device capable of bending the most rigid particles produced by the K500 cyclotron and of operating at very small angles, including 0°. It was constructed from magnetic elements and a scattering chamber obtained from other laboratories and has been used for a variety of purposes. These include experiments involving giant resonances, the properties of exotic

nuclei and high lying excitations in nuclei. The Reaction Product Mass Separator(RPMS) was also finished during this period and has been used in several measurements on the decay properties of light exotic nuclei. As higher energies and heavier beams from the NSCL accelerators make it possible to produce nuclides farther from the valley of stability, studies of the detailed properties of these exotic nuclei will form an important part of the program of the NSCL. The RPMS will be the central instrument in this program. In addition, two smaller scattering chambers were completed and used in experiments: (1) a thin-walled chamber with a large array of neutron detectors for studies of reactions producing neutrons and (2) a general purpose chamber for the coincident measurement of gamma rays and charged particles.

There has also been substantial development of ancillary equipment to increase the efficiency of laboratory operation. The computer system for data acquisition and analysis was completed, and a large effort has been devoted to increasing its speed and convenience. General purpose programs have been written to provide a framework which encompasses the special requirements of individual experiments. A new fast (and "smart") data acquisition system has been implemented; it provides very high data rates with options for software gates prior to recording of data on tape. The electronics pool has been greatly augmented during this period, both by purchase of commercial units and by laboratory construction of units not available commercially. While the pool is not yet adequate for the worst case situation, delays due to inadequate electronics are now much less frequent than at the beginning of the period.

2. Scientific Operation

During the past three years the laboratory has been operated as a national user facility, based on the K500 cyclotron. The resources devoted to K500 operation in the latter part of this period have been significantly reduced by the demands of the high priority Phase II construction project. Nevertheless, we have been able to operate a successful research program and to provide beams for an average of 75 hours per week during 1984 and 1985, sufficient to sustain a program of about 3800 hours of beam time per year and to meet the most urgent demands of the users group.

During this period the operation of the Program Advisory Committee was put on a regular basis, and four meetings of the committee were held to review proposals and recommend allocation of beam time. We require written proposals, with no oral presentation. This procedure is efficient, in the sense that travel is minimized, and appears to work well. The K500 provides beams of the lighter heavy ions that are unique in the U.S. and demand from users has been high, about twice the available time.

3. Nuclear Science

During the past three years the NSCL user facility and NSCL personnel have played an important role in research on nuclear reactions and nuclear structure at the frontiers of heavy ion physics; we list here some of the more important results: (1) One of the first experiments at the NSCL showed that the yield of intermediate mass fragments in heavy ion collisions closely follows a power law in the charge number Z, suggesting that the fragments are emitted from a system near its critical point. Other experiments, performed by NSCL personnel at LBL, showed that the fragment energy distributions were characterized by the same temperature for different fragments, suggesting that they had a common source. These provocative results have stimulated many investigations aimed at determining the mechanism of fragment emission and whether a nuclear liquid-gas phase transition can be observed. (2) A new technique, based on measurements of the Boltzmann factor for emitting systems, was developed and applied both to long lived and short lived systems. The resulting temperatures are far below those obtained from measurements of energy spectra and call into question the meaning of temperature in heavy ion collisions. (3) Neutral pion production has been observed for several targets with 35 MeV/nucleon incident ^{14}N ions. It appears that single particle interactions are inadequate to yield the concentration of energy needed to produce pions with the observed cross section; collective phenomena of some sort are required. (4) Very recently, high energy (>100 MeV) photons have been observed following collisions of ^{14}N ions with a variety of targets; the cross sections do not show the behavior with angle and target mass expected if the photons were produced by coherent phenomena. (5) It has been shown that the onset of nuclear transparency expected on simple theoretical arguments, and observed

in C+C collisions above 20 MeV/nucleon, also occurs for heavier targets. The phenomenon appears to be a general property of nucleus-nucleus reactions in this energy range. (7) Mass measurements for medium weight nuclei far from stability yielded results important for understanding the astrophysical rp process and the Coulomb energy anomaly. (8) Lifetimes of a number of very neutron rich light nuclei were measured using the RPMS. (9) Cross sections for the (^{6}Li,^{6}He) reaction at small momentum transfer were shown to be proportional to the Gamow-Teller strength of a transition, demonstrating that this reaction will be a new and versatile probe for spin strength in nuclei. (10) A program of spherical shell model calculations has produced many interesting results, including evidence for quenching of the nuclear spin operator based on comparisons with observed beta decay strength.

4. ECR Source

Most NSCL experiments have involved beams with A≤22 and energies of 40 MeV/nucleon or less. However, developments during the present grant period will greatly extend this range. Improvements in the voltage holding capabilities of the radio frequency and deflector systems are expected to permit particle energies of at least 45 MeV/nucleon and probably higher, and a greater change will occur when beams from the MSU room temperature electron cyclotron resonance (RT-ECR) ion source become available in the near future.

Detailed design of the ECR source began in November 1984 and it was completed in August 1985. Since then it has been under development and has recently produced world-record amounts of highly charged krypton ions (for example Kr^{19+}). At the time of writing, the injection line is complete, and injection into the K500 cyclotron is expected momentarily. With few exceptions, we expect that the future program of the facility will involve the ECR source.

C. List of Publications

A list of publications describing work performed under this grant is given in the separately bound Appendix AP-1.

D. Relation to Present Proposal

The present proposal is a continuation of the proposal summarized above. However, during the proposal period, construction of the Phase II system (comprised of the K800 cyclotron and related detection equipment) will be completed, and operation will involve a much more powerful facility than at present.

The proposal also includes an expanded program of accelerator and instrumentation physics, building on the laboratory's long term committment to the development of technology for nuclear science and expanding the longstanding Ph.D. program in Accelerator Physics at MSU.

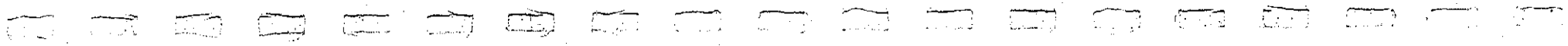

I. INTRODUCTION AND SUMMARY

This proposal requests funds for continuing support of the scientific program of the National Superconducting Cyclotron Laboratory (NSCL). The program includes operation of the laboratory as a national user facility, research in nuclear science and accelerator/instrumentation physics by the MSU scientific staff, and continuing development of the research capabilities of the laboratory. In addition to these activities, part of the NSCL staff is presently engaged in construction of the Phase II facility: a K800 cyclotron, a new beam transport system and a set of major experimental devices. Although the construction project is separately funded, a brief report describing its status is included as useful background information.

The three-year period of this proposal, 1 November 1986 through 31 October 1989, will see three increases in the power of laboratory facilities: addition of an Electron Cyclotron Resonance (ECR) source to the K500 cyclotron (K500+ECR facility); completion of the K800 cyclotron with ECR injection and a limited portion of the Phase II experimental area; and finally, completion of the full Phase II facility. When the initial Phase II facility is available in 1987, intense and precise beams with energies up to 200 MeV/nucleon for the lighter ions and 50 MeV/nucleon or more for the heaviest ions will be available, permitting the first systematic studies in an almost unexplored territory of energy and mass. Upon completion of the remaining Phase II facilities, a full complement of detection equipment for exploiting these unique beams will be available. The most important goal of the laboratory during this period is to bring the Phase II facility into timely and efficient operation, while operating a user facility based on the state-of-the-art capability of the K500+ECR and, then, the initial Phase II system.

During the past three years the K500 cyclotron has played an important role in research on nuclear reactions and nuclear structure at the frontiers of heavy ion physics. One of the first experiments done on the K500 showed that the yield of intermediate mass fragments closely follows a power law in Z (or A), suggesting that the fragments are emitted from a system near its critical point. This provocative result stimulated many investigations

aimed at determining whether a nuclear liquid-gas phase transition could be observed.

Other systematic measurements applied a new technique for obtaining nuclear temperatures (based on measurements of the Boltzmann factor for emitting systems) first to long lived systems and then to short lived ones; the resulting temperatures are far below those obtained by classical techniques, calling into question the concept of temperature in intermediate-energy heavy-ion collisions. Measurements of neutral pion production at incident energies of 35 MeV/nucleon established that collective phenomena must be responsible for the concentration of energy needed to produce a particle with a rest mass of 140 MeV. Very recently, high energy photons have been observed over a range of angle, energy and charge, following collisions of ^{14}N ions with a variety of targets; the observed energy and charge dependence appear to establish that the photons are not produced by coherent phenomena, but their origin is still unknown.

Research on nuclear structure has also been fruitful. It has been shown that the onset of nuclear transparency observed in C+C collisions above 20 MeV/nucleon is a general phenomenon, occurring also for heavier targets. It has also been shown that at 35 MeV/nucleon (^{6}Li,^{6}He) cross sections are proportional to the Gamow-Teller strength of a transition, providing a new and versatile probe for spin strength in nuclei. The long standing NSCL program on the properties of exotic nuclei has yielded nuclear masses important for understanding the astrophysical rp process, and the first observations of the decay properties of several light nuclei, using the Reaction Product Mass Separator(RPMS).

Most NSCL experiments to date have involved beams with $A \leq 22$, and energies of 40 MeV/nucleon or less. This will change in the near future. The voltage holding capability of the K500 RF and extraction (deflector) systems has risen during the past two years, and recent improvements in the design of rf couplers and the corona rings that protect the main rf insulators should permit particle energies of at least 45 MeV/nucleon and probably significantly higher (45 MeV/nucleon was achieved briefly in the past, but heating of the rf structure associated with the corona rings prevented long term operation at this energy). However, a greater change will occur when beams from the MSU room temperature ECR source (RT-ECR) become available in March 1986. Since its completion at the end of August

1985, the source, shown in Fig. 1, has been under development and has recently achieved world class performance; it is now producing world-record amounts of highly charged krypton ions, (for example, of Kr^{19+}, which will give energies of over 25 MeV/nucleon with the K500). ^{40}Ar energies over 40 MeV/nucleon will also become available. We anticipate that a large fraction of the program will use these heavier beams. Presently the injection line from the ECR to the K500 cyclotron shown in Fig. 2 is almost complete.

Of course, much higher energies will be available when the K800 cyclotron is finished. The anticipated energies for several combinations of ECR sources and cyclotrons are shown in Fig. 3, where they are compared with the performance of several competing accelerators and with the performance anticipated for the coupled-cyclotron facility in the original Phase II proposal of 1978. This figure illustrates an important issue for future development of the NSCL: whether the performance of advanced ECR sources will be sufficiently good that it will not be necessary to couple the K500 and K800 cyclotrons (as was originally proposed) to obtain the desired performance. Coupling carries with it significant costs in terms of the overall efficiency of the facility because of the more complicated operation and the lower reliability that accompanies the use of two state-of-the-art machines rather than one, especially during the start up phase of the facility.

The curves on Fig. 3 involve the assumption that the charge state for a given intensity scales as $\sqrt{r}$, the square root of the radius of the plasma region in the ECR source. The present MSU source serves as an experiment to determine whether the intensity of high charge state ions follows this rule; r is approximately 5/3 of that for the source at LBL. Should the MSU source's output follow this scaling, the (RT-ECR)+K800 combination will be a very powerful facility, although it will not reach the high energies for ions with A = 20 to 130, of the coupled NSCL facility proposed in 1978. To do so requires the development of an advanced ECR source, labeled SC-ECR, since superconducting(SC) technology will almost certainly be employed for production of its magnetic fields. This source may be large in size(if $\sqrt{r}$ scaling is verified for the RT-ECR source as has been assumed for the curves of Fig. 3) and/or high in frequency and power (following the directions of Geller and his collaborators at Grenoble).

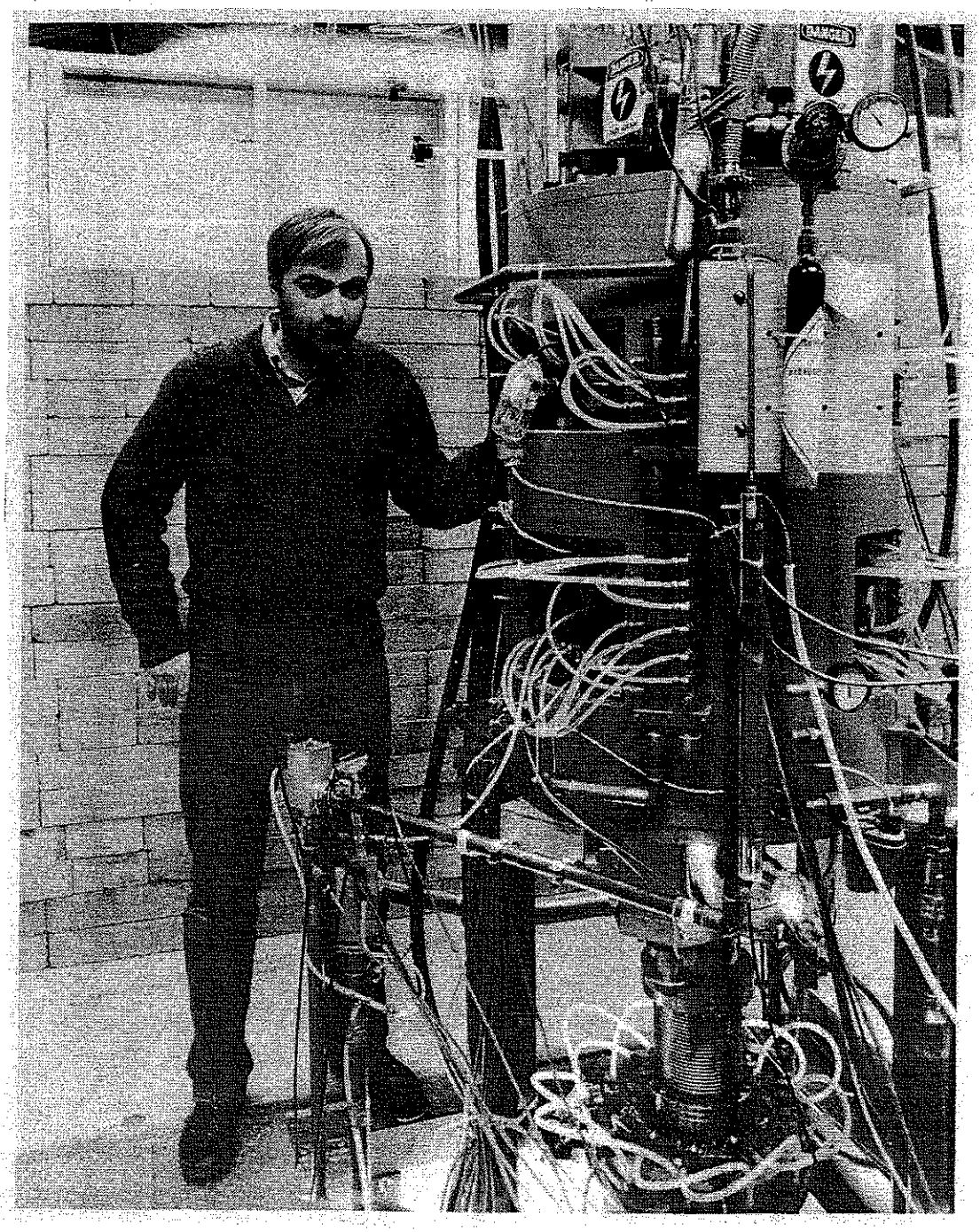

Fig. 1. Photograph of the NSCL room temperature ECR source. The source is vertical with beam extraction from the bottom of the source.

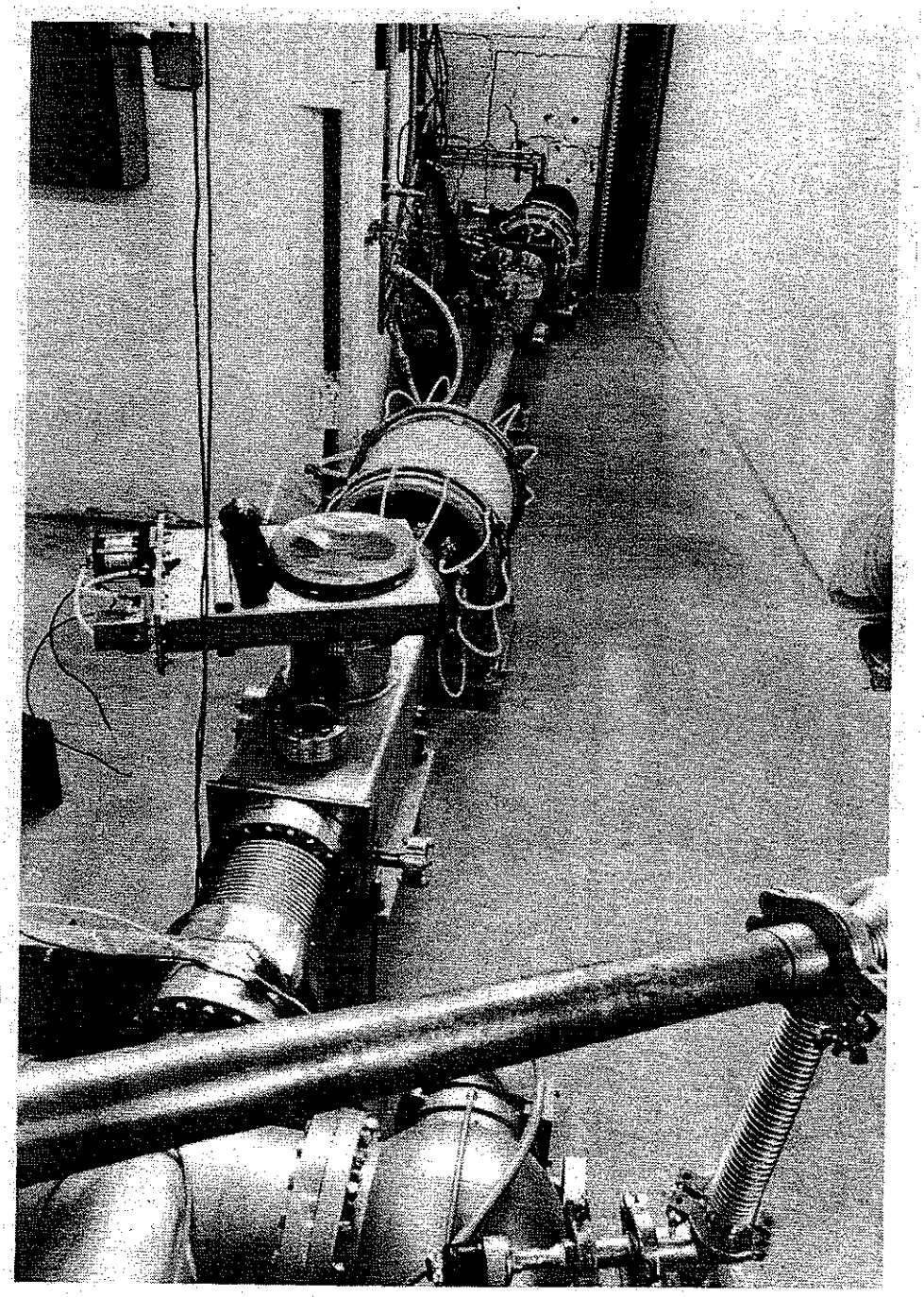

Fig. 2. Beam line leading from the ECR source shown in Fig. 1 to the K500 cyclotron. The cylindrical elements are the focusing solenoids. After passing through the shielding wall shown at the far end of the line, a 90^{o} vertical bend in the line leads into the center of cyclotron.

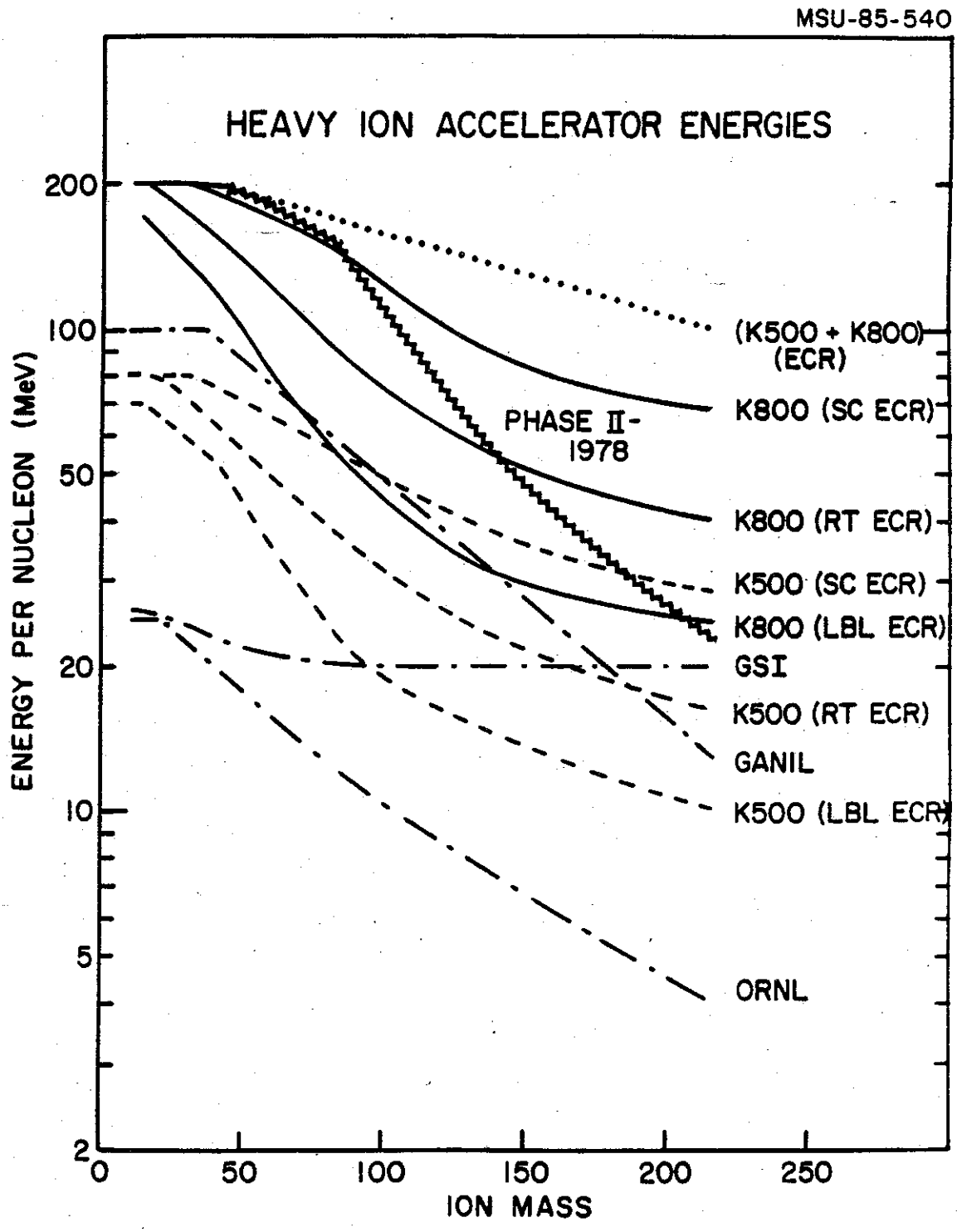

Fig. 3 Performance of NSCL accelerator and ECR systems compared with the performance of other operating accelerators, the initially proposed (1978) NSCL coupled cyclotron system and a limiting coupled system using an ECR source for injection (K500+K800(ECR)). The intensity of the NSCL accelerators is 10^{11} particles per second (within a factor of three), except for the K500+K800 (ECR) combination for which it is about 10^{9} particles per second.

Since it is not possible at present to determine whether the ultimate performance from the NSCL accelerators can be obtained without coupling, through use of an advanced ECR source, or whether coupling of the K500 and K800 machines will be necessary, we plan to proceed as follows. The K800 will be put into initial operation with the RT-ECR source. Concurrently, development of an advanced ECR will proceed, following directions based on our experience with the RT-ECR source and the experience of other ECR groups. Should the SC-ECR performance approach that implied by Fig. 3, (corresponding, for example, to Pb^{50+} from the source) then it is unlikely that coupling would extend the energy range sufficiently to be worthwhile. The curve shown for coupled operation is, essentially, an upper limit, corresponding to beams of less than 1 particle nanoampere that are suitable mainly for experiments with 4π detectors. If such source performance is not obtained, a decision on whether to couple can then be made based on much better information about the intrinsic interest of the physics in the extended energy range than is now available. Furthermore, the K800 accelerator will have had additional operating time and should operate more reliably than it will immediately after its commissioning.

Until the coupling issue is resolved, it is crucial that both accelerators remain available. Later, if a decision is made not to couple the K500 and K800, then two cyclotrons and two ECR sources will be available, and it will be necessary to decide whether to operate both accelerator systems at the NSCL or whether to relocate the K500 to another laboratory. It appears to us that there are strong arguments for dual operation. The K500 + RT-ECR is a powerful facility. Its beams will be adequate for many experiments, and parallel operation will increase the productivity of the laboratory. It will serve as a backup for the K800, and would be valuable for counter testing and for set up of experiments. Operation of the K500 should not add greatly to the overall cost of operating the laboratory, if the machine is not stressed to its ultimate performance and if maintenance and repairs are given lower priority so they can be fitted in between maintenance of the K800. Ultimately, whether simultaneous operation is desirable would be determined by the benefits and the cost of K500 operation as determined by experience.

Turning to the status of the Phase II project, work on all major items is moving forward vigorously. At the time of writing, the major step of

freezing the design of the K800 extraction system has just been taken and mechanical layout of cryostat penetrations for the extraction orbit and extraction magnetic focusing elements is beginning. The magnet proper has been operational since the spring of 1984 but is disassembled at the moment for installation of trim coils, which is complete (see Fig. 4), and for the installation of trim coil leads, which is in process. During this disassembly, cuts are also being made in the outer yoke as required for the external beam path and the extraction orbit focusing elements. The cuts in the yoke and cryostat also include holes where the injected beam from the K500 would enter, should coupling be implemented. Fabrication work on the copper liners which cover each pole is now in midstream. Covers for the hills are complete and are being assembled on a large aluminum jig which models the pole tip; copper sections to line the bottoms of the magnet valleys are about to be added, after which the array of parts will be welded into a single envelope. The large copper weldments that make up the dee stems and the outer resonators are on order from various commercial vendors, with deliveries scheduled during the next several months. The rather intricate sliding shorts that are the primary tuning element of the resonators are designed at the conceptual level and detailed drawings for external fabrication of components are being prepared. A first layout of the aluminum form that will be used for fabricating the dees has been made and fabrication drawings for the form should be completed in a few weeks. Overall, the cyclotron has come to a stage where the dominant remaining activity is final assembly. Assembly is highly manpower intensive and is complicated by the small size of the cyclotron which limits the number of people who can effectively work on the system at one time. Based on the time taken to complete the K500 from a similar stage of construction, we estimate that about one year's work remains before first beam tests.

Another major part of the Phase II project is the extensive beam transport system, consisting of 60 quadrupoles plus six $\pm 16°$ switching dipoles. The beam transport system makes extensive use of superconducting technology as does the S800 spectrograph. Cost studies led us to use magnetic fields in the range of two Tesla or less for these magnets, while still utilizing superconducting coils; at Phase II momenta (1.6 GeV/c) such magnets are less costly, both in construction costs and in operation, than are either conventional magnets or higher field superconducting magnets. At

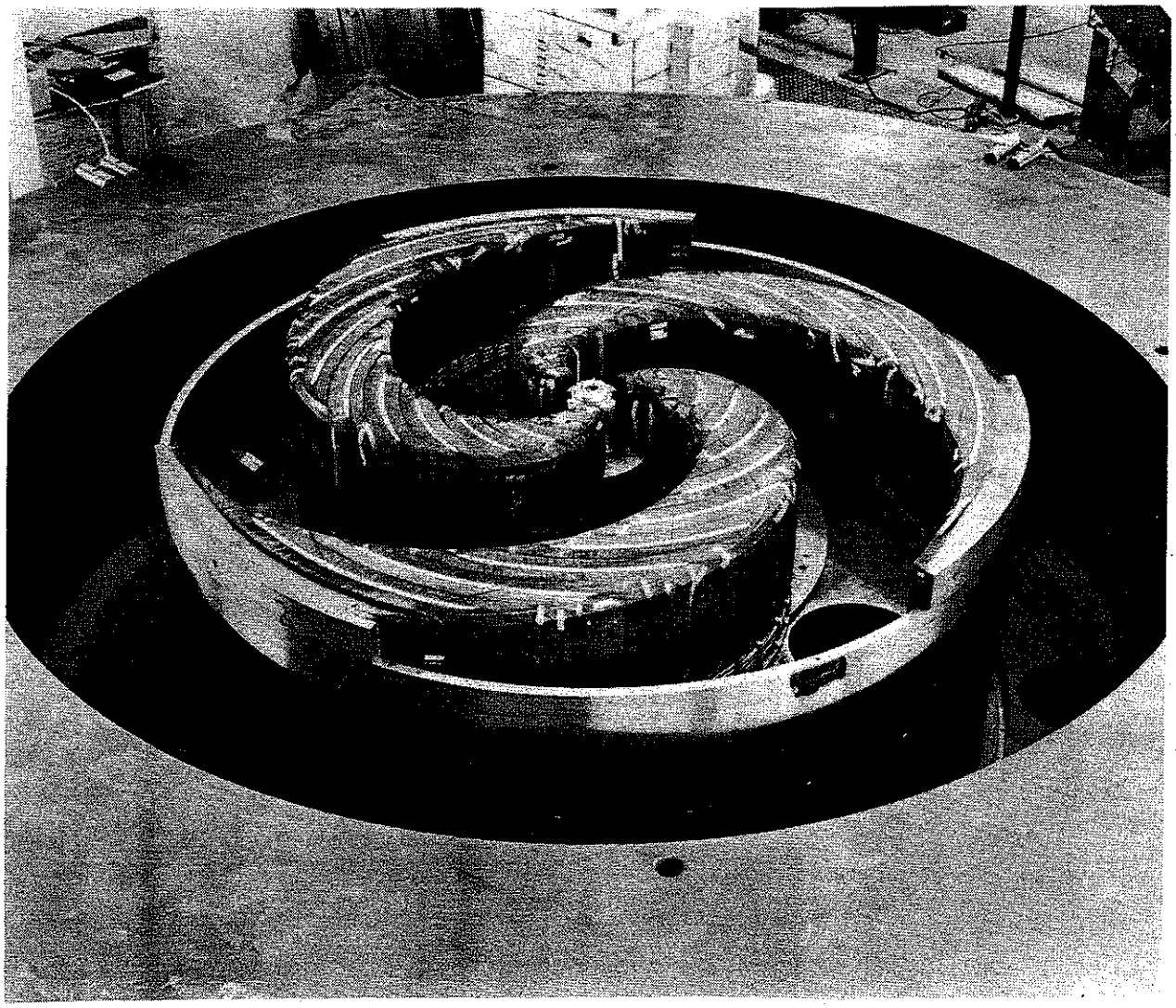

Fig. 4. Photograph of the bottom half of the K800 magnet, showing the spiral hills of the magnet with the trim coils installed.

this time the magnet designs of the spectrograph dipoles and the beamline magnets are nearly complete. Emphasis has been placed on efficient cryogenic performance.

A prototype superconducting quadrupole has been built and tested, both cryogenically and magnetically. The magnet ran to full field with no quenches; the measured magnetic fields are of high quality, and the cryogen holding times are greater than one week. A prototype superconducting switching dipole magnet is also near completion and will be tested soon. The dipoles require higher operating currents than the quadrupoles and will be operated in the persistent mode to achieve the desired cryogenic efficiency.

The other major items of the Phase II project are a large general purpose scattering chamber and a 4π detector. The scattering chamber is a horizontal cylinder, 92" in diameter by 120" long, with internal components supported on a beam cantilevered through bellows from the outside to provide easy access to detection equipment. Delivery of the stainless steel chamber is expected within two months; machining is complete and the chamber awaits leak checking at the vendor's facilities. Design of other components is under way.

The 4π detector is characterized by its large dynamic range and is capable of detecting charged products ranging from fission fragments to several hundred MeV protons. The individual detector modules are sandwiches consisting of parallel plate avalanche detectors, followed by a Bragg curve detector, followed by fast-slow plastic phoswich scintillation detectors. Design and prototyping has been completed for all these elements. The major mechanical structures, including the vacuum vessel, detector mounts, and cradle, are being assembled (see Fig. 5). Orders have been placed for all the long lead-time procurements, including the scintillator telescopes and the CAMAC electronics. Work is proceeding on the design of front end electronics, various fixtures for assembly and storage of the detector subarrays, and the target mechanism. We expect to construct the first detector subarray in March, and the entire detection system should be complete near the end of the year; performance tests and first experiments will be done with beams from the (RT-ECR)+K500 facility.

Some explanatory comments about the main body of the proposal are perhaps helpful. In Section II, we describe operation of the facility,

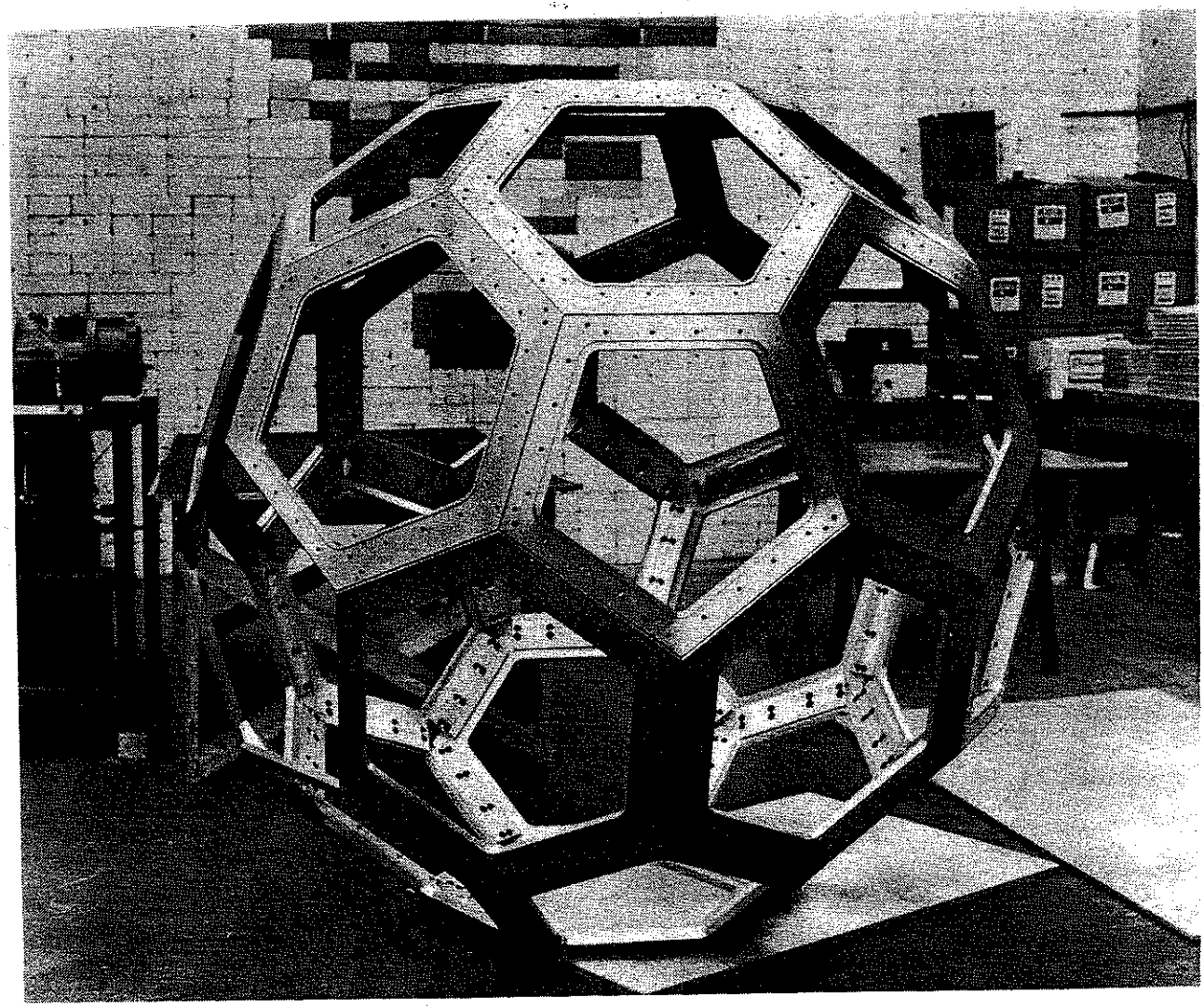

Fig. 5. The frame on which the individual detectors of the 4π detector will be mounted.

including its technical and scientific aspects. This section includes a historical perspective, a description of the status of the facility and directions of its evolution, a description of the operation of the Program Advisory Committee, a list of the proposals allocated beam time on the facility and a description of User Group operations. Interest of users in the facility has been high with an oversubscription of the available time by a factor of two, even with the limitation to low mass beams. We anticipate still greater user interest as heavier, higher energy projectiles become available in the near future.

In Section III.A and III.B, we review the research in nuclear science carried out by the MSU group. The program includes a broad range of topics, from the study of mechanisms of heavy ion reactions, to the study of "simple" excitations in nuclei, to the study of reactions of interest for astrophysics. As in the past we have emphasized the research that has been done, believing that in a field moving as rapidly as heavy ion physics, it is difficult to judge what will be interesting in three or four years and that the best predictor of future performance is past performance. When reasonable predictions are possible, we indicate the directions which we think our research will take during the next few years. Of course the total program of the facility will be greatly affected by the individual decisions of its outside users.

Sections III.C and IV describe the ongoing program in accelerator and instrumentation physics. The laboratory has been involved in such research since its inception. Major results include the first precision sector focused cyclotron for light ions and the K500 and K800 superconducting cyclotrons that are the heart of the NSCL facility. However, there have been many other developments which, when taken together, constitute a large contribution to the technique of modern nuclear physics. These include the development of energy-loss techniques yielding unprecedented resolution in the Enge split-pole spectrograph; of superconducting beam transport systems; of superconducting spectrographs; of beam-swinger-based charge exchange and neutron scattering techniques; of automatic nuclear emulsion scanners; of charge-coupled-device cameras for streamer chambers; of unique fast front ends for data acquisition computers; of a large reaction product mass separator; and of a 4π detector with an extremely large dynamic range. The laboratory has unique expertise and facilities for the construction of

large superconducting magnets. These have been used in the construction of coils for the K500 cyclotron, the K800 cyclotron and the beam line quadrupoles and dipoles. The facilities have also been made available to others: the superconducting coil for the Texas A&M cyclotron was wound here. We intend to maintain this facility as a national resource.

These accomplishments support the thesis that the laboratory has developed a level of expertise over a broad range of nuclear instrumentation that is probably unmatched at any U.S. university. Also rare among universities is the fact that the laboratory and the Physics Department have for many years offered a doctoral program in accelerator physics that has led to a total of six Ph.D.'s; of these, five are still involved in nuclear technology. Presently, there are three graduate students in accelerator physics.

Given the strength of the instrumentation activity at MSU and the NSCL, and the national demand for individuals with instrumentation expertise, both for basic research and for applications of nuclear technology, this seems a propitious time to expand our activities in instrumentation research and in the training of students and postdoctoral researchers in this field. This will lead to the development of new technology for nuclear science, benefitting not only the NSCL, but the field in general. Frontier science will depend on advanced technology that is not commercially available. Those trained in this technology will be in great demand and the instrumentation developed here will push forward the boundaries of what is technically possible.

As is described in Section IV of this proposal, the instrumentation effort will initially be involved with detailed analyses associated with initial operation of the K800-based facility and with the design and construction of advanced ECR sources. As the program shifts to routine operation, the efforts of the instrumentation research group will broaden to include studies of new detection apparatus for nuclear science and to studies of advanced accelerator systems. These studies will probably include beam cooling systems and accelerators (using magnetic fields in the 8 to 10 Tesla range) that can produce beams of 500 to 1000 MeV/nucleon.

A discussion of some implications of the transition from construction of Phase II, to its operation is contained in Section V. During the period

of the proposal, this transition will affect almost all of the 58 members of the technical staff now involved in construction activities.

Section VI discusses capital equipment items, divided into two categories. The first includes the relatively small items needed to maintain, retrofit and develop existing facilities; those needed to improve the present facility; and those needed for the ongoing research program. The second category includes the computer equipment to meet two critical needs of the laboratory: additional computer power to handle data analysis for the extremely complex reaction experiments that are at the heart of the experimental program and, during the third year of the proposal period, a replacement for the aging VAX780 that is the control processor of the NSCL computer system. Finally, in Section VII the budget for the first year is presented, with detailed justification. Budgets for the later years are scaled from this, with an accounting for the shift of manpower to operations, changes in equipment needs, and inflation.

In past years the NSCL has supported some theoretical work that is closely connected to experiment and could be justified in terms of the overall productivity of the experimental program. The largest part of this support is for the shell model program of B.A. Brown and his associates. This program has been very productive and we are often told that it is a national resource for nuclear physics. We again request support for this theory effort.

Although direct support for the remainder of the theory program at MSU is not requested in this proposal, the theory group provides important support to the experimental program. Professor George Bertsch has been active in almost all areas of interest to experimenters in the NSCL and is an important laboratory resource. He is currently funded by the NSF Theory Program and by MSU through his Chair: a John A. Hannah Distinguished Professorship. Professor Olaf Scholten is on leave at Groningen for the next year. Professor Joseph Kapusta, presently at the University of Minnesota, will be joining us in August, and we are presently recruiting to fill two additional tenure stream nuclear theory positions in the Department of Physics and Astronomy. These arise from the return of H. Toki and H. Stöcker to their native countries. Upon his retirement, Professor H. McManus's position will also be filled by a nuclear theorist. This availability of positions should make it possible for us to build a very

strong program in theory. The laboratory provides indirect support to the theoretical program, mainly through use of the laboratory computers for work in which experimenters have a direct interest or are collaborating with the theorists involved. We intend to continue this support.

The University strongly supports an expansion of the effort in theoretical nuclear physics; we have just received a grant from the MSU Foundation to fund a $1,200,000 addition to the laboratory, approximately half of which will be devoted to nuclear theory.

Later sections of the proposal present data of various sorts. Section VIII lists the senior laboratory staff. This list differs from those submitted previously because the laboratory has instituted a new personnel system for senior members of the scientific/technical staff who do not hold tenure stream appointments in the Departments of Physics or Chemistry. In this system individuals are appointed as Assistant, Associate or Full Professor (NSCL); Physicist, Staff Physicist or Senior Physicist; and Engineer, Staff Engineer or Senior Engineer. Beginning appointments generally involve a six year probationary period which can end in the award of a continuing appointment backed by grant funds.

As in previous proposals the group of principal investigators includes all tenured full professors whose research is supported by the grant. Most of these individuals devote all of their research effort (60% of their total time) to research supported by the NSF operating proposal. Exceptions to this are Professor Scott, who presently devotes 10% of his time to research in nuclear science, the remainder being spent in administrative duties as Associate Provost of the University; and Professors Austin, Blosser and Nolen, who devote part of their time to construction activities--this effort will decrease toward the end of this grant period. Also included as Principal Investigators are the two individuals directly responsible for facilities which most closely affect users of the NSCL: Richard Au, responsible for the computer systems and data acquisition, and Peter Miller, responsible for cyclotron operation.

A list of current and pending support is given in Section IX, and the separately bound appendices contain the list of publications describing work at the NSCL, a list of advanced degrees based on work at the NSCL and the Curricula Vitae of the Principal Investigators and other senior scientific staff. As in previous proposals, these lists are based on the immediate

past three year period, 1983-1985, inclusive; papers submitted for publication during this period, but not yet published, are also included to give a more complete indication of the work carried out. The listing includes published NSCL related work by outside users of the facility as well as that by MSU staff. Even during its formative years, the NSCL has played an important role in nuclear science, as can be seen from the total of over 100 invited papers based on experimental work by NSCL staff and by users of the NSCL.

The NSCL has contributed significantly to the education of the next generation of nuclear scientists. The listing of Ph.D.'s awarded 1983-1985 shows that 12 students have received their Ph.D.'s for work at the NSCL. One of the MSU students, Dr. Barbara Jacak, received a prestigious Oppenheimer Fellowship at Los Alamos National Laboratory.

II. LABORATORY OPERATION

The first successful extraction of beam from the K500 cyclotron occurred on August 31, 1982; initial experiments began shortly thereafter, and following a brief pause, regular operation started in January 1983. Since March 1984 the K500 has operated on a seven-days-a-week schedule. There have been three planned shutdowns. During the first of these, from June to December 1983, a number of improvements were made to improve the reliability of operation; during a three week shutdown in November-December 1985, improvements on the rf structure were made; and during the third, presently in progress, the axial injection line for ions from the room temperature ECR source is being installed. We expect to resume operation in March.

During this period, reliability of operations has been affected by the simultaneous construction program: we have been unable to devote the amount of time that would be desirable to improvements in the K500, nor have we been able to respond to breakdowns with the priority and concentration of manpower that would be warranted under normal conditions. Nevertheless, we have succeeded in providing beam for an average of about 75 hours per week during 1984 and 1985, sufficient to sustain a program of about 3800 hours of beam time per year, and to meet the most urgent demands from the users group. As is clear from other sections of this proposal, the resulting program has been very productive in terms of results that have influenced our understanding of heavy ion physics and the directions of future research in the field.

The future will see a substantial change in the scope of operations, with a much greater concentration of laboratory resources on operation of the facility as the Phase II systems come on line. In this section of the proposal we review the progress that has been made during the past three years in operating and developing the facility and the anticipated developments for the next three years.

A. Facility Operation and Development

1. K500 Operation

Development of the K500 cyclotron has focused on two goals: improved and more reliable performance and testing of design concepts for the K800 cyclotron. Many small improvements have been made, but the major effort has been devoted to improvements in the voltage holding capability of the radio-frequency system and the deflectors of the extraction system. The achievable voltages have limited the energy performance of the facility for the lighter ions and associated effects have been responsible for much of the unscheduled down time of the accelerator.

Improvements made in the rf system include: (a) new outer conductor contacts (fingers) for the sliding short planes in the coaxial dee stems and the transmitters--these have essentially eliminated previous frequent failures of these systems, (b) a new planar design for the rf coupler insulator that appears to have eliminated the second most common rf failure mode, (c) upgrade of the driver and final anode power supplies with more reliable components and a more conservative design, (d) improvements in the low level electronics to provide better phase control and improve protection of components during dee and coupler sparking, and most recently, (e) improved dee-stem corona-ring joints to reduce heating of the rf structure at high voltages.

Significant improvements have also been made in the deflector system, mainly through the replacement of ceramic insulators with grooved sapphire insulators. In the test stand, the deflectors now hold voltages compatible with the design goals of the K500. However, these voltages are not yet obtained when the deflectors are installed in the K500. Further improvements in the shape of the deflector shoe (negative electrode) and ground plane geometry are under way to lower maximum voltage gradients and reduce possibilities of deflector contamination by particulate material, respectively (see Section IV.E). At present, the deflector does not normally limit K500 energies.

Other K500 improvements include a pulsed power supply for the ion source (pulsing increases the intensity of higher charge state ions whenever the experiment can tolerate a duty factor less that 100%); air locks and

improved drive mechanisms for the beam probes; and development of a technique for determining the centering of the beam from the phase delay of the beam modulation produced by pulsing the source. Phase selecting slits were also installed (see Section IV.D).

Beams presently available from the accelerator are shown in Table II.1. Generally, development of a new beam is straightforward, requiring 12 hours or less, if it lies within the voltage and magnetic field range of previously developed beams, so we can usually make available whatever beams an experiment requires. Table II.2 shows the beams actually provided to experimenters in 1985; the most commonly used ion was ^{14}N, at 35 or 40 MeV/nucleon. The largest qualitative change anticipated when the ECR source becomes operational is that beams of high energy ions up to at least Krypton will become available. Operation with a PIG source will remain possible, with the source inserted from the top of the cyclotron instead of from the bottom as at present.

Figure 1 shows the beam-on hours of the accelerator, which have averaged approximately 75 hours per week over the past two years. Total hours were less in 1985 than in 1984 (3553 hrs vs 4328 hrs) because the facility was shut down for four weeks for improvements and because of problems with impurities in the liquid helium system (see below). The effects of the helium contaminant appeared suddenly and continue as a problem at this time. The contaminant causes blockages at restricted orifices (e.g. valves) in the liquid helium lines that eventually block flow of liquid helium to the K500. Operation is hampered (though experiments can run with lowered efficiency) by loss of liquid helium flow to the coil or the cryopumps and by the valving procedures necessary to clear the blockage. This appears to be a novel helium system problem and the source of the contamination has proven to be elusive. We are now embarked on a dual approach to the problem: attempting to track down the source of the contamination through spectroscopic and other analytic techniques, and installing filters which will allow us to live with the contamination until its source is found and eliminated. More details are given in Section IV.I.

Table II.1. Beam List for K500 Cyclotron 04 Jun 1985

Ion	A	E/A [MeV/u]	Beam Current on Target of the Experiment: DC [pnA]	NC	Pulsed [pnA]	Duty Factor [%]	Notes
2 H 1+	2	53.0	10.0	1.4			r,d
3 He 1+	3	25.0	70.0	1.2			d
	3	30.0	90.0	1.2			d
	3	35.0	80.0	1.3			d
	3	40.0	70.0	1.4			d,x
4 He 1+	4	15.0	100.0	1.2			
	4	20.0	100.0	1.2			
	4	25.0	80.0	1.2			
	4	30.0	60.0	1.4			d
4 He 2+	4	54.0	10.0	1.4			r
6 Li 1+	6	10.0	50.0	1.2			
	6	12.0	50.0	1.2			
	6	14.0	50.0	1.2			
6 Li 2+	6	25.0	30.0	1.2			
	6	30.0	30.0	1.2			
	6	35.0	30.0	1.4			
7 Li 1+	7	8.0	50.0	1.2			
	7	10.0	50.0	1.2			
7 Li 2+	7	20.0	30.0	1.2			
	7	25.0	30.0	1.2			
	7	30.0	30.0	1.2			
12 C 3+	12	15.0	30.0	1.2			
	12	20.0	30.0	1.2			
	12	25.0	30.0	1.2			
12 C 4+	12	30.0	20.0	1.2			
	12	35.0	20.0	1.2			
	12	40.0	20.0	1.3			x
13 C 3+	13	15.0	30.0	1.2			d
	13	20.0	30.0	1.2			d
	13	25.0	25.0	1.2			d
13 C 4+	13	30.0	20.0	1.2			d
	13	35.0	18.0	1.2			d
14 N 3+	14	15.0	30.0	1.2			
	14	20.0	30.0	1.2			
14 N 4+	14	20.0	10.0	1.2	20	50	
	14	25.0	10.0	1.2	20	50	
	14	30.0	10.0	1.2	24	50	
14 N 5+	14	35.0	7.0	1.2	12	30	
	14	40.0	7.0	1.2	12	30	
	14	45.0	7.0	1.3	12	30	x
15 N 3+	15	15.0	30.0	1.2			d
	15	20.0	30.0	1.2			d
15 N 4+	15	20.0	10.0	1.2	20	50	d
	15	25.0	10.0	1.2	20	50	d
16 O 3+	16	15.0	30.0	1.2			
	16	17.0	30.0	1.2			
16 O 4+	16	20.0	10.0	1.2	25	30	
16 O 5+	16	25.0	7.0	1.2	16	40	
	16	30.0	7.0	1.2	20	40	
	16	35.0	7.0	1.3	18	40	
18 O 4+	18	15.0	10.0	1.2	25	30	d
	18	20.0	10.0	1.2	25	30	d
18 O 5+	18	25.0	7.0	1.2	16	40	d
	18	30.0	7.0	1.2	16	40	d
20 Ne 4+	20	15.0	1.0	1.5	8	10	
	20	20.0	1.0	1.5	8	10	
22 Ne 4+	22	15.0	1.0	1.5	8	10	
22 Ne 5+	22	24.5	0.5	1.5	3	10	
40 Ar 6+	40	10.0	0.5	2.0	3	10	
	40	12.0	0.5	2.0	3	10	d
40 Ar 8+	40	20.0	0.1	2.0	1	10	

r=Secondary radiation may require reducing intensity

d=Beam requires development

x=Beam suspended, pending upgrade of rf resonators

Table II.2. Beams Provided by the K500 Cyclotron
Jan. - Dec. 1985

Label	Ion	E/A	% time
1	2 D 1+	25	1.2
2	4 He 1+	25	3.8
3	6 Li 1+	14	1.5
4	6 Li 2+	25	0.5
5		35	7.8
6	7 Li 1+	10	1.6
7	7 Li 2+	25	1.9
8		35	0.
9	12 C 2+	10	0.5
10	12 C 3+	15	1.6
11	12 C 4+	25	0.9
12		35	4.8
13	14 N 2+	8	3.9
14	14 N 3+	15	4.4
15	14 N 4+	20	5.9
16		25	0.5
17		30	3.3
18	14 N 5+	35	24.7
19		40	13.1
20	16 O 4+	25	0.2
21	16 O 5+	30	0.3
22		35	2.9
23	16 O 6+	35	1.3
24	18 O 5+	30	1.3
25	20 Ne 4+	20	0.
26	20 Ne 5+	25	2.5
27	20 Ne 6+	30	0.5
28	22 Ne 5+	20	1.5
29		24.6	7.1
30	22 Ne 6+	30	0.3
31	40 Ar 8+	20	0.
		Total:	100.0

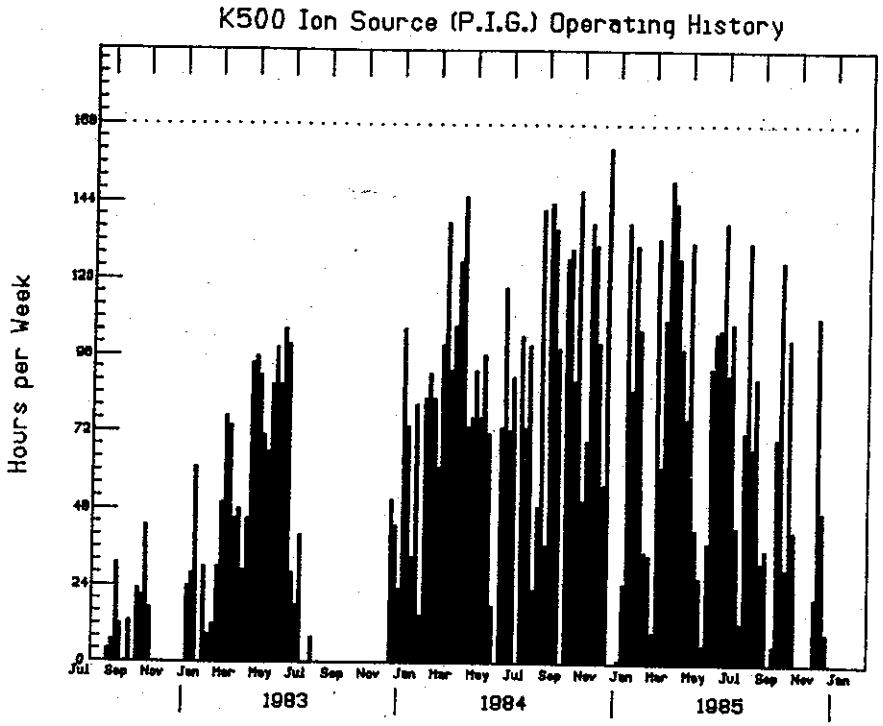

Fig. 1. Graph of beam hours per week as a function of time.

2. Experimental Apparatus

A map of the Phase I experimental area is shown in Fig. 2. The 60" scattering chamber has been the workhorse of the Phase I program, but several other devices were commissioned during the past three years. The S320 spectrograph is an easy to use device that performs very well within its limitations of solid angle and resolution (1 msr and 1.5×10^{-3} respectively). It is capable of bending the most rigid particles from the K500 cyclotron and of operating at small angles, including 0°; it is the second most heavily used facility in the laboratory. The Reaction Product Mass Separator (RPMS) was completed and has been used in several measurements of the decay properties of light exotic nuclei. It will be extremely valuable in the future program of the NSCL, as higher energies and heavier beams make it possible to produce nuclei far from the valley of stability and to measure their detailed properties, rather than simply establishing their stability or non-stability as has been the focus of most studies to date. A special purpose thin-walled chamber, with a large array

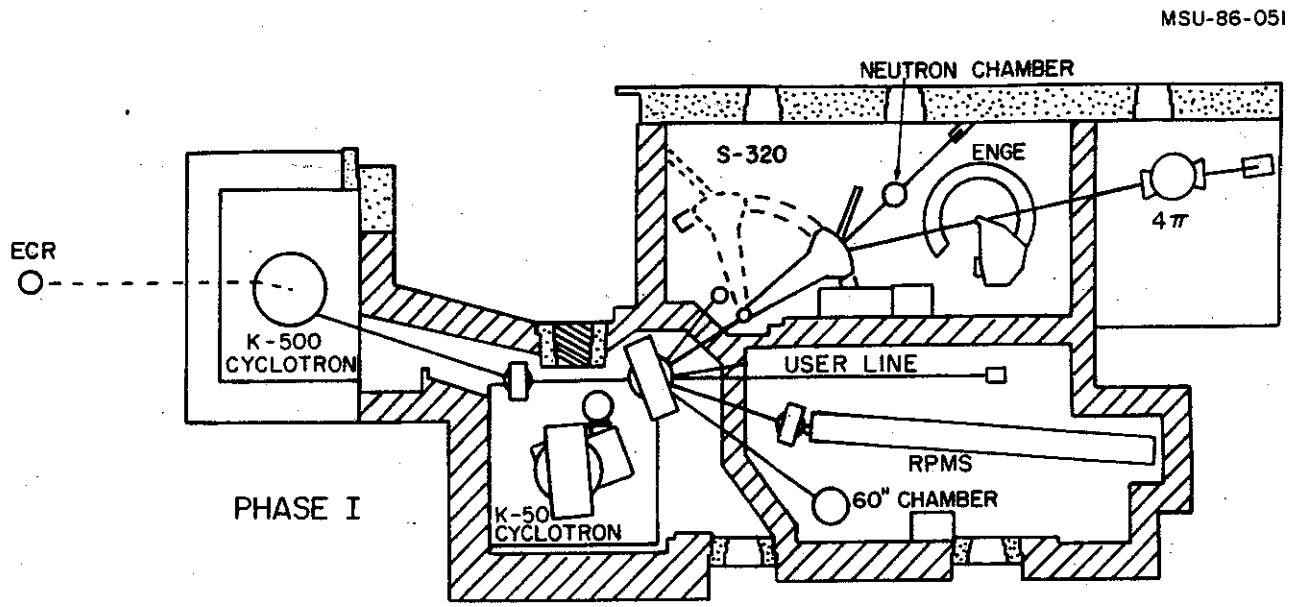

Fig. 2. Phase I experimental areas.

of neutron detectors, was built for the study of reactions producing neutrons. A general purpose chamber was developed for observation of gamma rays in coincidence with charged particles and has been used in several experiments, including those to determine nuclear temperatures by observation of the Boltzmann factor for long-lived nuclear states. The users' line has been heavily used, not only for this gamma ray chamber, but also for devices furnished by outside users: for example, a large Pb-glass spectrometer for measurements of subthreshold π^{o} production, and a polarimeter for measuring the circular polarization of γ rays produced in heavy ion reactions.

Most of these devices will also be used during Phase II operation. However, the Enge and S320 spectrometers may be phased out as more powerful devices are developed or if there is demand for additional general purpose users lines.

3. Computation and data processing

Much of the work at the NSCL is computer intensive. Experiments often require large numbers of detectors operating at high data rates and may yield 100 or more high density tapes from a week of running. This places heavy demands on the computer systems for both data acquisition and analysis. In addition, there is a heavy load of theoretical calculations relevant to the experimental and construction programs, and finally, word processing and accounting functions take a significant portion of the available CPU cycles. During the past three years there have been a number of incremental changes in the system of VAX computers that existed at the beginning of the period, and one major addition, an FPS-164 array processor. Figure 3 shows the present configuration of the computer system: the major elements are a VAX 780 for general use, a VAX 750 for data analysis, two VAX 750's for data acquisition, and a VAX 750 which serves as host for the FPS 164 and as a test machine.

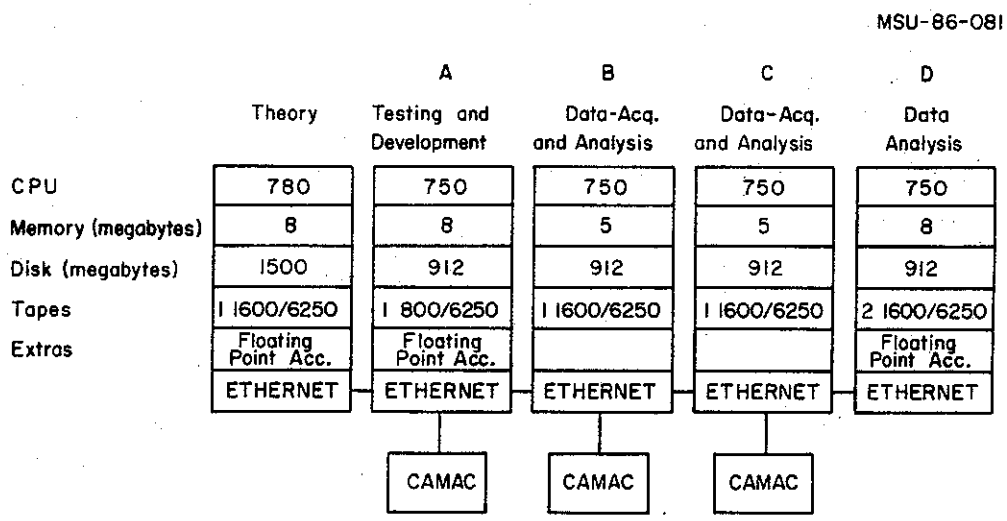

Fig. 3 Schematic diagram of the data acquisition and analysis system.

It had been thought that the Analysis 750 would serve the computer needs for data analysis, but it soon became clear that neither a single computer, nor the available disk space, was sufficient to handle the data from the large experiments that quickly became the norm. We therefore added additional disk storage (0.5 Gbyte) to each of the 750's and with the decreasing cost of memory have been able to increase memory on the 780 and two of the 750's to the full complement of 8 Mbytes. With these changes and the addition of one high density tape drive, all of the 750's are available for data analysis when experiments are not being run. As a result, the short term requirements for data analysis are approximately in balance with capacity.

This situation will change as experiments become larger (for example, those that use the 4π array) and as experiments routinely take advantage of the fast data taking system described below. To meet what would otherwise be an analysis bottleneck, we propose to construct and bring on line a variant of the Fermilab Advanced Computer Project: microprocessors (eventually 128 of them) will be connected in parallel on their own network, providing an increase in analysis speed by a factor of at least 50 over that of a single VAX 750. Data storage will also become a limitation; laser disk systems appear to be the preferred solution. These additions are discussed in Section VI.

The FPS 164 computer is a pipelined device, which, for many programs, can provide an order of magnitude increase in computational power compared to a VAX 780. It arrived in the laboratory in October 1984, and after a series of hardware difficulties, finally remedied by the vendor, it now operates well. The FPS was funded to make possible the computer-intensive calculations needed in the design of the K800 extraction system (see Section IV). With the completion of these calculations, the device will be used for computations directly relevant to the nuclear science program. For example, the large Boltzmann-Uehling-Uhlenbeck calculations, used for the description of intermediate energy reactions, would be essentially impossible to perform with adequate statistics (they use Monte Carlo methods) at VAX speeds.

Another important limitation concerned the data acquisition system in place three years ago. It became clear that the total data acquisition rate was often limited by the data handling capability of the LSI-11/23 based computer front ends. This translated immediately into an inefficient use of

beam time: if beam intensity must be decreased by a factor of two so the acquisition system can handle the event rate, data taking times are doubled. We have developed and put into operation a fast system based on MC68010 microprocessors and the VME bus. Data rates approximately five times those for the previous system have been obtained. For example, the actual event time, including the 80 μsec ADC conversion time, is 160-200 μsec for 5 to 12 parameter experiments. A further development (shown in Fig. 4), which eliminates transfer rate limitations on the CAMAC serial highway and elsewhere, is nearly complete. Significant efforts have also been expended to provide standard routines for the usual needs of data acquisition, taping, and display. In connection with the front-end improvements, we are writing software to reduce the detailed CAMAC knowledge required of a user when programming a new data acquisition task.

An Ethernet network was installed between all the machines to facilitate the sharing of data, as well as program and data transfer, and to reduce redundant files. This network also extends to the computer that runs the Computer Assisted Design system and permits its use for data analysis when it is not in use for its priority design function. Future expansion of the network will be both internal and external in nature. We intend to join the CAMAC systems so that data entering them can go to two or more computers independently. This will permit the focusing of additional computing power on a given problem. We will link our computers to the upcoming MSU network and thereby to the ARPANET and BITNET networks available on campus. This will allow outside users to interact with the laboratory machines and provide access to the NSF Supercomputer Centers.

Toward the end of the proposal period it will probably be necessary to replace the VAX 780, as this device nears the end of its design life and DEC support wanes. When this occurs, we propose to trade it in for a more capable processor; a more detailed discussion of this item is given in Section VI.D.

B. Transition to Phase II

We expect to have external beams for experiments from the K800 cyclotron during the first year covered by this proposal. The ion source for the first beams will be the room temperature ECR source; operation of the

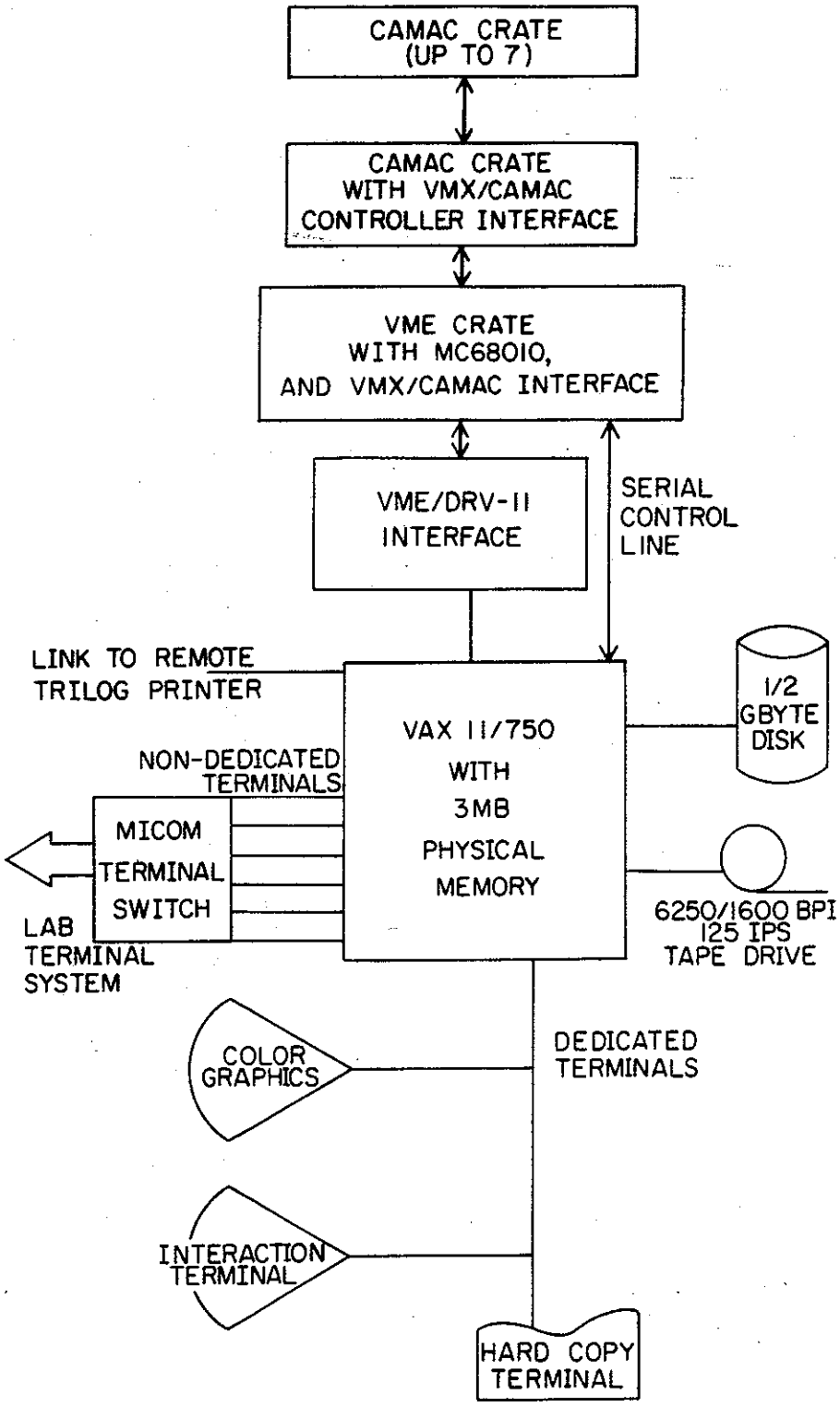

Fig. 4 Diagram of the new NSCL fast data acquisition system (an improvement of that described by A. Vander Molen, R. Au, R. Fox and T. Glynn, Nucl. Instr. Meth. A236, 359(1985)).

K500 with that source is expected in March, and we will have considerable operating experience when K800 operation begins.

Two major pieces of experimental apparatus will be ready for use with these higher energy beams: a 92" diameter by 120" long scattering chamber and a 4π array of multidetector telescopes. Details of these devices are given in Section III.C.1. Since the completion of the 4π array is planned for January 1987, there will be an opportunity to test and debug the array, and to carry out a number of experiments with beams from the K500+ECR facility prior to K800 operation. The array is being assembled at the target location chosen for these experiments, just east of the current 'north vault'.

Our current plan for the transition period, between initial operation of the K800 and completion of the many beam lines and experimental vaults planned for Phase II, differs somewhat from what might have seemed to be optimum a month ago. At that time our plans predicted completion of the K800 cyclotron late in 1987 and of the Phase II beam line system in mid 1988. In this situation it was not clear whether an interim target area for initial experiments was a wise investment of manpower, even though the manpower requirements are small. It might be better to delay experiments for the six months required to finish the beamlines, devoting this time to cyclotron development and shakedown, and then embark on the full-blown experimental program. However, as discussed in Section IV, we have been able to freeze the design of the extraction system earlier than expected, allowing a rearrangement of the construction procedure that moved up the planned K800 completion date by about four months. This of course has a cost: the necessary manpower for an accelerated K800 schedule must come from the other large project, the superconducting beamline system, and it will be correspondingly delayed. Nevertheless, we have decided to take this path; the K800 is intrinsically a very complicated system, and it seems advisable to move to operation as soon as is feasible.

Given this decision, the need for an interim system that will make use of the new beams from the K800 seems highly desirable; else we may have unique beams available for an extended period with no place to use them. Presently we are re-examining the beamline layout to determine whether a revision would allow us to deliver beam to one or two vaults that would be a

permanent part of the final system with a small complement of beamline magnets. That would be an ideal solution to the problem.

But in any case it appears that early delivery of beam to a limited experimental area is highly desirable, whatever detailed form this takes. During the early part of this period, beams from the K500 cyclotron can be directed to all present apparatus. As beam line elements become available we will extend the Phase II system in a phased manner until the total system is available. We would then devote a major effort to the completion of the S800 spectrograph and its beam analysis system. This unique device, with its large solid angle (20 millisteradians) and its remarkable capabilities for both energy and angular resolution, as well as the ease of operation which results from decoupling the energy analysis plane from the scattering plane, will add a new dimension to our study of nuclei with heavy ion beams.

During this interim period the advanced ECR source will begin operation, and this configuration will be used both to test that source's operation and to carry out an experimental research program. As has been discussed in the Introduction, we will then decide whether it is desirable to build the coupling line between the two cyclotrons to obtain still higher performance. The beam line layout preserves the necessary space to accomplish this coupling.

C. Scientific Operation

The NSCL has been operating as a national users facility since the first beams were obtained from the facility. As such, beam time is allocated by the Scientific Director of the NSCL (presently Sam Austin, Co-Director of the laboratory), based on recommendations of a Program Advisory Committee (PAC). A request for beam time is initiated by a proposal submitted to the laboratory, normally in response to a call for proposals issued approximately twice per year. These proposals are reviewed by the PAC in meetings held at MSU. There are no oral presentations, but Principal Investigators are encouraged to discuss their proposal with members of the PAC, and PAC members often call PI's to clear up issues that arise either before the PAC meeting or during it. The Scientific Director notifies PIs of their time allocations shortly after the PAC meeting.

This procedure is efficient in the sense that a great deal of travel is eliminated, and it appears to have worked well. Of course the effectiveness of any PAC process depends on the members of the PAC, and we feel that in this respect we have been unusually fortunate. Members are chosen by the Scientific Director following advice of the user community and of the Executive Committee of the Users Group. Presently the PAC is evolving into its asymptotic form where one member is replaced following each meeting; with a PAC of six members, each member will serve for six meetings or about three years. The members of the PAC to date are listed in Table II.3.

The Users Group is represented by an Executive Committee whose four elected members serve three year terms; this group elects its own chair. A fifth (non-voting) member of the Committee is appointed by the Scientific Director of the NSCL to serve as liaison to the laboratory. The Committee organizes the Annual Meeting of the Users Group which is held at the fall meeting of the Division of Nuclear Physics, normally attends site visits of NSF groups to the NSCL, and is consulted on issues of importance to the Users Group. In particular, the Executive Committee has had the opportunity to comment on the relevant sections of this proposal. Table II.4 lists members of the Executive Committee to date.

Finally we append to this chapter Table II.5, a list to date of proposals approved for use of the NSCL. There has been strong competition for beam time with an average ratio of time requested to time awarded of about 2 to 1, averaged over the past four PAC cycles. An average PAC meeting considers 26 proposals with requests for 3210 hours of beam time and awards a total of 1700 hours(excluding reserve time which is not usually run). These proposals involve 7 countries, 22 institutions and 92 individuals. A total of 201 scientists, including 32 postdoctoral scientists and 59 graduate students, have been involved in experiments approved to date.

Table II.3. Meetings and Members of the NSCL Program Advisory Committee

Meetings To Date:

PAC-1	February 1982
PAC-2	September 30, 1983
PAC-3	July 2, 1984
PAC-4	January 13-14, 1985
PAC-5	July 28-29, 1985
PAC-6	April 6-7, 1986

PAC Members

Members serve for about six PAC Meetings with one member leaving the PAC after each meeting. The Scientific Director of the NSCL is Convenor of the Committee. PAC members to date and the meetings at which they have served are:

H.C. Britt (LANL)	1,2
D. Cline (Rochester)	1,2,3,4,5
S.E. Koonin (CalTech)	1,2,3,4,5,6
P. Paul (Stony Brook)	1,2
D.K. Scott (MSU)	1,2,3
J. Cramer (Washington)	3,4,5,6
V. Viola (Indiana)	3,4,5,6
W. Benenson (MSU) Non-voting Chair 1,2,3	4,5,6
P. Siemens (Texas A&M)	5,6
F. Stephens (LBL)	6

Table II.4. NSCL User's Executive Committees

Members of the User's Executive Committee serve three-year terms, beginning November 1 (formerly two-year terms beginning October 1). Members are elected each year from the general membership of the User's Group, and a non-voting liaison representative from MSU is appointed by the Director of the NSCL. Committees to date are:

July 1, 1982 - September, 1982

F. Becchetti -- University of Michigan
A. Galonsky -- Michigan State University
J. Huizenga -- University of Rochester, Chair
V. Viola -- Indiana University
G.M. Crawley -- MSU, Liaison

October 1, 1982 - September 30, 1983

F. Becchetti -- University of Michigan, Chair
J. Kolata -- Notre Dame University
V. Viola -- Indiana University
D. Youngblood -- Texas A&M University
A. Galonsky -- MSU, Liaison

October 1, 1983 - September 30, 1984

J. Kolata -- Notre Dame University, Chair
F. Prosser -- University of Kansas
R. Tickle -- University of Michigan
D. Youngblood -- Texas A&M University
A. Galonsky -- MSU, Liaison

October 1, 1984 - October 31, 1985

J. Kolata -- Notre Dame University
L. Lee -- SUNY, Stony Brook
F. Prosser -- University of Kansas
R. Tickle -- University of Michigan, Chair
A. Galonsky -- MSU, Liaison

November 1, 1985 - October 31, 1986

D. Kovar -- Argonne National Lab
L. Lee -- SUNY, Stony Brook
F. Prosser -- University of Kansas, Chair
R. Tickle -- University of Michigan
A. Galonsky -- MSU, Liaison

Table II.5. Experiments Allocated Time at the NSCL

APPROVED EXPERIMENTS NSCL PAC1

Heavy Target Fragmentation at Intermediate Energies - G.T. Seaborg, W. Loveland, T.T. Sugihara, R.H. Kraus, Jr., K. Aleklett, P.L. McGaughey, H. Kudo, D.J. Morrissey; LBL, Oregon State, Studsvik, and MSU.

Cellular Microirradiation: Cell Survival vs. LET - W.C. Parkinson, J. Bardwick, F.L. Vaughan; Univ. of Mich.

Energy Dependence of Light Particle Production - G.D. Westfall, D. Ardouin, G.M. Crawley, M.V. Curtin, C.K. Gelbke, L. Harwood, B. Hasselquist, B.V. Jacak, D.K. Scott, M.B. Tsang; MSU and Univ. of Nantes.

Study of Light Nuclear Fragments from ^{12}C and ^{20}Ne Induced Reactions - N. Anantaraman D. Ardouin, G.M. Crawley, M.W. Curtin, C.K. Gelbke, L.H. Harwood, B.E. Hasselquist, B.V. Jacak, D.J. Morrissey, L. Panagiotou, D.K. Scott, G.D. Westfall; MSU.

Search for Coherent Pion Production in Reactions Between Light Nuclei - P. Braun-Munzinger, P. Paul, A. Sandorfi, L. Ricken, J. Stachel, Pei Hua Zhang, F. Obershain, G. Young, E. Grosse; Stony Brook, GSI, and BNL.

Studies of Evaporation-Fission Competition for Highly Excited Lanthanides and Actinides - W.U. Schroder, J.R. Birkelund, M.K. Butler, J.R. Huizenga, J.P. Kosky, W.W. Wilcke, D. Hilscher, Hahn-Meitner; Rochester.

Search for Multiparticle Jets in Heavy Ion Collisions - B.E. Hasselquist, G.M. Crawley, G.D. Westfall, C.K. Gelbke, W.G. Lynch, M.B. Tsang, L. Harwood, R. Fox, R.S. Tickle; MSU and Univ. of Michigan.

Linear Momentum Transfer in Incomplete Fusion Reactions Followed by Fission - C.K. Gelbke, B.B. Back, J. Kasagi, W.G. Lynch, M.B. Tsang, K.L. Wolf, Z.R. Xu, V.E. Viola, D. Fields, C.B. Chitwood, D.R. Klesch, H. Utsunomiya, K. Kwiatkowski; MSU, ANL, Indiana.

Neutron and Gamma-Ray Emission in Deep Inelastic Collisions - A. Galonsky, C.K. Gelbke, G. Caskey, J. Kasagi, M. Mallory, B. Remington, B. Tsang, J.J. Kolata, A. Kiss, F. Deak, Z. Seres; MSU, Notre Dame, Budapest.

Use of ^{13}N in Studies on Denitrification and Nitrogen Fixation - K. Schubert, J.M. Tiedje, J. Nolen, M. Betlach, P. Cornell, M. Boland, D. Myrold, T. Parkin, D. Morrissey, A. Sexstone, G.P. Robertson; MSU.

Complete and Incomplete Fusion Reactions at E_{Lab} >10 MeV/u - K.L. Wolf, D.G. Kovar, R. Janssens, C.K. Gelbke, G.D. Westfall, H. Ikezoe, G. Rosner, G. Stephans, B. Wilkins, B.V. Jacak; ANL, MSU.

Very High Energy Particle Production - F.D. Becchetti, J. Janecke, P. Lister, G.D. Westfall, A. Nadasen, H. van der Plicht, B. Sherrill; Univ. of Mich., MSU.

Search for Low-Energy Intermediate-Mass Fragments in ^{14}N and ^{20}Ne Induced Reactions - C.K. Gelbke, W. Lynch, D.J. Fields, C.B. Chitwood, H. Utsunomiya; MSU.

Study of the Energy Dependence of the Fragmentation Process Near 0° - L.H. Harwood, G.D. Westfall, N. Anantaraman, B.V. Jacak, A. Davenport, B. Hasselquist, H. Utsunomiya; MSU.

APPROVED EXPERIMENTS NSCL PAC2

Cellular Microirradiation: Cell Survival vs. LET - W.C. Parkinson, J. Bardwick, F.L. Vaughn; Univ. of Michigan.

Absorptive Fragmentation of 20 MeV/u - ^{4}N Projectiles - H. Utsunomiya, D.J. Morrissey, R.A. Blue, L.H. Harwood, R.M. Ronningen, J. van der Plicht; MSU.

Complete and Incomplete Fusion at Intermediate Energies - G.T. Seaborg, W. Loveland, T.T. Sugihara, K. Aleklett, D.J. Morrissey; LBL, Oregon State Univ., MSU, SRL Studsvik.

Spallation and Fragmentation of Medium-A Targets by Heavy Ions, N.T. Porile, Y.H. Chung, J. Herrmann, D.J. Morrissey, Purdue; MSU.

Particle Response Function to High Excitation Energy - G.M. Crawley, J.E. Duffy, R. Tickle, S. Gales, E. Gerlic, C.P. Massolo, J. Finck; MSU, Univ. of Mich., IPN/Orsay, UNLP/Argentina, Central Mich. Univ.

Study of Multi-Particle Correlations and Search for Jets in Intermediate Energy Heavy Ion Collisions - Z.M. Koenig, G.D. Westfall, G.M. Crawley, B.E. Hasselquist, B.V. Jacak, R.S. Tickle, H. Utsunomiya; MSU, and Univ. of Mich.

Mass Measurements of Proton Rich Nuclei Using the (^{7}Li,^{8}He) Reaction - B. Sherrill, W. Benenson, K. Beard, B.A. Brown, E. Kashy, J.A. Nolen Jr., A.D. Panagiotou, J. van der Plicht; MSU.

Test of the Validity of the Assumption of Thermal Equilibrium in Heavy Ion Collisions - D.J. Morrissey, W. Benenson, J. van der Plicht, E. Kashy, A.D. Panagiotou, H. Utsunomiya, B. Sherrill, R. Ronningen, R. Blue; MSU.

Neutral Pion Production at $E_{lab} \leq 35$ MeV/u - P. Braun-Munzinger, P. Paul, L. Ricken, J. Stachel, P.H. Zhang, T. Awes, F. Plasil, F. Obenshain, G.R. Young; Stony Brook, Oak Ridge.

$^{12}C(^{6}Li,d)$ and $(^{7}Li,t)$ ^{16}O: Study of α-Cluster States in ^{16}O - F. Becchetti, J. Janecke, P. Lister; Univ. of Michigan.

Giant Resonances Excited with High Energy ^{6}Li Scattering - J. van der Plicht, W. Benenson, G. Crawley, E. Kashy, B. Sherrill, K. Beard, H. Utsunomiya; MSU.

Investigation of Denitrification Using 13-N - J.M. Tiedje, D. Morrissey, J. Nolen, G. Phillip Robertson, D. Myroid, U. Ronner, G. Mileski, C. Rice; MSU.

Measurement of Total Reaction Cross Sections at 15 to 35 MeV/A - J.G. Cramer, L.H. Harwood, R.A. Loveman, W.G. Lynch, A.J. Lazzarini, A.G. Seamster, J. van der Plicht; Univ. of Washington, MSU.

Decay Measurements of Neutron Rich Isotopes Produced by Fragmentation of ^{22}Ne Beams - J. Nolen, L.H. Harwood, M.S. Curtin, W.E. Ormand, Z.Q. Xie; MSU.

Measurements of Intermediate Mass Fragments to Study Liquid-Gas Phenomena - M.S. Curtin, D.K. Scott, C.B. Chitwood, D.J. Fields, C.K. Gelbke, B.V. Jacak, W. Lynch, A.D. Panagiotou, M.B. Tsang; MSU.

Giant Resonance Studies Using Inelastic Scattering of 35 MeV/A ^{14}N - Umesh Garg, W.G. Lynch, A. Galonsky, J. van der Plicht, D.H. Youngblood; Univ. of Notre Dame, MSU, Texas A&M.

Neutron Emission in Deep-Inelastic Scattering - G. Caskey, A. Galonsky, B. Remington, M.B. Tsang, J. Kasagi, A. Kiss, F. Deak, Z. Seres, J. Kolata, J. Hennefeld, C.K. Gelbke; MSU, Tokyo Inst. Tech., Eotvos Univ., Notre Dame, CRI Budapest.

Investigation of Light Particle Correlations for ^{14}N Induced Reactions - W. Lynch, C.B. Chitwood, D.J. Fields, C.K. Gelbke, M.B. Tsang, D.R. Klesch, F. Plasil, T.C. Awes, G.R. Young; MSU, ORNL.

Exclusive Studies of Low-Energy, Intermediate-Mass Fragments in the ^{14}N + ^{238}U Reaction at E/A = 35 MeV - Vic Viola, K. Kwiatkowski, M. Fatyga, B. Tsang, B. Lynch, C.K. Gelbke, C. Chitwood, D. Fields, D. Klesch; IUCF, MSU.

Pion Production Far Below the N-N Threshold - K. Beard, W. Benenson, E. Kashy, B. Sherrill, J. van der Plicht; MSU.

Emission of Low energy Intermediate Mass Fragments - C.K. Gelbke, D.J. Fields, C.B. Chitwood, D.R. Klesch, W.G. Lynch, M.B. Tsang; MSU.

Elastic Scattering of ^{6}Li Ions - A. Nadasen, P. Schwandt, F. Becchetti, J. Janecke, G. Ciangaru, C.W. Wang; Univ. Of Mich., IUCF, Univ. of Maryland.

An Exploratory Study of the (^{6}Li, ^{6}He) Reaction at 25 and 35 MeV/nucleon - N. Anantaraman, S.M. Austin, A. Galonsky, J. van der Plicht, C.C. Chang, G. Ciangaru; MSU, Maryland.

Partial Wave Distributions in Total Momentum Transfer Reactions at 35 MeV/u - J.B. Natowitz, M.N. Namboodiri, P. Gonthier, H. Ho, R.P. Schmitt, G.

Berkowitz, K. Hagel, D. Fabris, G. Nebbia, Z. Majka; Texas A&M, LLNL, Hope College, Max Planck Inst., Heidelberg.

Study of Charge-Exchange Reaction (^{12}C, ^{12}N) at 35 MeV/Nucleon - N. Anantaraman, S.M. Austin, L.H. Harwood, A.D. Panagiotou, J. van der Plicht, A.F. Zeller; MSU.

APPROVED EXPERIMENTS NSCL PAC 3

Projectile Fragmentation and Correlated Multiparticle Emission - D. Horn, R. Bougault, G.C. Ball, E. Hagberg, G.D. Westfall, Z.M. Koenig, D. Fox; AECL, ORNL, MSU.

Elastic Scattering of ^{6}Li Ions - A. Nadasen, P. Schwandt, R.E. Warner, F. Becchetti, J. Janecke, P. Lister, A.A. Cowley and S. Mills; U. of Michigan, IUCF, Oberlin, CSIR (Faure, South Africa).

Mass Measurements of Proton-Rich Nuclei - W. Benenson, B. Sherrill, B.A. Brown, E. Kashy J.A. Nolen, J. van der Plicht, C. Bloch, J.S. Winfield; NSCL.

Giant Resonances Excited with High Energy ^{6}Li Scattering - J. van der Plicht, W. Benenson, G. Crawley, E. Kashy, B. Sherrill, H. Utsunomiya, J. Winfield; NSCL.

Exploratory Study of Deep-Lying Two-Proton-Hole States by $^{148}Sm(^{6}Li,^{8}B)$ - A. Saha, N. Anantaraman, G.M. Crawley, J. van der Plicht, J. Winfield, R.S. Tickle; Northwestern Univ., NSCL, U. of Michigan.

Test for Statistical Equilibrium in Heavy Ion Collisions - D.J. Morrissey, W. Benenson, E. Kashy, H. Utsunomiya, J. van der Plicht, B. Sherrill, C. Bloch, R. Blue, R. Ronningen; NSCL.

Importance of Direct vs. Thermal Contributions - G.D. Westfall, Z.M. Koenig, D. Fox, D. Horn, R. Bougault; NSCL, Chalk River.

Nonequilibrium Emission from 25 and 35 MeV/u ^{16}O + ^{58}Ni - Peter L. Gonthier, G.D. Westfall, H.Ho, R.S. Tickle, Z.M. Koenig, D. Fox, M. Kort, D. Mogdrige, A. Cummins; Hope College, Max-Planck-Institut,(Heidelberg), U. of Michigan, NSCL.

Determination of γ-ray Polarization Associated with Non-Equilibrium Light Particles at Intermediate Energies - W. Trautman, M.B. Tsang, C.B. Chitwood, D.J. Fields, C.K. Gelbke, W.G. Lynch, R. Ronningen, J. Pochodzalla; Brookhaven, NSCL.

Search for Pion Precursor Effects through Isovector Charge-Exchange on ^{14}C - J.S. Winfield, S.M. Austin, Z.P. Chen, A. Galonsky, B. Sherrill; NSCL.

Investigation of Denitrification Using ^{13}N - James M. Tiedje, D. Morrissey, J. Nolen, G.P. Robertson, U. Ronner, M. Klug, C. Rice, E. Aerssans; Crop & Soil Sciences (MSU), Kellogg Biological Station (MSU), NSCL.

In-Beam Gamma-Ray Spectroscopy of Odd-Odd Deformed Nuclei in the Re Region - Wm.C. McHarris, W. Olivier, Wen-Tsae Chou, Jane Kupstas-Guido; NSCL.

Giant Resonance Studies Using Inelastic Scattering of 35-40 MeV/A ^{14}N - Umesh Garg, W.G. Lynch, A. Galonsky, M.B. Tsang, J. van der Plicht, W.A. Hollerman, M.W. Drigert, D.H. Youngblood; Notre Dame, Texas A&M, NSCL.

Measurement of Target Residues from Collisions of ^{14}N(40 MeV/u) with ^{60}Ni and ^{107}Ag - N. Anantaraman, J. Wilczynski, W.G. Lynch, M. Maier, K. Siwek-Wilczynska, M.B. Tsang, J. Winfield, R.S. Tickle; NSCL, U. of Michigan.

Pion Production Far Below the N-N Threshold - K. Beard, W. Benenson, E. Kashy, D. Morrissey, J. van der Plicht, J. Winfield, B. Sherrill, C. Bloch; NSCL.

Particle Response Function to High Excitation Energy - G.M. Crawley, J.E. Duffy, J. van der Plicht, R. Tickle, S. Gales, E. Gerlic, C.P. Massolo, J. Finck; U. of Michigan, IPN(Orsay) UNLP (Argentina), Central Michigan, NSCL.

Lifetime Measurement of ^{6}He - J. Nolen, L.H. Harwood, Z.Q. Xie, B. Sherrill, D. Mikolas, R.G.H. Robertson; NSCL, LANL.

Measurement of Final State Interactions Between Non-Equilibrium Light Particles in Coincidence with Full Momentum Transfer Trigger - W.G. Lynch, C.K. Gelbke, C.B. Chitwood, D.J. Fields, P. Pochodzalla, M.B. Tsang; NSCL.

Limitation of Linear Momentum Transfer in Nucleus-Nucleus Collisions - Vic Viola, K. Kwiatkowski, M. Fatyga, M.B. Tsang, C. Chitwood, C.K. Gelbke, D. Fields, D. Klesch; IUCF, NSCL.

Decay Measurements of Neutron Rich Isotopes Produced by Fragmentation of O Beams - J. Nolen, L.H. Harwood, M.S. Curtin, W.E. Ormand, Z.Q. Xie; MSU.

Decay Measurements of Neutron Rich Isotopes Produced by Fragmentation of O Beams - J. Nolen, L.H. Harwood, M.S. Curtin, W.E. Ormand, Z.Q. Xie; MSU.

APPROVED EXPERIMENTS NSCL PAC4

^{22}Al Mass Measurement - W. Benenson, J.S. Winfield, C. Bloch, E. Kashy, J.A. Nolen, Jr., B. Sherrill, J. Stevenson, J. van der Plicht; NSCL.

Associated Neutron Multiplicities in Intermediate Energy Collisions - W. Benenson, D.J. Morrissey, C. Bloch, E. Kashy, G. Caskey, A.I. Galonsky, B. Remington, J. Heltsley, L. Heilbronn; NSCL.

Forward Angle Measurements of Projectile Fragmentation - G. Crawley, G. Westfall, R. Ronningen, S. Angius, V. Rotberg, D. Fox, D. Cebra, Pereira,

Sala, Szanto de Toledo, A. Menchaca-Rocha, M. Brandan, M.and A. Etchegoyen; NSCL; USP, Brazil; Univ. of Chile; CNEA, Buenos Aires.

Production of Unstable Nuclear Resonances - G.D. Westfall, D. Cebra, R.S. Tickle, D. Fox, Z. Koenig; NSCL, Univ. of Michigan.

Nucleus-Nucleus Photon Bremsstrahlung - J. Stevenson, W. Benenson, K. Beard, C. Bloch, E. Kashy, D.J. Morrissey, B. Sherrill, J.S. Winfield; NSCL.

Beta Decay of ^{9}C - R. Sherr, J.A. Nolen Jr., Z.Q. Xie, E. Kashy, W. Benenson, B.A. Brown, D. Mikolas, J. Stevenson, L.H. Harwood, J.D. Brown, Princeton; NSCL.

Structures at Very High Excitation Energy Observed in Heavy Ion Inelastic Scattering - S. Gales, S. Austin, W. Benenson, G.M. Crawley, J. van der Plicht, J. Winfield, H. Wu, Z. Chen, V. Borel, S. Fortier, IPN, Orsay; NSCL.

Measurement of Total Reaction Cross Sections in Nucleus-Nucleus Collisions - J.G. Cramer, R.A. Loveman, D.D. Leach, W.G. Lynch, T. Murakami, D.R. Tieger, M.B. Tsang, J. van der Plicht, Univ. of Wash; Univ. of Colo; NSCL.

Target Dependence of ^{22}Ne Projectile Dissociation at 25 MeV/Nucleon - H. Utsunomiya, D.J. Morrissey, L.H. Harwood, E.C. Deci; NSCL, Alma College.

Particle Response Function to High Excitation Energy - G.M. Crawley, J.E. Duffy, J. van der Plicht, R. Tickle, S. Gales, E. Gerlic, C.P. Massolo, J.E. Finck; NSCL, Univ. of Michigan; IPN, Orsay; Central Michigan University.

In-Beam Gamma-Ray Spectroscopy of Odd-Odd Deformed Nuclei in the Re Region - W.C. McHarris, W. Olivier, Wen-Tsae Chou, J. Kupstas-Guido, D. Mason; NSCL

Survey of the Production of Intermediate Mass Fragments - S.M. Austin, Z. Chen, C.K. Gelbke, W.G. Lynch, J. Pochodzalla, D.K. Scott, M.B. Tsang, J.S. Winfield, H. Wu, K. Kwiatkowski, V.E. Viola; NSCL, Indiana University.

Study of Spin Transfer Strength with the (^{6}Li,^{6}He) Reaction - J.S. Winfield, S.M. Austin, N. Anantaraman, Z.P. Chen, A. Galonsky, J. van der Plicht, H.L. Wu, C.C. Chang, G. Ciangaru; NSCL, Univ. of Maryland, Schlumberger Well Services, TX.

Lifetime Measurements of Neutron-Rich Light Isotopes - J.A. Nolen, L.H. Harwood, M.S. Curtin, Z.Q. Xie, B. Sherrill, B.A. Brown, J. Stevenson; NSCL, KMS Fusion.

Fragmentation and the Emission of Particle Unstable Complex Nuclei - W.G. Lynch, C.B. Chitwood, D.J. Fields, C.K. Gelbke, J. Pochodzalla, M.B. Tsang; NSCL.

Investigation of Soil Nitrogen Transformations Using 13-N - J.M. Tiedje, D. Morrissey, J.A. Nolen Jr., G.P. Robertson, C. Rice, E. Aerssens, S.N. Huang, P. Groffman, U. Ronner, M. Klug, G. Walker; MSU, NSCL.

APPROVED EXPERIMENTS NSCL PAC5

High Spin Spectroscopy in Neutron Rich Rare Earth Nuclei Using Heavy Ion Induced Tranfer Reactions - J.X. Saladin, D. Morrissey, R. Blue, R. Ronningen, E. Deci, C. Baktash, I. Lee, C. Knott, M. Kaplan, M. Metlay; NSCL, Alma College, ORNL, U. of Pittsburgh.

Decay of a High Spin Isomer in ^{178}W and the Question of Triaxial Behavior - J.X. Saladin, C. Baktash, I.Y. Lee, R. Blue, R. Ronningen, C. Knott, M. Kaplan, M. Metlay; University of Pittsburgh, ORNL, NSCL.

Lifetime Measurements of Neutron-Rich Light Isotopes - J. Nolen, J. Stevenson, J. Winfield, Z.Q. Xie, D. Mikolas, L. Harwood, M.S. Curtin, S. Heckman, B. Sherrill, B.A. Brown; NSCL, KMS Fusion.

Search for ^{12}C Clusters in ^{28}Si via ^{12}C-^{12}C Quasi-Elastic Scattering - A. Nadasen, R.E. Warner, A. Galonsky, F.D. Becchetti, J.W. Janecke, K.T. Hecht; University of Michigan, Oberlin College.

Very-High Energy Light-Particle Production $\Theta = 0°$ - F. Becchetti, J. Janecke, P. Schulman, P. Lister, R. Stern, D. Kovar; University of Michigan.

A Test for Statistical Equilibrium in Binary Reactions of ^{14}N with ^{12}C. D.J. Morrissey, W. Benenson, C. Bloch, R. Blue, E. Kashy, R.M. Ronningen, A. Tam; NSCL.

Systematics of Single-Nucleon Transfer Cross-Sections for $^{12}C + ^{208}Pb$ - J.S. Winfield, S.M. Austin, G.M. Crawley, Z.P. Chen, H.L. Wu, C.C. Chang; NSCL, U. of Maryland

Charged Particle Multiplicities Associated with High Energy Gamma Emission - E. Kashy, J. Stevenson, C. Bloch, W. Benenson, D.J. Morrissey, G. Westfall, J. Winfield, A. Tam, A. Lampis, D. Cebra, D. Fox; NSCL.

Large Angle Correlations of Light Particles - D. Fox, G.D. Westfall, D. Cebra, J. van der Plicht, D. Horn; NSCL, Chalk River.

Transition from Bound to Unbound Systems - D. Cebra, G. Westfall, D. Fox, J. van der Plicht, S. Angius, G. Crawley, S. Tanaka; NSCL.

Nucleus-Nucleus Photon Bremsstrahlung (Renewal of 85007) - J. Stevenson, W. Benenson, K. Beard, C. Bloch, E. Kashy, A. Lampis, D.J. Morrissey, M. Samuel, A. Tam, J.S. Winfield; NSCL.

Determination of the Circular Gamma-Ray Polarization Associated with the Emission of Intermediate Mass Fragments - M.B. Tsang, D.J. Fields, C.K. Gelbke, H.M. Xu, W.G. Lynch, T. Nayak, R. Ronningen, T. Shea, W. Trautmann, W. Dunnweber; NSCL, GSI, U. of Munchen.

Search for ^{10}He - J. Stevenson, J. Nolen, W. Benenson, L. Harwood, S. Heckman, E. Kashy, A. Lampis, D. Mikolas, M. Samuel, A. Tam, J.S. Winfield, Z.Q. Xie; NSCL.

High-Spin Particle-Hole Stretched States with the (α, ^{3}He) & (α,t) Reactions - C.C. Chang, J.S. Winfield, N. Anantaraman, A. Galonsky, J. van der Plicht, F. Khazaie, D.H. Zhang, P. Bonerg, G. Ciangaru; University of Maryland, Schlumberger Well Services.

Feasibility of Exciting $\Delta T=1$, $\Delta S=1$ Transitions by the (^{6}Li, ^{6}Li* [3.56 MeV]) Reaction - N. Anantaraman, S.M. Austin, D.J. Morrissey, R.M. Ronningen, J.S. Winfield, Z. Chen, H.L. Wu; NSCL.

Structures in Inelastic Scattering - S. Gales, S.M. Austin, W. Benenson, G. Crawley, J. Winfield, J. van der Plicht, S. Fortier; IPN, NSCL.

Beta Decay Branching Ratios of 17C - D. Mikolas, J. Stevenson, R.A. Blue, B.A. Brown, M.S. Curtin, L. Harwood, S. Heckman, J. Nolen, R. Ronningen, C. Scripter, B. Sherrill, J. Winfield, Z.Q. Xie; NSCL.

III. STAFF RESEARCH: NUCLEAR SCIENCE AND INSTRUMENTATION.

INTRODUCTION

The staff research in nuclear science section of this proposal is divided into three main parts:

A. Nuclear Reactions

B. Nuclear Structure and Nuclear Astrophysics

C. Instrumentation

Even a glance at the list of topics listed under these main headings shows the breadth of interests at the NSCL, which range from light-ion and heavy-ion physics to astrophysics. Nevertheless, the main emphasis of the laboratory, and therefore of this proposal, is the use of heavy ions both as a probe of nuclear structure and as a means of studying the mechanisms of the fascinating and little understood nucleus-nucleus reactions.

In the nuclear reactions section, there is considerable emphasis on understanding the role of equilibration and whether the "temperature" of short-lived nuclear systems is a viable concept. Early measurements using γ-rays to determine the relative population of bound nuclear states found surprisingly low "temperatures" and this issue is now being vigorously pursued by observing correlated emission of both charged particles and neutrons from unbound states (Section A4). Another new result discussed in this section is the production of very high energy gamma-rays (50-130 MeV) in heavy ion collisions. The energy and Z dependence of the production process does not appear to agree with any of the current theoretical predictions (Section A1). Another area which will become increasingly prominent is the study of complete events measured with various kinds of 4π detectors. A large 4π charged-particle detector and a 4π γ-ray detector are under construction and development is also proceeding on the use of CCD cameras for complete event analysis. These studies, (Section A3) particularly with heavier beams, should improve our understanding of the nuclear equation of state and possibly point to ways of detecting phase transitions in nuclear matter.

In the area of nuclear structure research, the investigation of spin-dependent phenomena will continue but now mainly using heavier projectiles (Section B1). The NSCL has pioneered a number of such studies in the past. The long standing interest in exotic nuclei will also be pursued, including the production and characterization of new species using the RPMS. A number of new β-decay lifetime measurements have been completed recently (Section B2). The RPMS should be even more useful with the higher energy and heavier beams which will soon be available. there is also considerable interest in studying simple excitations at high excitation energy. The NSCL has a history of research in nuclear astrophysics and a number of areas of current interest are described in Section B5. Finally, the operating grant has long supported a program of theoretical research, mainly involving large basis shell model calculations and their applications, that is closely related to the experimental program. The present interest and future directions are described in Section B4.

The third main section describes various instrumentation projects, some of which (S800 Spectrograph, 4π array, Large Scattering Chamber) are designed particularly for use in Phase II (Section C1). Ongoing instrumentation projects including nuclear electronics development and the production of ^{13}N for biological applications are described in Section C2.

As a useful guide to the reader, we shall outline some of the principles we have used in presenting the staff research. Most projects are ongoing so that the text includes a description of work already carried out plus an indication of future directions, especially with regard to the high energy beams from the K500 and ECR combination. There are a few projects for which the work is essentially complete and no further work is planned. Such projects are included in the proposal to demonstrate past accomplishments and to amplify the summary of previous work given earlier. We believe that this is an extremely important element in evaluating a proposal, expecially a renewal proposal. Finally, there are some new projects for which only the future plans are described.

Since some of the nuclear science experiments involving NSCL staff are carried out in other laboratories, we have included

descriptions of this work. In the list of authors we have generally included the names of people who are involved to a significant degree in a particular project. The NSCL personnel includes graduate students, post-doctoral fellows and staff members where appropriate. In many cases, both for work carried out at the NSCL and especially for work carried out at other laboratories, physicists who are not associated with the NSCL are involved. Their names have therefore been included as co-authors of particular projects and their affiliation has been referred to in each case.

As this proposal is being prepared, the injection line from an ECR ion source to the K500 cyclotron is being installed. This combination of the K500 cyclotron and ECR source will provide higher energy and more massive beams very soon. Present plans call for completion of the K800 cyclotron early in 1987. Beams from the K800, also with an ECR source, should therefore be available before the end of the first grant year.

III.A.1.a. PRODUCTION OF HIGH ENERGY GAMMA-RAYS

W. Benenson, E. Kashy, R. Smith, J. Stevenson,
D.J. Morrissey and J.S. Winfield

During the last year, we have developed an experimental program to study high energy gamma rays (E_γ>20 MeV) in heavy ion collisions. The high energy gamma ray yield in these collisions is surprisingly large[1]. For example, the reaction ^{14}N+Pb→γ at E/A=40 MeV has a total cross section for production of these gammas of about 0.5mb, which is much greater than for pions in the same energy range. The gamma ray spectra extend to at least 120 MeV, which for certain light target cases we have studied, implies that as much as 40% of the energy available is emitted as a single photon. Since the field is so new, the mechanism for high energy gamma ray production is completely unknown, but there are several interesting models in an early state of development.

Perhaps the most exciting possibility is that high energy gamma rays may be nuclear bremsstrahlung. Kapusta[2] first suggested that gamma rays might be produced by a bremsstrahlung process due to the sudden deceleration of the projectile in the early stages of the nuclear collision. This motivated Budiansky et. al.[3] to study high energy gamma rays from 2 GeV/A ^{40}Ar+Pb collisions at the LBL Bevalac. The large yield of gamma rays from π^0 decay precluded any definitive conclusions about bremsstrahlung in this experiment.

Recently Vasak et. al.[4] suggested that a bremsstrahlung process might produce both π^0's and γ's in intermediate energy heavy ion collisions. Observing this type of process would be particularly exciting because it would be an electromagnetic probe of the dynamics of the collision process. This has the advantage that the connection between the dynamics and the probe is well understood. In addition the nucleus is quite transparent to the gamma rays so the information is not destroyed by final state interactions.

First Observation of High Energy Gamma Rays:

In November 1984 we performed an exploratory experiment[1] to look for high energy gamma rays using the Enge spectrograph as an electron-positron detector. The technique used was to convert the gamma ray to an electron-positron pair directly after the target by backing the target with a thick γ→e+e- converter. The electron and positron energy spectra could then be measured using a specially designed focal plane detector on the focal plane of the magnetic spectrograph. Figure 1 shows measured positron spectra for 40 MeV/A ^{14}N+Cu using 3g/cm^2 converters of Be, Cu, and Pb with conversion efficiencies of 4, 13, and 24%, respecively. Note that the positron yield

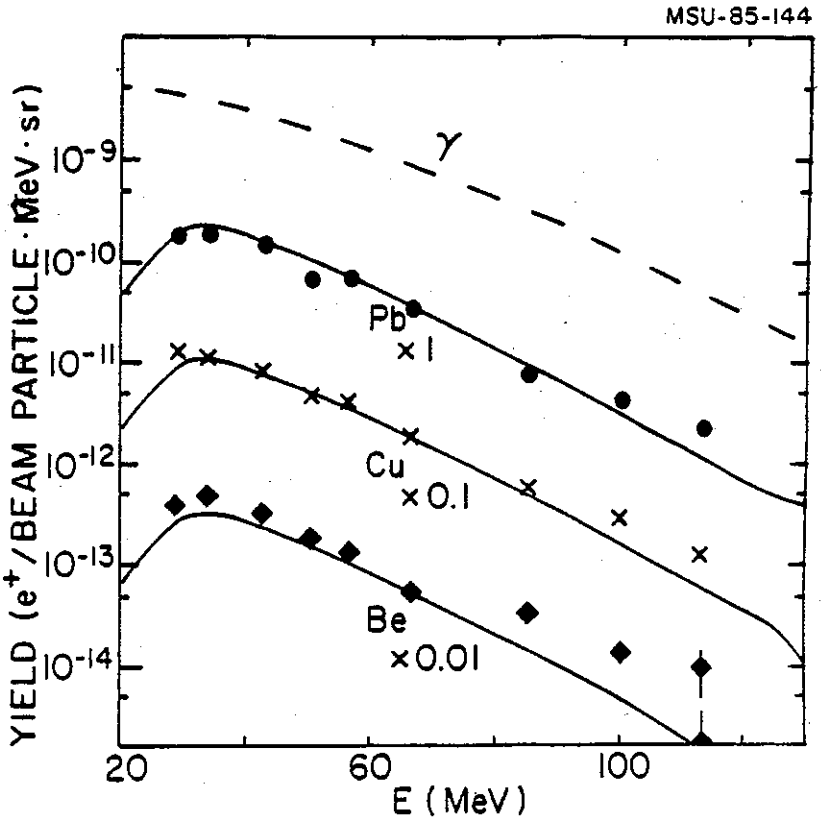

Fig. 1. The data points give the positron yield as a function of energy for ^{14}N+Cu at E/A=40 MeV for three different gamma ray converters at θ_{Lab}=17°. The dashed curve shows an assumed gamma ray yield assuming a thermal source, and the solid curves show the corresponding positron yields assuming all positrons are from gamma ray pair conversion.

extends beyond 100 MeV. The solid curve is the best fit gamma ray spectrum assuming a Planck form with a temperature of 12 MeV for the gamma ray

distribution. The dashed curves are calculated positron yields for each converter. The agreement for all three materials indicates that the positrons are being produced by the conversion of gamma rays to electron-positron pairs in the converter. Direct production of electron-positron pairs or high energy 'delta' electrons were found to be less than 2% of the gamma ray yield.

Gamma Ray Telescope design:

In January 1985 we began to design a telescope to measure gamma rays directly. The design objectives for the telescope were:

1) an energy range of 10 to 200 MeV, with a resolution of 10 to 20% FWHM.
2) a reasonably large solid angle of about 50 msr.
3) the ability to utilize high beam intensities and thick targets.
4) insensitivity to neutrons.

Large NaI or BGO detectors were ruled out due to their sensitivity to neutrons, as were lead glass detectors because of their poor resolution for gammas below 100 MeV. The design of the new γ-ray telescope is shown in Figure 2 .

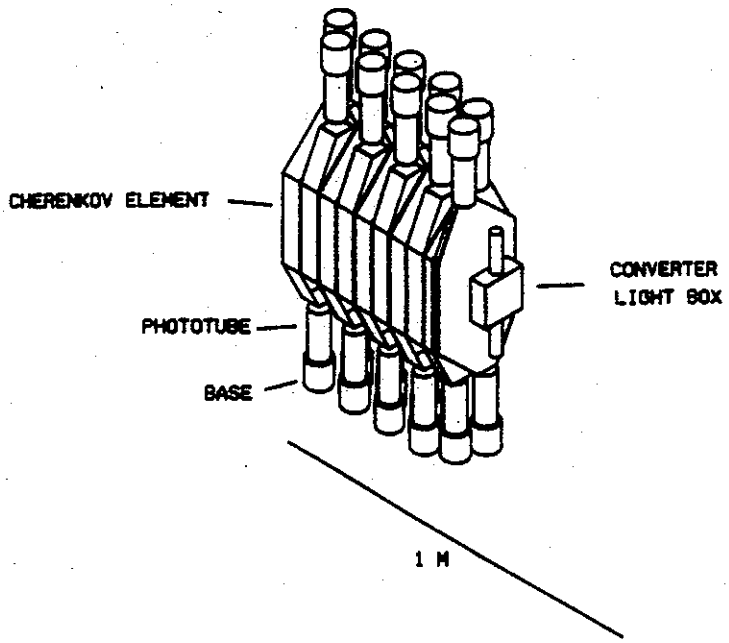

Fig. 2. High Energy Gamma Ray Telescope shown with the anticoincidence shield removed.The detector consists of a CsI active γ->e+e- converter,followed by 10 lucite cerenkov detectors arranged to form a range telescope.

It consists first of passive charged particle shielding followed by an anti-coincidence shield. The gamma ray is then converted to an electron-positron pair in an active CsI converter-scintillator. The electron-positron pair enters a plastic Cerenkov counter range telescope containing 10 segments with a total thickness of 43 cm. The pulse height information in the counters can distinguish between one or two $\beta=1$ particles in the counter. It is thus possible to measure the approximate range (and energy) of both particles of the pair to determine the gamma ray energy.

This detector was completed in June 1985 and used in a test run in July 1985. The only drawback in the original detector design was that its large size led to significant cosmic ray muon background. This was solved by putting the detector in a plastic scintillator anti-coincidence box. After the test run we decided that a second detector would be very useful and that eight elements of 33 cm. total length would be satisfactory. The second detector was completed in September 1985, and both detectors were used in a week long experiment in October 1985.

Inclusive Measurements:

In our July 1985 test run we measured the gamma ray yield for E/A=40 MeV ^{14}N on C, Zn and Pb targets at lab angles of $\theta=30°$, 90° and 150°. In our main run in October 1985 we made measurements for E/A = 20, 30, and 40 MeV ^{14}N + C, Zn and Pb at lab angles of $\theta=30°$, 60°, 120°, and 150°. The analysis of the test run data is complete. Gamma ray spectra for E/A=40 MeV ^{14}N+Pb are shown in Figure 3. The gamma ray yield extends to $E_\gamma>100$ MeV as observed in our previous experiment. The gamma ray energy spectra are clearly flatter than exponential and show little angle dependence. Figure 4 shows the angular distributions obtained for the three different targets. The Pb and Zn data are both close to isotropic, with the carbon data being significantly forward peaked. The yield for Pb is about 7 times larger than that of carbon implying an approximately $A^{2/3}$ target dependence. The nearly isotropic angular distribution and relatively weak target dependence are in disagreement with predictions of simple bremsstrahlung models which predict quadrupole angular distributions and a Z^2 dependence of the cross section (Z is the product of projectile and target charges for symmetric systems). Bertsch[5] has suggested that bremsstrahlung for small systems may

be dominated by incoherent proton-neutron bremsstrahlung which is isotropic and has a yield proportional to Z for symmetric systems. In Bertsch's model nucleus-nucleus bremsstrahlung becomes dominant at Z~50.

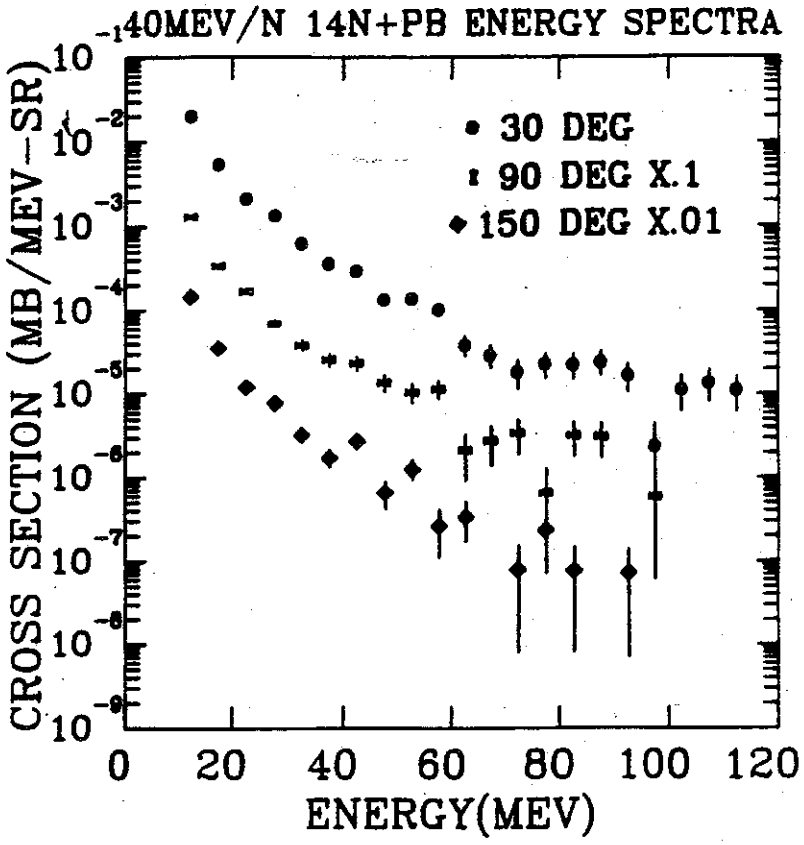

Fig. 3. The gamma ray energy spectrum from ^{14}N+Pb at E/A=40 MeV/A measured at lab angles of 30°, 90° and 150°.

Future Plans for Inclusive Measurements:

Clearly the most important step for future inclusive gamma ray measurements is to obtain data with heavy projectiles over a wide range of beam energies. Data with 40 MeV/A ^{40}Ar beams from the ECR+K500 will be interesting, but Pb beams from the ECR+K800 combination will probably be required to look for coherent nucleus nucleus bremsstrahlung.

Beyond experiments at MSU, we have an experiment approved at the LBL Bevalac to make inclusive measurements with E/A=100 MeV ^{139}La+La collisions. This experiment will be difficult because of the low beam intensities available but will give us an early look at what we may learn with K800 beams.

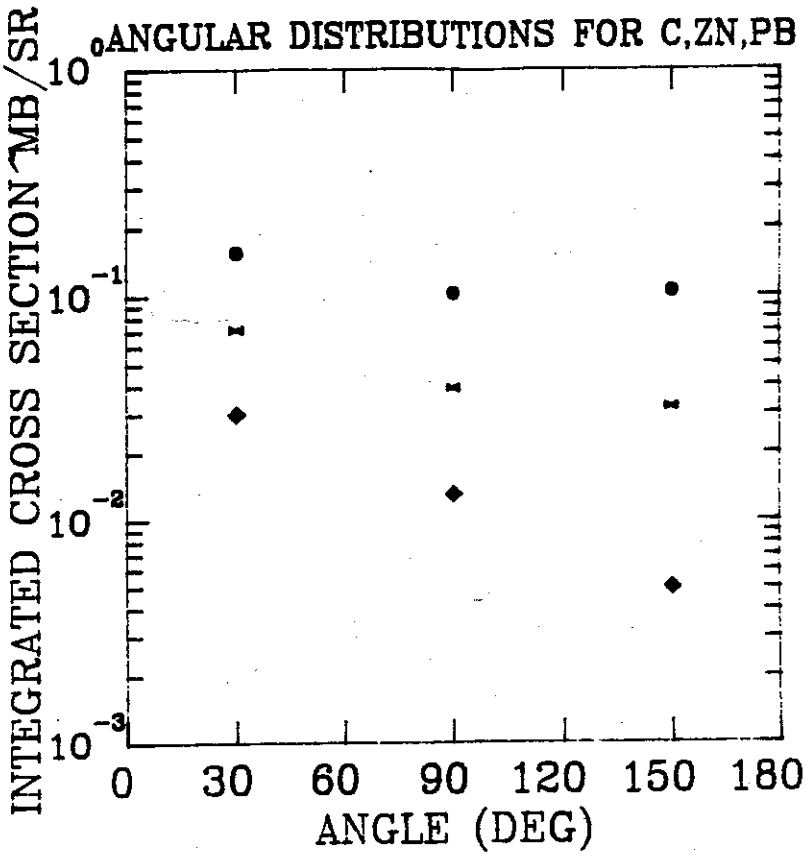

Fig. 4. A plot of the integral gamma ray yield with E_γ>12 MeV as a function of angle three targets Pb, Zn and C.

Associated Charged Particle Multiplicities:

The rather featureless character of the inclusive gamma ray data make it hard to draw conclusions about the production mechanism. The simultaneous observation of any other quantity associated with the collision will help characterize the reaction mechanism. Possible observables include the charged particle multiplicity and the energy and isotope distribution of intermediate mass fragments. Nucleus-nucleus bremsstrahlung is clearly associated with central collisions, and therefore we expect charged particle multiplicities larger than the untriggered ones.

At the last NSCL PAC meeting, a large experiment was approved to measure the charged particle multiplicity associated with high energy gamma rays. The two high energy gamma ray detectors will be placed on one side of the beam line 30 cm. away from the target. An array of 16 phoswich scintillator charged particle detectors placed on the opposite side of the beam line would sample the charged particle yield over an angular range of 20° to 90°. With each charged particle telescope having a solid angle of 20 msr. and the gamma telescopes covering 100 msr. each, a coincidence rate of

2 counts/sec can be obtained. This should make measurement of associated charged particle multiplicity and angular distributions possible. This experiment is tentatively scheduled to run in May 1986.

High Energy Gamma-Ray Trigger for the 4π Array:

The MSU 4π array will simultaneously detect virtually all charged fragments from a collision. One of the principal objectives of the detector is to study central collisions. If high energy gamma rays prove to be associated with central collisions, they could provide a trigger for the 4π array for central events. Or turning the problem around, differences in charged particle topology associated with high energy gamma rays will help determine the gamma ray production mechanism.

We plan to build a high energy gamma ray module which would replace one of the 30 large modules which form the 4π detector. Design goals for the detector are that it should have an active solid angle of 250 msr. and 30% efficiency. Prototype elements of the detector will be tested toward the middle of 1986 with completion of the detector scheduled for late in 1986.

References:

1. K.B. Beard, W. Benenson, C. Bloch, E. Kashy, J. Stevenson, D.J. Morrissey, J. van der Plicht, B. Sherrill and J.S. Winfield Phys. Rev. C 32,1111(1985).
2. J.I. Kapusta, Phys. Rev. C 15,1580(1977).
3. M.P. Budiansky, S.P. Ahlen, G. Tarle, And P.B. Price, Phys. Rev. Lett. 49,361(1982).
4. D. Vasak, W. Greiner, B. Mueller, Th. Stahl and M. Uhlig, Nucl. Phys. A428,291(1984).
5. Che Ming Ko, G. Bertsch and J. Aichelin, Phys. Rev. C 31,2324(1985).

III.A.1.b. INCLUSIVE MEASUREMENTS OF NON-COMPOUND PARTICLE EMISSION

J. Aichelin,[a] S.M. Austin, C.K. Gelbke, W.G. Lynch and M.B. Tsang

Intermediate energy nucleus-nucleus collisions are characterized by the increasing importance of particle emission prior to the attainment of full statistical equilibrium of the composite nuclear system. We have continued to investigate the characteristics of precompound particle emission over a broad energy range.[1-4] The rather successful description of inclusive light particle cross sections in terms of simple moving source parameterizations and the systematic variation[5,6] of the slopes ("temperature" parameters) of the energy spectra with projectile energy (see following section) were suggestive of statistical particle emission from highly excited subsets of nucleons. Statistical model calculations[7] for the decay of highly excited nuclear systems predicted non-negligible probabilities for the emission of intermediate mass fragments, i.e. complex nuclei of masses A≈6-40. Such decay processes are of particular interest since they might provide key information on the entropy production[2] in nuclear collisions and on the liquid-gas phase transition of nuclear matter.[8] We have, therefore, investigated the emission of intermediate mass fragments over a large range of energies.[2-4] (See following section for description of inclusive measurements of complex fragment emission at Bevalac energies.)

At present, the emission of intermediate mass fragments is not fully understood. A variety of models have been proposed, including the cold shattering of the target nucleus, sequential and non-sequential statistical emission from highly excited subsets of nucleons, the coalescence from a hot gas of nucleons, and the statistical formation of clusters near the critical point in the liquid-gas phase diagram of nuclear matter. Only a few attempts were made to describe differential cross sections. We have investigated two different models,[4] both based on the assumption that a local region of excitation is formed in the region of geometrical overlap of target and projectile. In the first model, energetic nucleons originating from this region pass through and destabilize the cold target spectator

matter, thereby shattering it into intermediate mass fragments. In this model, the momentum distributions of the emitted fragments are determined by the intrinsic Fermi motion, the momenta of absorbed "hot spot nucleons", and the Coulomb repulsion between the outgoing fragments; the shapes of the energy spectra are definitely determined by non-thermal processes.

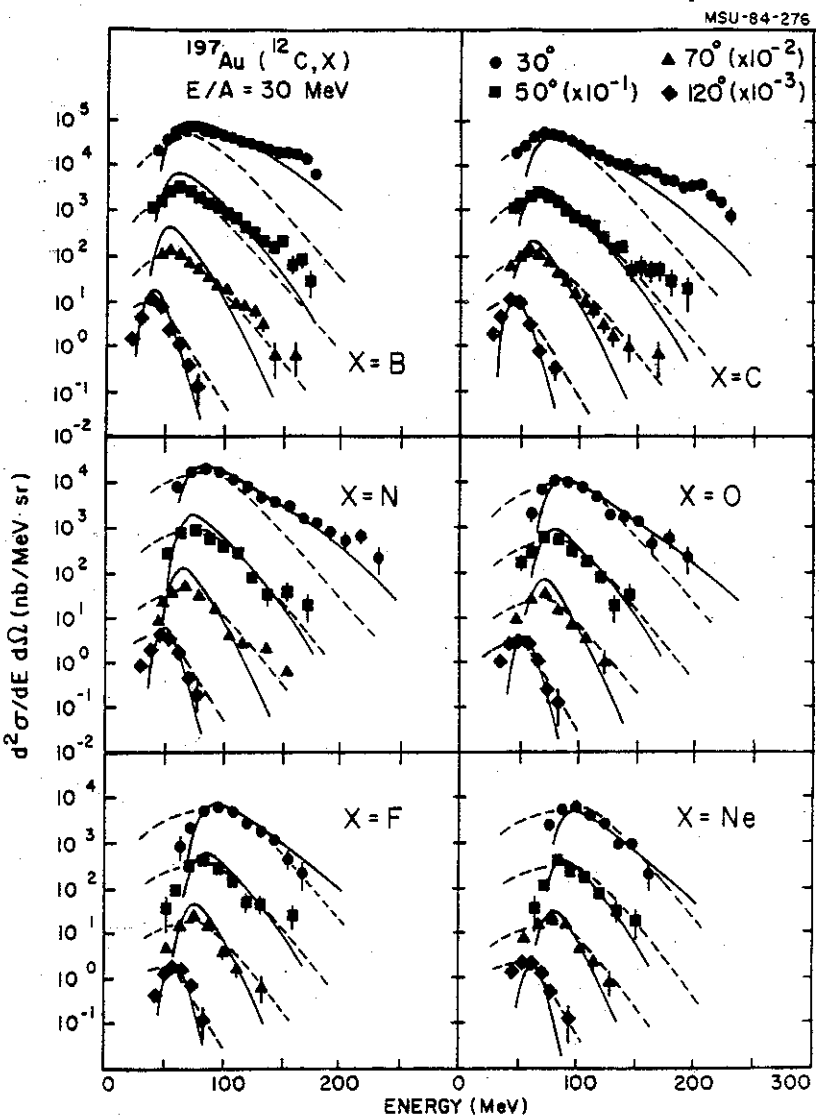

Fig. 1. Differential cross sections for the emission of B, C, N, O, F, and Ne nuclei in ^{12}C induced reactions on ^{197}Au at E/A=30 MeV. The spectra were measured at θ_{lab} = 30°, 50°, 70°, and 120°. The calculations are described in the text. (Ref. 4)

The differential cross sections calculated from the model are compared to data for the $^{12}C+^{197}Au$ reaction at E/A=30 MeV (see dashed curves in Figure 1). As an alternative model, we have assumed that the initial local excitation decays statistically by particle emission while equilibrating with the surrounding target spectator matter (see solid curves in Figure 1). In this model, the energy spectra are determined by the competition between precompound particle emission and equilibration of the remaining residual system. Again, the energy spectra have non-thermal contributions from Fermi-motion and Coulomb interactions. Moreover, this model implies that the energy spectra have varying contributions from different stages of the reaction; the slopes of the energy spectra cannot be associated with a single temperature. This latter effect is illustrated more clearly in Figure 2, in which calculated contributions from different stages of the reaction are depicted.[4]

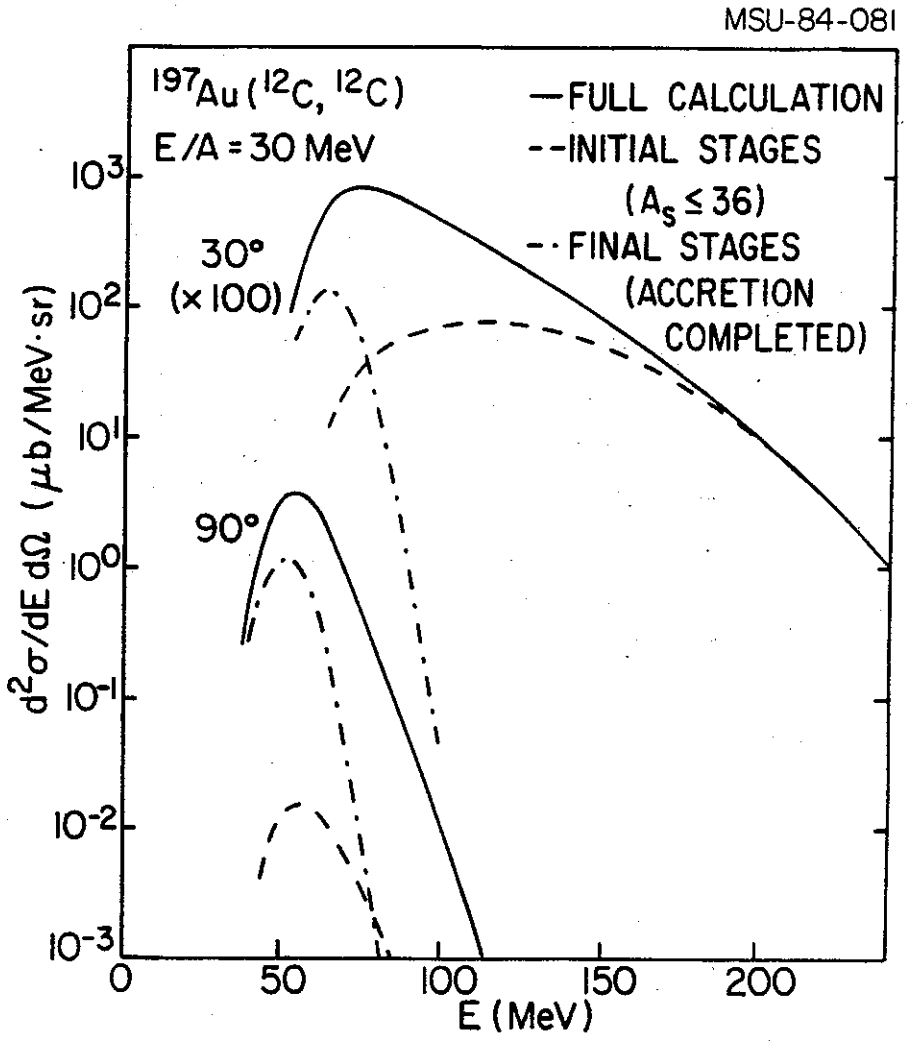

Fig. 2. Contributions to energy spectra from different stages of the reaction as calculated for the hypothetical emission from a hot spot which is in the process of equilibration with the surrounding target spectator matter. (Ref. 4)

The two models discussed above make conflicting assumptions concerning the mechanism leading to the emission of intermediate mass fragments. Yet, both can describe the qualitative trends of the data reasonably well. Clearly, more data are needed. As a first step, we plan to measure the energy dependence of intermediate mass fragment cross sections with the higher energies available at MSU. Dramatic differences of the elemental yields are, for example, predicted by models which assume that the production of complex nuclei contains key information about the liquid gas phase transition of nuclear matter. To resolve this issue, one must also assess the influence of secondary processes, such as sequential decay, upon the experimental observables. The importance of both secondary processes and reaction dynamics must be addressed by coincidence measurement similar to those discussed in later sections. In particular, we want to elucidate the extent to which thermalization is achieved during the various stages of the reaction. This information is essential to any statistical calculation.

a. Max-Planck Institut für Kernphysik, Heidelberg, W. Germany

References:

1. G.D. Westfall, Z.M. Koenig, B.V. Jacak, L.H. Harwood, G.M. Crawley, M.W. Curtin, C.K. Gelbke, B. Hasselquist, W.G. Lynch, A.D. Panagiotou, D.K. Scott, H. Stöcker and M.B. Tsang, Phys. Rev. C29,861(1984)
2. B.V. Jacak, G.D. Westfall, C.K. Gelbke, L.H. Harwood, W.G. Lynch, D.K. Scott, H. Stöcker, M.B. Tsang, and T.J.M. Symons, Phys. Rev. Lett. 51,1846(1983)
3. C.B. Chitwood, D.J. Fields, C.K. Gelbke, W.G. Lynch, A.D. Panagiotou, M.B. Tsang, H. Utsunomiya and W.A. Friedman, Phys. Lett. 131B,289(1983)
4. D.J. Fields, W.G. Lynch, C.B. Chitwood, C.K. Gelbke, M.B. Tsang, H. Utsunomiya and J. Aichelin, Phys. Rev. C30,1912(1984)
5. T.C. Awes, G. Poggi, S. Saini, C.K. Gelbke, R. Legrain, and G.D. Westfall, Phys. Lett. 103B.417(1981)
6. G.D. Westfall, B.V. Jacak, N. Anantaraman, M.W. Curtin, G.M. Crawley, C.K. Gelbke, B. Hasselquist, W.G. Lynch, D.K. Scott, M.B. Tsang, M.J. Murphy, T.J.M. Symons, R. Legrain, and T.J. Majors, Phys. Lett. 116B,118(1982)
7. W. Friedman and W.G. Lynch, Phys. Rev. C28,16,960(1983)
8. M.W. Curtin, H. Toki, and D.K. Scott, Phys. Lett. 123B,289(1983)

III.A.1.c. INCLUSIVE MEASUREMENTS OF INTERMEDIATE RAPIDITY FRAGMENTS.

G.D. Westfall, M.R. Maier and H. van der Plicht

The study of nuclear matter at high excitations and densities can yield information concerning the equation of state of nuclear matter. One way to study nuclear matter systematically in different states is to vary the excitation and density of the matter produced by simply varying the beam energy. Thus one may prepare nuclear matter in different excitations and study the properties of hot, dense nuclear matter.

Light Particle Inclusive Measurements:

A problem that must be solved if one is to address this type of physical phenomena with inclusive reactions is the separation of the participant particles from the spectator particles. We accomplished this separation by measuring spectra of light particles the energies of which were high compared to target evaporation energies and at angles which were large compared with those of projectile fragmentation. To simplify further the large amount of data we measured, as well as the vast amount of work extant in the literature, we chose a particular angular and energy range to select the participant particles as well as suppressing the unwanted target-like and projectile-like particles.[1,2] The moving source parameterization reduces a complete set of data for one type of emitted fragment, projectile nucleus, incident energy, and target nucleus to three parameters: the temperature τ, the production cross section σ_0, and the velocity of the emitting source β.

As an example of how inclusive spectra and the moving source fits pertains to these data, the energy spectra of light particles from 35 MeV/nucleon ^{12}C+Au reactions is shown[3] as a function of energy/nucleon in Fig. 1. The moving source fits are shown as solid lines. An example of light particle spectra from higher energies is shown in Fig. 2 in which 137 MeV/nucleon ^{40}Ar+Au leading to protons is shown along with moving source fits.[4] In Fig. 3 the results from applying the moving source

parameterzation to a wide spectrum of light particle data from ^{16}O- and ^{20}Ne-induced reactions on heavy targets (Au, Pb, and U) are shown as a function of energy per nucleon above the coulomb barrier.[3] This plot includes light particle inclusive measurements done at the NSCL at 25, 30, and 35 MeV/nucleon. The parameters vary smoothly with incident energy and the values from different particles are very similar suggesting that all the particles are emitted from a common source. However, the light particles do not tell the entire story; they can originate from peripheral as well as central collisions.

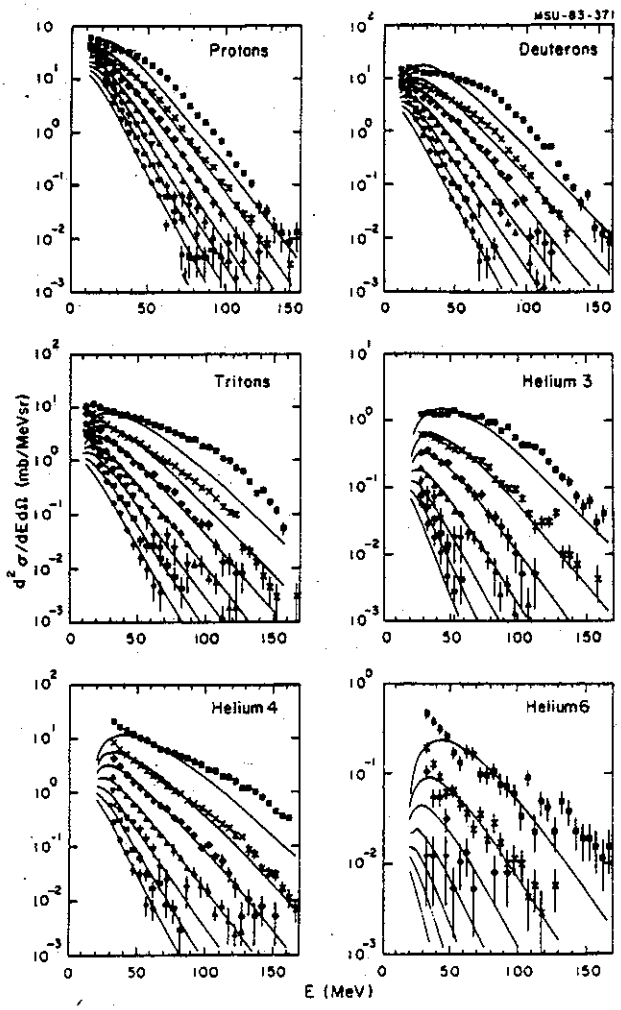

Figure 1.

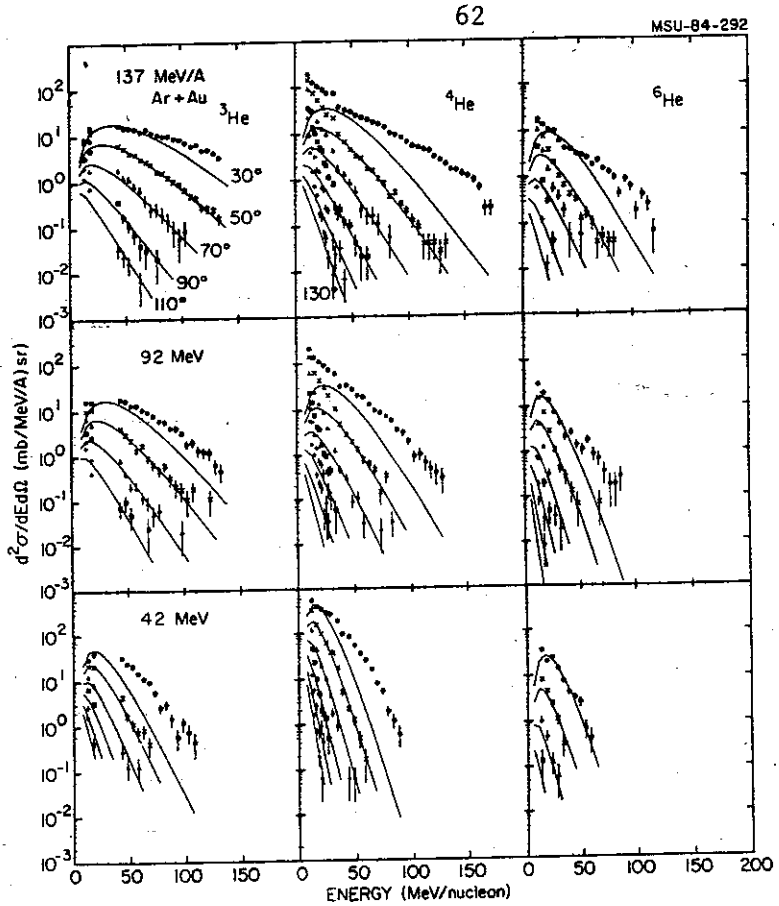

Figure 2.

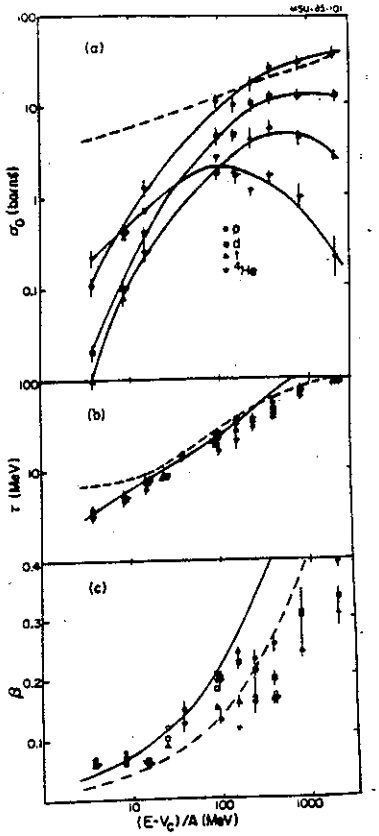

Figure 3.

Intermediate Rapidity Complex Fragments

The origins of light nuclei (complex fragments) observed at intermediate rapidities from high energy nucleus-nucleus collisions are not understood as well as emission of nucleons. The relative production cross sections and energy spectra of these fragments may carry signatures of various phenomena evolution of the reaction.[3-6] The production of light nuclei has been described in terms of the coalescence model,[7] chemical equilibrium models,[8-10] and intranuclear cascade calculations.[11,12] The most successful is the coalescence model, which has been applied to spectra from nucleus-nucleus collisions ranging in incident energy from 9 MeV/nucleon to 2 GeV/nucleon. This model has also been applied not only to light particles (d,t,^{3}He,^{4}He) but also to complex fragments ($6 \leq A \leq 14$) from intermediate energy nucleus-nucleus collisions.[13] Surprisingly, the simple scaling relation predicted by this model is found to hold for fragments up to A=14. The extracted coalescence radii are independent of the observed fragment and incident energy, and the interaction volumes deduced from the coalescence radii agree with recent particle-particle correlation studies.[14-15]

We intend to measure the cross sections for emission of complex fragments from high energy (400 and 800 MeV/nucleon) nucleus-nucleus collisions. This measurement is designed to determine whether the production cross sections for complex fragments at intermediate rapidities can provide information on the entropy produced in these reactions. The entropy produced when a high energy nucleus interacts with a target nucleus can be extracted by comparing the quantum predictions of a statistical model calculation to the production cross sections of emitted fragments. The entropy produced is predicted to increase with bombarding energy which implies that the relative production of complex fragments should decrease dramatically. Measurements carried out previously at 42, 92, and 137 MeV/nucleon give entropies that increase slightly with increasing bombarding energy, but the higher energies are necessary to determine conclusively if the concept of extracting state variables, such as entropy, from complex

fragment production is a useful one. These measurements will be carried out using the HISS spectrometer at the LBL Bevalac.

References:

1. G.D. Westfall, B.V. Jacak, N. Anantaraman, M.V. Curtin, G.M. Crawley, C.K. Gelbke, B. Hasselquist, W.G. Lynch, D.K. Scott, M.B. Tsang, M.J. Murphy, T.J.M. Symons, R. Legrain, and T.J. Majors, Phys. Lett. 116B,118(1982).
2. B.E. Hasselquist, G.M. Crawley, L.H. Harwood, B.V. Jacak, Z.M. Koenig, G.D. Westfall, J.E. Yurkon, R.S. Tickle, J.P. Dufour, and T.J.M. Symons, Phys. Rev. C 32,145(1985).
3. G.D. Westfall, Z.M. Koenig, B.V. Jacak, L.H. Harwood, G.M. Crawley, M.W. Curtin, C.K. Gelbke, B. Hasselquist, W.G. Lynch, A.D. Panagiotou, D.K. Scott, H. Stöcker, and M.B. Tsang, Phys. Rev. C 29,861(1984).
4. B.V. Jacak, G.D. Westfall, C.K. Gelbke, L.H. Harwood, W.G. Lynch, D.K. Scott, H. Stöcker, M.B. Tsang, and T.J.M. Symons, Phys. Rev. Lett. 51,1846(1983).
5. B.V. Jacak, H. Stöcker, and G.D. Westfall, Phys. Rev. C 29,1744(1984).
6. D.J. Morrissey, W. Benenson, E. Kashy, B. Sherrill, A.D. Panagiotou, R.A. Blue, R.M. Ronningen, J. van der Plicht, and H. Utsunomiya, Phys. Lett. 148B,432(1984).
7. H.H. Gutbrod, A. Sandoval, P.J. Johansen, A.M. Poskanzer, J. Gosset, W.G. Meyer, G.D. Westfall, and R. Stock, Phys. Rev. Lett. 37,667(1976).
8. J. Gosset, H.H. Gutbrod, W.G. Meyer, A.M. Poskanzer, A. Sandoval, R. Stock, and G.D. Westfall, Phys. Rev. C 16,629(1977).
9. M.-C. Lemaire, S. Nagamiya, S. Schnetzer, H. Steiner, and I. Tanihata, Phys. Lett. 85B,38(1979).
10. J. Gosset, J.I. Kapusta, and G.D. Westfall, Phys. Rev. C 18,844(1978).
11. V.D. Toneev and K.K. Gudima, Nucl. Phys. A400,173c(1983).
12. H. Kruse, B.V. Jacak, J.J. Molitoris, G.D. Westfall, and H. Stöcker, Phys. Rev. C. 31,1770(1985).
13. B.V. Jacak, D. Fox, and G.D. Westfall, Phys. Rev. C 31,704(1985).
14. D. Beavis, S.Y. Fung, W. Gorn, A. Huie, D. Keane, J.J. Lu, R.T. Poe, B.C. Shen, and G. VanDalen, Phys. Rev. C 27,910(1983).
15. H.A. Gustafsson, H.H. Gutbrod, B. Kolb, H. Löhner, B. Ludewigt, A.M. Poskanzer, T. Renner, H. Riedesel, H.G. Ritter, A. Warwick, F. Weik, and H. Wieman, Phys. Rev. Lett. 53,544(1984).

III.A.1.d. NEUTRONS FROM HIGH ENERGY NUCLEUS-NUCLEUS COLLISIONS

G.D. Westfall, D.J. Morrissey and A. Galonsky

The study of neutrons emitted from high energy nucleus-nucleus collisions can provide detailed information concerning the reaction mechanisms of these collisions. The main advantage of measuring neutron spectra rather than charged particle spectra is that the Coulomb interaction does not distort the emission pattern of the neutrons. This effect is most pronounced when very heavy projectile and target nuclei are used and when the neutron spectra are measured at rapidities very near the projectile and target rapidities.

Measurements of neutron spectra at zero degrees and wider angles have been carried out for several incident energies (200, 400, and 800 MeV/nucleon) and several projectile-target combinations (Ne+NaF,Pb; Nb+Nb; Au+Au).[1] The momentum spectra at zero degrees required more than one Gaussian to describe the entire spectrum. The measured double differential cross section in the rest frame of the projectile for 800 MeV/nucleon is shown in Fig. 1 as a function of the momentum of the neutron in that frame. The three Gaussians are shown separately as well as summed.

One of these three Guassians can be identified with the fermi momentum of the projectile. Another of the Gaussians was identified with central collisions. A very narrow Gaussian was required to fit the data at momenta near the beam velocity. This narrow component could be due to single nucleon-nucleon scattering or due to the decay of a nuclear resonance. The widths extracted for momenta near the beam velocities for the other systems studied was very similar.

We plan to extend these high energy measurements to energies available at NSCL. At incident energies between 30 and 100 MeV/nucleon one expects drastic changes because the interaction between a projectile nucleus and a target nucleus must change from dominantly a mean field interaction at low energies to single nucleon-nucleon scattering at high energies. By performing a systematic study of neutron spectra at zero degrees, one could gain insight into the fragmentation process at intermediate energies, especially since this narrow component is dominated by nucleon-nucleon scattering rather than excitation and decay.

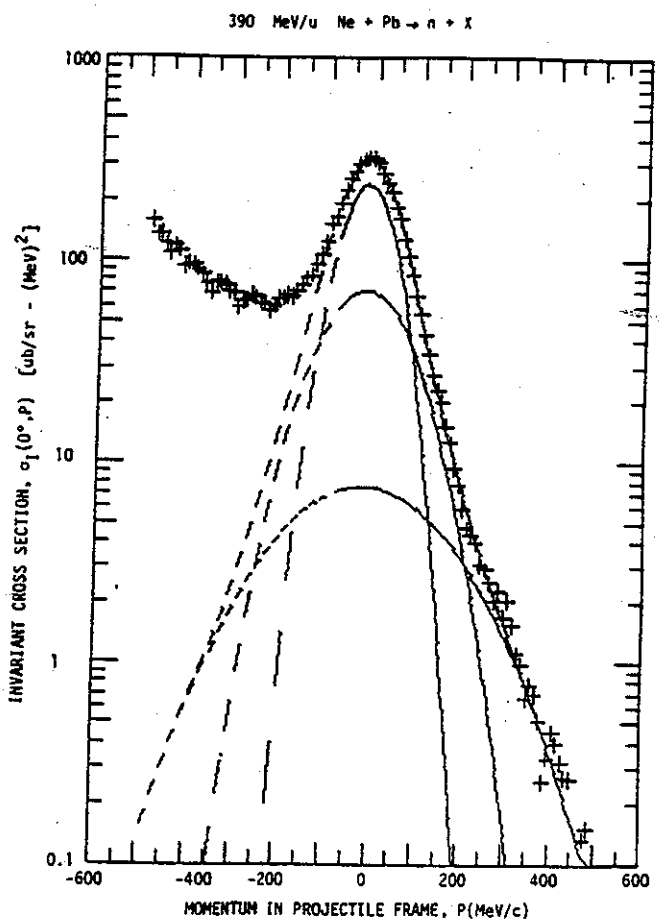

Figure 1.

These experiments would be carried out using the S320 spectrometer to measure the residual projectile nucleus in coincidence with the neutrons produced at zero degrees. By selecting the degree of centrality using the residual projectile fragment as an indicator, one can study the dependence of the zero degree peak on the impact parameter of the collision as well as in dependence on incident energy.

References:

1. R. Madey, J. Varga, A.R. Baldwin, B.D. Anderson, R.A. Cecil, G. Fai, P.C. Tandy, J.W. Watson, and G.D. Westfall, Phys. Rev. Lett. 55,1453(1985).

III.A.1.e. REACTION MECHANISMS OF HEAVY-ION COLLISIONS STUDIED VIA NEUTRON EMISSION

A. Galonsky, C.K. Gelbke, B.A. Remington[a], M.B. Tsang, F. Deak[b], A. Kiss[b], and Z. Seres[c]

When nuclei collide with a kinetic energy of several hundred MeV, a large part of that kinetic energy may be converted into short-lived excitation energy. Fast de-excitation is accomplished mainly through emission of nucleons and of light nuclei up to the alpha particle. Among these particles only neutrons follow paths that are free of Coulomb distortions as they leave the region of interaction. At least in principle, then, neutrons should carry a clean message of the early stages of the reaction. Indeed, the use of their special property in fragment-neutron coincidence experiments[1-5] has generated a great deal of information about reaction mechanisms. From neutron spectra measured in coincidence with light fragments, we can obtain information concerning the dynamic as well as the statistical aspects of heavy ion reactions at intermediate energies.

We have measured neutron spectra in coincidence with light fragments from the reactions of ^{14}N with Ho, Ni, and C at E/A = 35 MeV. One of the experimental set-ups, shown in Fig. 1, consisted of 10 neutron scintillation detectors around the outside of a thin-walled steel scattering chamber and six Si telescopes within the chamber. Each neutron detector had a thin, charged-particle anticoincidence scintillator in front of it. The shadow bars shown in the figure were in place part of the time for measurement of background--mostly neutrons scattered into the detectors by the floor. Ten percent is a typical value for the background. The detection efficiency is energy dependent, and again 10% is a typical value for this quantity.

When a neutron was in coincidence with a fragment, the neutron energy was determined from the time difference between the two particles plus the time of flight of the fragment. The latter time could easily be computed

from the telescope signals; they fixed the element and isotope and also the energy of the fragment.

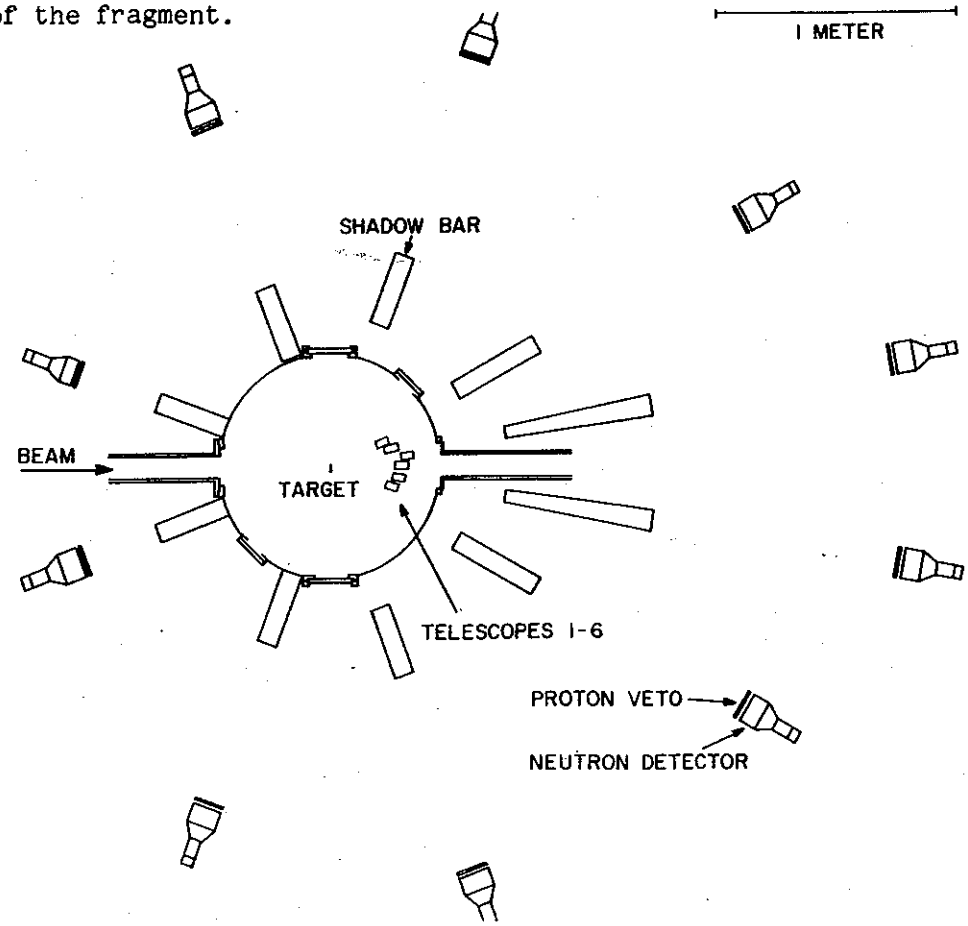

Fig. 1. Typical layout of the experiment .

Fragments were detected at six angles between 7° and 30°. The energy spectra of boron fragments from the reaction of ^{14}N with Ho are shown in Fig. 2. The character of the spectrum changes drastically from 7° and 10°, where a quasi-elastic peak dominates, to 30°, where there is only an exponential decrease. The spectra of other fragments--lithium, berylium, and carbon--have features similar to those of the boron spectra. In the extreme there are clearly two kinds of collisions, peripheral and central, and by choice of angle either one can be emphasized over the other.

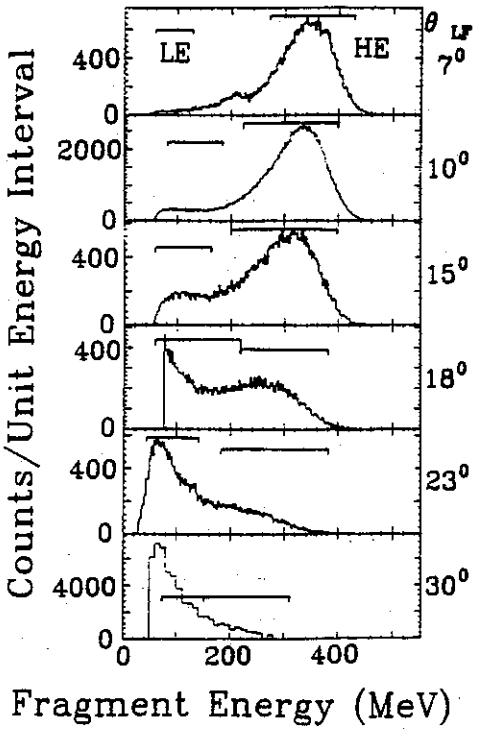

Fig. 2. Spectra of boron fragments from the Ho target at angles of 7° to 30°. The low-energy (LE) and high-energy (HE) gates used to produce coincident neutron spectra are indicated.

From a peripheral collision we might expect to see neutrons from a surface hot spot whose decay might then create a left-right asymmetry of the emitted neutrons. Figure 3 shows a neutron velocity scatter plot for coincident high energy boron fragments detected at 10°. The arrow in the figure indicates the average velocity vector of the boron fragments. There are more high velocity neutrons at middle angles (70° and 110°) on the side of the beam opposite that of the detected boron,[6] than on the same side. Since the boron fragments are close to the grazing angle, presumably undergoing positive-angle scattering, neutrons from a stationary surface hot spot would be shielded by the target and would produce the reverse asymmetry. What is required is a dynamic effect wherein the source acquires transverse momentum, perhaps balancing some of the transverse momentum of the boron fragment.

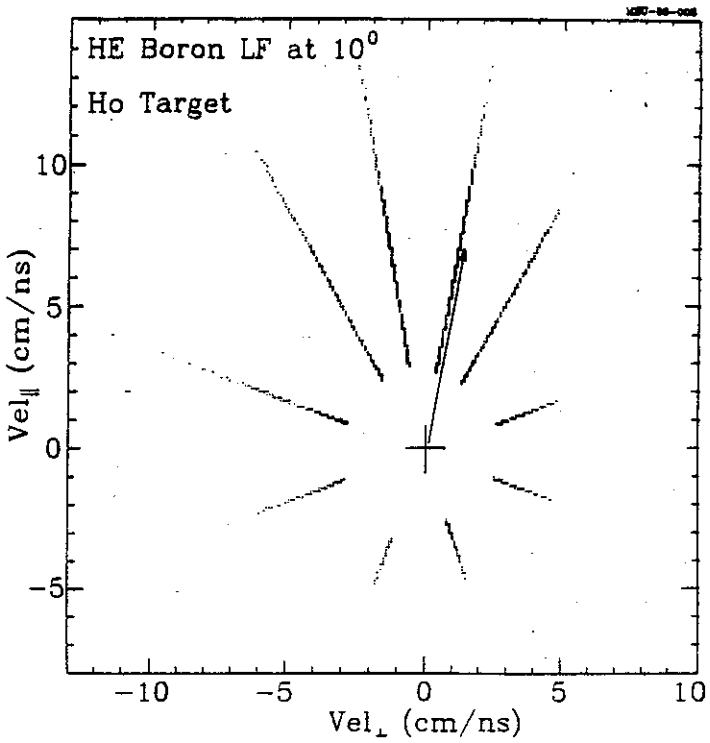

Fig. 3. Velocity scatter plot for neutrons detected at ±10°, ±30°, ±70°, ±110°, and ±160°. The neutrons are in coincidence with quasi-elastic boron fragments at +10°, that is, at 10° to the right.

Other aspects of the data may be seen in the neutron multiplicity spectra of Fig. 4 where the neutrons are in coincidence with lithium fragments of energies 14 to 28 MeV/u at 10°. The two topmost spectra are for ±10°; the lower ones are for successively larger angles. We focus on three features of the data. 1) At the lowest energies the cross section decreases at about the same rate for all angles; even the absolute values are constant to within a factor of two. 2) The high energy neutrons are very forward peaked. 3) The spectra at ±10° are approximately equal below 15 MeV and above 50 MeV, but between 15 and 50 MeV the +10° spectrum is much higher than the -10° spectrum. Spectra gated by other fragments (Be, B, or C) at 10°, whether of high energy or low energy, exhibit similar features. Enhancement of the neutron cross section at +10° arises from kinematic focusing of the neutrons emitted in sequential decay of the excited parent fragments, as discussed in Sec. A4(d).

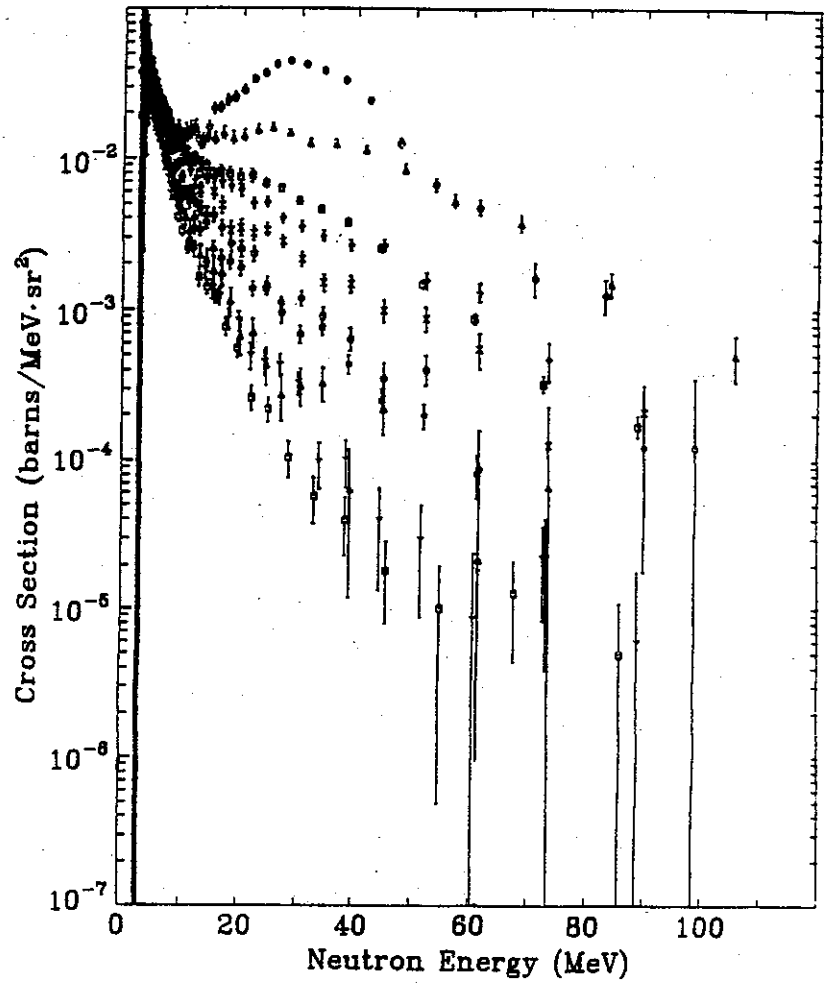

Fig. 4. Neutron energy spectra at angles ranging from 10° (+10° topmost) to 110°. The neutrons are gated by lithium fragments at +10° having E/A = 14-28 MeV.

In order to understand the origin of those neutrons not resulting from sequential decay of the light fragment, we have fitted the neutron spectra with two moving, thermal sources--a slowly-moving, target-like source (TLS) and an intermediate-rapidity source (IRS). Those spectra containing significant contributions from fragment sequential decay were not included in the fits. In general, the two-source model fits all the data except the contribution from excited fragments. The results for one case, boron emitted at 10° with energy 210-400 MeV, are shown as solid and dashed curves in Fig. 5.

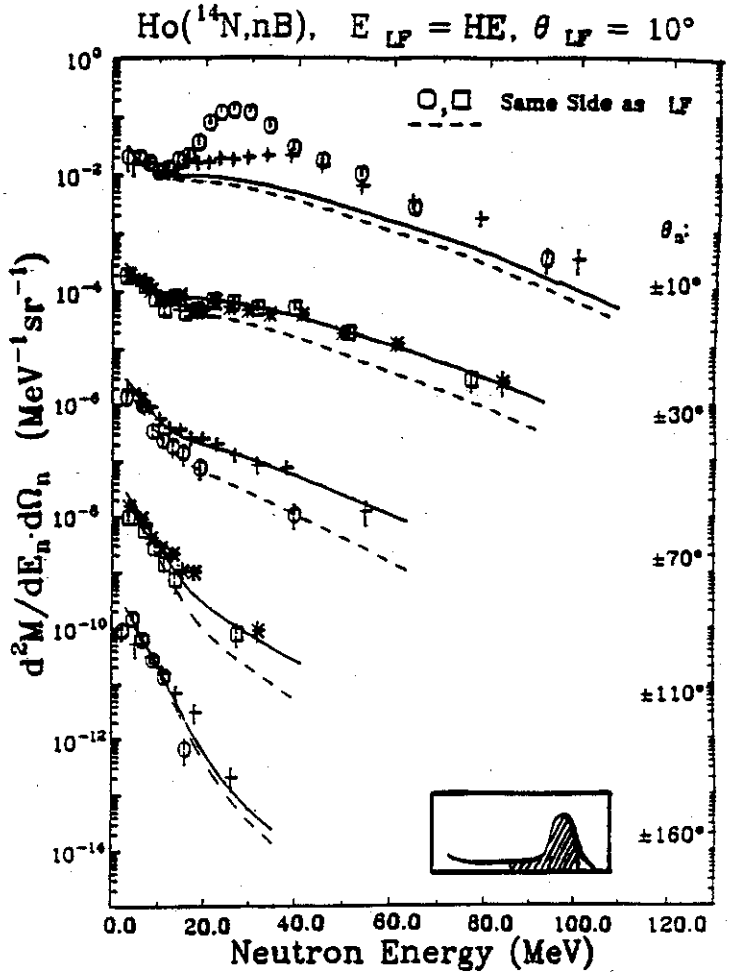

Fig. 5. Neutron energy spectra at in the indicated angles between 10° and 160°. The neutrons are gated by boron fragments at +10° having energy between 210 and 400 MeV. (See insert.) The vertical scale is correct for the spectrum at the top. For each subsequent spectrum below it the scale should be multiplied by 100. The curves are results of two-source fits to all the data except those at 30°, 10°, and -10°.

In the fitting procedure each source has four parameters to be determined--a strength, a temperature, a direction, and a speed. The TLS is responsible for the almost-isotropic, low-energy neutrons. The temperature is found to be independent of the angle and of the species of the coincident fragment and depends only slightly on the loss of kinetic energy and on the identity of the target nucleus. The temperature is 2-3 MeV when the target is Ho and about 3-4 MeV when the target is Ni.

Assuming a given mass for the source, the strength, or multiplicity, of a thermal source depends only on its temperature. We would therefore expect there to be no dependence of multiplicity upon fragment angle. When we look at the multiplicities, however, (Fig. 6) we see that they increase with angle. The reason is that we measure an "associated" multiplicity, a

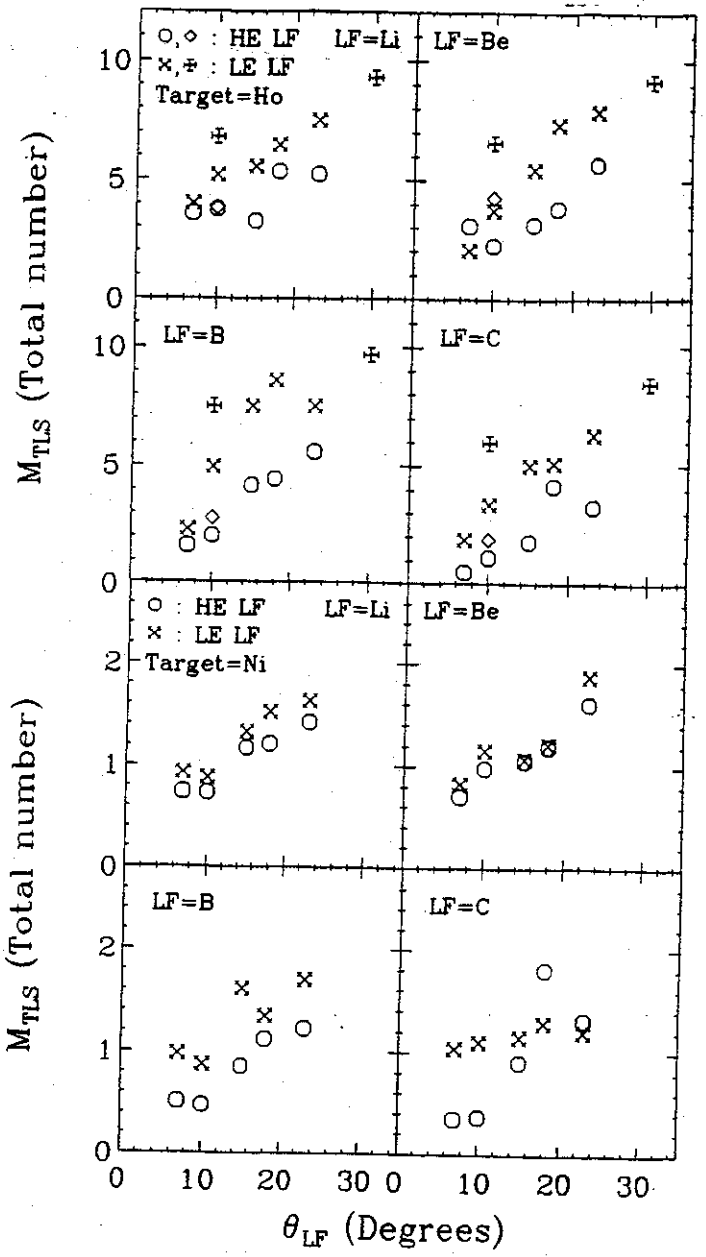

Fig. 6. Plot of M_{TLS}, total associated multiplicity, versus fragment angle for the Ho target (top four) and Ni target d(bottom four). Each quadrant represents a different fragment. The diamond and cross plotting symbols correspond to an independent set of data and analysis. Open symbols correspond to high-energy (HE) fragments and closed symbols to low-energy (LE) fragments. (Note the differences in scale between the Ho and the Ni values.)

multiplicity per detected fragment. The true multiplicity of the source is higher. This point has not always been appreciated,[5] but Fig. 6 makes it clear. Particularly at small angles there are processes, such as projectile fragmentation, that produce a fragment without a neutron-emitting TLS partner. Will the curves level off at some fragment angle and give us the true multiplicity? Only future experiments will tell, and we plan to do those experiments. In the meantime we have resorted to calculation, using the compound-nucleus code CASCADE,[7] to estimate neutron multiplicity. The results, 12 for Ho and 2.3 for Ni, are consistent with our observations in that they are greater than our associated multiplicities, but we must note that we have used CASCADE at a much higher excitation energy (up to 195 MeV) than it has been tested at.

The other source, the IRS, moves very rapidly (at about half the projectile velocity) and its temperature is higher than the temperature of the TLS. The combination of high velocity and high temperature enables it to produce the forward-peaked, high-energy neutrons. A similar fast, hot source has been used rather successfully to fit the high-energy portions of inclusive charged particle spectra.[8] With a LE gate on the coincident fragment this source moves at 0°, but with a HE gate the IRS balances the transverse momentum of the quasi-elastic fragment by moving to the side opposite the fragment, thus producing the observed neutron asymmetry. [An enhancement at negative angles was also found in the emission of light charged particles (p,d,t,α). And calculations based on the Boltzmann-Uehling-Uhlenbeck equations[9] do produce an asymmetry of the correct sign. For more details see Sec. A4(c).]

The values of temperature and velocity, (actually E/A, which is proportional to the velocity-squared) derived from fitting the gated neutron spectra, are given in Figs. 7 and 8, respectively. It is a striking feature of these plots that no clear, systematic trends are observed for either the temperature or the velocity of the IRS as a function of the species, the energy, or the angle of the coincident fragment. It is as if the properties of the IRS--at least when it emits neutrons--were independent of how or when the fragment was produced. Perhaps the IRS emits neutrons at a very early stage of the interaction, before the final "fate" of the projectile has been determined. In peripheral collisions the projectile may break up downstream from the target nucleus,[10] hence decoupling the detected fragment from those

emitted early in the collision. In more central collisions perhaps the fragment itself is emitted from the IRS, but at a later time, after it has cooled and grown from the accretion of target nucleons.[11] Then once again the source of the fragment would have no memory of the early neutron emission.

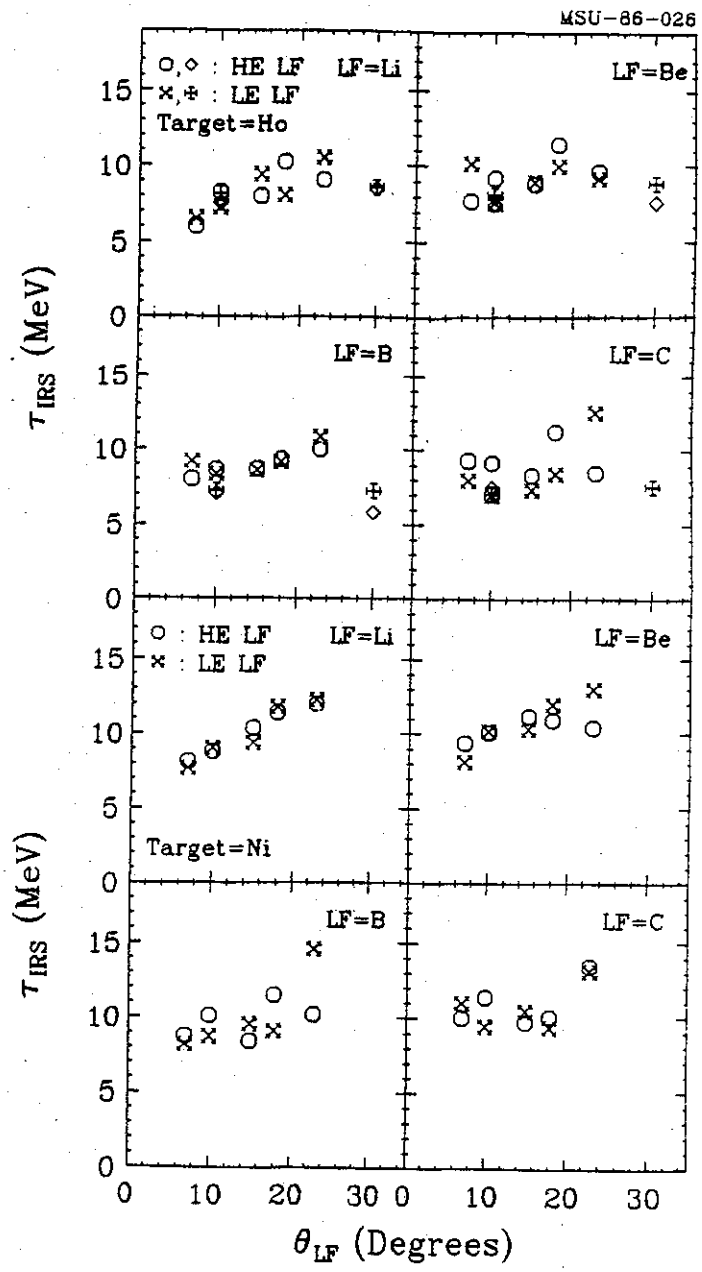

Fig. 7. IRS temperature parameter, τ_{IRS}, versus fragment angle. Symbols and format are the same as for Fig. 6.

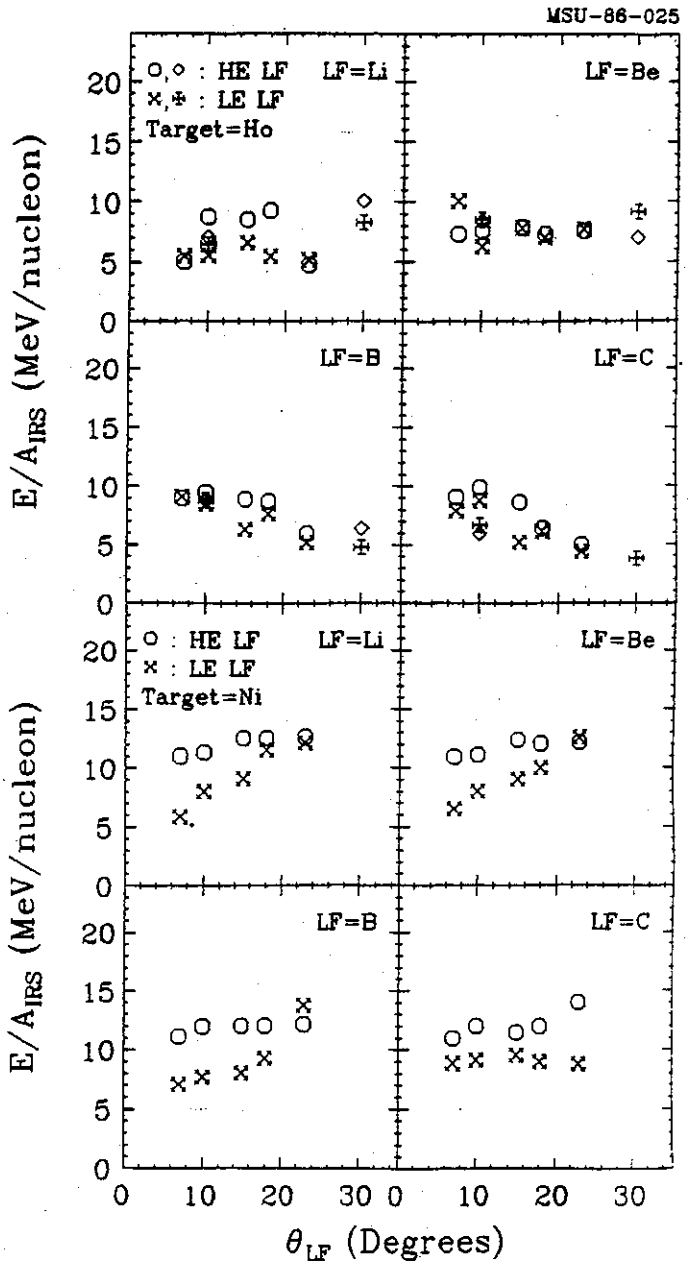

Fig. 8. IRS energy/nucleon, E/A_{IRS}, versus fragment angle. Symbols and format are the same as for Fig. 6.

Although the IRS is hotter than the TLS, its associated multiplicity is lower. The IRS emits only 1-2 neutrons per coincident fragment compared with 5-10 (Fig. 6) from the TLS. This must mean that the IRS is much smaller. In fact, since our fitting gave us the magnitude and direction of the IRS velocity, we determined its mass from momentum balance against the fragment in the peripheral collisions, with the result $A_{IRS} \leq 10\text{-}15$.

The insights we have obtained so far need to be explored in a broader arena. In connection with Fig. 6 we have already indicated that the

coincident light fragment will be observed at larger angles, at angles fed primarily by central collisions. If the "lantern" proposed in Sec. A1(e) is built, we can also study the neutron emission mechanisms in central collisions by triggering on fission fragments. Most important is the need to pursue similar studies with projectiles of greater mass and of higher energy in order to provide a global picture of the dynamical and statistical aspects of nucleus-nucleus reactions at intermediate energies. With ECR injection into the K500 Cyclotron followed by operation of the K800 Cyclotron, there will be a step-wise match between the goals of our neutron program and the development of beams at the NSCL. For use of the K800 beams we have already planned[12] to relocate our measurement area to a thin floor above the S800 pit.

Heavier projectiles should soon become available with ECR injection. With argon projectiles on target nuclei not too much heavier, (e.g. nickel) it should be possible to detect a target-like fragment in addition to the neutron and light (projectile-like) fragment that we have detected so far. The additional constraint on the kinematics should put to a stringent test the two-source model and any other model of the reaction.

Finally, we hope to measure singles, i.e., neutron inclusive spectra. Normally, inclusive measurements are simpler and are done before coincidence measurements. With neutrons such data are obtained by timing the neutron against the cyclotron rf. The energy resolution is limited by the time length of the beam bursts out of the cyclotron. Burst length in the old MSU proton cyclotron was less than 0.5ns, and we used it to do some interesting experiments utilizing the time-of-flight technique. In the K500 Cyclotron the burst length is more that 5ns, resulting in very poor energy resolution. However, the Ph.D. thesis project of Bruce Milton is to install internal phase slits in the K500. Particularly because inclusive measurements can be done with a low beam intensity, we expect that these phase slits will make this work possible. (Bunching of the ECR beam before injection is another possible way to produce sharp bursts.) We will choose cases representative of the reaction types--fission, strongly damped, and fragmentation--and carefully compare them with inclusive proton spectra. Each comparison between protons and neutrons should be made for the same reactants at the same bombarding energy. An early attempt[13] to do this for a fission reaction had an inconclusive result.

a Present address Rose-Hulman Institute of Technology
b Eötvös University, Budapest, Hungary
c Central Research Laboratory, Budapest, Hungary

References:

1. D. Hilscher, J.R. Birkeland, A.D. Hoover, W.U. Schroeder, W.W. Wilcke, J.R. Huizenga, A.C. Mignerey, K.L. Wolf, H.F. Breuer, and V.E. Viola, Phys. Rev. C 20,576(1979).
2. Y. Eyal, A. Gavron, I. Tserruya, Z. Fraenkel, Y. Eisen, S. Wald, R. Bass, C.R. Gould, G. Kreyling, R. Renfordt, K. Stelzer, R. Zitzman, A. Gobbi, U. Lynen, H. Stelzer, I. Rode, and R. Bock, Phys. Rev. C 21,1377(1980).
3. E. Holub, D. Hilscher, G. Ingold, U. Jahnke, H. Orf and H. Rossner, Phys. Rev. C 28,252(1983).
4. A. Gavron, J.R. Beene, R.L. Ferguson, F.E. Obenshain, F. Plasil, G.R. Young, G.A. Petitt, K. Geoffroy Young, M. Jääskelainen, D.G. Sarantites, and C.F. Maguire, Phys. Rev. C 24,2048(1981).
5. I. Tserruya, A. Breskin, R. Chechik, A. Fraenkel, s. Wald, N. Zwang, r. Bock, M. Dakowski, A. Gobbi, H. Sann, r. Bass, G. Kreyling, r. Renfordt, K. Stelzer and U. Arlt, Phys. Rev. C 26,2509(1982).
6. G. Caskey, A. Galonsky, B.A. Remington, M.B. Tsang, C.K. Gelbke, A. Kiss, F. Deak, Z. Seres, J.J. Kolata, J. Hinnefeld, and J. Kasagi, Phys. Rev. C 31,1597(1985).
7. F. Pühlhofer, Nucl. Phys. A280,267(1977).
8. B.V. Jacak, G.D. Westfall, C.K. Gelbke, L.H. Harwood, W.G. Lynch, D.K. Scott, H. Stöcker, M.B. Tsang and T.J.M. Symons. Phys. Rev. Lett. 51, 1846(1983).
9. J. Aichelin and G.F. Bertsch, Phys. Rev. C 31,1730(1985).
10. M.J. Murphy, S. Gil, M. Harakeh, A. Ray, A. Seamster, R. Vandenbosch, and T. Awes, Phys. Rev. Lett. 53,1543(1984).
11. D.J. Fields, W.F. Lynch C.B. Chitwood, C.K. Gelbke, M.b. Tsang, H. Utsunomiya and J. Aichelin, Phys. Rev. C 30,1912(1984).
12. NSCL Newsletter, March 1985, p.11.
13. J. Kasagi, S. Saini, T.C. Awes, A. Galonsky, C.K. Gelbke, G. Poggi, D.K. Scott, K.L. Wolf, and R.L. Legrain, Phys. Lett. 104B,434(1981).

III.A.1.f. FUSION AND FISSION REACTIONS

C.K. Gelbke, W.G. Lynch, M.B. Tsang,
B.B. Back,[a] K. Kwiatowski[b] and V.E. Viola[b]

Quasi-Fission Reactions: The concept of compound nucleus formation and decay becomes meaningless for angular momenta equal to or exceeding the value $\ell_{ZBf=0}$, for which the fission barrier vanishes. However, the cross sections for fusion-fission-like reactions may considerably exceed the sharp-cutoff limit for compound nucleus formation, $\sigma_{CN}^{max}=\pi k^{-2}\ell_{Bf=0}^2$, as calculated from the rotating liquid drop model. It was, therefore, suggested that a new "fast fission" or quasi-fission reaction mechanism occurred at angular momenta greater than or equal to $\ell_{Bf=0}$. In order to study the fission properties of composite systems at very high angular momenta and to search for experimental signatures of quasi-fission processes, we performed systematic investigations[1-3] of the energy dependence of fission fragment angular distributions for heavy-ion induced fusion-fission reactions. As an example, Figure 1 shows angular distributions measured[2] for reactions induced by ^{19}F, ^{24}Mg, and ^{28}Si on ^{208}Pb. Detailed analyses of these and other angular distributions[1-3] in terms of the standard transition state theory for fission revealed discrepancies with the saddle point shapes calculated from the rotating liquid drop model. These discrepancies become more pronounced with increasing projectile mass; they are, most likely, caused by the occurrence of quasi-fission reactions which proceed via the conditional saddle point.[3]

Linear momentum transfer in fusion-like reactions: As the relative energy of nucleus-nucleus collisions increases from the Coulomb barrier to beyond the Fermi energy, the influence of the dinuclear mean field on the reaction dynamics is expected to be modified by the effects of individual nucleon-nucleon collisions. The understanding of this transition energy region requires systematic experimental studies of global reaction properties as a function of bombarding energy. These, in turn, should provide valuable guidance for the future development of microscopic theories which consider both mean-field and nucleon-nucleon scattering aspects of the reaction. One

such global observation is the linear momentum transfer in fusion-like reactions.

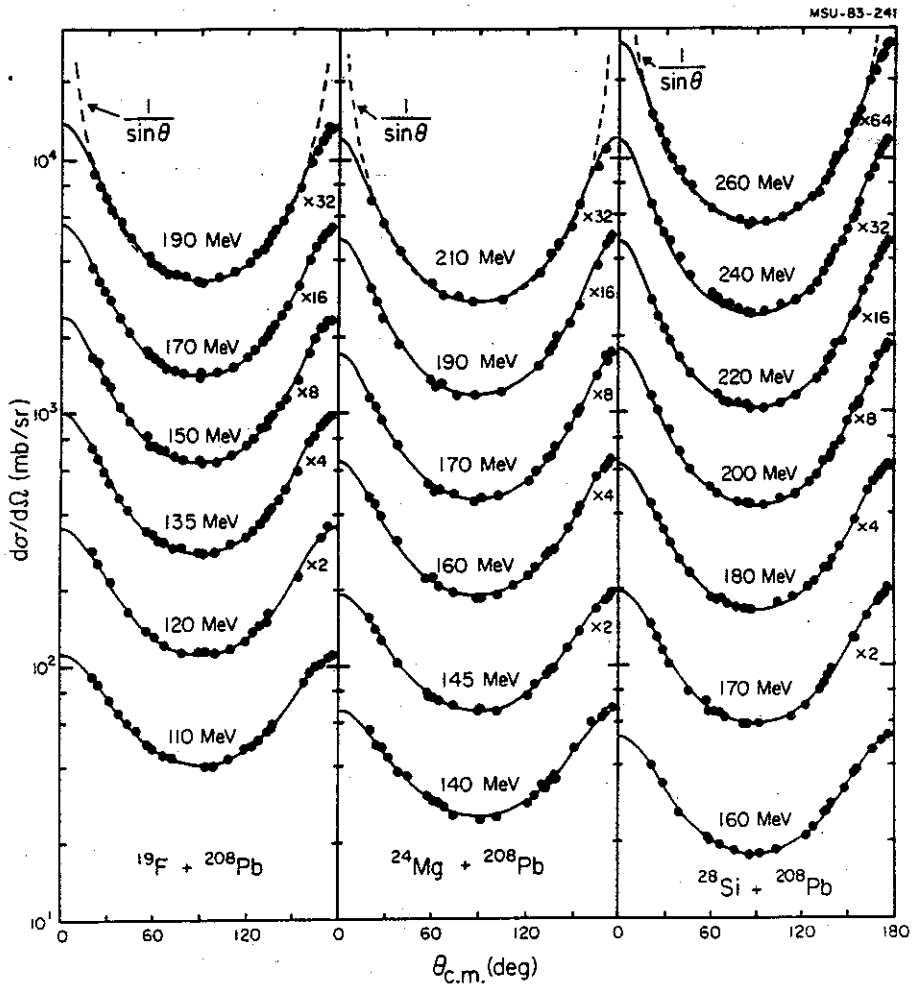

Fig. 1. Fission fragment angular distributions measured for ^{19}F, ^{24}Mg, and ^{28}Si induced reactions on ^{208}Pb. The solid curves are the results of global fits in terms of the transition state model. (Ref. 2)

Complete fusion of projectile and target nuclei implies, by definition, complete linear momentum transfer from the projectile to the composite nucleus. As the projectile energy is increased, the probability for complete fusion decreases markedly due to a rapid growth of fusion-like processes involving incomplete linear momentum transfer to the fusion-like residue and particle emission prior to the attainment of full statistical equilibrium of the composite system. We have investigated the energy dependence of incomplete fusion reactions by measuring the recoil velocities of fusion-like residues for reactions induced on lighter target nuclei[4] (in

collaboration with ANL) and by measuring the folding angles between coincident fission fragments for reactions induced on heavy target nuclei.[5,6] As an example, Figure 2 shows the evolution of fission-fragment folding angle distributions[6] for ^{14}N induced reactions on ^{238}U over a large range of incident energies. The increasing importance of incomplete fusion reactions with increasing beam energy is clearly evident.

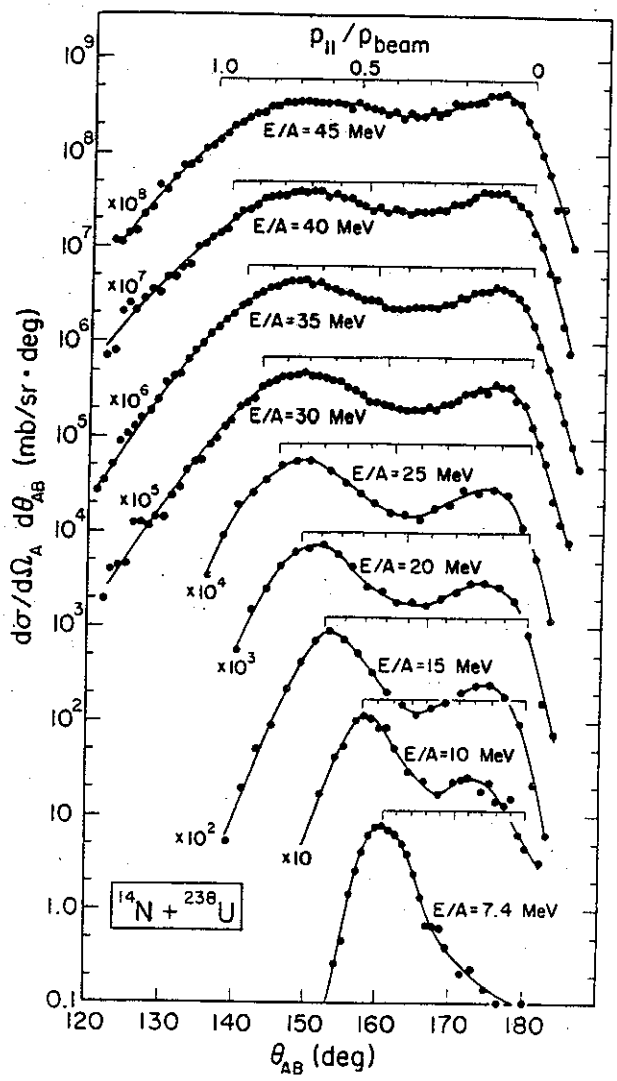

Fig. 2. Fission fragment folding angle distributions for ^{14}N induced reactions on ^{238}U. At each incident energy, a linear momentum transfer scale, $P_{\parallel}/P_{beam}$, is shown immediately above the data. (Ref. 6)

Figure 3 shows several quantities which can be extracted from the folding angle distributions: the most probable linear momentum transfer per projectile nucleon for the fusion-like component (Part a), the average value of the linear momentum transfer per projectile nucleon for the entire

distribution (Part b), and an upper limit for the ratio σ_{CF}/σ_R, where σ_{CF} and σ_R denote the complete fusion and total reaction cross sections, respectively (part c). (One should stress that this is a very conservative estimate of the upper limit for σ_{CF}/σ_R; the contributions from complete fusion are probably significantly smaller. Our measurements do not establish the occurrence of complete fusion at the higher bombarding energies where the very concept of complete fusion may be poorly defined.) As the relative velocity above the Coulomb barrier is increased, the linear momentum transfer per projectile nucleon decreases and is nearly independent of projectile.[5,6]

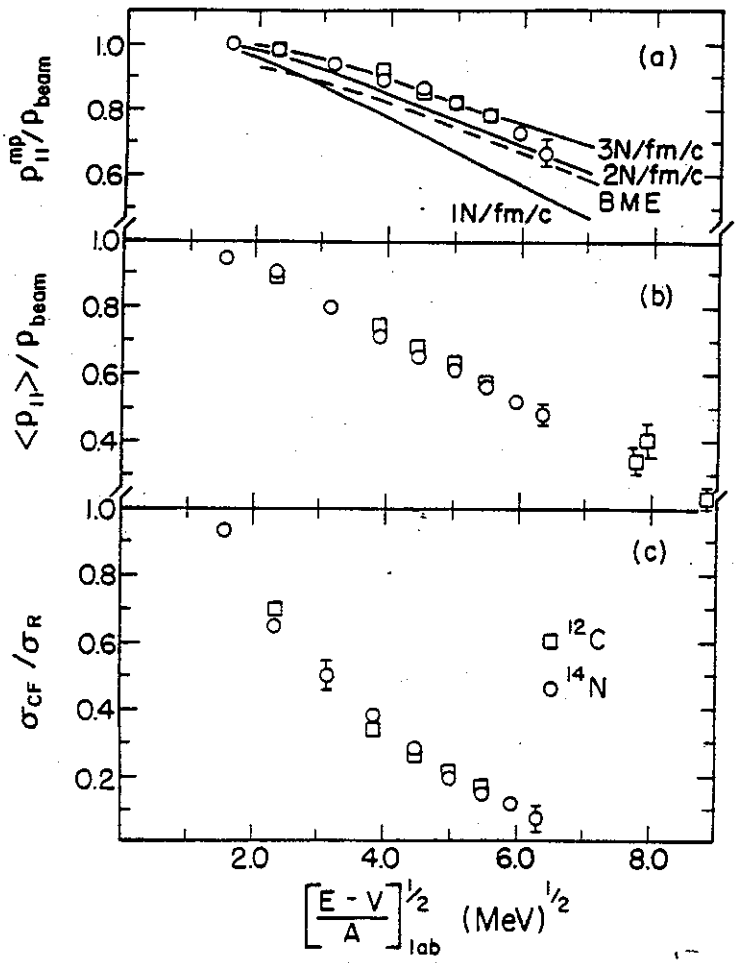

Fig. 3. Quantities extracted from the folding angle distributions shown in Figure 2. (a): Most probable linear momentum transfer per projectile nucleon for the fusion-like component. (b): Average linear momentum transfer per projectile nucleon for the entire distribution. (c): An estimate of the upper limit for the ratio σ_{CF}/σ_R, where σ_{CF} and σ_R denote the complete fusion and total reaction cross sections, respectively. (Ref. 6)

Incomplete momentum transfer for fusion-like reactions must be associated with processes which account for the missing momentum, such as precompound particle emission or absorptive breakup of the projectile. In order to illustrate the connection between precompound particle emission and incomplete linear momentum transfer, the solid and dashed lines in Figure 3a show the results from two model calculations which estimate the average linear momentum transfer carried away by precompound particle emission in central collisions. The dashed line shows the result obtained with a Boltzmann master-equation approach which includes emission of hydrogen and helium isotopes. The solid lines show the results of calculations which assume emission of particles from a localized region of excitation which is in the process of equilibration with the remainder of the composite system; three different rates of equilibration with the surrounding spectator matter are assumed. Future comparisons with more microscopic models which include more rigorously the effects of the mean field, nucleon-nucleon collisions and Pauli-blocking will be of considerable interest.

During the next three years, we intend to perform measurements of fission fragment folding angle distributions at higher energies and for heavier projectiles to complete our systematics of linear momentum transfer and to establish the range of energies for which fission fragment folding angle distributions can discriminate between peripheral and central collisions. As a future technical development, we plan to construct a high efficiency parallel plate fission detector similar to the "lantern" used by the GSI group. This detector would serve primarily as a central collision trigger in multiparticle correlation experiments. Finally we will measure fission folding angle distributions in coincidence with light particles detected with the MSU 4π detector in order to establish the correspondence between the light particle observables and the linear momentum transfer.

a. Argonne National Laboratory

b. Indiana University Cyclotron Facility.

References:

1. M.B. Tsang, D. Ardouin, C.K. Gelbke, W.G. Lynch, Z.R. Xu, B.B. Back, R. Betts, S. Saini, P.A. Baisden and M.A. McMahan, Phys. Rev. C 28,747(1983)
2. M.B. Tsang, H. Utsunomiya, C.K. Gelbke, W.G. Lynch, B.B. Back, S. Saini, P.A. Baisden and M.A. McMahan, Phys. Lett. 129B,18(1983)

3. B.B. Back, R.R. Betts, J.E. Gindler, B.D. Wilkins, S. Saini, M.B. Tsang, C.K. Gelbke, W.G. Lynch, M.A. McMahan, and P.A. Baisden, Phys. Rev. C 32,195(1985)
4. G.S.F. Stephans, D.G. Kovar, R.V.F. Janssens, G. Rosner, H. Ikezoe, B. Wilkins, D. Henderson, K.T. Lesko, J.J. Kolata, C.K. Gelbke, B.V. Jacak, Z.M. Koenig, G.D. Westfall, A. Szanto de Toledo, E.M. Szanto, and P.L. Gonthier, Phys. Lett. 161B,60(1985)
5) M.B. Tsang, D.R. Klesch, C.B. Chitwood, D.J. Fields, C.K. Gelbke, W.G. Lynch, H. Utsunomiya, K. Kwiatkowski, V.E. Viola, Jr. and M. Fatyga,Phys. Lett. 134B,169(1984)
6. M. Fatyga, K. Kwiatkowski, V.E. Viola, C.B. Chitwood, D.J. Fields, C.K. Gelbke, W.G. Lynch, J. Pochodzalla, M.B. Tsang, and M. Blann, Phys. Rev. Lett. 55,1376(1985)

III.A.1.g. SOURCE SHAPE PROBING BY BEAM-VELOCITY PIONS

Wm. C. McHarris
in collaboration with the Rasmussen/Crowe Group
Lawrence Berkeley Laboratory

In anticipation of high energy, heavy ion beams from the K800 cyclotron at NSCL, experiments are being carried out at other laboratories. This section describes some work being carried out at Lawrence Berkeley Laboratory. In addition to the π^+ experiments described here, we plan π^- experiments and a search for the possible existence of negatively-charged "pineuts," one or more π^- hadronically bound to neutrons.[1] A more complete discussion of the use of π^+s near beam velocity to probe transient nuclear shapes is given in a paper[2] to be published during the coming year.

We propose to use the Bevalac Beam-30 Janus spectrometer to measure simultaneously the one and two particle inclusive π^+ spectra near beam velocity for ^{139}La beams on La and on C targets. Our aim is to probe simultaneously the asphericity of the pion-source charge distribution by the one particle inclusive π^+ spectrum and the asphericity of the pion-source distribution by the Hanbury-Brown-Twiss correlation for two positive pions. The symmetric and extremely asymmetric beam-plus-target systems allow the large Coulomb-field corrections to be handled. The possibility of fleeting toroidal[3] or bubble nuclear systems can be probed on a very short time scale by the shape of the π^+ depression near beam velocity.

There have been a number of theoretical treatments[4] of the Coulomb effects on heavy-ion produced pion spectra, but they have been based generally on two or more charge distributions. Zajc,[5] when working with our group, concluded that the two-pion correlation was not seriously affected by the Coulomb fields of the nuclear pieces, provided the pion spectra were taken in a relatively small solid angle near 90° in the center-of-mass frame of a symmetric target-projectile system. The Coulomb shifts for each of the two pions may be considerable, but the velocity differences as the pions leave the nuclear surface map without much change into the velocity differences in the asymptotic final state. For data gathered over large solid angles, as in streamer-chamber work, and especially for pion momenta taken near 0°, the Coulomb changes in mapping pion momentum differences from

initial to final states may be large, not withstanding the symmetry of the system. Further, the corrections will depend on impact parameter, essentially an unmeasurable quantity.

Thus, we believe that the large Coulomb corrections to the two-pion correlation function can be handled best for heavy nuclei by studying very mass-asymmetric collision systems. Here the Coulomb corrections will be dominated by a single charge center, nearly independent of impact parameter. The ^{139}La + C seems ideally suited for our first studies, both for the above reasons and because its single-pion spectra have already been studied by the Hashimoto collaboration[6] with the HISS spectrometer, albeit at 800 A·MeV, which is lower than the maximum energy (for La^{48+}) of 1430 A·MeV at which we propose to run. We propose to set the trigger to accept all two-pion events and as large a fraction of one-pion events as the VAX-11/750 Q-system data acquisition allows.

There are a number of open questions[7] concerning Coulomb corrections to two-pion correlation studies. First of all, there are two separate Coulomb effects to be considered. One is the mutual repulsion of the two like-charged pions. This is referred to as the Gamow correction and is easily handled. The second is the interaction of the bulk charge distribution of the colliding heavy-ion system with the pions. The momentum difference of the two pions, as measured in the laboratory, needs to be mapped back into the momentum difference the pions had when leaving the strong-interaction region.

Some of us have worried that pion data near beam velocity would have serious Coulomb distortions due to projectile spectator charge. The corrections would depend on impact parameter and thus would be hard to make. The strong beam-velocity π^- peak studied by Sullivan and co-workers[8] via inclusive heavy-ion reactions should confirm this concern. The large-solid-angle streamer-chamber experiments have not been corrected for Coulomb distortions, and members of the group[6] have expressed belief that the beam-velocity π^- peak exists over such a small solid angle that the two-pion correlation will not be affected.[9]

We also plan to study the symmetric system, ^{139}La + La. This is a continuation of our studies of the mass dependence of the pion source parameters. The ^{139}La + La system has also been studied by the Hashimoto

collaboration at HISS.[6] Our proposed π^+ experiments are needed to complete and complement these others.

The JANUS dipole-dipole spectrometer, coupled to a VAX-11/750 Q-data-acquisition system, will be used to carry out the measurements. This spectrometer provides excellent spatial and momentum resolution (error in target trace-back ≈1 cm, $\Delta P/P < 2\%$) for pions having momenta greater than 150MeV/c; measurements centered at a laboratory pion angle nearr 0° have $\Delta\Omega \approx 1$ msr. Based on previous experiments, we expect that 120 hours of $3X10^6$ particles per pulse of ^{139}La with 1 gm/cm^2 targets would allow the acquisition of roughly 50,000 events for each of the two targets proposed. This would allow for a reasonable determination of the pion source parameters for these systems.

References:

1. Wm. C. McHarris and J.O. Rasmussen, Phys. Lett. 120B,49(1983).
2. J.O. Rasmussen, Wm. C. McHarris, and C.-Y. Wong, "Nuclear Shape Effects on Heavy-Ion π^- Spectra near Beam Velocity," to be submitted to Phys. Rev. C.
3. C.-Y. Wong, ORNL, preprint (1985).
4. S.E. Koonin, Phys. Lett. 70B,43(1977); M. Gyulassy, S.K. Kauffmann, and L.W. Wilson, Phys. Rev. C 20,2267(1979).
5. W. A. Zajc, Ph.D. Thesis, LBL-14864 (1982); W. A. Zajc et al., Phys. Rev. C 29,2173(1984).
6. Y. Miake et al., LBL Nuclear Science Division Annual Report, 1983-1984, LBL-18635, p. 101 (1985).
7. M. Gylassy and S. K. Kauffman, Nucl. Phys. A362,503(1981).
8. J. P. Sullivan, Ph.D. Thesis, LBL-12546 (1981); J. P. Sulivan et al., Phys. Rev. C 25,1499(1982).
9. T. J.Humanic, LBL-19420 (1985).

III.A.2.a. ROLE OF TWO BODY REACTIONS AT 20 MeV/A

D.J. Morrissey, R.A. Blue, L.H. Harwood and R.M. Ronningen

Experimental investigation of the binary nature of a nuclear reaction requires either a complete measurement of all products or at least a technique that identifies the mass and charge of both reaction partners. The combination of a mass-asymmetric reaction system in which the light fragment is identified in a conventional telescope consisting of Si surface barrier detectors, with high resolution γ-ray spectroscopy identifying the target-like fragments, adequately fulfills the requirements. We have begun a series of coincidence experiments at the NSCL and have completed measurements of the target-like fragment (TLF) γ-rays observed in coincidence with quasi-elastic projectile-like fragments (PLF) from the reaction of ^{14}N with ^{165}Ho and ^{164}Dy at 20 MeV/A[1].

Complete energy spectra of PLF's with $5 \leq Z \leq 8$ were obtained. Discrete γ-ray transitions from the heavy residues were observed with either of two high purity germanium (HPGe) detectors. In contrast to low energy heavy-ion reactions, at 20 MeV/A the present particle-γ coincidence technique was found to be limited to studies of the transfer of one or two units of charge because the excitation energy of the heavy residues becomes so high that a broad range of final residues are produced. Figure 1 shows the coincidence spectrum for the series of carbon isotopes. The transitions from the dominant reaction channels of neutron evaporation, xn, and rather weak channels of alpha plus neutron evaporation, αxn, are indicated in the figure. We also note that the ratio of the observable discrete γ-rays to background (continuum γ-rays) becomes poor and the number of reaction subchannels increases with decreasing mass number of PLF. In the upcoming year we will begin to use a Compton-suppressed germanium detector system in order to extend the measurements to larger charge (mass) transfer. This detector system is described in Section C1(e) of the proposal.

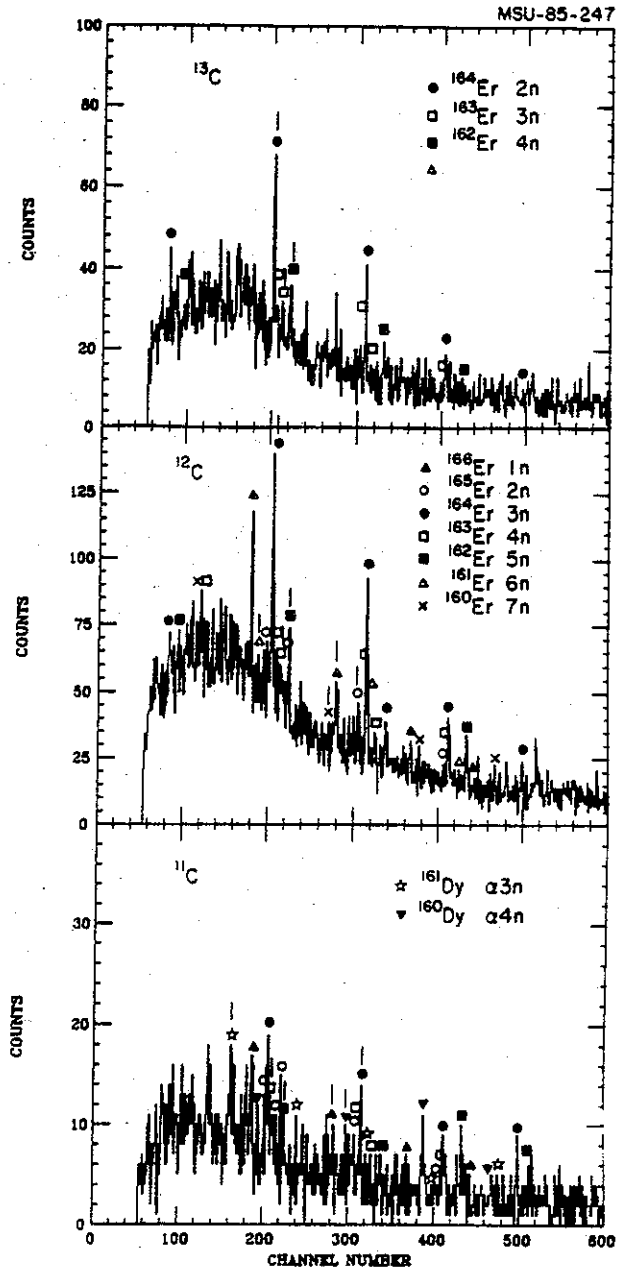

Fig. 1 Discrete γ-ray spectra from a HPGe detector in coincidence with ^{13}C, ^{12}C and ^{11}C from the reaction of ^{14}N + ^{165}Ho at 20 MeV/A. Each symbol uniquely represents one isotope in the three panels of the figure. Some of the γ-ray transitions used to obtain cross sections are marked with the bars.

Several models of projectile breakup have been suggested that describe the final momentum of PLF's lighter than the projectile in terms of two components, the fragment's fraction of the initial beam momentum and the momentum due to internal motion prior to breakup.[2,3] Overall, we have found that both calculations reproduce the experimental inclusive data acceptably well. We have made a more stringent test of the projectile breakup mechanism by comparing the observed TLF mass distributions with model predictions. The kinetic energy distribution predicted for a specific PLF was converted into an excitation energy distribution of a specific target-like fragment and then its evaporative statistical equilibrium decay was followed.[4] The relative isotopic distributions are compared to the data in Figure 2. In most cases the fits are unexpectedly good considering the

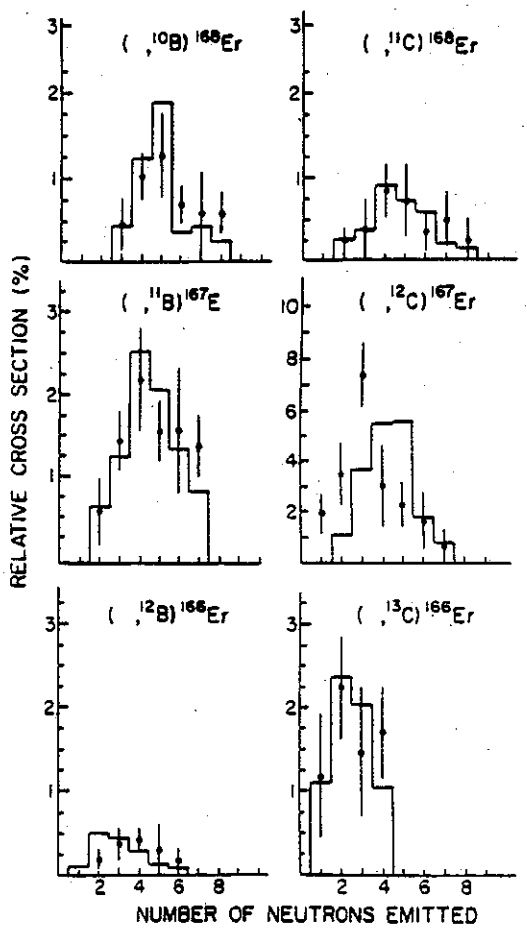

Fig. 2 Comparison of the observed isotopic distributions of TLFs (points) with a simple statistical evaporation calculation (histograms). Each panel is labeled with the PLF and primary TLF. The experimental cross sections are presented in relative percentages of the inclusive PLF cross section. The calculations were normalized to the TOTAL AREA in each panel.

simplicity of the assumptions. The average number and the range of evaporated neutrons are correctly predicted in four of the six cases. Only the centroids of the distributions calculated for fragmentation into mass 12 PLFs are different from the data by as much as two neutrons. Such differences may indicate the importance of sequential decay or other contributions to these PLF channels which are not present in the model calculations.

Additional information on the population of various ejectiles in specific bound states can give information on the question of the partition of the excitation energy between the reaction partners in asymmetric heavy-ion reaction systems. Previous studies have been based on an analysis of the charge distributions and neutron multiplicity in supposedly binary reactions of rather heavy systems,[5] as well as on the mass asymmetry of fission fragments.[6]

In conjunction with J. Wilczynski and K. Siwek-Wilczynska, we have studied PLF (fully identified by Z and A) in coincidence with discrete γ-rays during the measurement of the complementary information on target-like fragments in binary reactions at the NSCL,[7] described above. Energetic γ-rays corresponding to transitions of up to 6 to 8 MeV were detected in a set of four large volume bismuth germanate (BGO) scintillation detectors. Figure 3 (middle rows) show the kinetic energy spectra of the chosen ejectiles observed with the known γ-ray transitions. Samples of the inclusive energy spectra of these ejectiles are shown in the upper row of Fig. 3 for comparison. In the bottom row we plot the ratio of the excited state cross sections to the inclusive cross sections. This ratio represents the population of all bound excited states to the total production. It is interesting to note that the magnititude of this ratio does not differ much

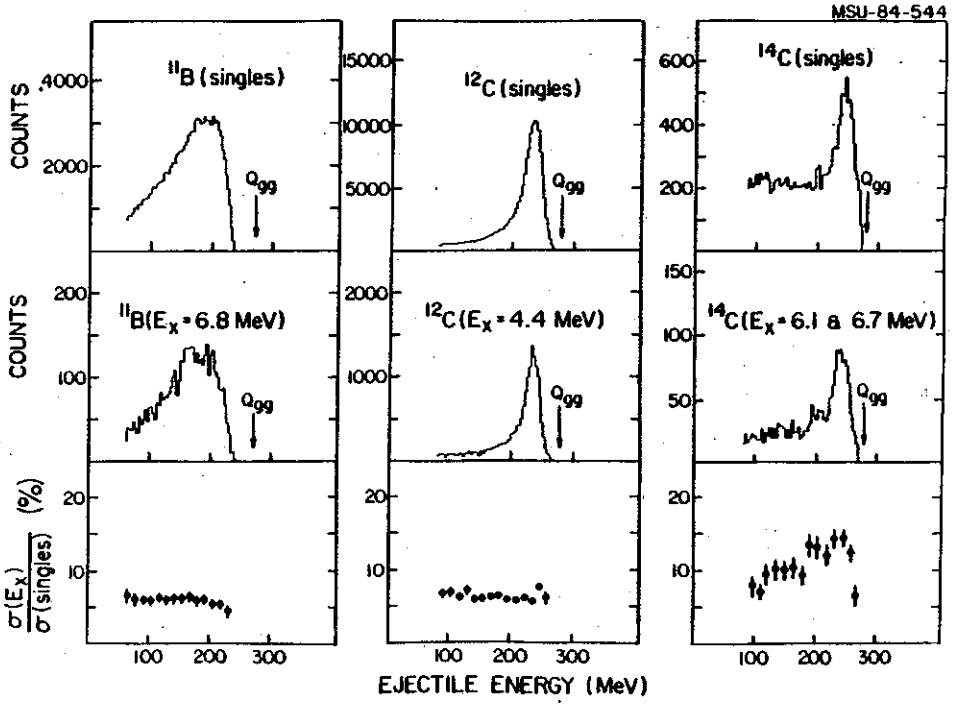

Fig. 3 Comparison of singles kinetic energy spectra of ^{11}B, ^{12}C and ^{14}C (top row) with those gated on the coincident photopeaks corresponding to specific ground state transitions in the same nuclei (middle row). The ratio of the cross sections for formation of the excited states to the inclusive cross sections for the same nuclei (bottom row).

from nucleus to nucleus, in spite of the fact that some of the observed nuclei have many excited states (viz. ^{11}B, ^{15}N) while others (viz. ^{12}C, ^{16}O) have relatively few.

It appears that the most interesting new result is that there is a clear difference in the energy dependence of this ratio between those reactions with PLF masses lower than that projectile, and those with the same or greater mass number. In the "stripping" reactions the ratio is essentially constant over the observed kinetic energy range, whereas in the "pickup and exchange" reactions the ratio decreases as the PLF kinetic energy decreases. This indicates that the total excitation energy produced in the reaction is not shared statistically but rather depends on the

direction of mass transfer. This is consistent with the Oppenheimer-Phillips mechanism[8,9] in which the transfered nucleons leave the parent nucleus near the ground state and bring all the excitation energy into the receiving nucleus. Redistribution of the excitation energy presumably relies on multiple transfers and thus the length of collision time.

Up to this point we have discussed our studies of projectile breakup and transfer to reactions at the grazing angle. The extended Serber model of the process[3] can also predict the angular distributions of beam velocity projectile-like fragments (PLF). However, there is notable lack of data available for comparison to the model. In addition, such cross sections are important in order to make the most efficient use of the RPMS at MSU during exotic isotope production runs.

We have recently measured the differential cross sections for isotope identified PLFs around the grazing angle for the reaction of 428 MeV ^{22}Ne with ^{197}Au, ^{165}Ho, ^{93}Nb and ^{27}Al. These measurements were performed at the NSCL using a cooled Si surface barrier telescope that was able to resolve completely those isotopes produced by the reaction in the range of ^{10}B to ^{23}Ne. Several isotopes showed a strong dependence on target mass, such as ^{21}F, ^{20}F and ^{18}O, which we attribute to direct reactions involving transfer of p, d and α particles, respectively. The remainder of the observed isotopes had nearly the same isotopic distribution for all four targets.

A small part of the data obtained in this experiment, shown in figure 4, is the differential cross section for ^{19}F and ^{16}O production with the ^{197}Au target as a function of laboratory angle. Also indicated on the figure are the extended Serber model calculations with two sets of input parameters. The curves have been independently normalized to the data at each angle, as the model does not predict absolute cross sections. The analysis of this data is in progress, and we expect to complete the analysis in the near future.

The present studies of transfer and fragmentation reactions were limited by the peak-to-background ratios in the γ-ray spectra. In the upcoming year we will begin a series of measurements of these reactions with the Compton suppressed spectrometer system developed in collaboration with

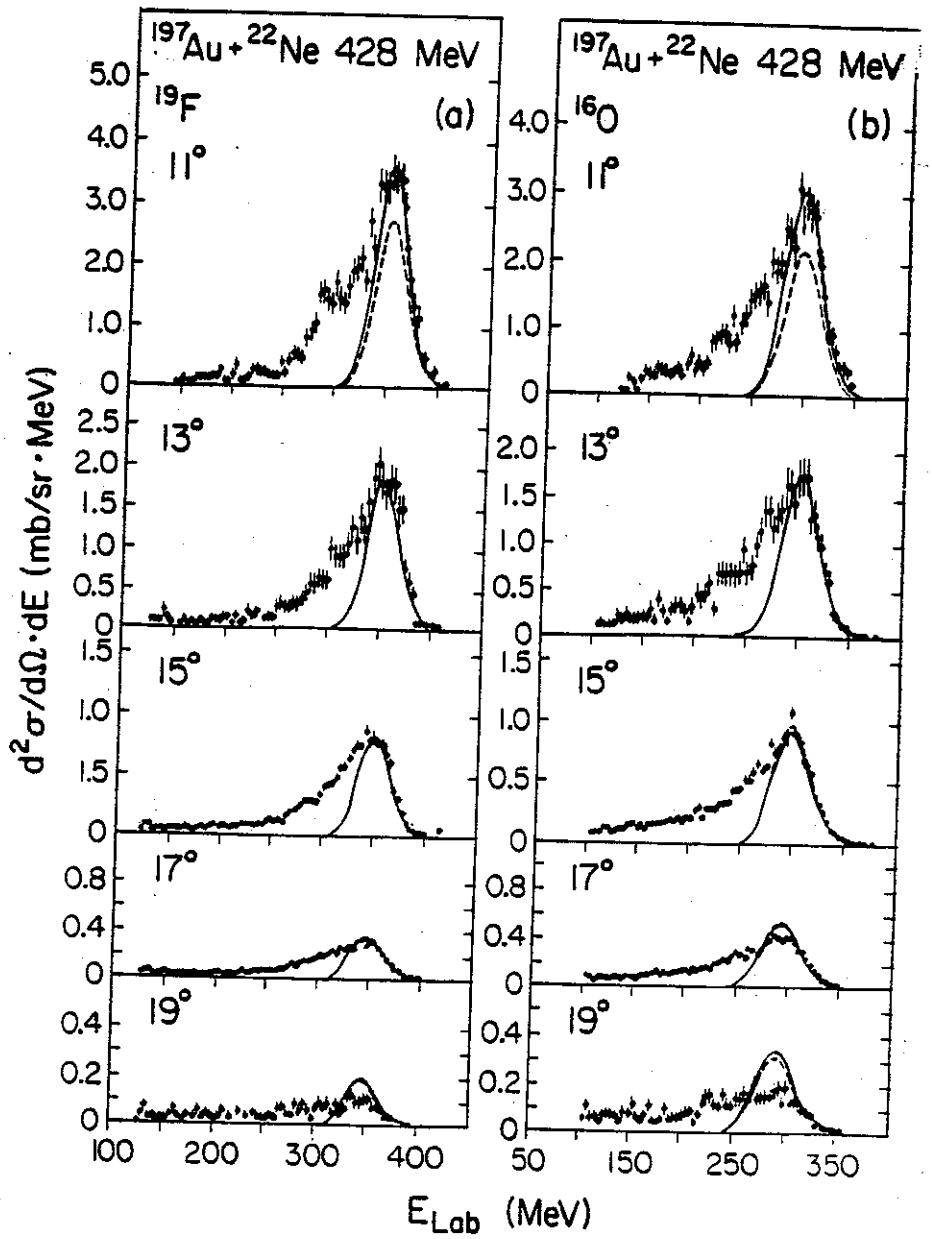

Fig. 4 Inclusive cross sections for production of ^{19}F and ^{16}O isotopes as a function of lab angle, see text.

J. Saladin (see sections B3a and C1e of this proposal). This device will provide a large solid angle for coincidence studies along with improved

spectral quality. In the first experiments we will study the products from the reaction of 10 MeV/A ^{22}Ne + ^{170}Er. Additional reaction mechanism studies will be aimed at understanding the role of momentum balance in these reactions and will focus on reactions with the the heaviest beams available from the K500/ECR system with energies in the range of 10 to 20 MeV/A, e.g. ^{40}Ar beams are useful in delivering large angular momenta into the TLFs and heavier beams such as ^{86}Kr or even ^{134}Xe can be used in "reverse kinematics" studies.

References:

1. H. Utsunomiya, et al. Phys. Rev. C 33,185(1986).
2. W.A. Friedman, Phys. Rev. C 27,569(1983).
3. H. Utsunomiya, Phys. Rev. C 32,849(1985).
4. F. Plasil, Oak Ridge National Laboratory Report ORNL-TM-6054, 1977, unpublished.
5. T.C. Awes, et al. Phys Rev. Lett. 52,252(1984).
6. R. Vandenbosch, et al. Phys. Rev. Lett. 52,1964(1984).
7. K. Siwek-Wilczynska, et al. Phys. Rev. C 32,1450(1985).
8. J.R. Oppenheimer and M. Phillips, Phys. Rev. 48,500(1935).
9. R. Serber, Phys. Rev. 72,1008(1947).

III.A.2.b. PROJECTILE FRAGMENTATION

G.D. Westfall, G.M. Crawley and H. van der Plicht

A great deal of information can be gained from the study of projectile fragmentation at forward angles. Some of the questions of interest are whether the two nuclei form a dinuclear system, or whether the projectile breaks up in the field of the target or decays in flight. In addition the detailed production cross sections for use in other types of experiments are of great importance. Systematic studies of projectile fragmentation have been carried out at energies below 20 MeV/nucleon[1] and at energies above 200 MeV/nucleon.[2,3]

However, there still is a lack of systematic studies of projectile fragmentation at intermediate energies. Studies have been carried out at GANIL[4] and at MSU[5,6] but these studies are not complete. At MSU the fragmentation of ^{14}N on C and Au targets has been studied by Harwood et. al.[5] Angular distributions that peak at angles of a few degrees were observed as shown in Fig. 1. This is in contrast to the situation at higher energies where the angular distributions continue to rise in to zero degrees. A more recent experiment by Angius et al.[6] where ^{16}O and ^{18}O fragmentation were studied at 35 MeV/nucleon show similar angular distributions.

In the future we propose to make detailed and systematic studies of projectile fragmentation phenomena. We plan to extract the parallel momentum widths, the perpendicular momentum widths, and the production cross sections as a function of projectile mass, target mass, and incident energy. The S320 spectrometer is the perfect tool for this task. These results will be compared with models such as those by Friedman[7] that predict very low momentum widths for given channels. The systematic results will be combined with those from higher and lower energies to produce a complete picture of this interesting reaction mechanism.

The natural extension of this work will be to measure several or all of the products from projectile fragmentation from the same event. This exclusive measurement can provide information concerning the decay of unstable resonances and the distribution of excitation energy tranferred to the projectile nucleus in these presumably peripheral collisions.

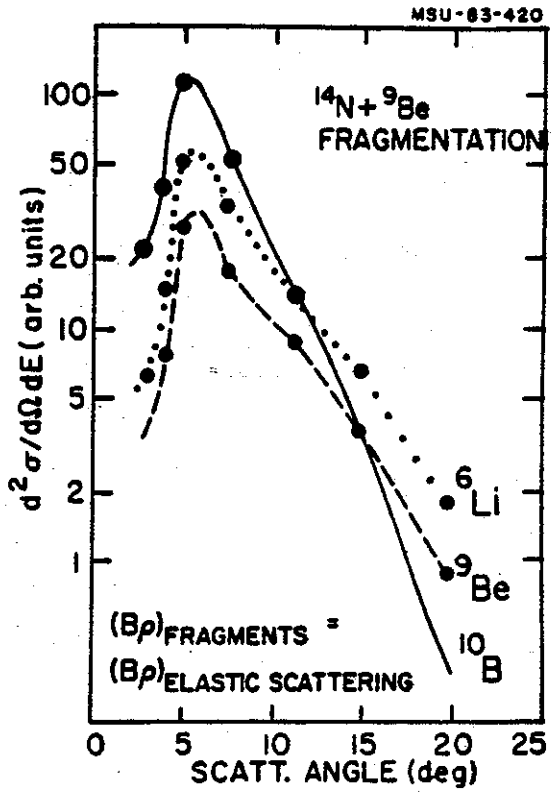

Figure 1.

One example of an exclusive projectile fragmentation experiment is the study of the break-up of ^{12}C into all of its final states, for which the neutrons are bound to some combination of charged particles, as was done at higher energies by Greiner et al.[8] By observing all the outgoing channels (e.g., 6 deuterons, 3 alphas, etc.) one can cover a very large range in excitation energies in the projectile nucleus before its breakup. These studies can provide a clear picture of the reaction mechanism independent of the later breakup processes. The S320 spectrometer will be used with a focal plane detector that can handle multiple particles simultaneously. To increase the acceptance, several of the exit points will be instrumented with these multi-hit focal plane detectors. The beams of interest are 100 and 200 MeV/nucleon ^{16}O and ^{40}Ar. Fragmentation of these beams has been studied extensively at lower energies ($\leq$30 MeV/nucleon) and higher energies ($\geq$200 MeV/nucleon).

References:

1. C.K. Gelbke, C. Olmer, M. Buenerd, D.L. Hendrie, J. Mahoney, M.C. Mermaz, and D.K. Scott, Phys. Rep. 42,311(1978).
2. Y.P. Viyogi, T.J.M. Symons, P. Doll, D.E. Greiner, H.H. Heckman, D.L. Hendrie, P.J. Lindstrom, J. Mahoney, D.K. Scott, H.J. Crawford, K. Van Bibber, G.D. Westfall, H. Wieman, C. MacParland, and C.K. Gelbke, Phys. Rev. Lett. 42,33(1979).
3. D.E. Greiner, P.J. Lindstrom, H.H. Heckman, B. Cork, and F.S. Bieser, Phys. Rev. Lett. 35,152(1975).
4. F. Rami, J.P. Coffin, G. Guillaume, B. Heusch, P. Wagner, A. Fahli, and P. Fintz, report CRN/PN.8407(1984).
5. L.H. Harwood, G.D. Westfall, N. Anantaraman, B. Hasselquist, B.V. Jacak, H. Utsunomiya, and A. Davenport, MSU Cyclotron Annual Report, 11(1983).
6. S.A. Angius, D. Cebra, G.M. Crawley, D. Fox, V. Rotberg, and G.D. Westfall, NSCL exp. 85004.
7. W.A. Friedman, Phys. Lett. B (1985).
8. J. Engelage et. al., BAPS, Asilomar 1985.

III.A.3.a. LIGHT-PARTICLE FISSION-FRAGMENT COINCIDENCES

C.K. Gelbke, W.G. Lynch, M.B. Tsang, K. Kwiatowski[a] and V.E. Viola[a]

Present information on non-compound particle emission in fusion-like reactions is consistent with the concept of statistical emission from highly excited subsets of nucleons. The corresponding single particle distributions can be rather well described in terms of isotropic Maxwellian distributions which are at rest in a frame moving with slightly less than half the beam velocity.[1,2] However, geometrical and dynamical effects are expected to lead to anisotropic particle emission. We have performed several experiments which clearly establish that non-compound particle emission is, indeed, highly anisotropic and occurs preferentially in the entrance channel scattering plane. These measurements are discussed in this section and in sections 3(b) and 3(c).

In order to investigate whether non-compound light particle emission is azimuthally symmetric about the beam direction, we have measured[3] coincidences between light particles and two correlated fission fragments resulting from the decay of the heavy target residue for ^{14}N induced reactions on ^{197}Au at E/A=30 MeV. Figure 1 shows the ratio of out-of-plane to in-plane coincidences between fission fragments and non-compound light particles. Clearly, non-compound light particles are preferentially emitted in the fission plane. The effect becomes more pronounced with increasing mass and energy of the emitted light particles.

For reactions induced on a Au target, fission fragments originate primarily from fusion-like collisions in which the major part of the projectile is absorbed by the target nucleus. Fission fragments will be preferentially emitted in the entrance channel scattering plane which is defined as the plane which contains the beam axis and which is perpendicular to the semiclassical orbital angular momentum vector for the relative motion of projectile and target nuclei.[3] Therefore, our measurements provide clear evidence for the preferential emission of non-compound light particles in the entrance channel scattering plane. The qualitative trend of increasing azimuthal asymmetries with increasing mass and energy of the outgoing particles can be understood in terms of a superposition of ordered transverse motion in the entrance channel scattering plane and random

(thermal?) motion of individual light particles. These effects are illustrated by schematic calculations[3].(See the dashed histograms and the dot-dashed curves in Figure 1.) Recent microscopic calculations with the Boltzmann-Uehling-Uhlenbeck equation have been able to reproduce the preferred emission of energetic light particles in the reaction plane.[4]

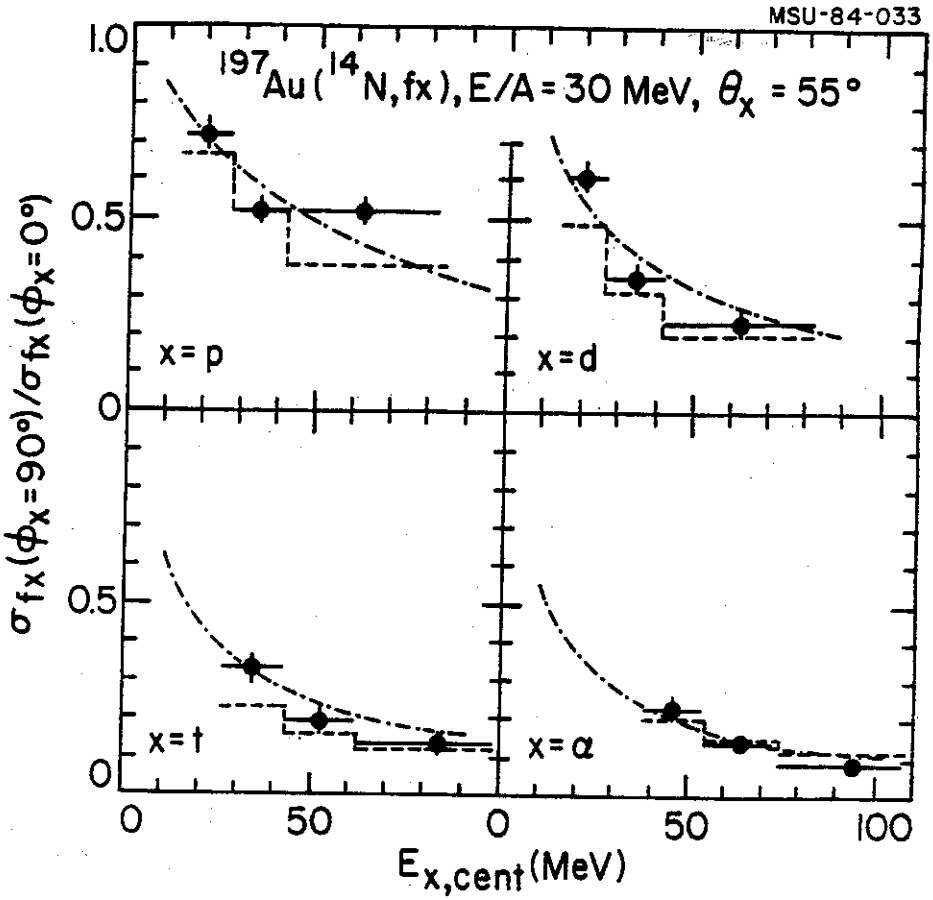

Fig. 1. Ratio of out-of-plane to in-plane coincidences between fission fragments and non-compound light particles emitted in the reaction $^{14}N+^{238}U$ at E/A=30 MeV.

The relative importance of mean field and nucleon-nucleon collision effects is expected to change significantly with beam energy. Since individual nucleon-nucleon collisions become less Pauli blocked at higher energies, we may expect increasing randomization and, consequently, more isotropic particle emission. We plan therefore to determine, at higher bombarding energies, the extent to which non-compound particle emission

preferentially occurs in the entrance channel scattering plane. Presently, however, it is not known whether coincident fission fragments will be sufficient to tag the entrance channel scattering plane at higher bombarding energies. For bombarding energies in excess of 50 MeV/A, it may be preferable to determine the azimuthal emission asymmetry with particle correlation techniques qualitatively similar to those described in the following section.

a. Indiana University Cyclotron Facility.

References:

1. T.C. Awes, G. Poggi, S. Saini, C.K. Gelbke, R. Legrain, and G.D. Westfall, Phys. Lett. 103B,417(1981)
2. G.D. Westfall, B.V. Jacak, N. Anantaraman, M.W. Curtin, G.M. Crawley, C.K. Gelbke, B. Hasselquist, W.G. Lynch, D.K. Scott, M.B. Tsang, M.J. Murphy, T.J.M. Symons, R. Legrain, and T.J. Majors, Phys. Lett. 116B,118(1982)
3. M.B. Tsang, C.B. Chitwood, D.J. Fields, C.K. Gelbke, D.R. Klesch, W.G. Lynch, K. Kwiatkowski and V.E. Viola, Jr., Phys. Rev. Lett. 52,1967(1984)
4. J. Aichelin and G. Bertsch, private communication

III.A.3.b. AZIMUTHAL CORRELATIONS BETWEEN LIGHT PARTICLES.

C.K. Gelbke, W.G. Lynch, J. Pochodzalla, M.B. Tsang, T. Awes,[a]
F.E. Obershain,[a] F. Plasil,[a] R.L. Robinson[a] and G.R. Young[a]

Additional information about the dynamic and geometric aspects of non-compound light particle emission can be obtained from investigations of light particle correlations at large relative momenta. In order to search for such correlations and to assess the importance of phase space constraints for small nuclear systems, we have measured azimuthal correlations between energetic light particles emitted in ^{16}O induced reactions on a light (^{12}C) and a heavy (^{197}Au) target at an incident energy of E/A=25 MeV. Figure 1 shows the azimuthal correlations between coincident light particles emitted at Θ_{lab}= 40° and 70°. For reactions on ^{12}C, there is a clear enhancement for the emission of two coincident light particles to opposite sides of the beam axis. These correlations may be understood in terms of the phase space constraints imposed by momentum conservation on finite nuclear systems. The solid lines show model calculations which illustrate this effect.[1,2]

Entirely different azimuthal correlations are observed for reactions on ^{197}Au (Fig. 1b). These correlations are nearly left-right symmetric about the beam axis and exhibit a characteristic "V"-shape corresponding to the preferential emission of energetic light particles in a plane which contains the beam axis. The preferentially co-planar emission of energetic light particles is consistent with the results shown in the previous section. The nearly left-right symmetric emission pattern, however, could not be anticipated. Again, the correlations become more pronounced with increasing mass of the detected light particles, consistent with the superposition of collective transverse motion in the reaction plane and random motion of individual particles. The solid and dashed lines correspond to simple model parameterizations of this effect.[1] Close inspection of the coincidence cross sections at ϕ=0° and ϕ=180° shows a small enhancement for the emission of coincident protons to opposite sides of the beam axis. Coincident deuterons and tritons, on the other hand, are preferentially emitted to the same side of the beam axis. At present, this effect is not entirely

understood. It might result from the competition of momentum conservation effects and absorptive (shadowing) effects.[1]

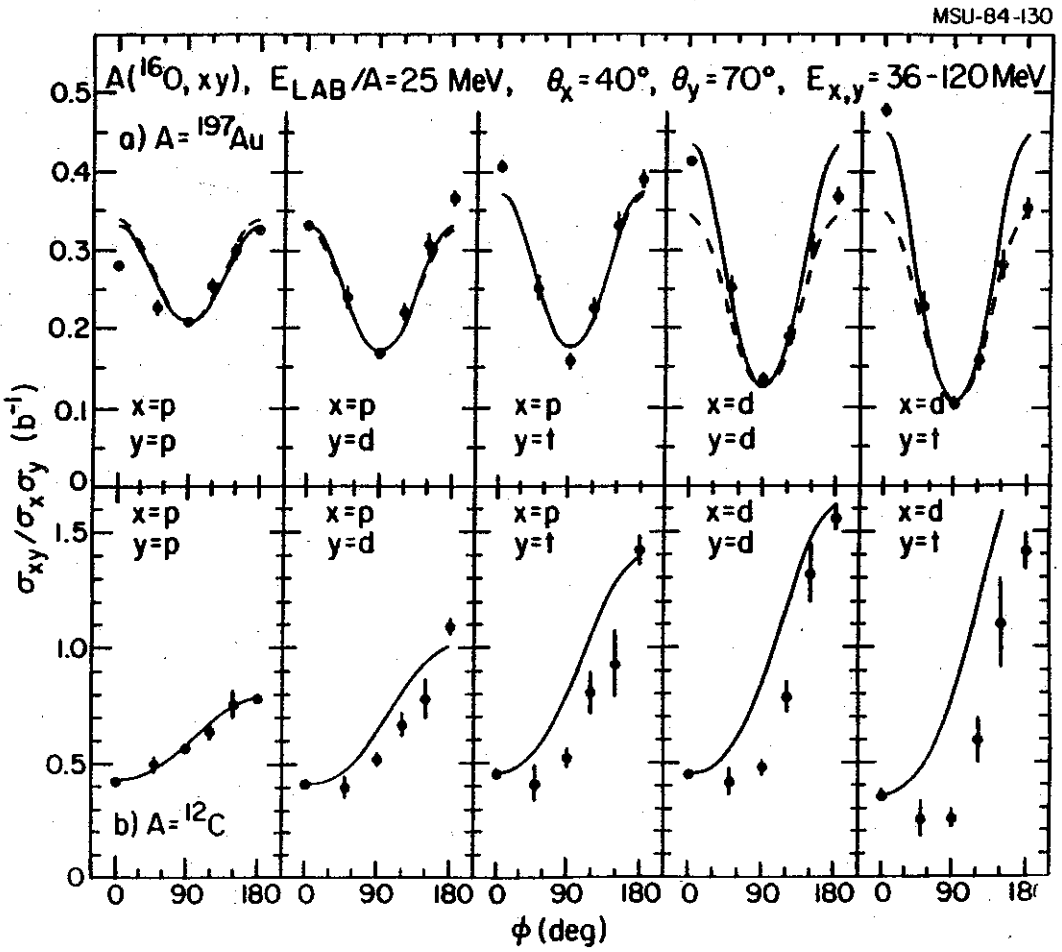

Fig. 1. Azimuthal angular correlations between coincident light particles emitted at θ_{lab} = 40° and 70° with respect to the beam axis for ^{16}O induced reactions on ^{12}C and ^{197}Au at E/A=25 MeV. A low energy threshold of 36 MeV was applied.

We plan to continue our investigations of light particle correlations at large relative momenta with heavier projectiles and at higher energies. Preliminary information for ^{40}Ar induced reactions on ^{197}Au at E/A=60 MeV indicates emission patterns which are considerably less coplanar. The coplanar emission of pre-equilibrium particles might then be the result of a delicate interplay of mean field effects and two-body collisions leading to thermalization. The relative importance of these factors is expected to be very different for reactions at higher energies (E/A >100 MeV) available

from the K800 cyclotron. We also plan to perform more detailed investigations of two-particle correlation functions at large relative momenta in coincidence with central collision triggers, which can be obtained by measuring the folding angles between correlated fission fragments at lower energies or by measuring the associated light particle multiplicities with the 4π array at higher energies. Such experiments can address the question whether the observed coplanar emission patterns of non-equilibrium light particles are primarily produced in peripheral collisions or in central collisions.

a. Oak Ridge National Laboratory

References:

1. M.B. Tsang, W.G. Lynch, C.B. Chitwood, D.J. Fields, D.R. Klesch, C.K. Gelbke, G.R. Young, T.C. Awes, R.L. Ferguson, F.E. Obenshain, F. Plasil and R.L. Robinson, Phys. Lett. 148B,265(1984)
2. W.G. Lynch, L.W. Richardson, M.B. Tsang, R.E. Ellis, C.K. Gelbke, and R.E. Warner, Phys. Lett. 108B,274(1982)

III.A.3.c. CIRCULAR POLARIZATION OF COINCIDENT GAMMA RAYS

C.K. Gelbke, W.G. Lynch, J. Pochodzalla, R.M. Ronningen,
M.B. Tsang and W. Trautman[a]

The preferential emission of non-compound particles in the entrance channel reaction plane may be understood in terms of the combined effects of the nuclear mean field and individual nucleon-nucleon collisions.[1] More detailed information about the interplay of mean-field and nucleon-nucleon collision effects can be obtained by measuring the circular polarization of γ-rays emitted from the heavy target residue in coincidence with non-compound light particles. By choosing the quantization axis along the direction of $\vec{k}_i \times \vec{k}_f$ and determining the sign of the circular polarization of γ-rays emitted perpendicular to the reaction plane, one may determine whether light particle emission occurs preferentially with positive or negative deflection angles. In our sign convention, positive deflection angles correspond to negative values of the polarization and negative deflection angles correspond to positive values of the polarization. If dynamic effects were negligible for non-compound light particle emission, the circular polarization of coincident γ-rays should be close to zero. Non-vanishing polarizations provide definitive evidence for dynamic mean-field effects; the sign of the measured polarization can determine whether the average mean field action is mainly attractive or repulsive.

We have performed measurements for ^{14}N induced reactions on ^{154}Sm at E/A=20 and 35 MeV[2], using two forward-scattering polarimeters[3] and four light particle detectors in a doubly symmetric geometry. As an example, Figure 1 shows the energy spectra of non-compound p, d, t and α-particles detected at $\theta_{lab}=30°$ and 60° (lower part of the figure) and the measured circular polarizations of coincident γ-rays (upper part of the figure). The polarizations measured in coincidence with protons are non-zero but small; rather significant positive polarizations are measured in coincidence with α-particles, indicating that they are emitted preferentially to negative deflection angles. Similar to the observation of increasingly anisotropic azimuthal distributions, the magnitude of the polarization increases with increasing mass of the detected light particles (p, d, t, α). Qualitatively

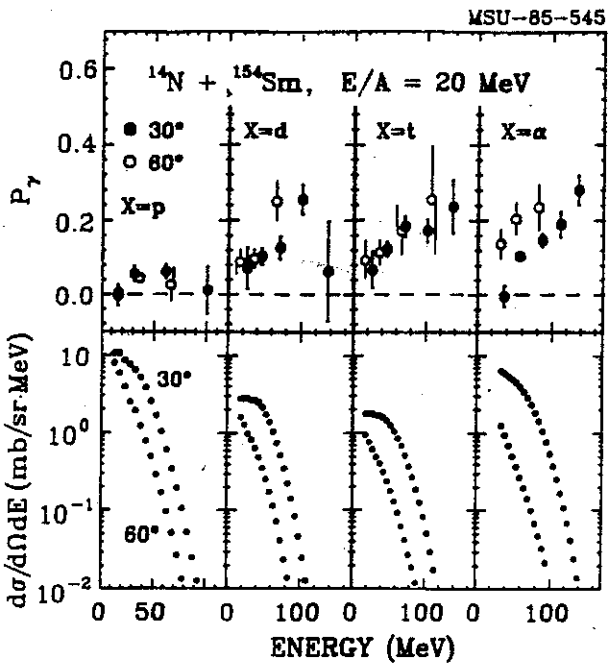

Fig. 1. Circular polarization of γ-rays measured in coincidence with non-compound protons and α-particles for ^{14}N induced reactions on ^{154}Sm at E/A=35 MeV (upper part of the figure). The energy spectra of the light particles are shown in the lower part of the figure; the light particle detection angles are θ_{lab}=30° and 60°.

similar observations are made at θ_{lab}=60° and at the lower beam energy of E/A=20 MeV. These measurements demonstrate the importance of the attractive mean field for non-compound single particle distributions. They are in qualitative agreement with the results from numerical calculations with the Boltzmann-Uehling-Uhlenbeck equation.[1] To illustrate this point, the upper half of Figure 2 shows the nucleon density at t=200 fm/c, calculated for a $^{14}N+^{154}Sm$ collision at E/A=35 MeV and at an impact parameter of 7 fm. The lower half of the figure provides the distribution of emitted nucleons as a function of the transverse momentum. The sign of the emission angle and hence the sign of the polarization is predicted correctly by these calculations. (This result does not change when the calculations are averaged over impact parameter.) A quantitative comparison with experiment is difficult at this time since the calculations do not yet include the emission of complex particles.

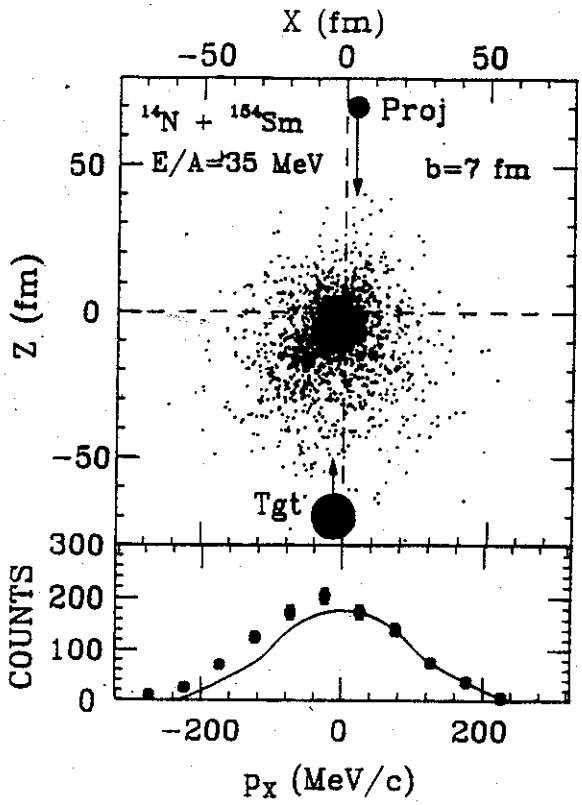

Fig. 2. Upper half of the figure: Nucleon density at t=200 fm/c calculated with the Boltzmann-Uehling-Uhlenbeck equation for a $^{14}N+^{154}Sm$ collision at E/A=35 MeV at an impact parameter of b=7 fm (t=0 corresponds to initial contact between projectile and target). The effects of the attractive mean nuclear field result in the preferential emission to negative deflection angles. Lower half of the figure: Distribution of nucleon as a function of the transverse momentum P_x (Nucleons in the residual nucleus are excluded from this plot). The solid curve corresponds to a distribution which is symmetric about P_x.

It will also be important to investigate the relative importance of positive and negative deflections for the emission of intermediate mass fragments. We plan to measure the circular polarization of γ-rays emitted in coincidence with intermediate mass fragments produced in ^{14}N induced reactions on ^{154}Sm at E/A=35 MeV. Since the average mean field is expected to become repulsive at higher energies, it would be very interesting to perform measurements at higher energies to determine whether the average deflection angle becomes positive. However, at present, it is not clear at which energy the γ-ray polarization technique ceases to provide useful information. We intend to exploit this technique at higher energies in

order to investigate whether the polarization does, indeed, decrease as expected.

a. GSI, Darmstadt.

References:

1. J. Aichelin and G. Bertsch, private communication
2. M.B. Tsang, R.M. Ronningen, T. Shea, Z. Chen, C.B. Chitwood, D.J. Fields, C.K. Gelbke, W.G. Lynch, T. Nayak, J. Pochodzalla, and W. Trautmann, to be published
3. W. Trautmann, C. Lauterbach, J. de Boer, W. Dünnweber, G. Graw, W. Hamann, W. Hering, and H. Puchta, Nucl. Instr. and Meth. 184 (1981) 449

III.A.3.d. COINCIDENCE STUDIES WITH INTERMEDIATE MASS FRAGMENTS.

C.K. Gelbke, W.G. Lynch, M.B. Tsang, T.C. Awes,[a] R.L. Ferguson,[a] F.E. Obershain,[a] F. Plasil[a] and G.R. Young[a]

Single particle inclusive measurements of the cross sections for the emission of intermediate mass fragments are not sufficient to characterize the emission mechanisms unambiguously. To investigate reaction dynamics, we have performed a series of coincidence measurements. Coincidences between intermediate mass fragments and heavy recoil nuclei were measured for ^{14}N-induced reactions on Ag at E/A=30 MeV, and for ^{32}S-induced reactions on Ag at E/A=23 MeV. For this latter reaction, we also measured coincidences with light particles. We have also performed triple coincidence measurements between intermediate mass fragments and two correlated fission fragments for ^{14}N-induced reactions on ^{238}U at E/A=35 MeV, in order to: address the question of decreasing cross sections for fusion-fission-like reactions at higher energies; search for azimuthally asymmetric emission patterns; and obtain information on the linear momentum transfer to the heavy target residue in these reactions. Most of these experiments are in the analysis stage. For the ^{32}S+Ag reaction, the analysis is close to completion; we will discuss some of the results.[1]

For ^{32}S-induced reactions on Ag at E/A=23 MeV, non-compound particle emission is an important feature of reactions producing intermediate mass fragments; both the inclusive intermediate mass fragment spectra and the spectra of coincident light particles contain large non-compound contributions. In Fig. 1, single light particle inclusive spectra are compared to corresponding coincidence light particle spectra for protons (upper half) and α particles (lower half) in coincidence with lithium (left side) and carbon (right side) fragments detected at Θ_x=27.5°, ϕ_x=0°. The light particle singles spectra are shown by the solid lines; the corresponding coincidence spectra are shown by solid points for ϕ_y=180° and open points for ϕ_y=90°. For the in-plane geometry, singles and coincidence spectra are of remarkably similar shape, indicating that the assumption of uncorrelated statistical emission is not strongly violated. The coincidence rate is reduced for the out-of-plane geometry and the out-of-plane coincidence spectra exhibit slightly steeper slopes.

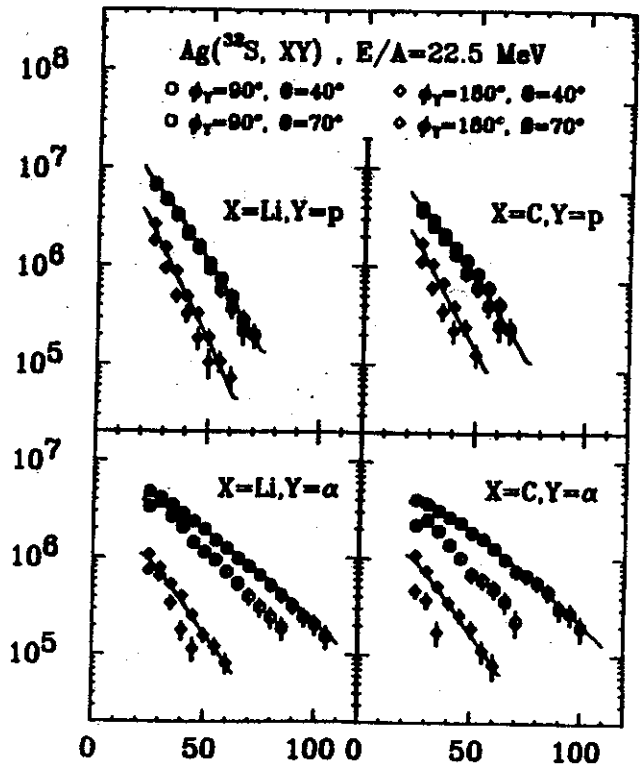

Fig. 1. Comparison of the shapes of singles and coincidence light particle spectra for ^{32}S-induced reactions on Ag at E/A=23 MeV. The solid lines show the shapes of single particle spectra; the open and solid points show spectra measured in coincidence with intermediate mass fragments for an out-of-plane ($\Delta\Phi$=90°) and an in-plane ($\Delta\Phi$=180°) geometry.

The systematic dependence upon the masses of the two-particle inclusive cross section and the scattering angles of the two particles can be examined with great sensitivity by constructing correlation functions. The correlation function can be strongly distorted by the sequential decay of particle unbound systems and final state interactions, particularly when the relative momenta of the two particles is small. In order to avoid such effects, we have excluded from the energy integrations those relative energies for which these effects are expected to be important.

Fig. 2 shows the dependence of the correlation function on the relative azimuthal angle, $\Delta\phi$, between alpha particles detected at θ_α=40° and intermediate mass fragments detected at θ_X=27.5° (open points) or θ_X=52.5° (solid points). The integrations in the correlation function are over particle energies above the thresholds, E_X/A_X > 5 MeV and E_α > 40 MeV. A pronounced minimum at $\Delta\phi$=90° can be clearly seen in the correlation function, indicating a strong preference for the emission of the coincident

intermediate mass fragment and alpha particle in a plane which contains the beam axis. The suppression of coincident particles at $\Delta\phi$=90° is more pronounced if the intermediate mass fragment is detected at the larger angle of θ_x=52.5°. Similar suppression of the angular correlation at relative azimuthal angles of 90° have been observed in light-particle correlations for ^{16}O-induced reactions on ^{197}Au at E/A=25 MeV (see Section A3(b). It suggests that intermediate mass fragments are also preferentially emitted in the entrance channel scattering plane and indicates that collective velocity components (as opposed to thermal velocity components) are not negligible.

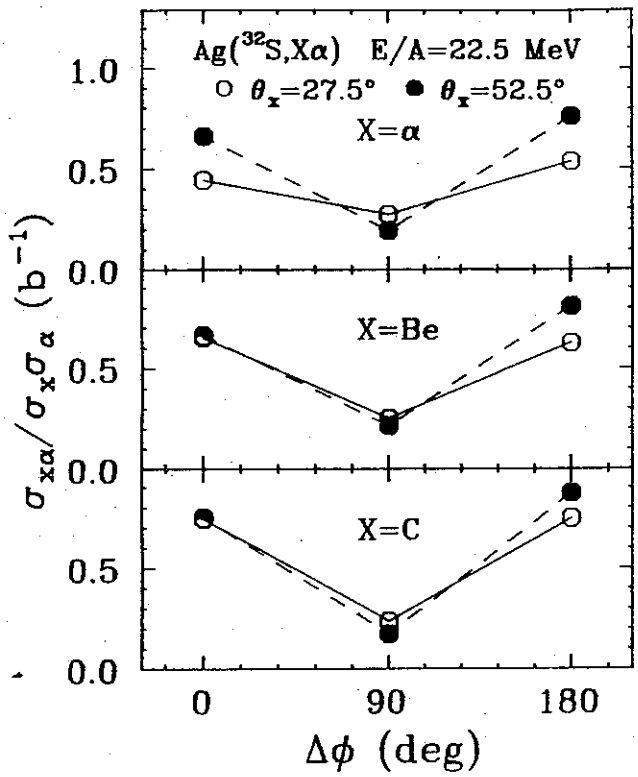

Fig. 2. Azimuthal correlation for concidence intermediate mass fragments and α particles for ^{32}S induced reactions on Ag at E/A = 23 MeV. The statistical errors are smaller than the data points. The lines are drawn to guide the eye.

Coincidence measurements[1] between intermediate mass fragments and heavy recoil nuclei indicate that the reactions are highly inelastic. For the ^{32}S+Ag reaction at E/A=23 MeV, between 200 and 400 MeV is deposited into intrinsic excitation of the emitted intermediate mass fragment or the heavy residual nucleus. The fragments are produced in reactions where more than

20% of the incident linear momentum is carried away by non-equilibrium particle emission. Nevertheless, absorptive breakup processes, for which a major part of the projectile emerges with beam velocity, can be excluded as a major reaction mechanism. The probability of detecting a heavy recoil nucleus in the reaction plane and on the opposite side of the beam axis is close to unity; the velocity distributions for the heavy recoil nuclei are well defined. This is consistent with multiplicity estimates obtained from the intermediate mass fragment-light particle coincidence measurements which indicate low multiplicities of intermediate mass fragments (the mean multiplicity of fragments with $Z \geq 3$ is of the order of 0.7). These low complex particle multiplicities are in qualitative agreement with statistical model calculations.[2]

In future experiments, we will pursue coincidence measurements between intermediate mass fragments in which both fragments are identified in order to determine the energy dependence of the multiplicity of intermediate mass fragments and to assess the relative importance of sequential decay processes leading to more than two heavy fragments in the exit channel. The unambiguous identification and characterization of true multi-fragmentation reactions at higher energies remains a challenging problem. For these experiments, we plan to use the heavier beams provided by the NSCL Phase II. These beams will make it possible to perform experiments with reverse kinematics. This technique will lead to considerable simplifications of the detection apparatus.

a. Oak Ridge National Laboratory.

References:

1. D.J. Fields, et al., to be published.
2. D.J. Fields, W.G. Lynch, C.B. Chitwood, C.K. Gelbke, M.B. Tsang, H. Utsunomiya and J. Aichelin, Phys. Rev. C30,1912(1984)

III.A.3.e. COMPLETE EVENT ANALYSIS OF NUCLEUS-NUCLEUS COLLISIONS

G.D. Westfall, G.M. Crawley, H. van der Plicht, M.R. Maier, and J. Yurkon

Recent results from sophisticated detection systems such as the Plastic Ball/Wall[1] and the Streamer Chamber[2] at the Bevalac at LBL have demonstrated the necessity of measuring as many particles from a high energy nucleus-nucleus collision as possible. These detection systems are able to study global variables such as kinetic energy flow, sphericity, and the dependence of the average transverse momentum on the rapidity. These quantities can provide strict tests for models that have successfully predicted the single particle inclusive data. Indeed, these experiments may have provided the first information that can be directly related to the equation of state of nuclear matter.[3]

Nucleus-nucleus collisions at NSCL energies (10 to 200 MeV/nucleon) produce events where up to 40 charged particles are emitted. Such an event is shown in Fig. 1 where a 100 MeV/nucleon Nb nucleus has interacted with a

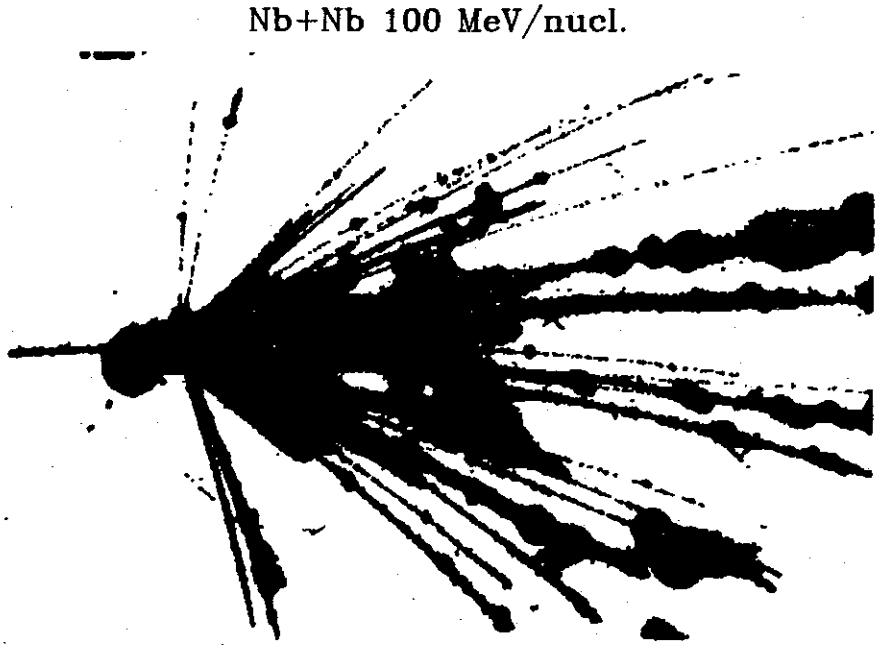

Figure 1.

Nb target. The multiplicity of charged particles clearly demonstrates the need for detection systems that not only can measure several particles in the final state but in fact must make every attempt to measure all of the charged particles. One can also see in this picture a fundamental difference between nucleus-nucleus collisions at NSCL energies and at Bevalac energies. At the lower energies, there are many particles that are obviously not protons. One must deal with a large number of particles that are complex fragments of many different energies.

One way to attack this problem is the solution provided by the NSCL 4π array. This apparatus can simultaneously detect light particles, fission fragments, target-like fragments, and pions. This detection system can trigger selectively on various classes of events and study them with very good statistics. In addition the 4π array can act as a filter for specialized modules such as small angle correlation detectors or high energy γ-ray detectors. A more complete description of the technical details and status of the 4π array are given in section C1(b).

We plan to carry out a large program of complete event measurements using the 4π array. The first experiments are planned to study 50 MeV/nucleon ^{40}Ca+Ca and Au to complement our previous inclusive measurements. A program of systematic measurements to map out the dependence of nucleus-nucleus collisions on incident energy, projectile and target nuclei with a variety of trigger conditions is also planned. We also have several special purpose modules planned for more focused experiments. For example, we plan to construct a small angle correlation device that will replace one of the hexagonal subarrays that has six detectors, with one containing 24 telescopes preceded by a position sensitive drift chamber array to accurately measure the relative momenta. The first experiments with the 4π array include the study of kinetic energy flow in collisions of 50 MeV/nucleon ^{40}Ca + ^{40}Ca. At this energy the compression effects are expected to be large compared with random thermal effects.

At higher energies, the systematic study of the global observables of average transverse momentum versus rapidity can yield detailed information on the equation of state. A collective sideward flow of matter is one of the features of high-energy nucleus-nucleus collisions predicted by calculations based on the nuclear fluid dynamics model,[4] the classical equations of motion,[5] and the microscopic Vlasov-Uehling-Uhlenbeck (VUU)

equations of motion,[5] and the microscopic Vlasov-Uehling-Uhlenbeck (VUU) theory.[6] In contrast, this sideward flow is not predicted by standard microscopic intranuclear cascade models,[7] which, however, have been quite successful in describing inclusive data. Sideward collective flow has recently been observed in 400 MeV/A Nb + Nb[8] and 770 MeV/A Ar + Pb[9] reactions.

To determine the degree of sideward collective flow, the data will be analyzed to extract flow angles from the diagonalization of the kinetic energy flow tensor.[10] In addition, the data will also be analyzed using the new transverse momentum technique recently proposed by Danielewicz and Odyniec.[11] Once the flow angle and/or the transverse momentum spectrum has been determined, nuclear fluid dynamics or VUU calculations[12] can be used to extract the nuclear equation of state. Figure 2 shows the predictions of a

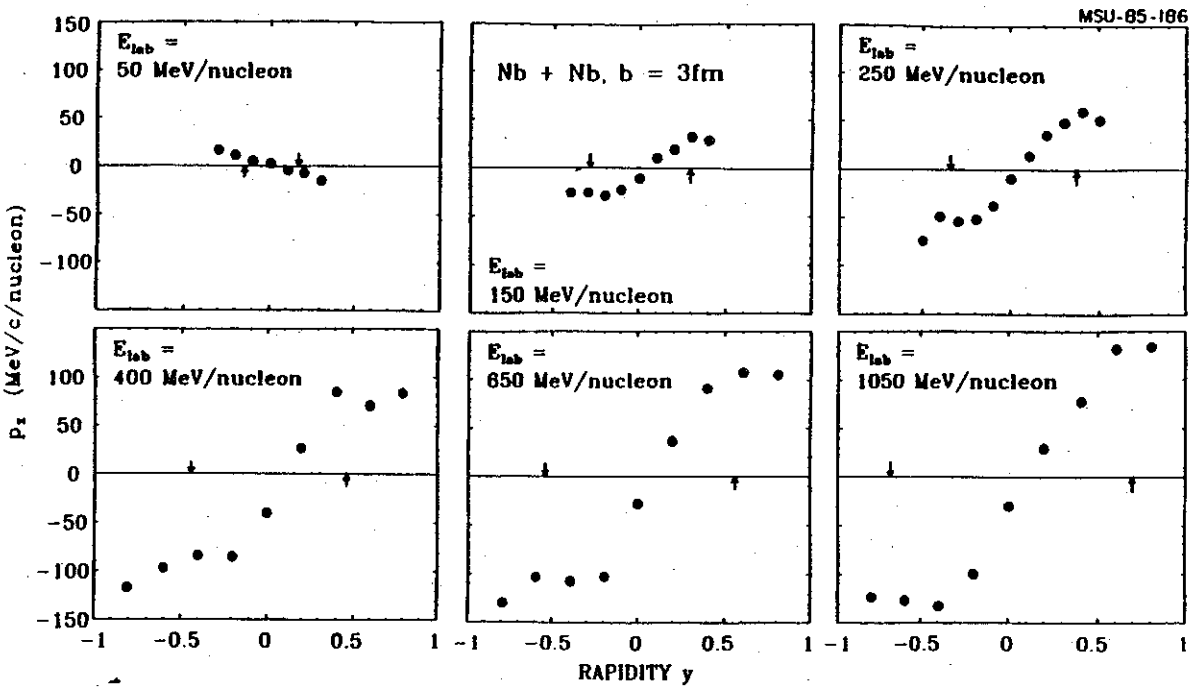

Figure 2.

VUU calculation[13] with a stiff equation of state (compressibility coefficient K = 375 MeV) for P_x vs. rapidity y as a function of energy for the system Nb + Nb. Note the increase in P_x at energies greater than 100 MeV/A and the sign reversal between 50 and 150 MeV/A. It will be interesting to see if similar behavior is observed in the systems we propose for study.

References:

1. H.H. Gutbrod, H. Löhner, A.M. Poskanzer, T. Renner, H. Reidesel, H.G. Ritter, A. Warwick, F. Wiek, and H. Wieman, Phys. Lett. 127B,317(1983).
2. H. Ströbele, R. Brockmann, J.W. Harris, F. Riess, A. Sandoval, R. Stock, K.L. Wolf, H.G. Pugh, L.S. Schroeder, R.E. Renfordt, K. Tittel, and M. Maier, Phys. Rev. C27,1349(1983).
3. G. Buchwald, G. Graebner, J, Theis, J. Maruhn, W. Greiner, H. Stöcker, Phys. Rev. Lett. 52, 1594 (1984) and W. Greiner and H. Stöcker, Scientific American, January, 1985.
4. W. Scheid, H. Müller, and W. Greiner, Phys. Rev. Lett. 32,741(1974). H. Stöcker, J. Maruhn, and W. Greiner, Zeit für Phys. A290,297(1978).
5. A.R. Bodmer, C.N. Panos, and A.D. MacKellar, Phys. Rev. C22,1025(1980).
6. H. Kruse, B.V. Jacak, and H. Stöcker, Phys. Rev. Lett. 54,289(1985).
7. J. Cugnon, Nucl. Phys. A387,191c(1982). Z. Fraenkel, Nucl. Phys. A428, 373c(1984).
8. H.A. Gustafsson, J. Gutbrod, B. Kolb, H. Löhner, B. Ludewigt, A.M. Poskanzer, T. Renner, H. Rredesel, H.G. Ritter, A. Warwick, F. Weik, H. Wieman, Phys. Rev. Lett. 52,1590(1984).
9. R.E. Renfordt, D. Schall, R. Bock, R. Brockmann, J.W. Harris, A. Sandoval, R. Stock, H. Ströbele, D. Bangert, W. Rauch, G. Odymec, H.G. Pugh, L.S. Schroeder, Phys. Rev. Lett. 53,763(1984).
10. M. Gyulassy, K.A. Frankel, and H. Stöcker, Phys. Lett. 110B,185(1982).
11. P. Danielewicz and G. Odyniec, Phys. Lett. B (to be published).
12. J. Molitoris and H. Stöcker, Phys. Rev. C32,346(1985).
13. H. Stöcker, and J. Molitoris, to be published.

III.A.3.f. STUDY OF CENTRAL COLLISIONS USING A STREAMER CHAMBER WITH CCD CAMERAS

S. Angius, G.M. Crawley, C. Djalali, M.R. Maier, V. Rotberg, D.K. Scott, R.S. Tickle[a], G.D. Westfall.

A complementary device to the 4π array for studying central events with high granularity is a triggered streamer chamber. In such a device it is possible to obtain much better spatial definition than is possible in a counter array but of course at the sacrifice of statistical accuracy. We have developed a system for recording central events in a streamer chamber which consists of three charged coupled devices (CCDs) which allow digital information to be recorded directly on magnetic tape. A description of this CCD development project is given in Section C1(c).

Using these CCD cameras, we propose to study central and near-central collisions of medium mass projectiles like Nb, La and Au on equal mass targets over a range of energies from 50 MeV/A to 200 MeV/A. The first of these studies has been approved by the Bevalac PAC, and a production run is scheduled in Feb 1986. Using a lighter projectile, we will also study collisions of Ar on targets of KCl, Nb, and Au at 200 MeV/A. Collisions such as these offer a unique opportunity to investigate the properties of hot, compressed nuclear matter. A major goal of our proposed work will be to determine the equation of state of nuclear matter under the conditions of high temperature and density. Knowledge of the nuclear equation of state, which at present is sketchy at best, has important applications in the understanding of neutron stars[1] and supernovae[2] and in testing and constraining nuclear matter theories. More detailed information on the investigation of the nuclear equation of state is given in Section A3(e).

The behavior of the equation of state at values of $\rho/\rho_0 < 2$ is a topic of particular interest on account of recent attempts to determine the behavior at higher densities. Some of the trends are shown in Fig.1, which compares a variety of theoretical and experimental results.[3] Encompassed by the shaded region are the experimental measurements from a comparison of the excitation function for pion production, with the prediction of a cascade model which does not explicitly include compressional effects. The deduced compressional energies are in rough agreement with the equation of state

required in a VUU calculation to describe experimental data on hydrodynamic flow. Although the methods of interpreting the data are still

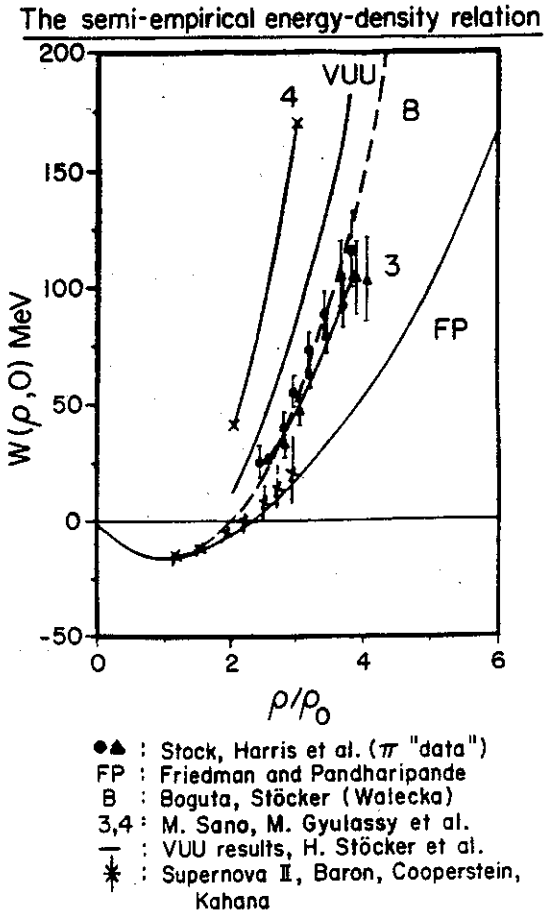

Figure 1.

controversial, it seems that the two experimental determinations are consistent; certainly there is a greater variation between the different theoretical approaches which are also shown in the Figure. The best agreement is with the calculations of Brockman et al., who use a relativistic Breuckner Hartree-Fock model. This implies that the equation of state is stiffer than, for example, the theory of Friedman-Pandharapande (labelled FP). On the other hand the theoretical equation of state predicted by Friedman and Pandharapande is necessary for understanding the dynamics of the supernova bounce (shown by the crosses along the FP-line).[14] In fact the traditional model of supernovae does not lead to densities in excess of $\rho \sim 1.5\ \rho_0$, whereas the more recent work of Baron, Cooperstein and Kahana predicts the bounce at $\rho \sim 2.5\text{-}3\ \rho_0$.[15] Both approaches require a

moderately soft equation of state. It is now of paramount importance to extend the heavy ion measurements into the region $\rho < 2.5\ \rho_0$ in order to determine whether the implied trend continues in disagreement with the dynamics of supernovae. Another source of the discrepancy might come from the fact that the high energy heavy ion collisions take place at high temperatures, whereas a supernova occurs at lower (but non-zero) temperatures at the same density. If there is a temperature dependence of the mean potential energy per baryon, it may contribute to the apparent discontinuity.

In a central or near-central heavy-ion collision, there is initially a compression and heating of the system, followed by an expansion with approximately constant entropy and decreasing temperature. Statistical and hydrodynamic considerations predict that if the state of the nuclear system ends its compression stage within a certain limited range of conditions, the temperature may subsequently decrease to the vicinity of the critical temperature (T_c), estimated to be 10-14 MeV for finite nuclei. Above the critical temperature the nuclear system exists only in the gaseous phase, but below T_c both the gaseous and liquid phases can coexist. This raises the possibility that evidence for a gas - liquid phase transition may be observed. Such an observation would greatly add to our understanding of nuclear matter at low densities and moderate temperatures. The occurrence of a phase transition, however, might be prevented by the finite size of the system and insufficient time.[4] In any event, the topic is of such importance that it should be carefully investigated experimentally.

The experimental signature of any movement of the expanding nuclear system towards a phase transition may be reflected in the relative abundances of nucleons and light- and medium-mass fragments as some critical excitation energy is reached. One of our primary measurements, which will now be possible with our new CCD system, will be of the exclusive charge distribution Y(Z) of fragments emitted in central collisions as a function of the system mass and the incident energy. Inclusive measurements of Y(Z) have been previously carried out and the results have stirred a controversy among theorists concerning their interpretation. One important limitation of the early experiments is their averaging over impact parameters which intermingles proton and light fragment yields from peripheral collisions with intermediate mass fragments from more central events. Our exclusive

measurements of Y(Z), as a function of the total charge multiplicity, will allow the selection of near-central collisions for direct comparison with theoretical results. Exclusive measurements of Y(Z), tagged with multiplicity, are essential to understand the collision processes as a function of the impact parameter and should help unravel the longstanding puzzles of the liquid-gas transition and the entropy.

In central collisions it is expected that the yield of medium mass fragments should reach a maximum relative to light fragments[5] at a given incident energy. Such behavior is indeed expected for phase transitions other than the transition from liquid to gas. A percolation theory of nuclei breakup,[6] for example, yields similar results, as does the finite molecular dynamical calculations of Vincentini et al.[7] A prediction of the percolation model is that the apparent power law dependence of the fragment mass distribution should pass through a minimum as a function of the average multiplicity of light fragments. The minimum power law exponent as a function of multiplicity can be determined in principle as a function of incident energy, in contrast to the case for most of the inclusive measurements conducted in the intermediate energy regime to date. It is important to keep in mind, however, that there is a wide variation in the predicted energy regime for the liquid-gas phase transition. In the work of Glendenning et al.,[8] the best estimate is that the transition lies at 330 MeV/nucleon. By combining the work proposed in this section with measurements of other groups at higher energy, there is hope that the existence or non-existence of a phase transition can be established. The outcome of these experiments may be relevant to the observation of phase transitions of a more exotic nature, such as the transition from the hadronic phase to a quark-gluon plasma. Some of the uncertainties surrounding finite size effects and time scales are common to both the high and low energy phase transitions.

Another question of considerable importance concerns nuclear stopping power, i.e. the degree to which colliding nuclei stop each other. Stopping power is directly related to a degradation of the initial longitudinal momentum in the collision. Colliding nuclei are somewhat transparent in the standard intranuclear cascade model[9] which predicts a forward-backward prolate distribution of fragment momenta in the participant center of mass following the collision. On the other hand, a very short mean free path and

total stopping is assumed by the hydrodynamic model,[10] which predicts considerably more sidewards deflection of the incident momentum flux than does the cascade model. An experimental study[11] of stopping power and collective flow in the Ar + Pb reaction at 772 MeV/A has shown that the predictions of the hydrodynamic model agree qualitatively with the data whereas the standard cascade model disagrees. In a recent theoretical analysis of the same reaction using the Vlasov-Uehling-Uhlenbeck theory, the predictions of stopping power and collective flow are shown to be in accord with the experimental data.[12] As observed experimentally, the theory predicts total stopping of the Ar projectile for small impact parameters.

As a corollary to the analysis for sidewards collective flow discussed in section A3(e), we will extract from the experimental data information concerning stopping power, mean free path, and the degree to which thermalization is attained. Because our proposed experiments will study collisions of both symmetric and asymmetric systems over a range of masses and energies, the results will represent a significant challenge to a broadly consistent theoretical interpretation. Thermalization requires both isotropy and Maxwell-Boltzmann energy distributions. We have chosen both symmetric and asymmetric systems for study and they present somewhat different problems in the analysis. In the symmetric case, the results are complicated by nucleons in the surface "corona" regions of the colliding nuclei[13] while in the asymmetric case choice of the proper participant center of mass is non-trival.

As well as the physics projects described here, an additional motivation for our work with the Bevalac streamer chamber and CCD cameras is to explore the feasibility and utility of constructing a streamer chamber at the NSCL. In many ways the visual information available from a streamer chamber makes it an ideal tool for the investigation of a new energy region. The studies most appropriate for a streamer chamber at Phase II energies would be the selection of specific event topologies and the study of negative pion production. The CCD readout should provide Z and A separation up to around mass 20, which would allow this device to attack such questions as the emission of complex fragments which may be a signature of critical phenomena.

a. University of Michigan.

References:

1. M. Nauenberg and G. Chapline, Astrophys. Journ. 179,277(1973).
2. H.A. Bethe, G.E. Brown, J. Applegate, and J.M. Lattimer, Nucl. Phys. A324,487(1979).
3. R. Stock, Proceedings of the Workshop on Intermediate Energy Heavy Ion Physics, Oak Ridge National Laboratory Publication CONF-8509176, p. C3.
4. D.H. Boal, Phys. Rev. C30,119(1985).
5. A.D. Panagiotou, M.W. Curtin, H. Toki, D.K. Scott and P.J. Siemens, Phys. Rev. Lett. 52,496(1984).
6. W. Bauer, D.R. Dean, U. Mosel and U. Post, Phys. Lett. 105B,53(1985).
7. A. Vincentine, G. Jacucci and V.R. Pandharapande, Phys. Rev. C31,1783(1985).
8. N.K. Glendenning, L.P. Csernai and J. Kapusta, LBL report LBL-20465(1985).
9. J. Cugnon, Nucl. Phys. A387,191c(1982).
   Z. Fraenkel, Nucl. Phys. A428, 373c(1984).
10. W. Scheid, H. Müller, and W. Greiner, Phys. Rev. Lett. 32,741(1974).
    H. Stöcker, J. Maruhn, and W. Greiner, Zeit für Phys. A290,297(1978).
11. R.E. Renfordt, D. Schall, R. Bock, R. Brockmann, J.W. Harris, A. Sandoval, R. Stock, H. Ströbele, D. Bangert, W. Rauch, G. Odyniec, H.G. Pugh, L.S. Schroeder, Phys. Rev. Lett. 53,763(1984).
12. J.J. Molitoris and H. Stöcker, MSU preprint MSUCL 504 (1985).
13. H. Ströbele, R. Brockman, J.W. Harris, F. Riess, A. Sandoval, R. Stock, K.L. Wolf, H.G. Pugh, L.S. Schroeder, R.E. Renfordt, K. Tittel, and M. Maier, Phys. Rev. C27,1349(1983).
14. B. Friedman and V.R. Pandharapande, Nucl. Phys. A361,502(1981).
15. E. Baron, J. Cooperstein, and S. Kahana, Phys. Rev. Lett. 55,126(1985).

III.A.4.a. NUCLEAR TEMPERATURE MEASUREMENT VIA EXCITED STATES

W. Benenson, E. Kashy, D.J. Morrissey and G.D. Westfall

An important component of heavy-ion research involves characterization of the "nuclear temperature" produced in various reactions. This concept implies the production of nuclear matter with some internal (thermal) energy all of which is in a state of equilibrium. The equilibrium should extend over all the degrees of freedom of the nuclear matter, and the observation of a consistent "temperature" among these various degrees of freedom would be a clear signal of the equilibrium. Until recently, researchers relied heavily on measuring the temperature indicated by Maxwell-Boltzmann velocity distributions, i.e., thermalization of kinetic energy degrees of freedom. By extension, we expect that the isotopic distributions of fragments produced by such thermal matter should also be indicative of the temperature through their Q-value dependence, sometimes called chemical equilibrium, and thirdly that excited states of any nuclear fragments should also be populated in accordance with the temperature. It is this latter idea, thermal production of bound, nuclear excited states, that we have developed and explored over the past few years. The first results were obtained for the excited state populations of lithium and beryllium fragments produced in the reaction of 35 MeV/A ^{14}N + Ag.[1,2] Recent extensions of these studies have been made by Pochodzalla, et al.,[3] who have measured unbound excited state populations with a particle correlation technique and by Galonsky et al. who have used a charged particle plus neutron coincidence technique, as discussed in the following sections.

We have extended our first measurements to the following projects:

1) the reaction of 20 and 25 MeV/A ^{14}N + Ag,

2) an auxillary measurement of the neutron multiplicity associated with the light fragments from the same reaction at 20 and 35 MeV/A,

3) the reaction of 6, 7, 8, 12, 15, 20 and 25 MeV/A ^{14}N + C, including a recent measurement of the excited state populations in which two-body kinematics were required,

4) and the reaction of 137 MeV/A ^{40}Ar + ^{197}Au at the LBL BEVALAC. In addition, we have beam time approved at TRIUMF to study fragment population

distributions in the reaction of 500 MeV protons with Ag. Each of these projects is discussed below after a brief introduction.

The distribution among their excited states of fragments emitted from a system in thermal equilibrium depends on the temperature of the system and the energy level spacing. For a two level system at constant volume the ratio of the populations is given simply by the Boltzmann factor. The distribution of the populations of the bound states of observable nuclear systems, such as ^{7}Li, ^{8}Li and ^{7}Be nuclei, will be modified by the statistical weights of the states and by any feeding from higher lying states that γ-ray decay and from more massive nuclei that particle decay. Such decays can have a significant effect on the population distribution and, in general, depend on nonstatistical nuclear structure effects. In the simplest picture of emission of these nuclei in thermal equilibrium with no feeding by particle decay, the ratio, R, of the populations of two states is:

$$R = \frac{(2\, j_{ex} + 1)}{(2\, j_{gs} + 1)}\; e^{-\Delta E/kT} \qquad (1)$$

where j_{gs} and j_{ex} are the spins of the ground and excited states, respectively, ΔE is the energy spacing between the states and kT is the nuclear temperature. This ratio is not directly measurable because the lifetimes of the γ-ray emitting states are short. However, the fraction of the observed nuclei that emit γ-rays, f=R/(1+R), can be obtained from particle-γ-ray coincidence measurements. The variation of this fraction with temperature can be seen for several examples in Figure 1.

All our measurements of the fractions of nuclei in excited states were performed at the NSCL, with the exception of the 137 MeV/A ^{40}Ar measurement which was carried out at the BEVALAC. The fractions were determined by a comparison of the γ-ray coincidence counting rate to the inclusive counting rate of each nucleus. The details of the experimental arrangement have been presented in references 1 and 2. Briefly, the light nuclei were completely identified, Z, A and kinetic energy being measured in one of a set of four Si surface barrier detector telescopes, and the γ-rays were detected in a set of eight 7.6 x 7.6 cm NaI(Tl) detectors. The solid angle of each particle detector was generally quite large, about 25 millisteradians, and

the total photopeak efficiency of the γ-ray array was 4.5 percent. As the fraction depends on the ratio of the counting rates, it only depended on the value of the coincidence efficiency of the γ-ray detector array.

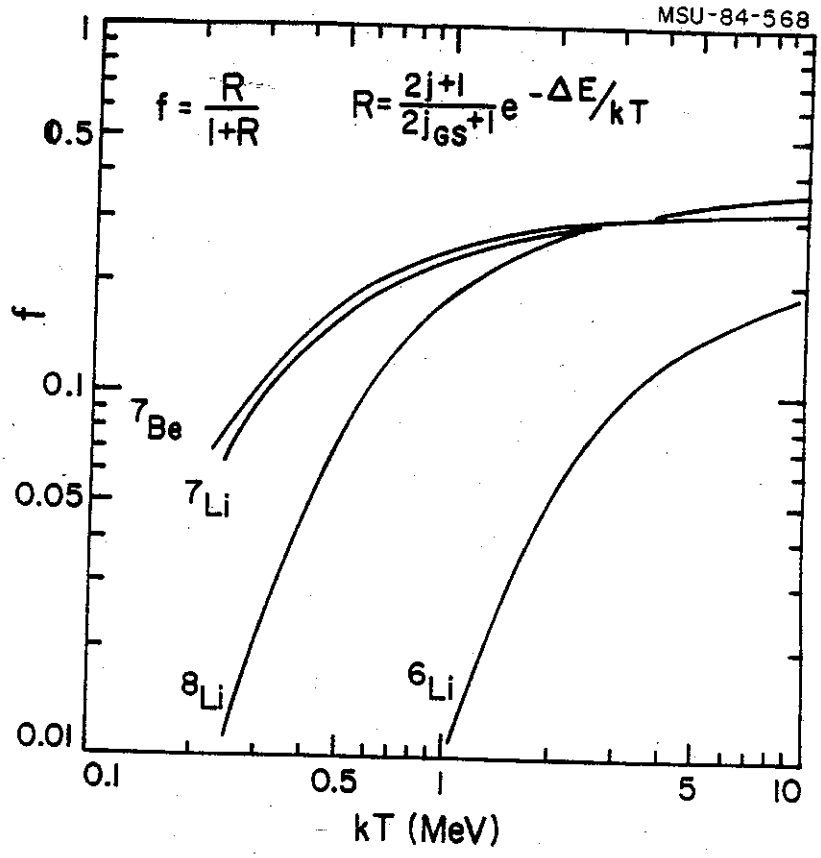

Fig. 1. Calculated values of the fraction of emitted nuclei in their excited states as a function of temperature. [MSU-84-568]

The $^{14}N + ^{12}C$ Reaction:

This compound nucleus reaction has been well studied, and approximately half of the reaction cross section is known to go into the compound nucleus channel, a large fraction of which goes to formation of lithium and beryllium nuclei, as discussed in references 4 and 5. Thus, studying the $^{14}N + ^{12}C$ reaction allows us to check the validity of this technique to measure nuclear temperatures by excited state production. We were able to study this reaction over a large range of bombarding energies, from 6 to 25 MeV/A, due to the relatively high cross sections for producing these fragments. The analysis of the data is in progress and we will only describe the results from the reaction at 8 MeV/A.

At most energies, lithium, beryllium and boron nuclei were detected at eight angles ranging from 30° to 65° in 5° steps. The inclusive kinetic energy spectra, shown in figure 2 for the 8 MeV/A reaction, are generally exponential in shape. As a preliminary test for emission from the compound

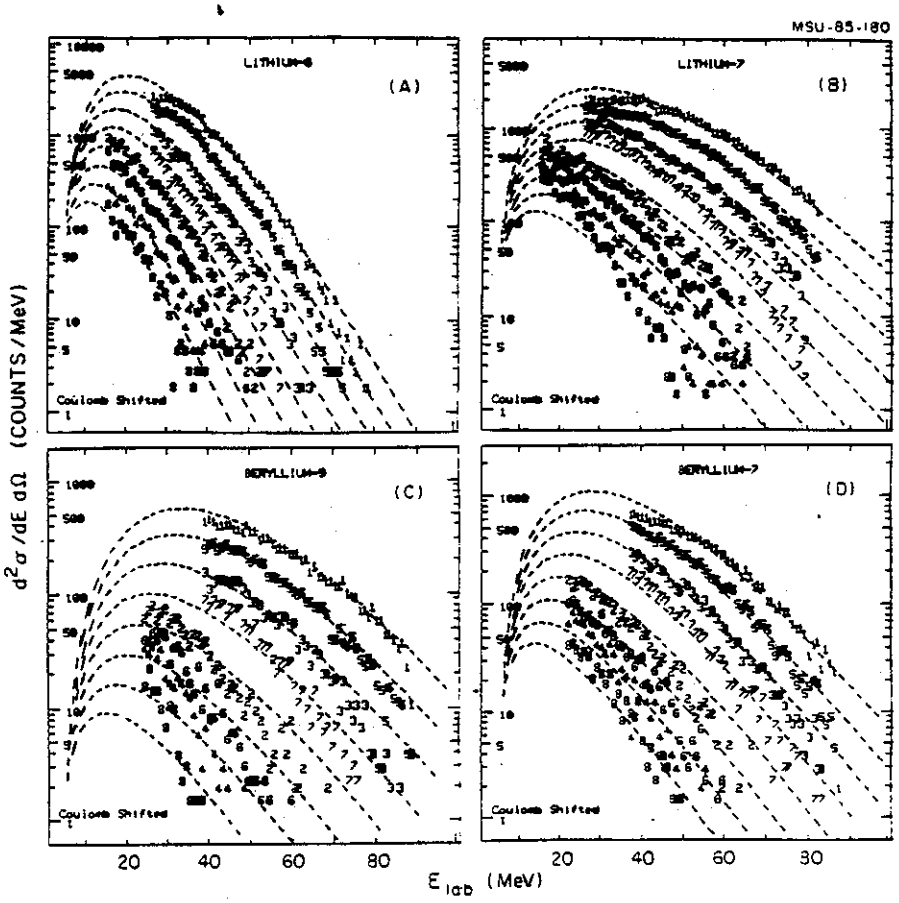

Fig. 2. Kinetic energy distributions of fragments from thereaction of 8 MeV/A ^{14}N + C. Dotted curves represent single moving-source fits,or compound nucleus emission.

nucleus, we fitted the kinetic energy spectra for each isotope to those expected from a single moving source. Such a fit has three independent parameters, the source velocity and temperature and the total cross section. The velocity of the source with the lowest chi-squared value ($\beta = v/c$ of 0.071 to 0.075, depending on isotope) agreed very well with that of the compound nucleus (0.0718). The fitted temperature was in agreement with that expected for a degenerate Fermi gas (approximately 4.7 MeV for ^{26}Al). This agreement indicates that these fragments are produced by the compound nucleus mechanism and we should find that the excited state populations are also indicative of this temperature. However, the fits to the ^{7}Li kinetic energy spectra were noticeably poorer than those to the other isotopes. For example, the shapes of the spectra at 30° and 35° were much flatter than those predicted by a single source model. This indicates that the ^{7}Li fragments have been produced by more than one reaction mechanism as well as having been contaminated by the misidentification of the double alpha decay products from ^{8}Be as ^{7}Li fragments. In subsequent bombardments, we have measured the isotopic cross sections as a function of detector solid angle in order to assess the extent of contamination.

The fraction of ^{7}Be nuclei in the excited state was found to be 0.28±0.05, while the "apparent fraction" of ^{7}Li was 0.04±0.01. This indicates that the population of the excited state of ^{7}Be is approximately what one would expect for a temperature of 4 MeV. The population of the ^{7}Li excited state is well below the expected saturated value which would be consistent with the spectral shape of the inclusive data. Preliminary indications are that the contamination of ^{7}Li by ^{8}Be decay is severe in this isospin 0 reaction and the "corrected fraction" will be close to that of ^{7}Be. These results indicate that the new population distribution method of measuring nuclear temperatures is valid.

Reactions of ^{14}N + Ag:

The lithium and beryllium fragments for the reaction of 20, 25 and 35 MeV/A ^{14}N with Ag were measured at three angles. An analysis of these inclusive kinetic energy spectra obtained at 35 MeV/A in terms of a single moving source indicated a temperature of 12±2 MeV and a source velocity of

2.2±0.3 cm/ns. These values are completely consistent with similar analyses of inclusive data of this type. However, in this reaction the fraction of ^{7}Li (after correction for the misidentification of ^{8}Be) and ^{7}Be products in their excited states were lower than those in the compound nucleus reaction, independent of angle. The results are:

Energy	f(^{7}Be)	f("^{7}Li")	corrected f(^{7}Li)
20 MeV/A	0.083 ± 0.022	0.051 ± 0.015	0.08 ± 0.02
25 MeV/A	0.164 ± 0.036	0.101 ± 0.023	0.155 ± 0.04
35 MeV/A	0.20 ± 0.06	0.10 ± 0.01	0.15 ± 0.02

We also note that the corrections for the ^{8}Be decay have brought the ^{7}Li results into agreement with those for ^{7}Be. These fractions indicate "temperatures" that are less than 1 MeV and much lower than those obtained from the inclusive kinetic energy spectra. They are, however, in good agreement with the ^{8}Li temperature also measured in this experiment.

Our results have stimulated several theoretical groups to propose models to explain the low apparent temperatures based on either thermodynamic equilibrium during the expansion of the zone of emission[6] or by perturbation of the populations by particle decay among the members of the initial thermodynamic equilibrium ensemble.[7] Neither model is able to explain our results completely. A more complete discussions of the comparison of the model results to our data in reference 2. A study of the identical system by Chitwood, et al.,[8] gave a temperature of ≈4 MeV for particle unbound states in similar nuclei. However, the threshold energy for detection of unbound Li and Be fragments was 55 MeV much higher than the 17 MeV threshold in the present experiment. Consequently, the two results are not necessarily inconsistent with each other but rather both show smaller populations than those expected from the "slope temperature." The possibility that the population distributions may depend on fragment kinetic energy is an intriguing possibility suggested by these results.

The Reaction of ^{40}Ar + ^{197}Au:

One explanation of the low temperatures obtained in the ^{14}N + Ag experiments performed at MSU is that at these beam energies equilibrium is

not reached but rather the process is a complex many staged one. For this reason we attempted to carry out an identical experiment at higher energies at the BEVALAC for ^{40}Ar + ^{197}Au at E/A = 137 MeV. This is a system that has been very thoroughly studied by Jacak, et al.,[9] and appeared to agree extremely well with the thermal model. The experiment was run on the Low Energy Beam Line in March of 1985. The apparatus was almost identical to that described in reference 2 except that thicker Si detectors were used, and four BGOs were added to the eight NaI gamma detectors. Although the experimental spectra appeared to be as clean as those obtained at MSU at lower energies (because the gamma ray multiplicity is not very different), there was no sign of peaks corresponding to the production of Li or Be nuclei in excited states. This was partly due to the statistics, which were limited by the breakdown of the BEVALAC about one third of the way through the run, but a quite low upper limit of about 600 keV could be set on the temperature from excited state production. This is a very similar result to that obtained at lower energies, although the temperature determined from the slope of the energy distributions is about three times higher.

Proton Induced Reactions at Intermediate Energies:

The spallation of Ag by protons at 500 MeV gives spectra for the intermediate mass fragments which are very similar to that obtained for ^{14}N at the same total energy. Studies with the cascade model seem to indicate that this reaction can be very well understood and should have a strong thermal component. Unlike the heavy ion case, the effect of the Pauli principle is minimal, and one is studying in this case the expansion of hot low density nuclear matter. Therefore we have decided to study the excited state production for 500 MeV p + Ag at TRIUMF. One week of beam time has already been approved for a gamma ray experiment, but we are currently modifying the proposal to include the study of unbound or resonant excited states. For this we will use an array of plastic scintillator phoswiches with a multiwire proportional counter. The experiment will be run next summer at TRIUMF.

Future Studies of Nuclear Temperatures and Excited State Populations:

We have undertaken a large experimental investigation of the relationship between the populations of nuclear excited states and

temperature in a wide variety of reactions. Because several measurements have only recently been completed, we will spend the upcoming year analyzing and interpreting our results. We can only suggest a few possibilities for the direction of future work. We have seen that the populations of the excited states of ^{7}Li and ^{7}Be nuclei are increasing with bombarding energies from 20 to 35 MeV/A in the reaction of ^{14}N + Ag. This trend will be explored up to the limits of the K500 cyclotron. We are beginning to investigate actively the possibilities of using additional nuclei in these studies; a prime candidate is ^{10}B. This isotope has five states that decay by γ-ray emission in a complicated branching pattern. We have already observed significant production of this isotope in the ^{14}N + ^{12}C system and relatively low production in the intermediate energy reactions. Future experimental work with this and other similar isotopes will require a much more efficient γ-ray detector. We recognize that all of the reactions we have studied so far have been induced by a "light" heavy-ion, ^{14}N. With the operation of the K500 coupled to an ECR ion source early in 1986, we expect to repeat some of these pioneering studies with higher mass beams such as 40 MeV/A ^{40}Ar, or 20 MeV/A ^{86}Kr. Recent studies with such massive beams using "reverse kinematics" have indicated that fragment emission is occuring from apparently equilibrated composite systems.[10,11]

Perhaps the most important task for the upcoming years is a synthesis of all the results of temperature measurements by the various techniques. At present, we see substantial discrepancies; first, between the population distributions and the kinetic energy distributions, and second between the distribution of bound and unbound states. What the result of this synthesis will be is not clear, but certainly our measurements of the excited state populations of these fragments have played an important role in forcing a re-evaluation of the extent of equilibration in heavy-ion reactions.

References:

1. D. J. Morrissey, W. Benenson, E. Kashy, B. Sherrill, A. D. Panagiotou, R. A. Blue, R. M. Ronningen, J. van der Plicht and H. Utsunomiya, Phys. Lett. 148B,423(1984).
2. D. J. Morrissey, W. Benenson, E. Kashy, C. Bloch, M. Lowe, R. A. Blue, R. M. Ronningen, B. Sherrill, H. Utsunomiya and I. Kelson, Phys. Rev. C 32,877(1985).
3. J. Pochodzalla, W.A. Friedman, C.K. Gelbke, W.G. Lynch, M. Maier, D. Ardouin, H. Delagrange, H Doubre, C. Gregoire, A. Kyanowski, W. Mittig,

A. Peghaire, J. Peter, F. Saint-Laurent, Y.P Viyogi, B. Zwieglinski, G. Bizard, F. Lefebvres, B. Tamain, and J. Quebert, Phys. Rev. Lett. 55,177(1985).

4. J. Gomez del Campo, J. A. Biggerstaff, R. A. Dayras, D. Shipira, A. H. Snell, P. H. Stelson and R. G. Stokstad, Phys. Rev. C 29,1722(1984).
5. R. G. Stokstad, M. N. Namboodiri, E. T. Chulick, J. B. Natowitz and D. L. Hanson, Phys. Rev C 16,2249(1984).
6. D. Boal, Phys. Rev. C 30,749(1984).
7. H. Stöcker, private communication; H. Stöcker, G. Buchwald, G. Graebner, P. Subramania, J. A. Maruhn, W. Greiner, B.V. Jacak and G. D. Westfall, Nucl. Phys. A400,63(1983).
8. C.B. Chitwood, C.K. Gelbke, J. Pochodzalla, Z. Chen, D.J. Fields, W.G. Lynch, R. Morse, M.B. Tsang, D.H. Boal, and J.C. Shillcock, NSCL Report MSUCL-543
9. B.V. Jacak, et al. Phys. Rev. Lett. 51,1846(1984).
10. W. Mittig, A. Cunsolo, A. Foti, J.P. Wieleczko, F. Auger, B. Berthier, J.M. Pascuad, J. Quebert and E. Plagnol, Phys. Lett. 154B,259(1985).
11. R.J. Charity, M.A. McMahan, D.R. Bowman, Z.H. Liu, R.J. McDonald, G.J. Wozniak, L.G. Moretto, S. Bradley, W.L. Kehoe, A.C. Mignerey, and M.N. Namboodiri, Lawrence Berkeley Lab Report LBL-20383, submitted for publication (1985).

III.A.4.b. LIGHT PARTICLE CORRELATIONS AT SMALL RELATIVE MOMENTA

C.K. Gelbke, W.G. Lynch, J. Pochodzalla and M.B. Tsang
In collaboration with scientists from ORNL[a], GANIL[b], Simon Frasier University[c], and the University of Wisconsin[d].

Light particle correlations at small relative momenta provide information about the space-time characteristics of the emitting system and the population of particle unbound states. Our major research effort over the last three years has been devoted to the investigation of these correlations.

For intermediate energy nucleus-nucleus collisions, particle emission occurs prior to the attainment of full statistical equilibrium of the composite system.[1,2] In the absence of a complete dynamic treatment, recourse is often taken to models, based on the assumption of statistical particle emission from subsets of nucleons characterized by their average velocity, space-time extent, and excitation energy or "temperature". The experimental determination of the detailed characteristics of these subsets is clearly important. Detailed investigations of the degree of thermalization are also desirable at higher energies, where promising attempts were made to determine the nuclear equation of state from multiplicity gated pion production cross sections.[3,4]

Most attempts to extract temperatures are based on analyses of the kinetic energy spectra of the emitted particles.[5] The interpretation of such spectra can, however, be complicated by sensitivities to the collective motion[6] and the temporal evolution of the emitting system.[2] (see also Section A1(a)). An alternative determination of the "emission temperature", i.e. the temperature at the point at which particles leave the equilibrated subsystem, was first suggested by Morrissey et al.,[7] and is based on the relative population of states.[8-11] Information about the space-time extent of the emitting system can be obtained from two-particle correlation functions.[12-16]

Two-Particle Correlation Functions: The two-particle correlation function, $R(q)$, is defined in terms of the singles yields, $Y_1(\vec{p}_1)$ and $Y_2(\vec{p}_2)$, and the coincidence yield, $Y_{12}(\vec{p}_1,\vec{p}_2)$:

$$Y_{12}(\vec{p}_1,\vec{p}_2) = C \cdot Y_1(\vec{p}_1) Y_2(\vec{p}_2)[1+R(q)] \quad . \qquad (1)$$

Here, $\vec{p}_1$ and $\vec{p}_2$ are the laboratory momenta of particles 1 and 2, respectively: q is the momentum of relative motion, and C is a normalization constant. The experimental correlation functions are obtained by inserting the measured yields into eq. 1 and summing both sides of the equation over all energies and angles corresponding to a given constraint. First exploratory measurements of light particle correlations at small relative momenta were performed for ^{16}O induced reactions at E/A=25 MeV, using a simple array of six ΔE-E telescopes each consisting of a silicon ΔE-detector and a NaI E-detector. Figure 1 shows the two-proton correlation function measured[13] for $^{16}O+^{197}Au$. The curves in the figure are the results

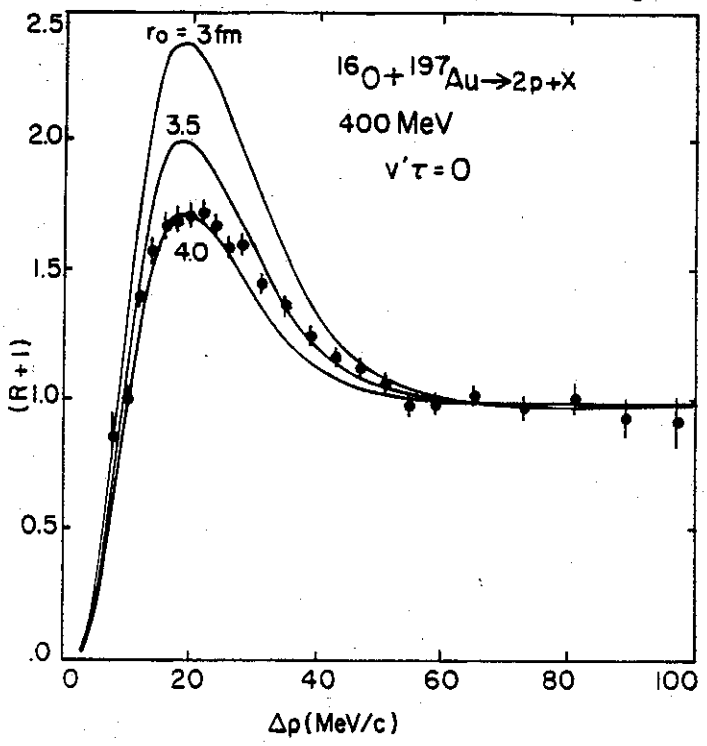

Fig. 1. Experimental two-proton correlation function (1+R(q)) measured for ^{16}O induced reactions on ^{197}Au at E/A=25 MeV. (Notation: q=Δp, Ref.13)

of model calculations[12] for the case of incoherent emission from a source of negligible lifetime and spatial density $\rho(r)=\rho_0 \cdot \exp(-r^2/r_0^2)$. For intermediate energy nucleus-nucleus collisions, these measurements provided the first experimental evidence for particle emission from localized subsets of nucleons. The investigation of the energy dependence of the two-proton correlation function revealed that the correlations become more pronounced

with increasing energy of the coincident particles, suggesting that more energetic particles originate from sources of relatively small space-time extent, whereas low energy particles are primarily emitted at the later, more equilibrated stages of the reaction.[13]

Information about the space-time extent of the emitting source may, in principle, be extracted from any two-particle correlation function. The simultaneous investigation of several different correlation functions could then provide a valuable test of the consistency of the method and could, in addition, provide information about the densities at which different degrees of freedom go out of equilibrium.[14] Figure 2 shows the first attempt to extract such information from the two-deuteron correlation function. The calculations shown in the figure were based on two different sets of

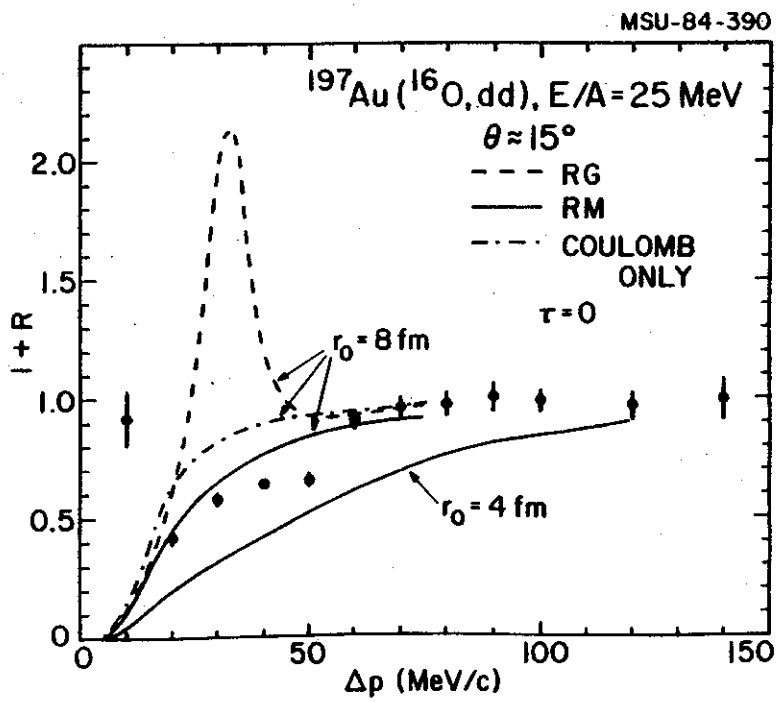

Fig. 2. Two-deuteron correlation function maesured for ^{16}O induced reactions on ^{197}Au at E/A=25 MeV. The solid and dashed curves correspond to calculations based on two different set of phase shifs. (Notation: q=Δp, Ref.14)

published phase shifts.[17,18] The data clearly favor the more recent set of phase shifts[18] which was extracted by a coupled channels R-matrix approach. Significantly larger source radii are extracted from the two-deuteron

correlation function than for the two-proton correlation function, possibly indicating that deuterons go out of equilibrium at a lower densities than protons.[14]

Population of Unbound States: As the excitation energy per nucleon is increased, new decay modes should become important such as the emission and subsequent decay of particle-unstable nuclei.[19-21] A consistent treatment of complex particle emission in intermediate nucleus-nucleus collisions is not yet available. For the decay of an equilibrated compound nucleus, however, the problem has been formulated in sufficient detail to warrant experimental investigation.[19,21] A first such attempt[22] was made for the case of ^{16}O induced reactions on ^{12}C and ^{27}Al at E/A=25 MeV. For these light targets, the single particle inclusive energy spectra at forward angles are compatible with considerable contributions from statistically emitting compound residues. (This stands in contrast to the negligible contributions at forward angles from compound-like residues observed for ^{197}Au.) This investigation showed that the two-proton correlations measured for these lighter targets were entirely consistent with statistical model calculations.[22]

The first determinations of "emission temperatures" from the relative yields of particle unbound states were performed for ^{40}Ar induced reactions on ^{197}Au at E/A=60 MeV by studying the decays: $^{6}Li^{*}\rightarrow\alpha+d$, $^{8}Be^{*}\rightarrow\alpha+\alpha$, $^{8}Be^{*}\rightarrow p+^{7}Li$, $^{5}Li\rightarrow p+\alpha$, $^{5}Li^{*}\rightarrow d+^{3}He$.[9,10] These measurements were performed with an improved hodoscope consisting of 13 elements. To illustrate the quality of the data, Figure 3 shows the $p+^{7}Li$ correlation function.[10] Emission temperatures of T≈4-5 MeV were extracted; they are considerably lower than the temperature parameters (T_0≈20 MeV) extracted from the kinetic energy spectra of the emitted light particles.[9,10] At present we cannot offer a quantitative explanation for this large discrepancy.

Emission Temperatures and Source Dimensions: The formal connection between the final state interaction model of Koonin[12] and statistical models has been established only recently:[16] to first order within the framework of equilibrium thermodynamics, the two-particle correlation function and the relative decay yields are independent functions of one variable each, the source volume and temperature, respectively. In this approximation, the two-particle correlation function and the relative population of states provide

independent information on the temperature and the space-time evolution of the emitting system.[16]

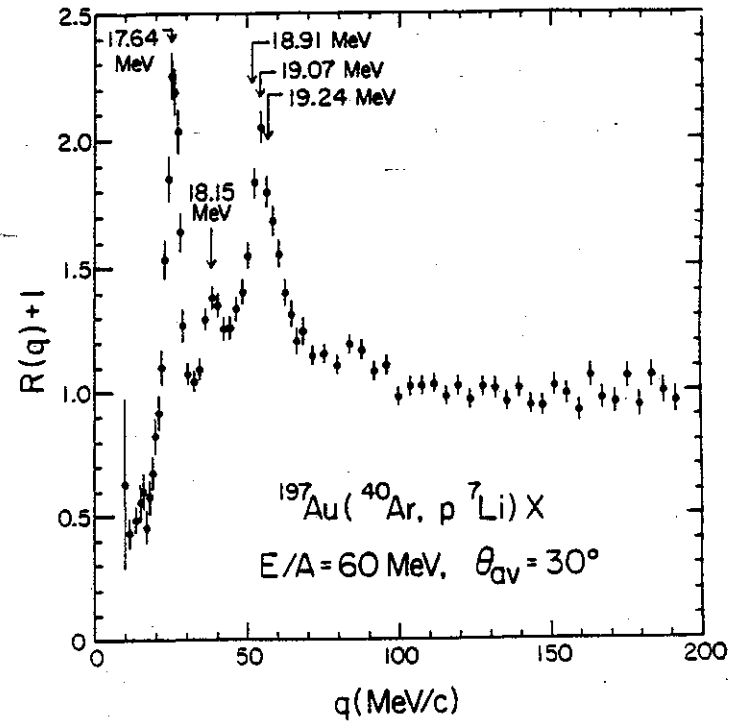

Fig. 3. Correlation function for coincident protons and ^{7}Li nuclei measured for ^{40}Ar induced reactions on ^{197}Au at E/A=60 MeV. (Ref. 10)

As an example, we briefly discuss the results of recent alpha-particle deuteron correlation measurements[11] performed at NSCL for ^{14}N induced reactions on ^{197}Au at E/A = 35 MeV. The experiment was performed with a close-packed hexagonal array of 13 ΔE-E telescopes, each consisting of a 400 μm thick Si detector and a 10 cm thick NaI detector. Each telescope subtended a solid angle of 0.94 msr; the angular separation between adjacent detectors was 6.1°. Measurements were performed with the center of the hodoscope positioned at laboratory angles of 35° and 50°.

Figure 4 shows the measured α-d correlation functions; in order to exhibit the energy dependence of these correlations, the following constraints were applied: $E_\alpha \geq$ 40 MeV, $E_d \geq$ 15 MeV and: 55 MeV < $E_\alpha+E_d \leq$ 100 MeV (left hand part), 100 MeV < $E_\alpha+E_d \leq$ 150 MeV (center part), 150 MeV < $E_\alpha+E_d \leq$ 220 MeV (right hand part). The α-d correlation functions exhibit two maxima corresponding to the T=0 state in ^{6}Li at 2.186 MeV ($J^\pi=3^+$, Γ=24 keV, $\Gamma_\alpha/\Gamma_{tot}$=1.00) and the overlapping T=0 states at 4.31 MeV ($J^\pi=2^+$, Γ=1.3 MeV, $\Gamma_\alpha/\Gamma_{tot}$=0.97) and at 5.65 MeV ($J^\pi=1^+$, Γ=1.9 MeV, $\Gamma_\alpha/\Gamma_{tot}$=0.74).

Calculations of the α-d correlation function corresponding to a generalization[15] of the final-state interaction model of ref. 12 are shown by the solid and dotted lines in Figure 4. A source of Gaussian spatial density, $\rho(r)=\rho_0 \cdot e^{-r^2/r_0^2}$, and negligible lifetime was assumed. The measured correlations do not exhibit a strong dependence on angle, but become more pronounced with increasing kinetic energies, $E_\alpha+E_d$, indicating that more energetic particles may originate from subsets of nucleons which are more localized in space-time. This feature is quantified by the estimated source radii summarized in Table 1.

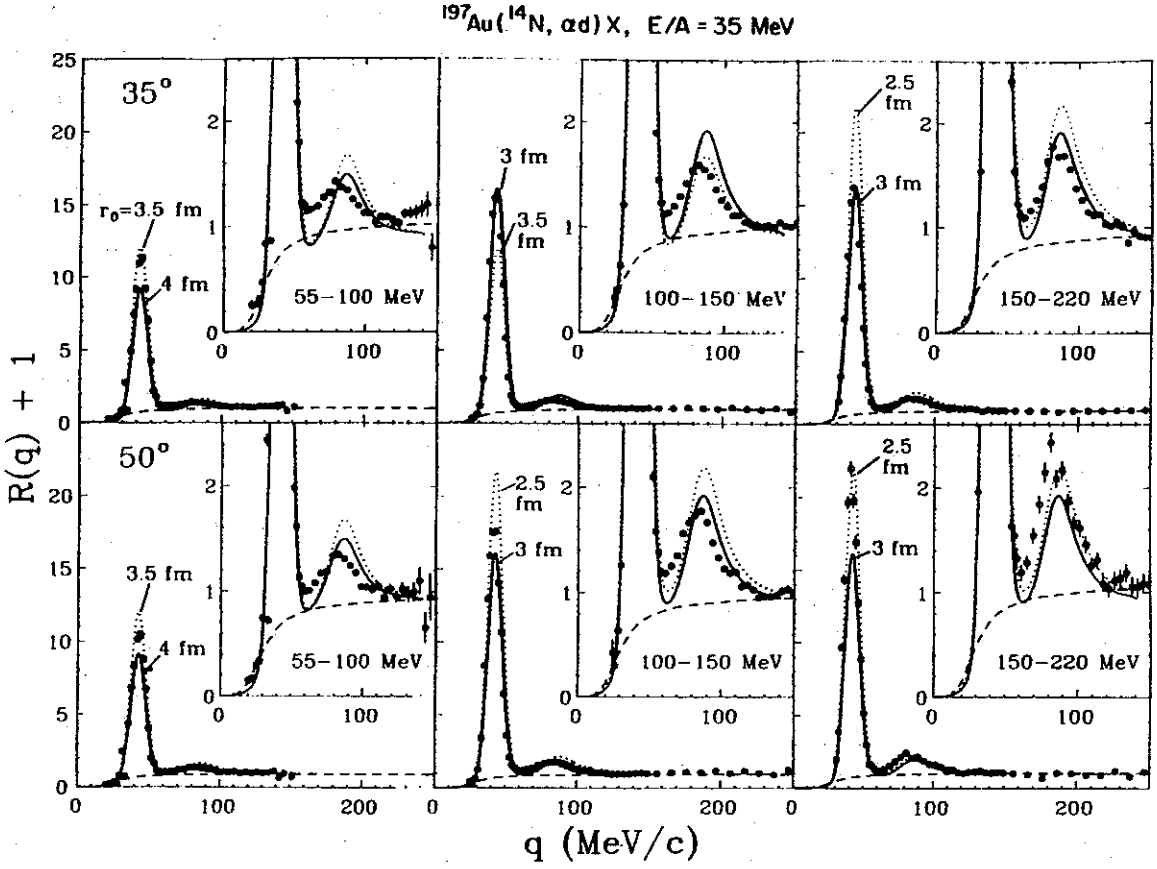

Fig. 4. Correlation functions measured for coincident deuterons and alpha particles for ^{14}N induced reactions on ^{197}Au at E/A=35 MeV. A detailed discussion of the figure is given in the text. (Ref.11)

Emission temperatures were obtained by comparing the experimental yield of particle unstable ^6Li nuclei with thermal calculations. The experimental yield of particle unstable decays $^6Li^* \rightarrow \alpha+d$, Y_c, was assumed to be given by $Y_c = Y_{\alpha d} - C \cdot Y_\alpha Y_d [1+R_b(q)]$, where the "background correlation function",[9] $R_b(q)$, is shown by the dashed lines in Fig. 4. The resulting yields are shown in Figure 5 as a function of the kinetic energy, $T_{c.m.}$, in the ^6Li

rest frame. The curves shown in the figure correspond to the theoretical coincidence yields, resulting from the decays of thermally emitted particle unstable ^{6}Li nuclei. The calculations incorporate efficiency and resolution of the hodoscope; for a detailed discussion see refs. 9-11. In order to

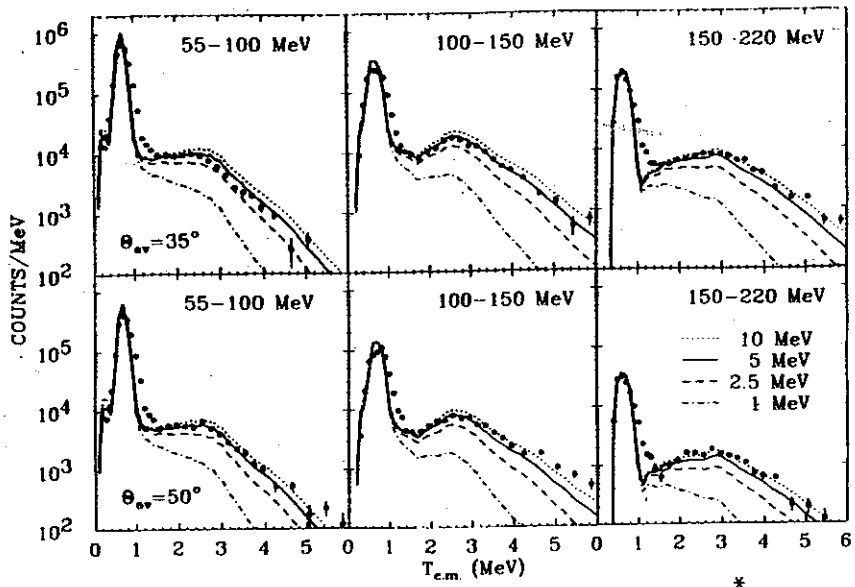

Fig. 5. Energy spectra resulting from the decay $^6Li^* \rightarrow \alpha+d$. A detailed discussion of the figure is given in the text. (Ref. 11)

extract emission temperatures, we have integrated the decay yields over the energy ranges of $T_{c.m.}$ = 0.25-1.45 and 1.5-6.25 MeV and compared the ratio of these yields to the corresponding theoretical ratio. The results are summarized in Table 1.

Table 1:

Emission temperatures and source radii extracted from the decay $^6Li^* \rightarrow \alpha+d$.

constraint on $E_1 + E_2$	θ = 35°		θ = 50°	
	T(MeV)	r_0(fm)	T(MeV)	r_0(fm)
55 - 220 MeV	4	3.4	4	3.6
55 - 100 MeV	4	3.8	3	3.9
100 - 150 MeV	4	3.0	5	2.8
150 - 220 MeV	7	3.0	9	2.7

Higher emission temperatures and smaller source radii are extracted for higher kinetic energies of the emitted particles. These findings are consistent with particle emission from a subsystem which is in the process of cooling and expanding. Cooling and expanding subsystems of high excitation could arise from the equilibration of participant matter with the surrounding cold target nuclear matter[2] or from an isentropic expansion as expected from intranuclear cascade calculations.[23]

The temperatures extracted from the α-d coincidence measurements shown in Figs. 4 and 5 are associated with considerable uncertainties (≈25%; see the discussion in ref. 9 due to uncertainties in the α-d background correlation function and due to the saturation of the coincidence yields at higher temperatures). More accurate temperature determinations can be made by measuring the relative populations of states separated by significantly larger energy intervals;[10] suitable decays are, for example: $^{5}Li_{0.0} \rightarrow \alpha+p$ and $^{5}Li_{16.7} \rightarrow d+^{3}He$, $^{8}Be_{3.0} \rightarrow \alpha+\alpha$ and $^{8}Be_{17.6} \rightarrow ^{7}Li+p$.

Three-Particle effects: Two-particle correlation functions can be affected by interactions with a third particle. We have recently isolated two such effects[24] in the α-p correlation function measured for ^{40}Ar-induced reactions on ^{197}Au at E/A=60 MeV. This correlation function is shown in Figure 6; it exhibits clear evidence for line shape distortions of the ^{5}Li decay spectrum which result from the Coulomb interaction with the heavy target residue. The lower part of the figure shows the splitting of the ^{5}Li-peak which depends on the relative magnitudes of the velocities of the decay products. The solid lines correspond to theoretical predictions of the effect.[24] The second anomaly in the α-p correlation function corresponds to the sharp peak at low relative momenta (q=15 MeV/c). This peak does not coincide with any known state of the α+p system; it can, however, be understood quantitatively[24] as due to the decay $^{9}B \rightarrow 2\alpha+p$.

Outlook: It is clear that we are only beginning to exploit measurements of two-particle correlations at small relative momenta. Much more can be learned with this technique. For example, little is known about the dependence of these correlations on the projectile energy. We plan to extend our measurements to higher projectile energies and heavier projectiles experiments with beams from the K500 and later the K800 cyclotrons. We plan

to complement these measurements with still higher energy experiments at the BEVALAC.

Our plans emphasize the investigation of two-particle correlations in coincidence with central collision triggers. Since all existing and planned multiplicity filters have restrictive count rate capabilities, it will be necessary to construct a more efficient detection system. This is one of our

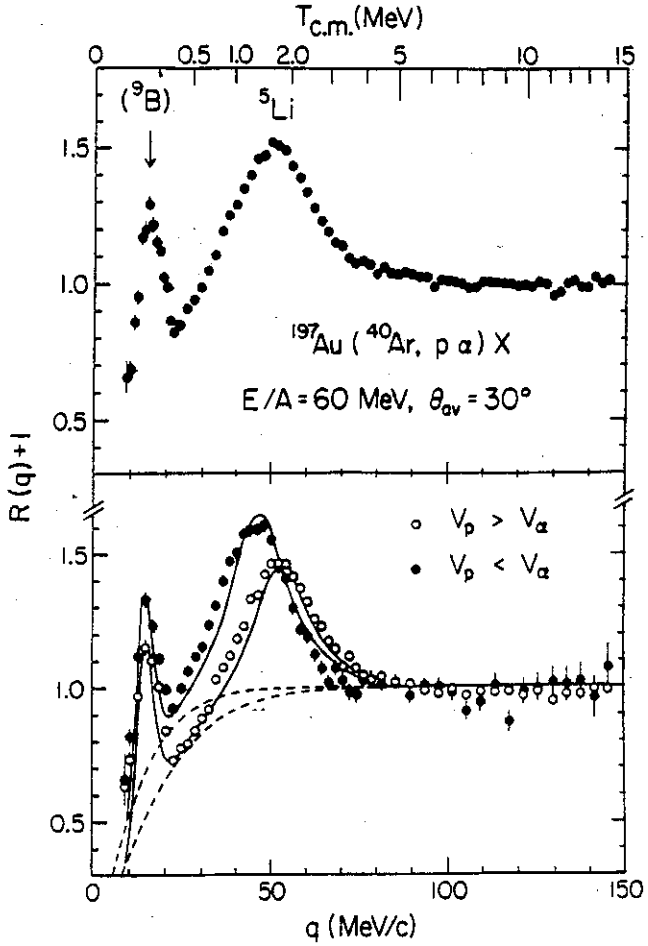

Fig. 6. Correlation function for coincident protons and α-particles measured for ^{40}Ar induced reactions on ^{197}Au at E/A=60 MeV. The upper part shows the energy integrated correlation function; the lower part shows the correlation functions subject to the constraints of $v_p > v_\alpha$ (open points) and $v_p < v_\alpha$ (solid points) in order to illustrate the line shape distortions resulting from the Coulomb interactions with the heavy target residue. The solid lines are theoretical line shapes. (Ref. 24)

major priorities. We plan to explore other two-particle correlations which have been inaccessible with the present apparatus. The extension of these measurements to the decays of much heavier fragments is discussed in Section A4(e). Correlations between neutrons and charged particles are discussed in both section A4(d) and (e). Finally, it will be important to have accurate calculations which incorporate the time dependence of the reaction, Coulomb final state interaction, and density fluctuations for the large variety of particle combinations for which two particle correlations can be measured.

a. See reference 13 for authors
b. See reference 9 for authors
c. D.H. Boal and J.C. Shillcock
d. W.A. Friedman and M.A. Bernstein

References:

1. B.V. Jacak, G.D. Westfall, C.K. Gelbke, L.H. Harwood, W.G. Lynch, D.K. Scott, H. Stöcker, M.B. Tsang, and T.J.M. Symons, Phys. Rev. Lett. 51,1846(1983)
2. D.J. Fields, W.G. Lynch, C.B. Chitwood, C.K. Gelbke, M.B. Tsang, H. Utsunomiya and J. Aichelin, Phys. Rev. C 30,1912(1984)
3. R. Stock, R. Bock, R. Brockmann, J.W. Harris, A. Sandoval, H. Stroebele, K.L. Wolf, H.G. Pugh, L.S. Schroeder, M. Maier, R.E. Renfordt, A. Dacal, and M.E. Ortiz, Phys. Rev. Lett. 49,1236(1982)
4. J.W. Harris, R. Bock, R. Brockmann, A. Sandoval, R. Stock, H. Stroebele, G. Odyniec, H.G. Pugh, L.S. Schroeder, R.E. Renfordt, D. Schall, D. Bangert, W. Rauch, and K.L. Wolf, Phys. Lett. 153B,377(1985)
5. G.D. Westfall, B.V. Jacak, N. Anantaraman, M.W. Curtin, G.M. Crawley, G.K. Gelbke, B. Hasselquist, W.G. Lynch, D.K. Scott, M.B. Tsang, M.J. Murphy, T.J.M. Symons, R. Legrain, and T.J. Majors, Phys. Lett. 116B,118(1982)
6. P.J. Siemens and J.O. Rasmussen, Phys. Rev. Lett. 42,880(1979)
7. D.J. Morrissey, W. Benenson, E. Kashy, B. Sherrill, A.D. Panagiotou, R.A. Blue, R.M. Ronningen, J. van der Plicht, and H. Utsunomiya, Phys. Lett. 148B,423(1984)
8. D.J. Morrissey, W. Benenson, E. Kashy, C. Bloch, M. Lowe, R.A. Blue, R.M. Ronningen, B. Sherrill, H. Utsunomiya, and I. Kelson, Phys. Rev. C 32,877(1985)
9. J. Pochodzalla, W.A. Friedman, C.K. Gelbke, W.G. Lynch, M. Maier, D. Ardouin, H. Delagrange, H. Doubre, C. Grègoire, A. Kyanowski, W. Mittig, A. Pèghaire, J. Pèter, F. Saint-Laurent, Y.P. Viyogi, B. Zwieglinski, G. Bizard, F. Lefèbvres, B. Tamain, and J. Quèbert, Phys. Rev. Lett. 55,177(1985)
10. J. Pochodzalla, W.A. Friedman, C.K. Gelbke, W.G. Lynch, M. Maier, D. Ardouin, H. Delagrange, H. Doubre, C. Grègoire, A. Kyanowski, W.

Mittig, A. Pèghaire, J. Pèter, F. Saint-Laurent, Y.P. Viyogi, B. Zwieglinski, G. Bizard, F. Lefèbvres, B. Tamain, and J. Quèbert, Phys. Lett. 161B(1985)275
11. C.B. Chitwood, C.K. Gelbke, J. Pochodzalla, Z. Chen, D.J. Fields, W.G. Lynch, R. Morse, M.B. Tsang, D.H. Boal, and J.C. Shillcock, Michigan State University preprint MSUCL-525
12. S.E. Koonin, Phys. Lett. 70B (1977) 43
13. W.G. Lynch, C.B. Chitwood, M.B. Tsang, D.J. Fields, D.R. Klesch, C.K. Gelbke, G.R. Young, T.C. Awes, R.L. Ferguson, F.E. Obenshain, F. Plasil, R.L. Robinson and A.D. Panagiotou, Phys. Rev. Lett. 51 (1983) 1850
14. C.B. Chitwood, J. Aichelin, D.H. Boal, G. Bertsch, D.J. Fields, C.K. Gelbke, W.G. Lynch, M.B. Tsang, J.C. Shillcock, T.C. Awes, R.L. Ferguson, F.E. Obenshain, F. Plasil, R.L. Robinson, and G.R. Young, Phys. Rev. Lett. 54,302(1985)
15. D.H. Boal and J.C. Shillcock, Phys. Rev. C (in press)
16. D.H. Boal, B.K. Jennings, and J.C. Shillcock, private communication
17. F.S. Chwieroth, Y.C. Tang, and D.R. Thompson, Nucl. Phys. A189 (1972) 1
18. G.M. Hale and B.C. Dodder, "Few-Body Problems in Physics, edited by B. Zeidnitz, Elsevier, Amsterdam, 1984, Vol. 2, p.433
19. W. Friedman and W.G. Lynch, Phys. Rev. C 28,16,960(1983)
20. M.A. Bernstein, W.A. Friedman, and W.G. Lynch, Phys. Rev. C 29,132(1984)
C.K. Gelbke, Comments Nucl. Part. Phys. 11,259(1983)
22. M.A. Bernstein, W.A. Friedman, W.G. Lynch, C.B. Chitwood, D.J. Fields, C.K. Gelbke, M.B. Tsang, T.C. Awes, R.L. Ferguson, F.E. Obenshain, F. Plasil, R.L. Robinson, and G.R. Young, Phys. Rev. Lett. 54,402(1985)
23. G. Bertsch and J. Cugnon, Phys. Rev. C 24,2514(1981)
24. J. Pochodzalla, W.A. Friedman, C.K. Gelbke, W.G. Lynch, M. Maier, D. Ardouin, H. Delagrange, H. Doubre, C. Grègoire, A. Kyanowski, W. Mittig, A. Pèghaire, J. Pèter, F. Saint-Laurent, Y.P. Viyogi, B. Zwieglinski, G. Bizard, F. Lefèbvres, B. Tamain, and J. Quèbert, Phys. Lett.161B(1985)256

III.A.4.c. MULTI-PARTICLE CORRELATIONS

G.D. Westfall, G.M. Crawley, H. van der Plicht and R.S. Tickle[a].

A great deal of information concerning the reaction mechanism of intermediate energy nucleus-nucleus collisions has been learned from the study of inclusive reactions. However, when detailed models are compared with these data, models incorporating radically different assumptions describe the data equally well. Thus, we have embarked on a series of experiments designed to select specific topological and kinematic situations to study questions such as the relative importance of direct versus thermal phenomena, the size of the emitting system, and the evolution of the participant zone as a function of the degree of centrality of the collision.

One of the most puzzling questions to be answered is the question of whether thermalization is reached in these collisions. Recent results by Morrissey, et. al.,[1] and by Pochodzalla, et al.,[2] demonstrate that the apparent temperature of the kinetic energy spectra does not agree with the apparent temperature of the complex fragments. In contrast, there is a large body of evidence that argues for thermalization, both kinetic and chemical, in intermediate energy nucleus-nucleus collisions. The most eloquent is the fact that both light particles and complex fragments appear to originate from a common source.[3]

The apparent thermal nature of inclusive spectra may be due to other effects besides thermalization, such as the fact that averaging over many separate events, each of which is not thermal or may not be thermalized, may produce spectra that on the average appear to be thermal. To remove this average over different types of events, we have undertaken a series of triggered experiments to select out a given type of event topology and study the light particle spectra associated with these phenomena. The two types of events selected are those in which an intermediate rapidity fragment (IRF) is emitted at large angles (which should signify a violent collision) and events in which a projectile-like fragment (PLF) survives the collision (which can be characterized as a grazing collision).

Proton spectra triggered on IRFs with $3 \leq Z \leq 6$ for 30 MeV/nucleon ^{12}C+Al are shown in Fig. 1.[4] Spectra for protons coincident with IRFs from 92

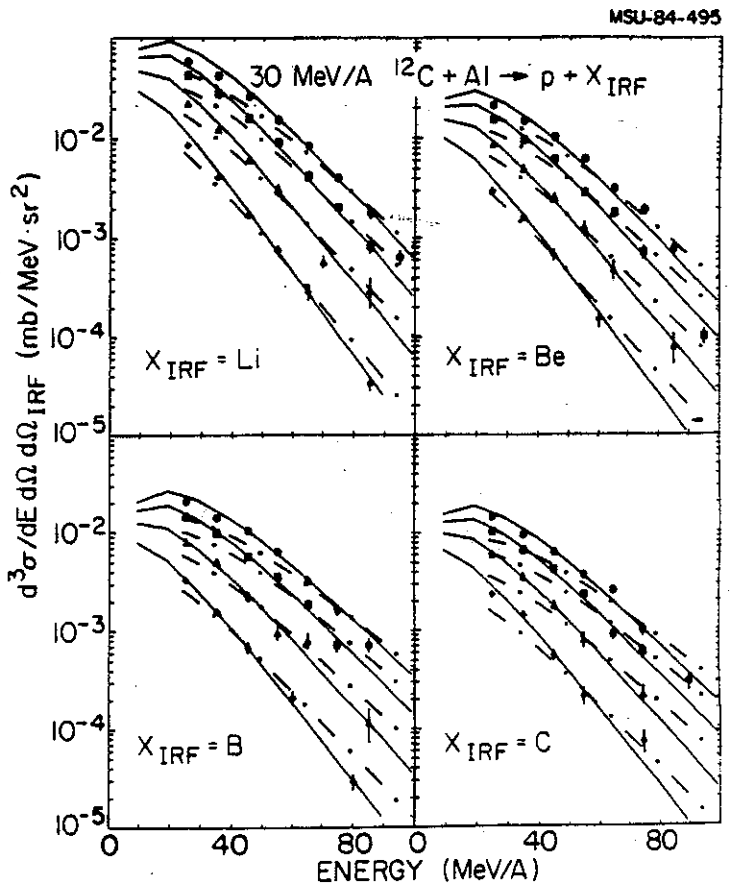

Fig. 1. Proton spectra from 30 MeV/A ^{12}C+Al triggered by intermediate rapidity fragments (IRF's). The spectra were measured at 45° (circles), 56° (squares), 71° (triangles), and 90° (diamonds). The solid lines represent moving source fits and the dot - dashed lines show momentum conservation model calculations.

MeV/nucleon ^{40}Ar+Au are shown in Fig. 2.[4] The inclusive light particle spectra have been included in the figures for comparison with the coincidence spectra. The coincidence spectra have the same general features as the inclusive spectra for all measured light particle-IRF combinations suggesting that these fragments have a common source. The solid curves in the Figs. 1 and 2 are moving source fits to the IRF-triggered data.

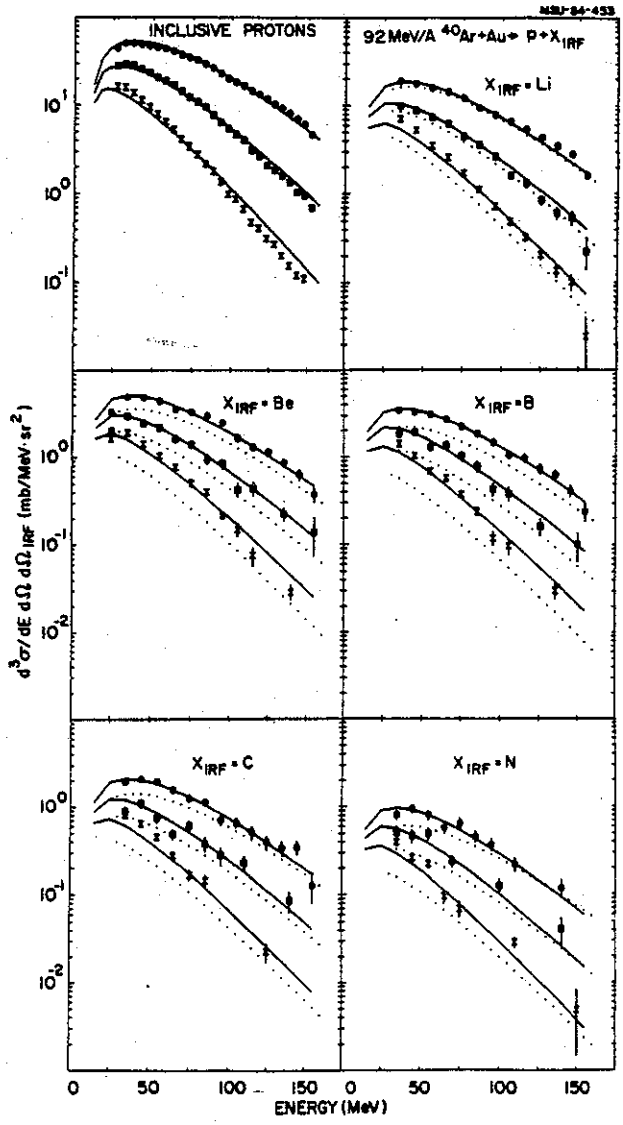

Fig. 2. Inclusive and intermediate rapidity fragment (IRF) triggered spectra for protons from 92 MeV/A ^{40}Ar+Au at 45° (circles), 67.5° (squares), and 90° (hourglasses). The solid lines represent moving source fits, and the dotted lines show the momentum conservation model.

These fits describe the data very well and only deviate significantly for the p-Li coincidences from both targets at 30 MeV/nucleon. The extracted temperatures and velocities for the IRF triggered light particle coincidence spectra are shown in Figs. 3 and 4 as ratios of the coincidence

values to the inclusive values. These ratios demonstrate that the extracted IRF-triggered temperatures tend to be about 5% higher than the inclusive temperatures at 92 MeV/nucleon, but are about the same at 30 MeV/nucleon. There does not appear to be any statistically significant variation in this parameter over the range of trigger fragments measured.

Figs. 3 and 4 also show that the extracted coincidence spectra

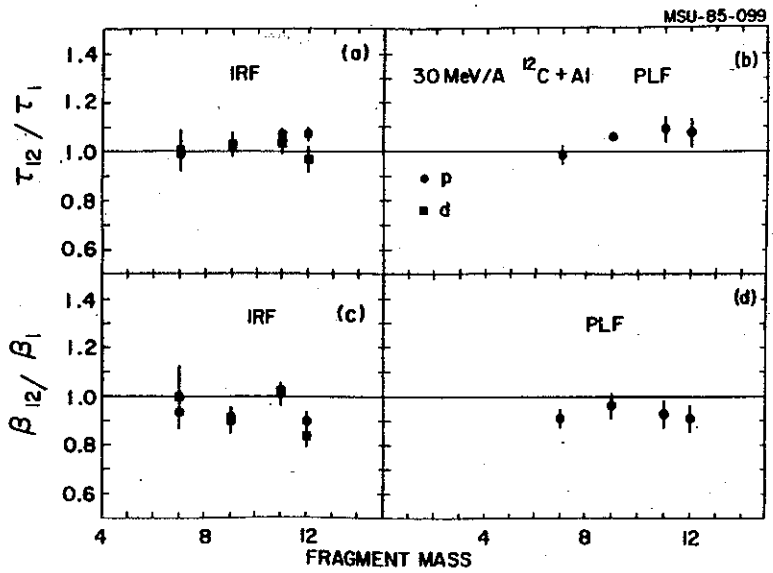

Fig. 3. Ratios of Moving source parameters extracted from triggered and inclusive proton and deuteron spectra from 30 MeV/A ^{12}C+Al. The trigger in (a) and (c) is intermediate rapidity fragments (IRF's), and in (b) and (d) it is projectile like fragments (PLF's).

Fig. 4. Ratios of moving source parameters extracted from triggered and inclusive p,d,t, ^{3}He and ^{4}He spectra from 92 MeV/A ^{40}Ar+Au. The trigger in (a) and (c) is intermediate rapidity fragments (IRF's), and (b) and (d) it is projectile like fragments (PLF's).

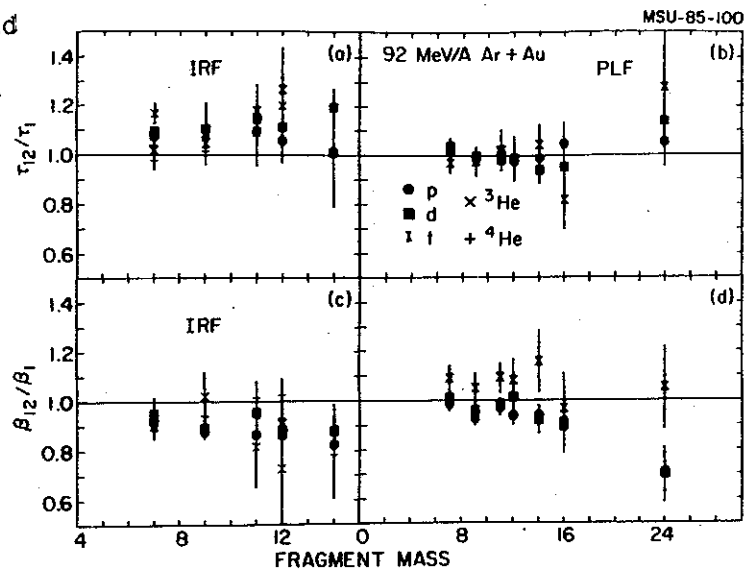

velocities tend to be lower than the inclusive velocities by about 10%. There are indications of a decrease in the velocity parameter with increased trigger fragment mass. There seems to be no significant dependence of the temperature and velocity parameters on the particular type of light particle measured. The apparent differences between the ^{3}He parameters and those of the other light isotopes may be due to the lower statistics of the ^{3}He spectra.

Coincidence spectra between protons and PLFs from 30 MeV/nucleon ^{12}C + Al are shown in Fig. 5,[4] and those for 92 MeV/nucleon ^{40}Ar + Au[4] in Fig. 6.

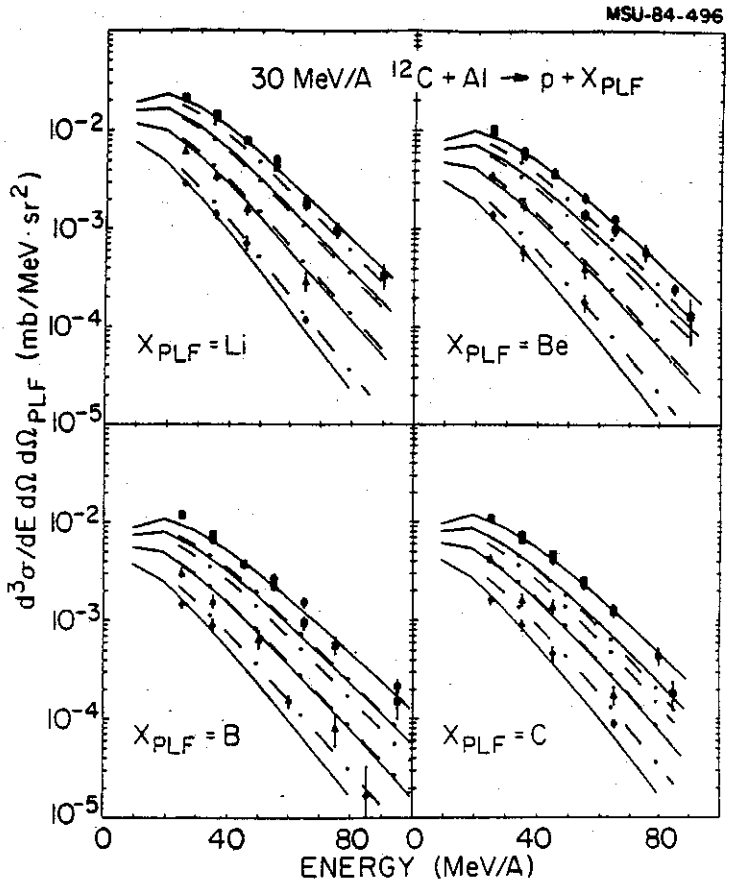

Fig. 5. Proton spectra from 30 MeV/A ^{12}C+Al triggered by projectile like fragments (PLF's). The spectra were measured at 45° (circles), 56° (squares), 71° (triangles), and 90° (diamonds). The solid lines represent moving source fits and the dot-dashed lines show momentum conservation model calculations.

The spectra for coincident fragments with $9 \leq Z \leq 15$ have been summed together to obtain reasonable statistics. The inclusive light particle spectra have been included in this figure for comparison with the coincidence spectra. The light particle coincidence spectra for the Li through N PLF triggers

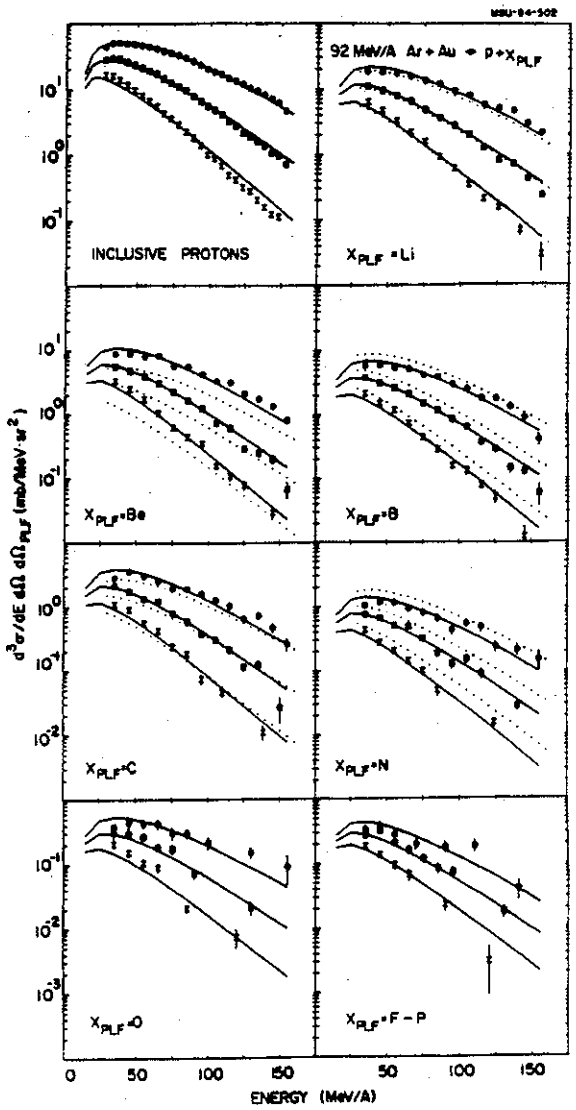

Fig. 6. Inclusive and projectile like fragment (PLF) triggered spectra for protons from 92 MeV/A ^{40}Ar+Au at 45° (circles), 67.5° (squares), and 90° (hourglasses). The solid lines represent moving source fits and the dotted lines show the momentum conservations model.

appear to be very similar to the inclusive spectra. It can be seen that the proton coincidence cross sections for the O and the F through P PLF triggers have a slightly flatter angular distribution than the inclusive cross sections characteristic of a lower source velocity.

The temperatures and velocities are plotted in Figs. 3 and 4 as ratios of the coincident values to the inclusive values. Note that the parameters for spectra summed over coincidences with F through P fragments are plotted at an approximate average mass of 24. As was true for the light particle - IRF spectra, the temperature parameter shows no variation with the PLF trigger fragment mass. In addition, source temperatures of the spectra triggered by PLFs are the same as the inclusive temperature. This constancy could reflect the fact that the PLF spectra at 13° may contain a large contribution from thermal sources. In contrast, the velocities show a clear trend toward decreasing velocities with increasing trigger fragment mass for the proton and deutron spectra. An apparent velocity 30% below the inclusive result is obtained for the average projectile mass of A=24 which is consistent with the concept of emission from an excited residual target nucleus.

Further evidence for thermalization comes from light particle correlation measurements by Fox, et. al.[5] In this experiment the relative contribution of direct vs. thermal components was studied in reactions of 40 MeV/nucleon ^{12}C + C, where in-plane vs. out-of-plane correlations were studied. Light particle telescopes were placed at $(\theta,\phi)=(45°,90°)$ and $(45°,180°)$ and another telescope was moved from $\theta=25°$ to 120° at $\phi=0°$. No peak was observed in the ratio of in- to out-of-plane proton-proton correlations at energies and angles corresponding to quasi-elastic scattering. In Fig. 7 the ratio of the in-plane to out-of-plane p-p coincidence spectra for the case of the movable detector at 45° is shown as a function of energy in the movable telescope. The correlations are integrated over all proton energies in the other two telescopes (one in-plane and one out-of-plane) covering the range from 10 to 160 MeV. This ratio is constant as a function of energy up to 60 MeV and then apparently

increases although the statistics are poor. The average value for the ratio at this angle is 1.08 ± 0.01. There is clearly no peak at 20 MeV in the ratio of in-plane to out-of-plane coincidence spectra as one would expect from free proton-proton scattering.

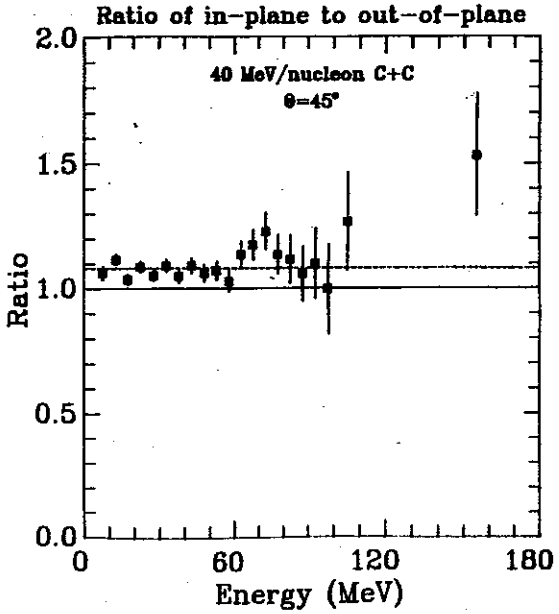

Fig. 7. Ratio of in-plane to out-of-plane proton-proton correlations as a function of energy, as measured in 40 MeV/A ^{12}C+C.

We have also extended the present measurements to target-like fragment/light particle correlations and projectile-like/light particle correlations where we were able to measure the coincident light particle spectra on both the same side and opposite side of the reaction plane as the trigger counters.[6] Preliminary analysis shows that a very strong effect is observed for light particles in coincidence with target-like fragments (TLFs) with $3 \leq Z \leq 7$ in which a strong enhancement in the opposite side emission was observed.

In the future we plan to extend these measurements to include incomplete fusion products in coincidence with light particles[7] as well as high energy gamma rays in coincidence with light particles.[8] In addition, we plan to study the correlation of light particles and complex fragments

from high energy nucleus-nucleus collisions using the HISS spectrometer. This work will complement our extensive program in inclusive measurements at these energies.

a. University of Michigan.

References:

1. D.J. Morrissey, W. Benenson, E. Kashy, B. Sherrill, A.D. Panagiotou, R.A. Blue, R.M. Ronningen, J. van der Plicht, and H. Utsunomiya, Phys. Lett. 148B,423(1984).
2. J. Pochodzalla et al., Phys. Rev. Lett. 55,177(1985).
3. B.V. Jacak, G.D. Westfall, C.K. Gelbke, L.H. Harwood, W.G. Lynch, D.K. Scott, H. Stoecker, M.B. Tsang, and T.J.M. Symons, Phys. Rev. Lett. 51, 1846(1983).
4. B.E. Hasselquist, G.M. Crawley, B.V. Jacak, Z.M. Koenig, G.D. Westfall, J.E. Yurkon, R.S. Tickle, J.P. Dufour, and T.J.M. Symons, Phys. Rev. C32,145(1985).
5. D.Fox, D.A. Cebra, Z.M. Koenig, J.J. Molitoris, P. Ugorowki, H. Stöcker, and G.D. Westfall, submitted to Phys. Rev. C,(1985).
6. Z.M. Koenig, G.D. Westfall, D. Fox, D. Cebra, J. Wilcyinski, K. Siwek-Wilcyinska, and R.S. Tickle, to be published.
7. D. Cebra, G.D. Westfall, D. Fox, H. van der Plicht, S. Angius, G.M. Crawley, NSCL exp.
8. J. Stevenson, E. Kashy, W. Benenson, R. Smith, G.D. Westfall, D. Cebra, D. Fox, U. Chen, NSCL exp.

III.A.4.d. NEUTRON EMISSION FROM DISCRETE STATES IN HEAVY-ION COLLISIONS

A. Galonsky, B.A. Remington,[a] A. Kiss,[b] F. Deak,[b] Z. Seres,[c]

A common way of parameterizing particle spectra is to assume thermal evaporation from hot, moving sources and then determine the temperatures and velocities of the sources. Within this framework we know that the low-energy part of a spectrum is populated by a relatively low-temperature, slowly-moving, target-like source.[1] The high-energy part of a spectrum is often attributed to an intermediate-rapidity source--a source of higher temperature and of speed about one-half the projectile speed.[2,3]

It has been recognized, however, that one mode of particle emission is not accommodated by this description. This occurs when a light fragment of the collision particle-decays from a discrete unbound state.[4-9] Then we have a moving source of particles of one specific energy. For example, a ^{13}C fragment ejected from the nuclear collision in its excited state at 6.87 MeV decays by emitting a neutron of 1.918 MeV with respect to the ^{13}C fragment. With respect to the laboratory, the neutron energy is determined by vector addition of the two velocities, and the extreme values of neutron energy can by quite far apart--3.2 and 20.7 MeV if the ^{13}C fragments have 10 MeV per nucleon.

In order to study the role of discrete, particle-unbound states, we measured neutron spectra in coincidence with light fragments resulting from collisions of ^{14}N projectiles at 35 MeV per nucleon with a ^{165}Ho target. The fragments were detected by ΔE-E silicon telescopes, one at an angle of +10° and another at -30° relative to the beam axis. NE 213 liquid scintillator counters were employed to detect the coincident neutrons, and the method of time-of-flight was used to determine the neutron energies. One of the neutron detectors was positioned at +10° and another one at -30° in colinear geometry with the corresponding ΔE-E telescopes.

Figure 1 shows neutron energy spectra in coincidence with boron fragments of 7-14, 14-21, 21-28, and 28-35 MeV per nucleon at 10° and 14-21

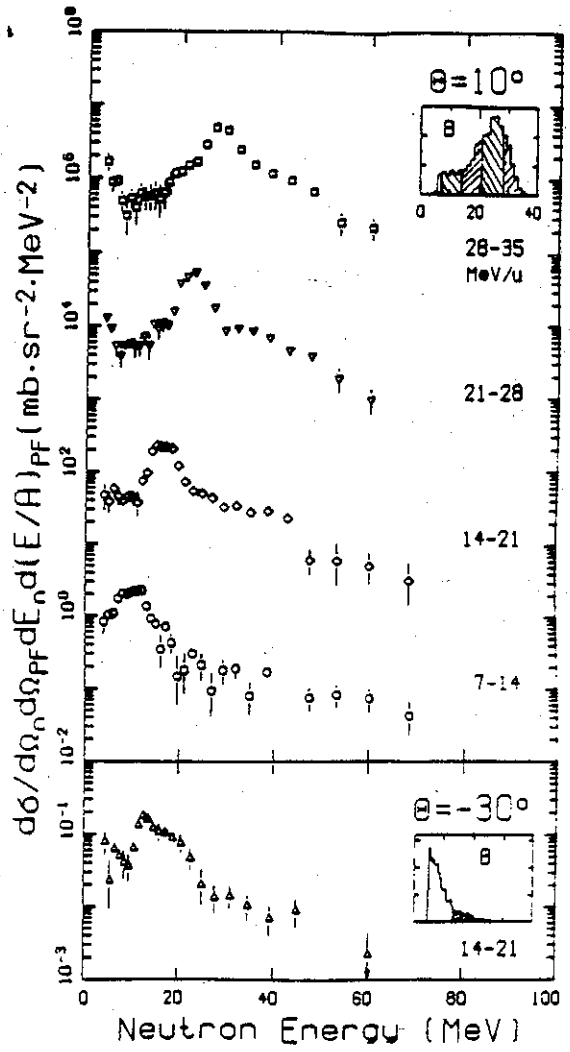

Fig. 1 Neutron energy spectra in coincidence with boron isotopes having energy per nucleon 7-14, 14-21, 21-28 and 28-35 MeV for +10° (upper part) and 14-21 MeV for -30° (lower part). The inserts show the corresponding boron energy distributions.

MeV per nucleon at 30°. In each spectrum one can see a dominant enhancement at neutron energies equal to the average energy-per-nucleon of the coincident fragment; the yield of the enhancement is about one-half of the total. The inserts in Fig. 1 display the corresponding boron energy distributions at 10° and 30° in coincidence with the neutrons. That the fragment distributions are clearly very different for the two cases, suggests different reaction mechanisms for 10° and 30°. Nevertheless, the enhancements dominate the neutron energy spectra at both angles. Similar structures, but with different widths and strengths, can be seen in neutron energy spectra coincident with reaction fragments of other light elements such as Li, Be, and C.

These enhancements, always correlated with the velocity of the fragment, suggest that the neutron spectra should be plotted as a function of the relative velocity between neutron and fragment. Such relative velocity spectra are shown in Fig. 2 for both fragments and neutrons

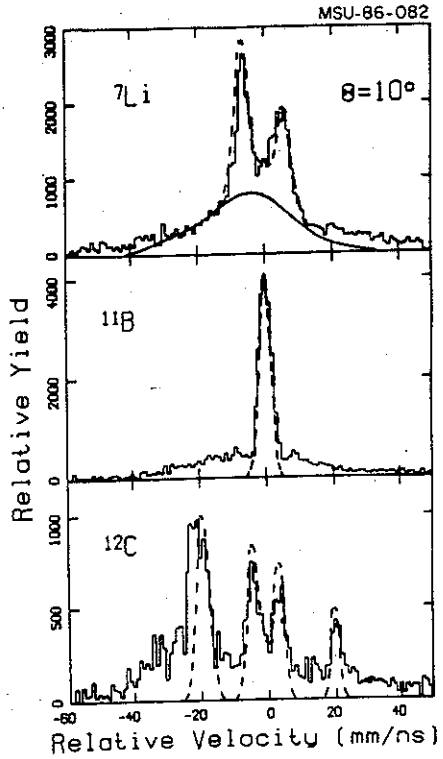

Fig. 2. Coincident fragment-neutron relative velocity spectra for ^{7}Li, ^{11}B and ^{12}C at +10°. The abcissa is fragment velocity minus neutron velocity. Dashed lines are results of Monte Carlo simulations of discrete neutron decays. For ^{7}Li there is also a simulation (solid line) of thermal emission of neutrons.

detected at 10°. The parent nuclei are ^{8}Li, ^{12}B, and ^{13}C. In each coincident event the velocity of the fragment was calculated from its measured kinetic energy after establishing its isotopic identity, and the velocity of the neutron was derived from its flight time.

Each relative velocity spectrum is dominated by structure caused by the decay of a particle-unstable nucleus. This structure is also observed at 30°. We have uniquely identified the discrete transitions responsible for the major peaks. The relevant parameters of those transitions are listed in Table I. For ^{11}B, where the decay energies are only 19 keV, there is a single peak centered at zero relative velocity--a simple case of kinematic focusing. But for ^{7}Li, where the decay energy is 222 keV, there is a pair of peaks centered about zero relative velocity. In this case the neutron detector solid angle is not big enough to capture all of the neutrons emitted from a fragment headed towards the detector. Instead, we get a forward peak ($v_f - v_n < 0$) and a backward peak.

Table I. Parameters of the levels in the neutron decays associated with the peaks in Fig. 2.

Detected Fragment	Parent State Nuclide	E_x(MeV)	Γ(keV)	Daughter E_x(MeV)	Decay E_{decay}(MeV)	Rel.Vel. (mm/ns)
^{7}Li	^{8}Li	2.255	33	0	0.222	7.0
^{11}B	^{12}B	3.389	3.1	0	0.019	1.9
^{12}C	^{13}C	6.864	6	0	1.918	20
^{12}C	^{13}C	9.500	5	4.439	0.114	5.0

The same is true for ^{12}C, but there are four prominent peaks corresponding to two transitions. The peaks at ±20 mm/ns in Fig. 2 arise from decay of the first unbound state of ^{13}C augmented by decays from a triplet of states 0.7 MeV higher. Here, the neutron energy is so high that we cannot resolve the individual states and there is a sizeable difference in the solid angles

for accepting forward and backward neutrons. The peaks at ±5 mm/ns correspond to decay from a more highly excited state, at 9.50 MeV, but to the 4.44-MeV state of ^{12}C rather than to the ground state. The solid angle for detecting the 4.44-MeV branch is much greater than for detecting the ground-state branch. In addition, it has recently been found in a ^{12}C (d,p) experiment that most of the wave function of the 9.50-MeV state consists of a neutron coupled to the 4.44-MeV state of ^{12}C.[10]

The actual shape of a line (or pair of lines) depends on many parameters of the experiment, such as the 3-dimensional finite geometry of the fragment and neutron detectors, the angular and energy distributions of the fragments, the experimental time resolutions of the fragment and neutron detectors, the recoil of the fragment from the decay of the parent, the pulse-height thresholds of the detectors, the energy dependence of the neutron detection efficiency, and the width and decay energy of the parent state. Estimating where necessary, we put these quantities into a Monte Carlo code for each of the transitions in Fig. 2. Normalizing each transition to the data, we obtained the results given by the dashed lines in the figure. The simulations do reproduce the most important features of the experimental spectra. For the lines at ±20 mm/ns in the ^{12}C spectrum the computation included only the first unbound state; the triplet above it accounts for the broadening of these lines.

Since discrete lines do not account for the entire spectrum in any case, we used the Monte Carlo code for ^{7}Li at 10° to determine whether a thermal spectrum could account for the continuum under the lines. The solid line in the top part of Fig. 2 is the result for an assumed source temperature of 2.5 MeV. The distribution of source velocities was that obtained from the measured spectrum of ^{7}Li fragments. The thermal contribution is about equal to that of the single discrete line. For the other isotopes in Fig. 2 the thermal part is relatively smaller. In all cases there may be contributions from other discrete transitions which are too small for unambiguous analysis with the velocity resolution and statistical accuracy we have achieved in this first experiment. At 30°, where central collisions dominate, discrete emission is equally important. This means that even in inclusive measurements not all of a spectrum has a thermal origin, and thermal parameters derived neglecting this fact are somewhat in error. The same is true of proton spectra.

Where more than one discrete state can be discerned in a relative velocity spectrum, it is interesting to determine the relative populations of the states. If these excited nuclei are boiled out of hot nuclear matter in thermal equilibrium, their populations are determined only by a Boltzmann factor that depends on the spins of the states and the temperature of the hot nuclear matter. Conversely, a measurement of the relative populations of two states of known spins determines the temperature. This idea has been used by Morrissey, et al.,[11] to analyze the gamma decays of excited ^{7}Li, ^{8}Li and ^{7}Be nuclei. These results are discussed in Section A4(a). Unexpectedly, the temperature determined from the relative populations of particle-stable excited states was much lower ($\approx$ 0.5 MeV) than the temperature determined by the slopes of the fragment energy spectra. There have been a number of conjectures about this discrepancy, but so far no clear solution has emerged. In any case, more data is clearly needed.

From the data in Fig. 2 it is obvious that we can determine a temperature with respect to excited ^{13}C nuclei. The preliminary result is 1.0 to 1.5 MeV. It should be remembered that these data are for fragments and neutrons emitted at 10°, an angle close to the grazing angle. The assumption of thermal equilibrium may not be valid at this angle. At 30°, where central collisions may dominate, we have data which are colinear, but of very low statistical accuracy. Nevertheless, the value extracted from those data is consistent with 1.0 to 1.5 MeV. We will soon extract a temperature from the slopes of the ^{13}C inclusive spectra to compare with these results.

These initial results occurred as a byproduct of a broader investigation of intermediate energy nucleus-nucleus collisions[12,13] which was partly discussed in Section A1(d). The neutron detection apparatus was certainly not optimized to study the relative populations of particle unbound excited states of emitted nuclei. For future experiments, we plan to collaborate with C.K. Gelbke and W. Lynch in the development of a highly efficient and granular neutron detection array. Our current plans involve the construction of approximately 30 NE213 liquid scintillator counters. The geometry and resolution of the array will be studied with existing Monte-Carlo codes to achieve the optimal dynamic range, detection efficiency, and energy resolution.

With the new array, we will be able to address a broad spectrum of issues:

We will measure the neutron decays of particle-unbound emitted fragments. For states where sufficient spectroscopic information exists, we will determine the relative populations of particle-unbound states that neutron decay. The neutron measurements will be combined with high-resolution, charged-particle coincidence studies (discussed in Section A4(b) to obtain emission temperatures for particle-unstable fragments and to determine the relative importance of direct-emission vs. secondary-decay processes in determining the observed yields and spectra of complex particles.[14-16] This latter issue is especially relevant whenever one attempts to relate the experimental observables to the thermodynamic properties of the excited nuclear system created in these collisions.

We will test conclusions obtained with charged particle correlation techniques concerning the space-time localization of the subsystems which emit energetic neutrons.[17] Direct comparisons of the n-n, n-p and n-α correlations with p-p and p-α correlations should help to test the consistency of the correlation analysis. In addition, these correlations should provide the ideal experimental constraints needed to refine calculations which predict the three-body Coulomb distortions of the two-particle correlation function at small relative momentum.[14,18]

a Eötvös University, Budapest
b Central Research Institute, Budapest
c Present address - Rose-Hulman Institute of Technology

References:

1. D. Hilscher, J.R. Birkelund, A.D. Hoover, W.U. Schröder, W.W. Wilcke, J.R. Huizenga, A.C. Mignerey, K.L. Wolf, H.F. Breuer and V.E. Viola, Jr., Phys. Rev. C 20,576(1979).
2. T.C. Awes, S. Saini, G. Poggi, C.K. Gelbke, D. Cha, R. Legrain and G.D. Westfall, Phys. Rev. C 25,2361(1982).
3. C.K. Gelbke, Nucl. Phys. A400,473c(1983).
4. A. Gavron, J.R. Beene, R.L. Ferguson, F.E. Obenshain, F. Plasil, G.R. Young, G.A. Petitt, K. Geoffroy Young, M. Jääskeläinen, D.G. Sarantites and C.F. Maguire, Phys. Rev. C 24,2048(1981).
5. I. Tserruya, A. Breskin, R. Chechnik, Z. Fraenkel, S. Wald, N. Zwang, R. Bock, M. Dakowski, A. Gobbi, H. Sann, R. Bass, G. Kreyling, R. Renfordt, K. Stelzer and U. Arlt, Phys. Rev. C 26,2509(1981)
6. E. Holub, D. Hilscher, G. Ingold, U. Jahnke, H. Orf, H. Rossner, Phys. Rev C 28,252(1983)
7. H. Ho, P.L. Gonthier, G.-Y. Fan, W. Kühn, A. Pfoh, L. Schad, R. Wolski, J.P. Wurm, J.C. Adloff, D. Disdier, A. Kamili, V. Rauch, G. Rudolf, F. Scheibling, A. Strazzeri, Phys. Rev. C 27,584(1983)

8. W. Lücking, R. Schreck, K. Keller, L. Lassen, A. Nagel and H. Gemmeke, Z. Phys. A320,585(1985)
9. B. Chambon, D. Drain, C. Pastor, A. Dauchy, A. Giorni, C. Morand, Z. Phys. A312,125(1983)
10. H. Ohnuma, N. Hoshino, O. Mikoshiba, K. Raywood, A. Sakagughi, G.G. Shute, B.M. Spicer, M.H. Tanaka, M. Tanifuji, T. Terasawa and M. Yasue, Submitted to Nucl. Phys., July 1985.
11. D.J. Morrissey, W. Benenson, E. Kashy, C. Bloch, M. Lowe, R.A. Blue, R.M. Ronningen, B. Sherrill, H. Utsunomiya and I. Kelson, Phys. Rev. C 32,877(1985).
12. G. Caskey, A. Galonsky, B. Remington, M.B. Tsang, C.K. Gelbke, A. Kiss, F. Deak, Z. Seres, J.J. Kolata, J. Hinnefeld and J. Kasagi, Phys. Rev. C 31,1597(1985).
13. B.A. Remington, Ph.D. Thesis, Michigan State University 1986.
14. M.A. Bernstein, W.A. Friedman, and W.G. Lynch, Phys. Rev. C 29,132(1984) and 30,412(E)(1984).
15. J. Gosset, J. Kapusta, and G.D. Westfall, Phys. Rev. C 18,L111(1984).
16. H. Stöcker, J. Phys. G. 10,L111(1984).
17. C.B. Chitwood, C.K. Gelbke, J. Pochodzalla, Z. Chen, D.J. Fields, W.G. Lynch, R. Morse, M.B. Tsang, D.H. Boal, J.C. Shillcock, Michigan State Univ. preprint MSUCL-525
18. J. Pochodzalla, W.A. Friedman, C.K. Gelbke, W.G. Lynch, M. Maier, D. Ardouin, H. Delagrange, H. Doubre, C. Gregoire, A. Kyanowski, W. Mittig, A. Peghaire, J. Peter, F. Saint-Laurent, Y.P. Viyogi, B. Zwieglinski, G. Bizard, F. Lefèbvres, B. Tamain, and J. Quebert, Phys. Lett. B. 161,256(1985).

III.A.4.e. EMISSION OF INTERMEDIATE MASS NUCLEI IN EXCITED STATES

C.K. Gelbke, W.G. Lynch, J. Pochodzalla, M.B. Tsang, D.J. Morrissey, D. Sarantites,[a] L.G. Sobotka,[a] M. Halbert,[b] and D. Hensley[b]

A variety of statistical models have been proposed to describe the emission of intermediate mass nuclei, including the sequential[1,2] or non-sequential[3-6] emission of particle stable and unstable complex nuclei, or the statistical formation of clusters near the critical point in the liquid-gas phase diagram of nuclear matter.[7-8] These calculations differ principally in the choice of the decay configurations which are assumed to be statistically populated. The variety of decay configurations currently used reflects major physics uncertainties associated with the detailed nature of the disassembly process. Most statistical calculations assume, when defining the phase space of decay configurations, that the excited states of the emitted fragments are unperturbed by the nuclear medium. This results in specific predictions about the relative populations of ground and excited states of the emitted fragments.

At present, experimental information is available only for the decay of light nuclei[9-12] (see detailed discussion in Sections A4(a) and (b)). In order to study the production of heavier nuclei in their excited states, experiments with higher resolution need to be performed.

We have already carried out a high resolution study of the relative population of particle stable states of fragments produced in ^{32}S induced reactions on Ag. A spectrum of γ-rays in coincidence with ^{10}B fragments is shown in Fig. 1; γ-rays from the 0.72, 1.74, and 2.15 MeV excited states are observed. Emission temperatures will be extracted following an assessment of the influence of sequential decay processes. Evidence for the importance of sequential decay processes is provided by Fig. 2 where the ^{7}Li-α correlation function for ^{40}Ar induced reactions on ^{197}Au at E/A=60 MeV is shown.[13]

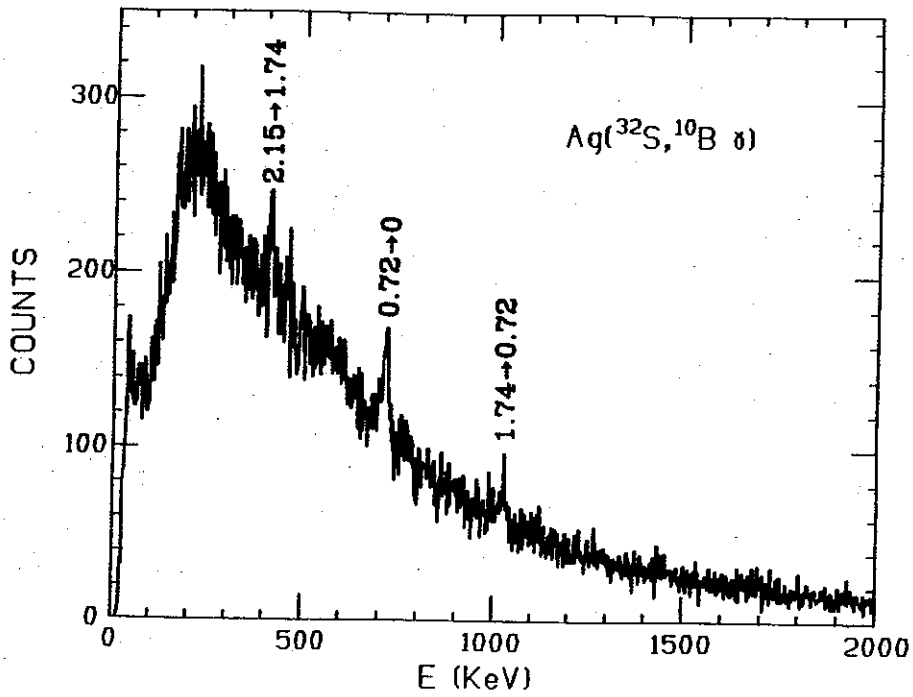

Fig. 1. Spectrum of γ-rays in coincidence with ^{10}B fragments for ^{32}S induced reactions on Ag at E/A=22.5 MeV. Transitions from states at .72, 1.74, and 2.15 MeV are indicated on the figure.

(See section A4(b) for a discussion of correlation function techniques.) The prominant peaks in the correlation function correspond to unresolved states in ^{11}B; almost 15% of the observed yield for particle stable ^{7}Li results from the decay of particle unstable ^{11}B fragments. Figure 2 clearly illustrates the need for higher resolution correlation measurements.

The excitation energy resolution in Fig. 2 was limited by the angular resolution of the hodoscope. At the NSCL, we are currently constructing a position-sensitive detection array with a design resolution of better than 50 keV in order to resolve the individual states of intermediate mass fragments with A≤16. For states where adequate spectroscopic information is available, we will test presently available statistical calculations.[1,14] Data measured with this device will be combined with data from the neutron detection array, discussed in section A4(d), to determine sequential feeding contributions to observed particle stable intermediate mass fragment cross sections. Branching ratios will be obtained for states with more than one decay branch.

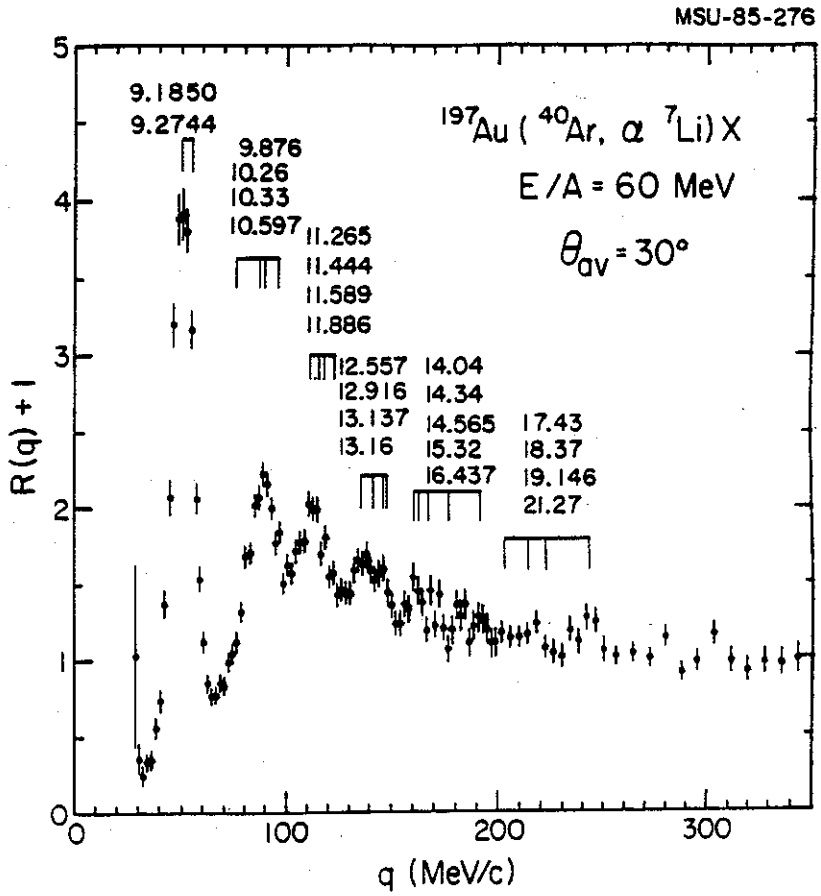

Fig. 2. Correlation function for coincident ^{7}Li and α particles emitted in ^{40}Ar-induced reactions on ^{197}Au at E/A=60 MeV. Locations of states in ^{11}B are indicated on the figure.

For the first experiment with this array, we plan to measure the yields of particle unstable states of nuclei with A=5-16 for ^{14}N induced reactions on Ag. This will permit an assessment of the importance of secondary emission processes for this reaction where the low emission temperature was reported.

a. Washington University, St. Louis.

b. Oak Ridge National Laboratory.

References:

1. D.J.Fields, W.G.Lynch, C.B.Chitwood, C.K.Gelbke, M.B.Tsang, H.Utsunomiya, and J.Aichelin, Phys.Rev.C,1912(1984).
2. W.A.Friedman and W.G.Lynch, Phys.Rev.C28,950(1983).
3. D.H.E.Gross, L.Satpathy, Meng Ta-chung, and M.Satpathy, Z.Phys.A309,41(1982).
4. J.Randrup and S.E.Koonin. Nucl.Phys.A356,223(1981).
5. G.Fai and J.Randrup, Nucl.Phys.A381,557(1982).
6. J.P.Bondorf, Nucl.Phys.A387,25c(1982).
7. J.E.Finn, S.Agarwal, A.Bujak, J.Chuang, L.J.Gutay, A.S.Hirsch, R.W.Minich, N.T.Porile, R.P.Scharenberg, B.C.Stringfellow, and F.Turkot, Phys.Rev.Lett.49,1321(1982).
8. R.W.Minich, S.Agarwal, A.Bujak, J.Chuang, J.E.Finn, L.J.Gutay, A.S.Hirsch, N.T.Porile, R.P.Scharenberg, B.C.Stringfellow, and F.Turkot, Phys.Lett.118B,458(1982).
9. D.J. Morrissey, W. Benenson, E. Kashy, B. Sherrill, A.D. Panagiotou, R.A. Blue, R.M. Ronningen, J. van der Plicht and H. Utsunomiya, Phys. Lett. 148B,423(1984).
10. J. Pochodzalla, W.A. Friedman, C.K. Gelbke, W.G. Lynch, M. Maier, D. Ardouin, H. Delagrange, H. Doubre, C. Gregoire, A. Kyanowski, W. Mittig, A. Peghaire, J. Peter, F. Saint-Laurent, Y.P. Viyogi, B. Zwieglinski, G. Bizard, G. Lefebvres, and B. Tamain, Phys. Rev. Lett 55,177(1985).
11. J. Pochodzalla, W.A. Friedman, C.K. Gelbke, W.G. Lynch, M. Maier, D. Ardouin, H. Delagrange, H. Doubre, C. Gregoire, A. Kyanowski, W. Mittig, A. Peghaire, J. Peter, F. Saint-Laurent, Y.P. Viyogi, B. Zwieglinski, G. Bizard, G. Lefebvres, and B. Tamain, Phys. Lett. 161B,275(1985).
12. C.B. Chitwood, C.K. Gelbke, J. Pochodzalla, Z. Chen, D.J. Fields, W.G. Lynch, R. Morse, M.B. Tsang, D.H. Boal, and J.C. Shillcock, Michigan State University preprint MSUCL-525.
13. J. Pochodzalla, W.A. Friedman, C.K. Gelbke, W.G. Lynch, M. Maier, D. Ardouin, H. Delagrange, H. Doubre, C. Gregoire, A. Kyanowski, W. Mittig, A. Peghaire, J. Peter, F. Saint-Laurent, Y.P. Viyogi, B. Zwieglinski, G. Bizard, G. Lefbvres, and B. Tamain, Proceedings of 4th International Conference on Nuclear Reaction Mechanisms, Varenna, Italy (1985), pg. 171.
14. D. Hahn, and H. Stöcker, to be published.

III.B.1.a. CHARGE EXCHANGE WITH HEAVY IONS

N. Anantaraman, S.M. Austin, J.S. Winfield, C.C. Chang[a],
G.C. Ciangaru[b], and S. Gales[c]

Heavy-ion charge exchange reactions[1-6] offer several advantages over (p,n) reactions as spectroscopic tools for the study of Gamow-Teller (GT) and other spin-dependent transitions in nuclei. Perhaps the most important advantage is the selectivity of the spin transfer channel for certain projectile-ejectile choices: for example, (^{6}Li,^{6}He) and (^{12}C,^{12}N) are both 0^+ to 1^+ transitions and hence should selectively excite $\Delta S=\Delta T=1$ transitions. Heavy-ion charge exchange reactions also allow the equivalent of both (p,n) and (n,p) reactions (or B^- and B^+). They may also give information about the location and strength of higher multipolarity spin resonances than GT, and may allow the study of more exotic phenomena such as double charge exchange.[7]

A disadvantage of charge exchange reactions with low-energy heavy ions is that the one-step process, which is of most interest for spectroscopic studies, must compete with a large amplitude for the sequential transfer of nucleons (e.g. one nucleon pickup and stripping). However, whereas two-step processes are found to dominate at beam energies of less than 10 MeV per nucleon, the one-step process is expected to become dominant at sufficiently high energies, since the cross sections for transfer decrease exponentially with increasing energy.[8] As a reference point, the (p,n) reaction at energies above 25 MeV appears to be well-described by a one-step mechanism.[9]

If the (^{12}C,^{12}N) and (^{18}O,^{18}F) reactions proceed by a one step mechanism, they will certainly be useful and perhaps unique spectroscopic probes of β^+ strength in nuclei. The reaction (^{12}C,^{12}N) is particularly suitable as a spectroscopic tool since ^{12}N (unlike ^{18}F) has no particle-stable excited states and hence peaks due to mutual excitation of target and projectile will be absent in the spectra.

Our program of heavy-ion charge exchange experiments at MSU has involved two reactions: (^{6}Li,^{6}He) at bombarding energies from 14 to 35 MeV/nucleon on several targets, which provided well-resolved states for studying $\Delta L=0$, $\Delta S=1$, $\Delta T=1$ (Gamow-Teller) transitions; and (^{12}C,^{12}N) at 35 MeV/nucleon on a ^{12}C target. These measurements were performed with the S-320 spectrograph. The main objective of both studies was to investigate

whether the reaction mechanism is dominated by the one-step process. This was done in the first case by checking the extent to which the cross sections for the various GT transitions, after being corrected for the mass dependence of distortion effects, had similar angular distributions and magnitudes proportional to the known B(GT) values. In the second case, we inferred the reaction mechanism by comparing measured cross sections to values expected for the one-step process.

Some results from the (^{6}Li,^{6}He) study are shown in Fig. 1. The magnitudes of the distortion-corrected cross sections at a fixed momentum

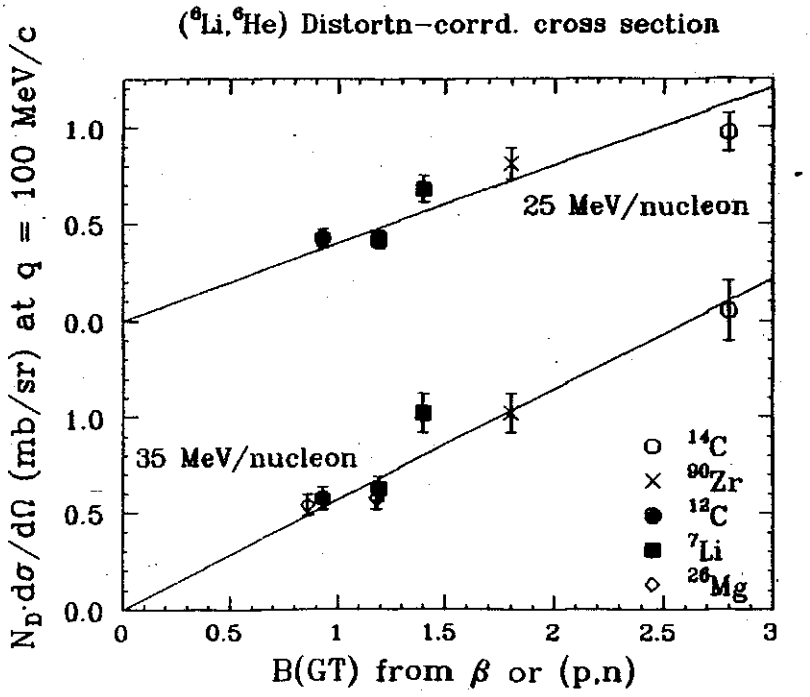

Fig. 1. Plot of distortion-corrected (^{6}Li,^{6}He) cross sections at 25 and 35 MeV/nucleon for a momentum transfer of 100 MeV/c vs. B(GT) values.

transfer (100 MeV/c), at both 25 and 35 MeV/nucleon, are found to be approximately proportional to the B(GT) values. The correlation is less good at 14 MeV/nucleon. From this and several other checks, we conclude

that the one-step process dominates the (^{6}Li,^{6}He) reaction at 25 MeV and that the observed section for a transition provides a good measure of B(GT).

We reach a different conclusion for the (^{12}C,^{12}N) reaction at 35 MeV/nucleon. The most prominent feature of the spectrum is a peak at 4.5 MeV which corresponds to the unresolved 4^- (4.52 MeV) and 2^- (4.46 MeV) states in ^{12}B. The angular momentum mismatch for the reaction (~4.5ħ) suggests that most of the contribution to this peak is from the higher spin state. Strong population of states near 4.5 MeV has also been observed in the ^{12}C(d,^{2}He)^{12}B reaction[10] and in the mirror nucleus ^{12}N by von Oertzen et al.[4].

Microscopic DWBA calculations for the one-step process have been performed for comparison with the four experimental angular distributions extracted. A test of the model lies in the extracted value of the strength of the interaction, $V_{\sigma\tau}$. The values of $V_{\sigma\tau}$ required to fit the data vary from 29 MeV for the ground state to an untypically large 320 MeV for the 2^+ state. The most accurate determination of $V_{\sigma\tau}$ in this energy range is probably the average value of 11.7±1.7 MeV obtained from a variety of (p,n) and (p,p') studies.[11] While it is true that the values of $V_{\sigma\tau}$ obtained here for (^{12}C,^{12}N) (with the exception of the transition to the 2^+ state of ^{12}B) are smaller than values obtained previously for projectiles with A>6 (but at lower energy), they are nevertheless larger than the accepted value of $V_{\sigma\tau}$ (≈12 MeV).

A rough estimate of the energy at which the ^{12}C-induced charge exchange reactions become mainly one-step in nature is indicated in Fig. 2. The solid line shows the calculated trend of the angle-integrated one-step (^{6}Li,^{6}He) cross section (using $V_{\sigma\tau}$=12 MeV) as a function of bombarding energy. The dashed line is the estimated trend of the sequential transfer process, based on calculations of transfer cross sections and the model of Madsen,[12] normalized by assuming that our measured cross section at 35 MeV/nucleon is essentially all sequential transfer. Figure 2 shows that the sequential transfer process becomes negligible at about 60 MeV/nucleon. This limit may be reduced to 50 MeV/nucleon if exchange effects are found to increase the predicted one-step cross section by 30%.

However, the one-step nature of heavy-ion charge exchange reactions with ^{12}C and heavier projectiles at intermediate energies still remains to be established experimentally, and the first experiments we plan with the K500 + ECR will have that goal. An obvious follow-up to our previous

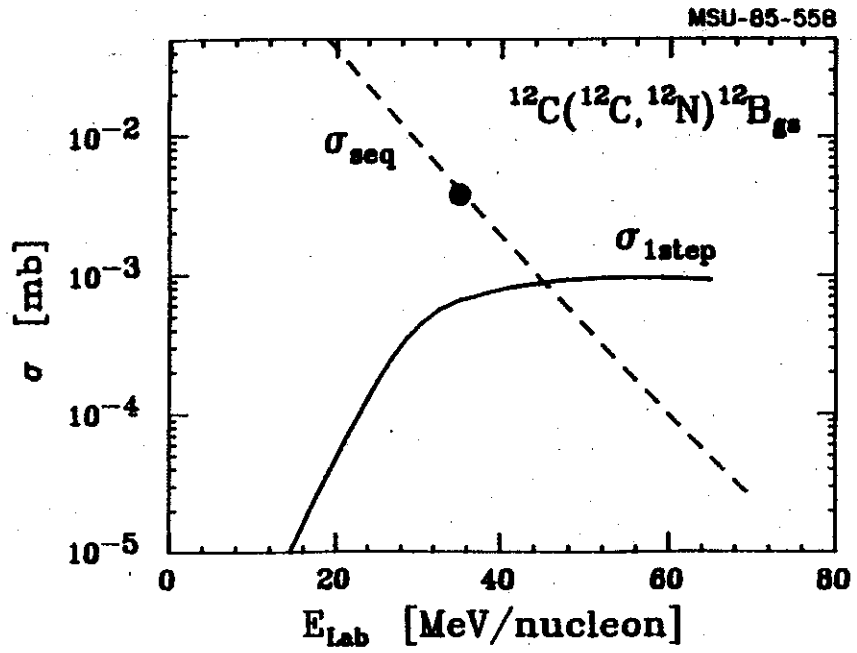

Fig. 2. Trends of the one-step and sequential transfer cross sections as a function of ^{12}C incident energy. The solid line (σ_{1step}) is taken from microscopic DWBA calculations. The dashed line is an estimate of σ_{seq}; this line is normalized to the data point which represents the observed cross section for $^{12}C(^{12}C,^{12}N)^{12}B_{gs}$ at 35 MeV/nucleon.

experiment would be to study the mechanism of $^{12}C(^{12}C,^{12}N)^{12}B$ at 50 or 60 MeV/nucleon and at higher energies, up to the 110 MeV/nucleon limit of the S320 Spectograph when the K800 becomes available. Another interesting system to study would be $^{26}Mg(^{12}C,^{12}N)^{26}Na$, since there are theoretical calculations for the B(GT,β^+) strength indicate that most of the low-lying β^+ strength is concentrated in one state at $E_x \approx 200$ keV, and intermediate-energy (p,n) measurements[13] for the analogue T=2 state in ^{26}Al yield the value of B(GT) with good accuracy. Hence this reaction should also be a good calibration case.

Most applications of the (^{12}C,^{12}N) and (^{18}O,^{18}F) reactions to spectroscopy will probably require the high resolution of the S-800 spectrograph and energies above 100 MeV/nucleon. An immediate goal, however, would be to measure β^+ strengths which are of especial interest to astrophysics in connection with the production of light elements in explosive nucleosynthesis and the detailed evolution of supernova explosions.[14] The initial experiment would be with a ^{56}Fe target since the region near mass 56 is fundamental to nuclear astrophysics (see Section C.3.a).

One topic of general interest is the evaluation of the β-decay sum rule[15] $S_-(GT) - S_+(GT) = 3(N-Z)$, where S_- is the strength for β^- and S_+ is the strength for β^+ decay. This sum rule will be substantially modified if "quenching", e.g. due to Δ degrees of freedom,[16] is important. It has been pointed out[17] that the same Δ-hole mechanism which quenches the GT strength in (p,n) reactions will <u>enhance</u> (n,p) transitions at very forward angles. Similar quenching and enchancement should also be expected in (^{12}C,^{12}B) and (^{12}C,^{12}N) reactions, respectively.

Because of the absence of non $\Delta S=1$ background, the ^{12}C-induced charge exchange reactions might be useful in studying both weaker GT transitions than is possible with (p,n) and higher-multipole spin-flip transitions. In particular, the kinematic conditions governing the heavy-ion charge exchange reactions will tend to favor the higher multipolarities in the same way that the 4^- state was so strongly selected in the $^{12}C(^{12}C,^{12}N)^{12}B$ reaction. It will be important to establish these reaction properties by studies above 100 MeV/nucleon.

a. University of Maryland
b. Schlumberger Well Services, Houston, Texas
c. IPN, Orsay

<u>References:</u>

1. G. Ciangaru, R.L. McGrath and F.E. Cecil, Phys. Lett. <u>61B</u>, 25 (1976)
2. W.R. Wharton and P.T. Debevec, Phys. Rev. C <u>11</u>, 1963 (1975)

3. A. Etchegoyen, D. Sinclair, S. Liu, M.C. Etchegoyen, D.K. Scott and D.L. Hendrie, Nucl. Phys. A397, 343 (1983)
4. W. von Oertzen, in "Lecture Notes of the Erice Summer School, 1984", (to be published by Interscience, New York); GANIL preprint P.84.15; W. von Oertzen et al., HMI annual report (1984) p. 53.
5. H.G. Bohlen, E.R. Flynn, A. Miczaika and W. von Oertzen, in Abstracts of Contributed papers, Int. Symposium on Highly Excited States and Nucl. Structure, edited by N. Marty and N. van Giai (Orsay, 1983), p. 76
6. B.T. Kim, A. Greiner, M.A.G. Fernandes, N. Lisbona, K.W. Low and M.C. Mermaz, Phys. Rev. C 20, 1680 (1979)
7. C. Brendel et al., Proc. 4th Int. Conf. on Nuclei Far From Stability, Helsingør, 1981 (CERN 81-09) p. 664
8. W. von Oertzen, Phys. Lett. 151B, 95 (1985)
9. W.A. Sterrenburg, Sam M. Austin, U.E.P. Berg and R.P. DeVito, Phys. Lett. 91B, 337 (1980)
10. D.P. Stahel, R. Jahn, G.J. Wozniak and J. Cerny, Phys. Rev. C 20, 1680 (1979); K.B. Beard, J. Kasagi, E. Kashy, B.H. Wildenthal, D.L. Friesel, H. Hann and R.E. Warner, Phys. Rev. C 26, 720 (1982)
11. S.M. Austin, in "The (p,n) reaction and the N-N force", ed. C.D. Goodman et al., (Plenum, New York, 1980)
12. V.A. Madsen and V.R. Brown, in "The (p,n) reaction and the N-N force," edited by C.D. Goodman et al., (Plenum, New York, 1980).
13. R. Madey, B.S. Flanders, B.D. Anderson, A.R. Baldwin, C. Lebo, J.W. Watson, S.M. Austin, A. Galonsky, B.H. Wildenthal and C.C. Foster, Phys. Rev. C, to be published.
14. G.M. Fuller, W.A. Fowler and M.J. Newman, Astrophysics Journal 252, 715 (1982); G.M. Fuller, ibid 252, 741 (1982); and priv. comm.
15. C. Gaarde et al., Nucl. Phys. A334, 248 (1980)
16. M. Rho, Nucl. Phys. A231, 497 (1974); A. Bohr and B.R. Mottelson, Phys. Lett. 100B, 10 (1981)
17. V.R. Brown, S. Krewald and J. Speth, Phys. Rev. Lett. 50, 658 (1983)

III.B.1.b. SPIN-FLIP TRANSITIONS

G.M. Crawley, A. Galonsky, B.A. Brown, V. Rotberg, C. Djalali,
N. Marty[a], A. Willis[a], M. Morlet[a]

Motivated by the observation of the Gamow-Teller resonance in the (p,n) reaction, first at MSU[1] and later at IUCF,[2] and guided by the experimental and theoretical investigations of the nucleon-nucleon effective interaction, we carried out the first successful search for the corresponding (p,p') transition in the parent nucleus early in 1981. This work was a collaboration between an MSU group and a group from the Institut de Physique Nucleaire, Orsay, France (N. Marty, A. Willis, M. Morlet and C. Djalali). The important experimental ingredients for success in this project were the bombarding energy of 200 MeV, where spin-flip processes are enhanced, and the ability to measure the inelastically scattered protons cleanly at small scattering angles, where the cross section for the ℓ=0 transition peaks. The large spectrometer at the Orsay synchrocyclotron and its focal plane detector which recorded the direction of the scattered particles made it possible to obtain the required small angle data.

The first measurements were made on the zirconium isotopes and a broad feature was observed in all four even-even isotopes studied.[3] This feature had the right excitation energy and angular distribution to be an ℓ=0 spin-flip transition. More recently, the spin-flip nature of this structure has been confirmed by spin-flip probability measurements[4] at LAMPF. We have subsequently measured the properties of such spin-flip transitions in a wide range of nuclei. Some of the highlights of the early work were the observation[5] of the single state in ^{48}Ca and its spreading as more protons were added in the N=28 isotones[6] and the observation of states with both lower and higher isospin in the nickel isotopes. These aspects have been discussed in our previous proposal and in a number of review articles.

More recently, due to improvements in the small angle capability of the spectrograph, we have been able to extend our measurements to heavier nuclei including the interesting case[7] of ^{208}Pb. A (p,p') spectrum taken on ^{208}Pb at 3° is shown in Fig. 1. In such heavy nuclei, Coulomb excited 1^- states have angular distributions which are very similar to those of ℓ=0 spin-flip transitions. However, it is possible to predict the magnitude of the (p,p') cross section, of such Coulomb excited states, quite accurately if the B(E1)'s are known. Thus, using the results from electromagnetic probes, which give quite accurate B(E1)'s up to about 8.5 MeV excitation energy, it is possible to extract spin-flip strength over this same energy region. We find that only about 30% of the total expected strength is observed below 8.5 MeV.

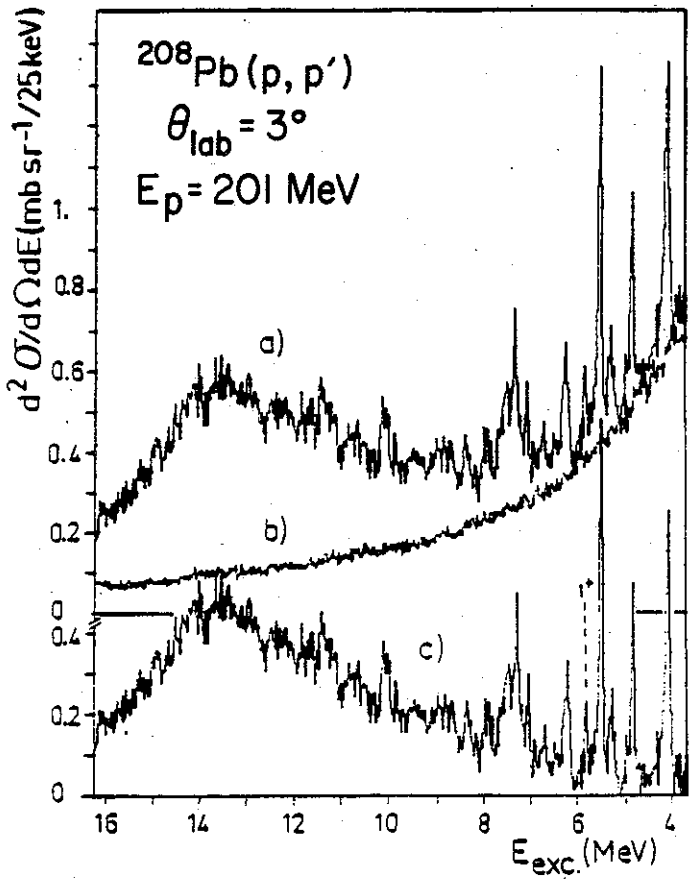

Figure 1.

As a consequence of the earlier studies on a broad spectrum of nuclei two questions arose. Why is the (p,p') strength only about one third of that predicted, even when fairly sophisticated wave functions are used, and why is there sometimes agreement with electron scattering results on the same nuclei and sometimes marked disagreement? Two suggestions have been advanced to explain the lack of observed strength ("quenching"). One is that the strength is spread more widely than is anticipated even in fairly sophisticated shell model calculations because of mixing with states from higher oscillator shells. The other is that the mixing is with a Δ-hole state at around 300 MeV excitation energy. Since all particles in the nucleus can participate, such mixing might be significant even though the energy denominator is so large. This latter explanation will only apply to isovector ($\Delta T=1$, 1^+) excitations, since these have the same quantum numbers as the Δ-hole excitation. Unfortunately,there is no general theoretical agreement, and very little experimental evidence as to the relative importance of these mechanisms. Experimentally, very little is known about isoscalar M1 states since these states are generally not excited in electromagnetic reactions. In intermediate energy (p,p') scattering, both isoscalar and isovector M1 states can be excited. We have therefore begun a program of studying both $\Delta T=1$ and $\Delta T=0$ excitations in light nuclei, particularly those with N=Z where such $\Delta T=1$ and $\Delta T=0$ excitations can be distinguished. The first case we studied[8] was ^{28}Si, where we compared measured cross sections for T=0 and T=1, 1^+ states separately with predictions using the wave functions of Brown, Wildenthal, et al. We found that the quenchings for both T=0 and T=1 states are the same. This result suggests that mixing with the Δ-hole state does not play an overwhelming role in the quenching of 1^+ strength and that the other explanation (higher configuration mixing) needs to be invoked. However more cases need to be examined to pin down the effect.

We have therefore obtained data on ^{16}O, ^{20}Ne, ^{24}Mg and ^{32}S. A representative spectrum from three of these targets is given in Fig. 2. The ^{16}O and ^{20}Ne data were obtained using a gas cell target with kapton windows. To maintain energy resolution, the cell had to be fairly thin and was therefore operated at pressures of three to four bars. The resolution becomes worse as the scattering angle increases but we were able to take usable data with this target between laboratory angles of 2° and 10°.

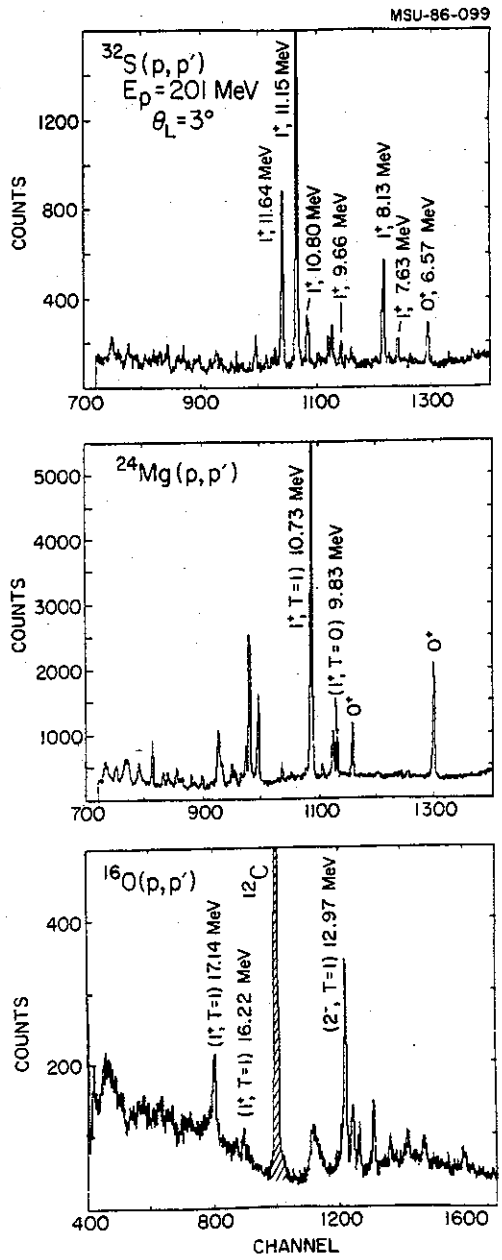

Figure 2.

In these light nuclei, the angular distributions identify the J^{π} and, for the 1^+ states, even the isospin character of the transitions quite clearly. For example, in Fig. 3, angular distributions for known 0^+, 2^+, 1^-, 1^+, T=1 and 1^+, T=0 states are shown. All these angular distributions

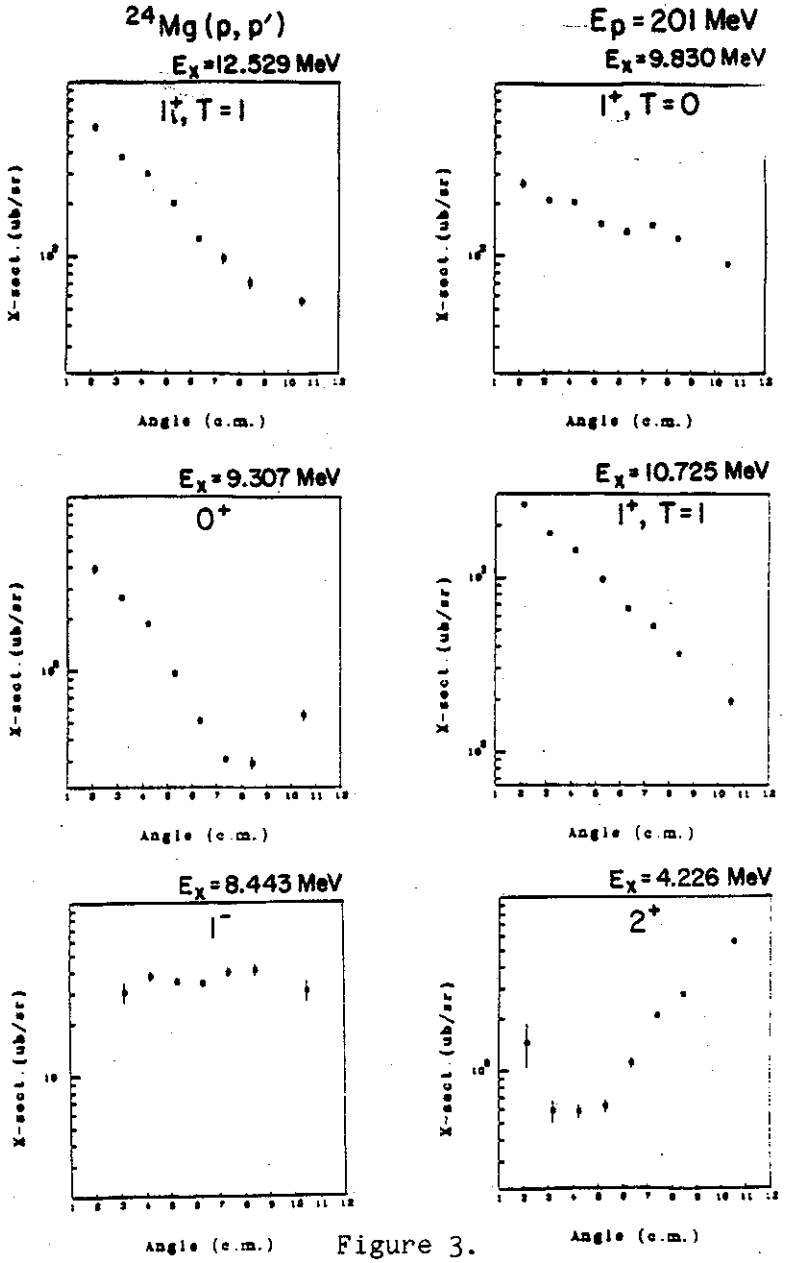

Figure 3.

are quite different and allow us to identify unknown states. We are in the process of making distorted wave calculations for a number of the 1^+ states using the wave functions of Brown and Wildenthal.

The second question raised was the comparison with electron scattering. In some cases, for example in the nickel isotopes, the agreement between proton and electron scattering seems to be quite good, but in other cases there seems to be serious disagreements. Perhaps the clearest example of this is the case of ^{51}V where the (p,p') measurements show a substantial broad but structured feature, whereas detailed (e,e') searches show no 1^+ strength in this region (Fig. 4). One possible explanation is that the (p,p') reaction is more selective of 1^+ transitions so that the peak-to-background ratio is better. In ^{50}Ti for example, where similar states can be compared, the proton peak-to-background ratio is about 10 times better than that for the (e,e') results. This means that, especially in the case of broad structures, it may be difficult to find the 1^+ strength in (e,e').

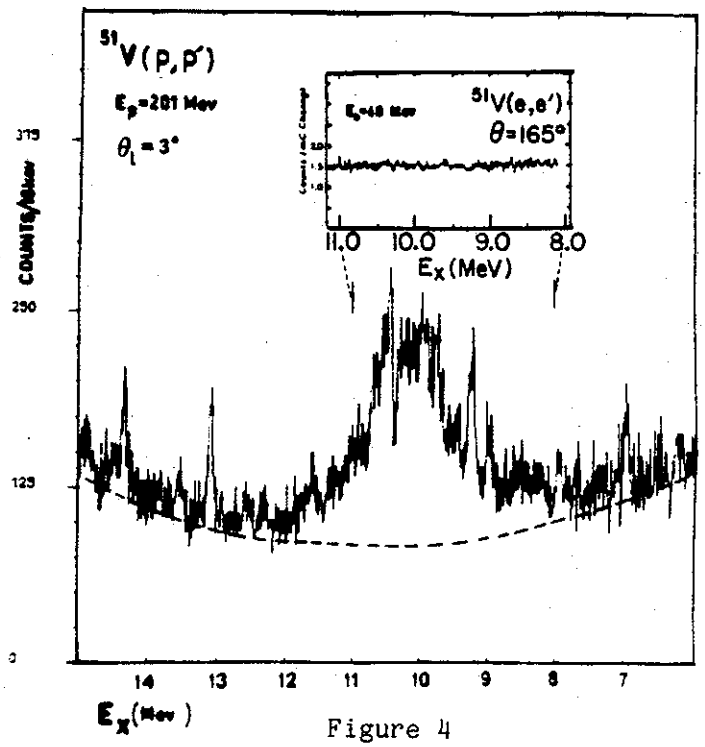

Figure 4

However, there is a more fundamental reason why there may be differences between proton and electron inelastic scattering. In electron scattering one measures B(M1), which contains both orbital and spin components, whereas in (p,p') one has only a spin component. Thus, for transitions where the orbital component can contribute (proton transitions), there may be differences between the electron and proton scattering results, especially since there can be interferance between the orbital and spin amplitudes.

Quite dramatic differences are observed in some cases -- for example, in the calcium isotopes. In ^{48}Ca, for the strong state at 10.2 MeV, there is rather good agreement between proton and electron scattering, which is expected since this transition is believed to be a predominantly neutron transition. However, for the other even-even calcium isotopes, and even for the weaker 1^+ states in ^{48}Ca, there are substantial differences between the proton scattering results (see Fig. 5) and the earlier electron scattering data. For example, in ^{42}Ca, there is a single strong 1^+ state observed in (e,e') at 11.2 MeV, whereas in (p,p') the 1^+ strength is divided over six or seven states and no one state is dominant. In ^{40}Ca, on the other hand, there appear to be two 1^+ states, one at 10.32 MeV and another near 12.09 MeV, which are quite strongly excited in (p,p'). In (e,e') on the other hand, the 12.09 MeV state is not observed. Such differences between proton and electron scattering could be used to obtain information on the spin versus orbital nature of particular transitions and, therefore, on the structure of the states.

We have recently applied this method to some low-lying 1^+ transitions observed in heavy deformed nuclei. These states were first observed in electron scattering[9] and were believed to be mainly orbital transitions arising from a collective "twisting" mode of oscillation of protons against neutrons. However, no direct proof could be given from inelastic electron scattering alone since both spin and orbital parts of the electromagnetic

interaction may contribute. If the states were mainly orbital they would not be excited in the (p,p') reaction.

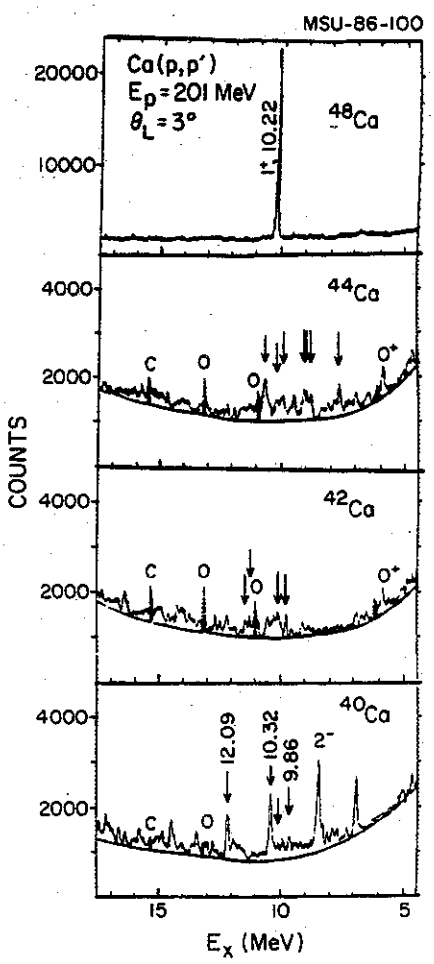

Figure 5.

Indeed, only upper limits on the cross sections for the (p,p') reaction on ^{154}Sm, ^{156}Gd and ^{164}Dy could be obtained. This suggested that the spin contributions to these excitations were small, thus supporting the earlier suggestion of a dominant orbital mode.

In addition, Zamick[10] has recently pointed out that low lying 1^+ states with strong M1 transition strength are not restricted to rare earth nuclei.

In an $f_{7/2}$ shell model calculation, he predicted a state at $E_x \sim 4$ MeV carrying a transition strength $B(M1)\uparrow = 1.7\ \mu_N^2$. Comparison of shell model and interacting boson type calculations also shows that low-lying 1^+ states in medium heavy nuclei should be considered of mixed symmetry in the proton-neutron degree of freedom, analogous to the states observed in heavier nuclei. This stimulated us to explore the role of spin and orbital excitation mechanisms in medium heavy nuclei, specifically in ^{46}Ti.

Spectra on ^{46}Ti from both (p,p') and (e,e') are given in Fig. 6. The energy of the state seen in (p,p') at 4.32 MeV agrees very well with the energy of the state excited by (e,e'). The shape of the measured angular

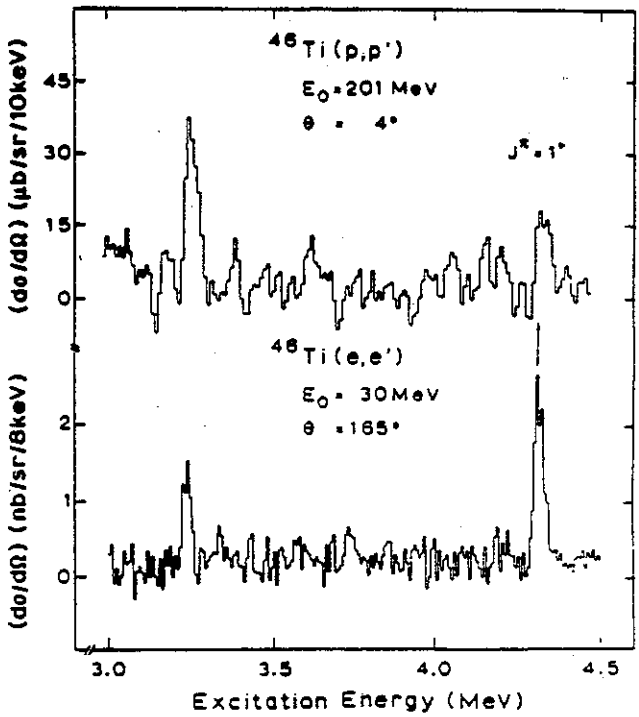

Figure 6

distribution of this state matches that predicted for the low lying 1^+ state by the shell model calculations of Brown. We obtain a $B(\sigma)$ value of $0.13 \pm 0.2\ \mu_N^2$, and the $B(M1)\uparrow$ value from the (e,e') measurement is $1.0 \pm 0.2\ \mu_N^2$. The ratio of orbital amplitude to spin amplitude, therefore, has the value

1.8 ± 0.6 or 3.8 ± 0.6 depending upon the phase between orbital and spin components. The ratio predicted by Zamick is 1.1, which is close to being within the experimental range for one choice of the phase but not for the other.

Thus for ^{46}Ti, a measured value of the spin contribution is obtained, in contrast to the situation in the three heavy target nuclei, where we could determine only an upper limit. For all four nuclei, we have shown that the spin contribution to the B(M1)↑ is generally smaller than the orbital contribution,a conclusion that supports the "twist" nature of these states.

There is still substantial data analysis and publication to be carried out for the work described above, but we believe that our experimental program at the Orsay synchrocyclotron is essentially complete. However there are a number of new directions that we plan to pursue at IUCF, using polarized proton beams at Saclay and possibly at the NSCL when the S800 spectrograph becomes operational. A brief outline of these directions is given below:

(i) The Calcium Isotopes:

In our earlier ^{48}Ca experiment, we were able to place an upper limit of about 3% of the main peak on any individual level. Only about seven other levels which could have 1^+ strength were identified (see Fig. 7). With better resolution, one could push these limits much more strongly. A new high resolution spectrometer is just coming on line at IUCF which should give a resolution of 10 keV with polarized protons at 200 MeV. This is an important case, because the quenching is substantial (30% of expected strength is observed) and also because ^{48}Ca is a nucleus for which accurate shell model wave functions are available. More stringent upper limits on the total amount of 1^+ strength observed would place more severe limits on the possible explanations of the quenching.

Time has already been approved for measurements on the calcium isotopes by the IUCF PAC, and we are eager to try to make small angle measurements with the new spectrograph.

(ii) The 2s-1d Shell Nuclei:

A more precise determination of both isovector and isoscalar spin-flip strength in s-d shell nuclei would be possible with improved resolution and polarized beams. The improved energy resolution would help to search for very fragmented strength by resolving weakly excited states and to measure the angular distributions more precisely over a wider range of angles thus allowing better J^{π} identification. In addition, the analyzing powers are expected to be different at small angles for isovector and isoscalar spin-flip transitions. Therefore their measurement should allow a better determination of the the isospin quantum number. Finally, at a later stage, the possibility of measuring spin-flip probabilities S_{nn} would greatly help to pin down the spin-flip strength in these nuclei.

(iii) Heavy Deformed Nuclei:

The capability of high resolution would also allow a more thorough investigation of the low lying 1^{+} states in the heavy deformed nuclei discussed earlier. It might then be possible actually to measure a cross section for such states, instead of the upper limit which is presently possible. If such a measurement could be made, the actual value of the spin to orbital contribution could be determined, and much tighter constraints could be placed on the model wave functions.

(iv) Inelastic Deuteron Scattering:

The deuteron is a potentially interesting probe since it only excites, at least in first order, isoscalar transitions. In general, the natural parity states are expected to dominate the spectra. However, because of the energy dependance of the N-N interaction, spin-flip transitions should be favoured

relative to non spin-flip transitions for incident energies of 200 to 400 Mev per nucleon. Furthermore, the analyzing powers A_y and A_{yy} should help distinguish between spin-flip and non spin-flip states. Elastic scattering measurements of polarized deuterons from different nuclei have been recently carried out at SATURNE,[12] and analyzed both microscopically and phenomenologically. These results can be used to analyze the inelastic scattering data.

The study of the isoscalar spin-flip response of nuclei leads to important information concerning the strength of the residual p-h interaction in the $\vec{\sigma}_p \cdot \vec{\sigma}_h$ channel. Experimentally, besides some discrete states observed in light nuclei, almost nothing is known about the isoscalar spin-flip strength in nuclei. So far, the only indication of a giant isoscalar spin-flip resonance ($\Delta L=1$) was obtained in a (π,π') experiment[11] on ^{12}C.

In a first phase, inelastic cross sections and analyzing powers will be measured at forward angles using 400 MeV polarized deutrons at SATURNE, for known spin-flip states in ^{12}C and ^{48}Ca. These transitions constitute test cases for understanding the reaction mechanism involved. In a second phase, by measuring spin-flip probabilities S_{nn}, the spin-flip cross section can be measured over a wide range of excitation energies in different nuclei. These spectra measured with good statistics can then be analyzed to extract the different spin-flip multipolarities involved. These latter experiments will be carried out at SATURNE in collaboration with a large group from Saclay, Orsay and Rutgers.

a IPN, Orsay

References:

1. R.R. Doering et al., Phys. Rev. Lett. 35,1691(1975)

2. C.D. Goodman et al., Phys. Rev. Lett.44,1755 (1980)and D.E. Bainum et al., Phys. Rev. Lett. 44,1751(1980).
3. G.M. Crawley et al., Phys. Rev. C 26,87(1982)
4. S.K. Nanda et al., Phys. Rev. Lett. 51.1526(1983)
5. G.M. Crawley et al., Phys. Lett. 127B,322(1983)
6. C. Djalali et al., Nucl. Phys A410,399(1983)
7. C. Djalali et al., Phys. Rev. C 31,758(1985)
8. N. Anantaraman et al., Phys. Rev. Lett. 52,1409(1984)
9. D. Bohle et al., Physics Letters 137B,27(1984) and Physics Letters 148B,260(1984)
10. L. Zamick , Phys. Rev. C 31,1955(1985)
11. L. Bland et al., Phys. Lett. 144B,328(1984)
12. Nguyen van Sen et al., Phys. Lett. 156B,185(1985)

III.B.1.c. STUDIES OF ISOVECTOR SPIN-FLIP STRENGTH BY THE (^{6}Li, ^{6}Li*) REACTION

N. Anantaraman, S.M. Austin, D.J. Morrissey,
R.M. Ronningen and J.S. Winfield

Studies of spin-flip strength by inelastic scattering of intermediate energy (200 MeV) protons have been successful in revealing concentrations of spin-transfer strength over a wide range of nuclei, as is shown in Section B1(b) of this proposal.[1] However, this technique does have some limitations: it is difficult to differentiate cleanly between 1^+ and 0^+ transitions (as well as 1^- transitions for A>90 where Coulomb excitation becomes important); natural parity transitions are excited, forming a large background under the giant 1^+ state and hiding weak 1^+ transitions; and the tail of the elastic peak makes it difficult to observe low-lying strength, especially for heavy nuclei where Rutherford scattering is intense.

It appears that the (^{6}Li, ^{6}Li*) reaction, leaving ^{6}Li in its $J^\pi = 0^+$, T=1 state at 3.56 MeV, with coincident detection of the isotropically emitted 3.56 MeV de-excitation gamma ray and the product ^{6}Li, is a probe without these disadvantages. Since the ground state of ^{6}Li is 1^+, T=0, the transitions have $\Delta S=1$, $\Delta T=1$, (i.e. they are pure spin-isospin transfer) so natural parity, isoscalar transitions will not appear. Nor will an elastic tail appear in the coincidence spectrum. Of course, the coincidence experiment will have its own difficulties: in particular, background in the gamma ray detectors will be severe unless the Faraday cup can be well-shielded.

Nevertheless, preliminary estimates indicate that the experiment will have a tractable counting rate, 25 to 50 counts per hour for strong transitions, even for the small (typically 0.65/msr) solid angle of the S320 spectrograph and a gamma detector consisting of four 3x3 BGO detectors. A feasibility study, examining the excitation of the strong 10.2 MeV, 1^+ state in ^{48}Ca (which has been studied by, e.g. (p,p'):ref. 2) at a ^{6}Li energy of 35 MeV/nucleon has received PAC approval. It is known that the isospin analog transitions, (^{6}Li, ^{6}He), are one-step reactions at this energy (see Section B1(a) of this proposal) and their cross sections were used to estimate the expected (^{6}Li, ^{6}Li*) cross sections. If these results

look promising, the 4π gamma ray hit detector presently under construction and the large solid angle of the S800 spectrograph, expected to be available toward the end of the proposal period, will each greatly increase counting rates and make this reaction a powerful probe for isovector spin strength in nuclei.

References:

1. C. Djalali et al., Nuclear Physics A410,399(1983).
2. G.M. Crawley et al., Phys. Lett 127B,322(1983).

III.B.1.d. MEASUREMENTS OF GAMOW TELLER STRENGTH FOR DOUBLE-BETA DECAYING NUCLEI

N. Anantaraman, Sam M. Austin, B.A. Brown and J.S. Winfield

Double β decay (denoted ββ decay)[1] can occur in two modes:

$$(Z,A) \rightarrow (Z+2,A) + e_1^- + e_2^- + \bar{\nu}_1 + \bar{\nu}_2 \qquad (2\nu)$$
$$(Z,A) \rightarrow (Z+2,A) + e_1^- + e_2^- \qquad (0\nu)$$

The first of these modes can be thought of as a second order process, a sequence of two normal β decays passing through (virtual) intermediate states of the nucleus (Z+1,A). The second is of great interest since it does not conserve lepton number, and can serve to measure or limit the mass of Majorana neutrinos and the presence of right handed currents in the weak information.

Recently there has been a renewed interest in these decays because limits on the (0ν) branch for ^{82}Se and ^{76}Ge decay have been used to place limits[1,2] on the mass of Majorana neutrinos and because the first direct electron counting experiment[3] has been performed for $^{82}Se \rightarrow {}^{82}Kr + 2e^- + 2\bar{\nu}$, with tentative results corresponding to a lifetime of $1.0 \pm 0.4 \times 10^{19}$ years. This is about a factor of 30 shorter than the lifetime obtained by geochemical methods. A detailed model calculation of the (2ν) lifetime[2] is in reasonable agreement with the direct counting result but not with the geochemical results. Since recent work[4] indicates that the lifetime inferred from the direct counting experiment is too short, a failure of the theoretical calculations seems likely.

In an attempt to provide constraints on the the calculations the neutron time-of-flight system at the Indiana University Cyclotron Facility was used[5] to obtain (p,n) spectra at 0°, 4° and 8° for ^{76}Ge, ^{82}Se and ^{128,130}Te with an energy resolution of 360 keV. The L=0 strength at 0° (low q) is closely proportional to the Gamow-Teller (GT) strength to the (virtual) intermediate states of the ββ process. Strength is observed to the giant GT resonance region and to narrow low-lying structures populated with $\approx 10^{-2}$ of the strength of the giant resonance. The spectrum for ^{82}Se is shown in Fig. 1.

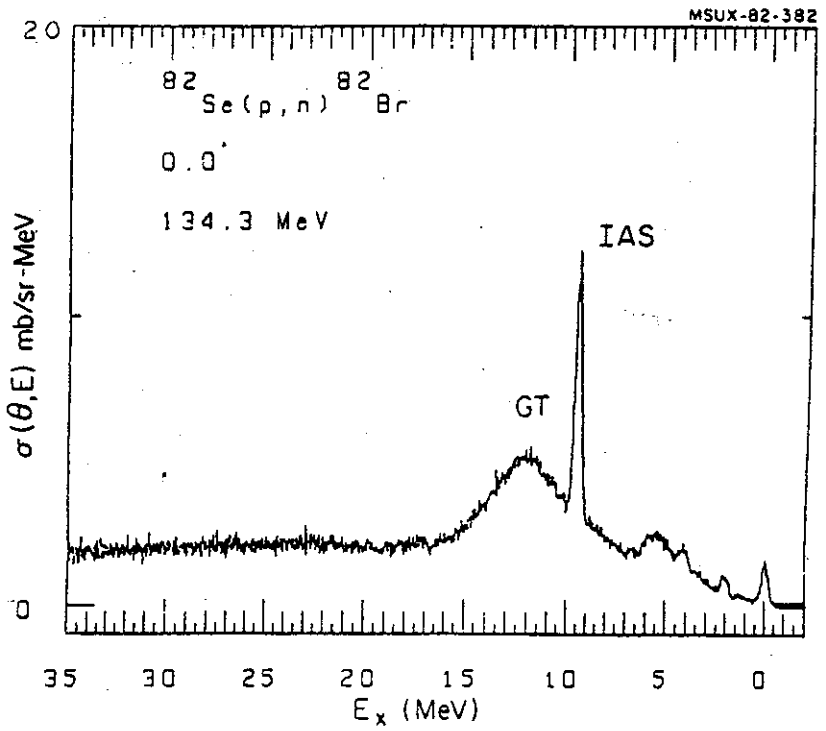

Fig. 1 Spectrum from the ^{82}Se(p,n) reaction at 135 MeV.

Further constraints will be obtained from a study of the reaction ^{76}Se(^{12}C,^{12}N)^{76}As at energies above 50 MeV/nucleon where the reaction is likely to be one step in nature (see section B1(a)). This proposed measurement will yield the GT strength leading to the ^{76}As intermediate system from ^{76}Se side, combining these results with the ^{76}Ge(p,n) results should allow us to place a limit on the total strength of the ^{76}Ge → ^{76}As (virtual) → ^{76}Se decay. Since the phases of the GT amplitudes are not determined, but only their magnitudes, this limit is based on the assumption that all amplitudes are in phase. Hence it will be meaningful only if the transition is quite collective. Fortunately this appears to be the case,[1,6] so we may hope to determine whether the theoretical estimates are reasonable.

References:

1. For a review of all aspects of this subject see W.C. Haxton and G.J. Stephenson, Prog. Part. Nucl. Physics 12,409(1984).
2. W.C. Haxton, G.J. Stephenson and D. Strottman, Phys. Rev. Lett. 47,133(1981).
3. M.K. Moe and D.D. Lowenthal, Phys. Rev. C22,216(1980).
4. M.K. Moe, Invited Talk, DNP/APS Asilomar, Oct. 1985.